AD_____

Award Number: DAMD17-99-1-9481

TITLE: Protein Kinase Pathways that Regulate Neuronal Survival and Death

PRINCIPAL INVESTIGATOR: Kim A. Heidenreich, Ph.D.

CONTRACTING ORGANIZATION: University of Colorado Health Sciences Center
Denver, Colorado 80291-0238

REPORT DATE: August 2004

TYPE OF REPORT: Final

PREPARED FOR: U.S. Army Medical Research and Materiel Command
Fort Detrick, Maryland 21702-5012

REPORT DOCUMENTATION PAGE

Form Approved
OMB No. 074-0188

1. AGENCY USE ONLY (Leave blank)	2. REPORT DATE	3. REPORT TYPE AND DATES COVERED
	August 2004	Final (1 Aug 1999 - 31 Jul 2004)

4. TITLE AND SUBTITLE
Protein Kinase Pathways that Regulate Neuronal Survival and Death

5. FUNDING NUMBERS
DAMD17-99-1-9481

6. AUTHOR(S)
Kim A. Heidenreich, Ph.D.

7. PERFORMING ORGANIZATION NAME(S) AND ADDRESS(ES)
University of Colorado Health Sciences Center
Denver, Colorado 80291-0238

E-Mail: Kim.heidenreich@uchsc.edu

8. PERFORMING ORGANIZATION REPORT NUMBER

9. SPONSORING / MONITORING AGENCY NAME(S) AND ADDRESS(ES)
U.S. Army Medical Research and Materiel Command
Fort Detrick, Maryland 21702-5012

10. SPONSORING / MONITORING AGENCY REPORT NUMBER

11. SUPPLEMENTARY NOTES

12a. DISTRIBUTION / AVAILABILITY STATEMENT
Approved for Public Release; Distribution Unlimited

12b. DISTRIBUTION CODE

13. ABSTRACT (Maximum 200 Words)

Loss of post-mitotic neurons from the adult brain underlies the pathology of neurodegenerative diseases and neurotoxin exposure. Neuronal cell death occurs by two mechanisms: necrosis and apoptosis. Apoptosis is a process whereby developmental cues and environmental stimuli activate a genetic program to implement a series of steps that culminate in cell death. An important aspect of apoptosis is that it can be halted and such interventions may rescue dying neurons. The overall goal of this project is to identify key protein kinases involved in regulating neuronal survival and apoptosis.

The progress made in these areas has resulted in 4 published manuscripts (plus 2 submitted articles) and 9 abstracts presented at national and international scientific meetings in 2002.

14. SUBJECT TERMS
Neurodegeneration, apoptosis, neurons, MEF2, IGF-I, lithium, death receptor, bim, intrinsic death pathway

15. NUMBER OF PAGES
110

16. PRICE CODE

17. SECURITY CLASSIFICATION OF REPORT	18. SECURITY CLASSIFICATION OF THIS PAGE	19. SECURITY CLASSIFICATION OF ABSTRACT	20. LIMITATION OF ABSTRACT
Unclassified	Unclassified	Unclassified	Unlimited

Table of Contents

Cover.....

SF 298.....

Table of Contents.....

Introduction.....1

Body.....1

Key Research Accomplishments.....8

Reportable Outcomes.....9

Conclusions.....14

References.....

Appendices.....

Final Progress Report-#DAMD17-99-1-9481, "Protein Kinase Pathways that Regulate Neuronal Survival and Death", August 1, 1999- July 31, 2004.

Task #1. The first task was to identify protein kinase cascades that are regulated by neurotrophic factors known to support the survival of neurons.
Task #2 The second task was to determine whether activation or inhibition of the neurotrophin- regulated kinases is necessary or sufficient to influence neuronal survival.
Task #3 The third task was to determine whether there is cross-talk between pro-apoptotic and anti-apoptotic signaling pathways.

Results

a) The proapoptotic effects of GSK-3β in primary neurons. Previous studies have established a key role for phosphatidylinositol (PI) 3-kinase in regulating trophic factor-dependent survival of neurons. The Akt protein kinase (also termed protein kinase B) has been implicated as the transducer of PI 3-kinase dependent survival signals generated by serum and certain growth factors. In response to PI 3-kinase activation, Akt binds to phosphorylated membrane lipids via its pleckstrin homology domain and is phosphorylated at threonine 308 and serine 473. Phosphorylation of Akt at these two sites leads to its activation and propagation of an anti-apoptotic signal. One of the downstream targets of Akt implicated in neuron survival is glycogen synthase kinase-3 (GSK-3). Although GSK-3 was originally identified as a kinase that phosphorylates glycogen synthase, subsequent studies have revealed that GSK-3 has a broader role in neurons. It phosphorylates a number of substrates not involved in glycogen metabolism including the initiation factor eIF2B, the microtubule-associated protein tau , and the transcription factors, CREB, c-myc, c-jun, and □ -catenin. GSK-3 β has been shown by complementation to be the mammalian homologue of the *shaggy* gene from *Drosophila melanogaster* that regulates cell-fate decisions during axial patterning and neurogenesis. GSK-3 β homologues in *Dictyostelium* and *Xenopus* also appear to regulate cell fate in development. Studies funded by this grant published in **Molecular and Cellular Biology 20:9356-9363,2000**, demonstrate that elevation of intracellular cAMP in rat cerebellar granule neurons leads to phosphorylation of GSK-3 β. The increased phosphorylation of GSK-3□ by PKA occurs at serine 9, the same site phosphorylated by Akt. Purified PKA is able to phosphorylate recombinant GSK-3 □ *in vitro*. Inhibitors of GSK-3 block apoptosis in these neurons and transfection of neurons with a GSK-3 β mutant that cannot be

phosphorylated interferes with the pro-survival effects of cAMP. These data indicate that activated PKA can directly phosphorylate GSK-3 β and inhibits its proapoptotic activity in neurons.

b) IGF-I regulation of CREB activity. In other studies, we collaborated with Dr. Jane Reusch to examine the potential role of CREB in mediating the trophic effects of IGF-I in neuronal cells. Activation of the nuclear transcription factor cAMP response element-binding protein (CREB) has emerged as a central determinant in neuronal functions. We examined whether IGF-I regulated the phosphorylation and transcriptional activation of CREB in rat pheochromocytoma (PC12) cells, a cellular model for neuronal differentiation. We found that CREB phosphorylation at serine 133 and its transcriptional activation as measured by a CREB-specific Gal4-CREB reporter and the neuroendocrine-specific gene chromogranin A was induced 2-3.3-fold by insulin-like growth factor (IGF)-I. This activation was significantly blocked ($p > 0.001$) by the dominant negative K-CREB or by mutation of the CRE site. IGF-I stimulated chromogranin A gene expression by Northern blot analysis 3.7-fold. Inhibition of MAPK kinase with PD98059, PI 3-kinase with wortmannin, and p38 MAPK with SB203580 blocked IGF-I-mediated phosphorylation and transcriptional activation of CREB by 30-50% ($p < 0.001$). Constitutively active and dominant negative regulators of the Ras and PI 3-kinase pathways confirmed the contribution of these pathways for CREB regulation by IGF-I. Cotransfection of PC12 cells with p38 β MAP kinase and constitutively active MAPK kinase 6 resulted in enhanced basal as well as IGF-I-stimulated chromogranin A promoter. IGF-I activated p38 β, which was blocked by the inhibitor SB203580. This is the first description of a p38 β -mediated nuclear signaling pathway for IGF-I leading to CREB-dependent neuronal specific gene expression. These studies also indicated that p38 β and p38 α have very distinct functions in neurons since p38 α is proapoptotic in PC12 cells. This work was published in the **Journal of Biological Chemistry 274:2829-2837, 1999**.

c) Akt up-regulates Bcl-2 expression through CREB. To determine potential anti-apoptotic genes that are regulated by IGF-I via CREB in PC12 cells, we examined the role of Akt on Bcl-2 expression in PC12 cells. A series of transient transfections using a luciferase reporter gene driven by the promoter region of Bcl-2 containing a CRE were carried out. Pharmacological inhibition of phosphatidylinositol (PI) 3-kinase, the upstream kinase of Akt,

with LY294002 led to a 45% decrease in Bcl-2 promoter activity. The reporter activity was enhanced 2.3-fold by overexpression of active p110 subunit of PI 3-kinase and inhibited 44% by the dominant negative p85 subunit of PI 3-kinase. Cotransfection with 3-phosphoinositide-dependent kinase (PDK1), which is required for the full activation of Akt, resulted in enhanced luciferase activity. Insulin-like growth factor I mediated induction of the bcl-2 promoter activity was decreased significantly by the dominate negative forms of p85 subunit of PI-3 kinase, PDK1, and Akt. These data indicate that the regulation of Bcl-2 expression by IGF-I involves a signaling cascade mediated by PI 3-kinase/PDK1/Akt/CREB. Furthermore, we measured the Bcl-2 mRNA in PC12 cells overexpressing Akt by real-time quantitative reverse transcription PCR using the TaqMan fluorogenic probe system. We observed a 2.1-fold increase in Bcl-2 mRNA levels in the Akt cell line compared with control PC12 cells, supporting the observation that enhanced CREB activity by Akt signaling leads to increased Bcl-2 promoter activity and cell survival. These results were published in the **Journal of Biological Chemistry 274:27529-27535, 1999.**

d) The transcription factors MEF2-A and -D regulate survival of rat cerebellar neurons. I other studies funded by this grant , we identified MEF2 as a transcription factor downstream of a depolarization-dependent, calcium-regulated pathway that controls neuronal survival. MEF2 transcription factors have been shown to regulate the development of skeletal, cardiac, and smooth muscle. MEF2 factors are present in the brain, but less in known about their function in nervous tissue. The MEF2 factors, MEF2-A,-B, -C, and-D, bind to DNA as homo- or hetero- dimers to regulate gene expression. Recently, we demonstrated that all four MEF2s are present in rat cerebellar granule neurons, and MEF2D was the prominent species. Gel shift mobility assays (EMSA) indicated that MEF2D and MEF2A were the major MEF2s bound to DNA in healthy neurons. When neurons were induced to undergo apoptosis by lowering extracellular potassium to 5mM, MEF2D and MEF2A were phosphorylated and a decrease in the MEF2/DNA binding complex was observed. Transfection of neurons with a dominant-inactive mutant of MEF2A induced apoptosis, whereas, the dominant-active MEF2 mutant blocked apoptosis. Thus, MEF2D and 2A are critical factors for survival of cerebellar granule neurons. These results were published in the **Journal of Neuroscience 21 (7): 6544-6552, 2001**. Ongoing studies are directed at identifying the protein kinase that phosphorylates the MEF2s and defining the neuronal genes that are regulated by MEF2s. We

extended our MEF2 studies by examining whether GSK-3β is the kinase regulating this pathway in dying neurons. To investigate a potential role for GSK-3β in MEF2D phosphorylation, we examined the effects of lithium, an uncompetitive inhibitor of GSK-3β, on MEF2D in granule neurons induced to undergo apoptosis. Lithium inhibited caspase-3 activation and DNA condensation and fragmentation induced by removal of depolarizing potassium and serum. Lithium suppressed the hyperphosphorylation and caspase-mediated degradation of MEF2D. Moreover, lithium sustained MEF2 DNA binding and transcriptional activity in the absence of depolarization. Unexpectedly, MEF2D hyperphosphorylation was not blocked by either forskolin, insulin-like growth factor-I, or valproate, three mechanistically distinct inhibitors of GSK-3β. These results suggest that lithium targets a novel kinase, different from GSK-3β, that phosphorylates and inhibits the pro-survival function of MEF2D in cerebellar granule neurons. Future studies will be aimed at identifying the protein kinase that induces hyperphosphorylation and degradation of MEF2. These results were published in the **Journal of Neurochemistry 85:1488-1499, 2003**.

The mechanism by which calcium influx regulates MEF2 activity in neurons is complex and involves multiple effector proteins that modulate MEF2 activity. We demonstrated that depolarization-mediated MEF2 activity and granule neuron survival are compromised by overexpression of the MEF2 transcriptional repressor histone deacetylase-5 (HDAC5). Furthermore, induction of apoptosis by removal of depolarizing extracellular potassium induced rapid cytoplasm-to-nuclear translocation of endogenous HDAC5. This effect was mimicked by addition of the calcium/calmodulin-dependent protein kinase (CaMK) inhibitor KN93 to depolarizing medium. Removal of depolarization or KN93 addition increased the mobility of HDAC5 on polyacrylamide gels, consistent with its dephosphorylation. Moreover, HDAC5 co-precipitated with MEF2D under these conditions. Induction of HDAC5 nuclear translocation by KN93 resulted in a marked loss of MEF2 transcriptional activity. MEF2 inactivation was followed by caspase-3 activation, microtubule disruption, and chromatin fragmentation. To selectively decrease CaMKII activity, cerebellar granule neurons were incubated with a fluorescein-labeled, phosphorothioate antisense oligonucleotide to CaMKIIα. Antisense to CaMKII□ decreased CaMKIIα protein expression and induced nuclear shuttling of HDAC5 in granule neurons

maintained in depolarizing medium. Selectivity of the CaMKIIα antisense was demonstrated by its lack of effect on CaMKIV-mediated cAMP-response element binding protein phosphorylation. Finally, antisense to CaMKII□ induced caspase-3 activation and apoptosis, whereas a missense control oligonucleotide had no effect on neuronal survival. These results indicate that depolarization-mediated calcium influx acts through CaMKII to inhibit function of the MEF2 repressor HDAC5, thereby sustaining high MEF2 activity in cerebellar granule neurons maintained under depolarizing conditions. This work was published in the **Journal of Biological Chemistry 278: 41472-41481, 2003**.

e) IGF-I and bFGF improve dopamine neuron survival and behavioral outcome in Parkinsonian rats receiving cultured human fetal tissue strands. In collaboration with Dr. Curt Freed, we investigated the effects of growth factors on survival of human dopamine neurons transplanted into Parkinsonian rats. To promote dopamine cell survival in human fetal tissue strands transplanted into immunosuppressed 6-OHDA lesioned rats, we preincubated tissue in insulin-like growth factor-I (IGF-I, 150 ng/ml) and basic fibroblast growth factor (bFGF, 15 ng/ml) in vitro for two weeks. Growth factor treatment did not affect the rate of homovanillic acid production in vitro but increased overall dopamine neuron survival in animals after transplant from 1240 + 250 to 2380 + 440 neurons ($p<0.05$). Animals in the growth factor-treated group had a significantly greater reduction in methamphetamine-induced rotation (66%) compared to control transplants (30%, $p<0.05$). We conclude that *in vitro* preincubation of human fetal tissue strands with IGF-I and bFGF improves dopamine cell survival and the behavioral outcome of transplants. These results were published in **Experimental Neurology 168:183-191, 2001**.

f) The impact of IGF-I signaling neuronal death machinery.

Another area in which we've made progress is understanding how neurotrophin signaling, in particular IGF-I, impacts on the intrinsic death machinery in neurons. Cerebellar granule neurons depend on insulin-like growth factor-I (IGF-I) for their survival. However, the mechanism underlying the neuroprotective effects of IGF-I is presently unclear. We have shown that IGF-I protects granule neurons by suppressing key elements of the intrinsic (mitochondrial) death pathway. IGF-I blocked activation of the executioner caspase-3 and the intrinsic initiator caspase-9 in primary cerebellar granule neurons deprived of serum and depolarizing potassium. IGF-I inhibited cytochrome C release from mitochondria and

prevented its redistribution to neuronal processes. The effects of IGF-I on cytochrome C release were not mediated by blockade of the mitochondrial permeability transition pore since IGF-I failed to inhibit mitochondrial swelling or depolarization. In contrast, IGF-I blocked induction of the BH3-only Bcl-2 family member, Bim, a mediator of Bax-dependent cytochrome C release. The suppression of Bim expression by IGF-I did not involve inhibition of the c-Jun transcription factor. Instead, IGF-I prevented activation of the forkhead family member, FKHRL1, another transcriptional regulator of Bim. Finally, adenoviral-mediated expression of dominant-negative AKT activated FKHRL1 and induced expression of Bim. These data suggest that IGF-I signaling via AKT promotes survival of cerebellar granule neurons by blocking the FKHRL1-dependent transcription of Bim, a principal effector of the intrinsic death signaling cascade. These results were published in **The Journal of Neuroscience 22: 9278-9297, 2002** .

g) The role of death receptor signaling in neuronal death.

In other experiments , we examined the involvement of death receptor signaling in granule neuron apoptosis by expressing adenoviral, AU1-tagged, dominant-negative Fas-associated death domain (Ad-AU1-FADD). Ad-AU1-FADD decreased apoptosis of granule neurons from 65±5% to 27±2% (n=7, $p<0.01$). Unexpectedly, immunocytochemical staining for AU1 revealed that <5% of granule neurons expressed FADD. In contrast, FADD was expressed in >95% of calbindin-positive Purkinje neurons (~2% of the cerebellar culture). Granule neurons in proximity to FADD-expressing Purkinje cells demonstrated markedly increased survival. Both granule and Purkinje neurons expressed insulin-like growth factor-I (IGF-I) receptors and FADD-mediated survival of granule neurons was inhibited by an IGF-I receptor blocking antibody. These results demonstrate that the selective suppression of death receptor signaling in Purkinje neurons is sufficient to rescue neighboring granule neurons that depend on Purkinje cell-derived IGF-I. Thus, the extrinsic death pathway has a profound, but indirect, effect on the survival of cerebellar granule neurons. These results were published in the **Journal of Biological Chemistry 277: 24546-24553, 2002.**

h) Neurotrophic factors regulate autophagic death of neurons.

In the past year, we have discovered a novel programmed death pathway in Purkinje neurons. Under the same conditions that induce apoptosis of granule neurons, the Purkinje neurons die by a slower programmed mechanism that involves activation of autophagy. We

demonstrated that the death process activated in cerebellar Purkinje neurons following trophic factor withdrawal is autophagic by several methods. The abundant cytoplasmic vacuoles that form in degenerating Purkinje neurons stain with lysosensor blue, a pH-sensitive dye that only fluoresces in acidic cellular compartments, and monodansylcadaverine, an autofluorescent drug that specifically accumulates in autophagic vacuoles. Also, in collaboration with Dr. Charleen Chu at the University of Pittsburg, we were able to demonstrate the appearance of multiple-membrane autophagic vacuoles in degenerating Purkinje neurons by transmission electron microscopy. In addition, a method for quantifying the degree of Purkinje neuron vacuolation was developed based on the size distribution of lysosensor-positive Purkinje vacuoles.

We were also able to demonstrate that death receptor signaling is involved in the regulation of Purkinje autophagy and death. Adenoviral dominant-negative FADD infection prevented the death and vacuolation of Purkinje neurons induced by trophic factor withdrawal. The addition of exogenous death ligand, TNF□, was able to induce death and vacuolation in Purkinje neurons. However, we were unable to find evidence implicating TNF□ as the mediator of death during trophic factor withdrawal as soluble death receptor-Fc proteins, ligand-neutralizing antibodies and chemical inhibitors of the TNF□ synthesis pathway did not increase the survival of Purkinje neurons undergoing trophic factor withdrawal.

The p75 neurotrophin receptor is implicated in mediating many diverse neuronal processes including cell cycle arrest, neurite extension, neuronal survival and neuronal death. p75ntr is highly expressed by Purkinje neurons during development and following axotomy of adult neurons. Nerve growth factor (NGF), one of the neurotrophin ligands for p75ntr is required for proper development and survival of many types of neurons both *in vivo* and *in vitro*, including Purkinje neurons. Since p75ntr is also a member of the death receptor family, we wished to examine if it was involved in the autophagic death of Purkinje neurons. Exogenous NGF increased survival and decreased vacuolation of Purkinje neurons undergoing trophic factor withdrawal. Conversely, NGF-neutralizing antibodies decreased survival and induced vacuolation of Purkinje neurons. Antisense to p75ntr had two effects on the cells in the culture. In cells maintained in complete media, antisense to p75ntr decreased the survival of both Purkinje and granule neurons. However, the antisense

increased survival and delayed the onset of vacuolation of Purkinje neurons following trophic factor withdrawal. These results are consistent with a model in which liganded p75ntr signals survival and unliganded p75ntr may engage an alternate pathway that signals death. These results were published in **Journal of Neuroscience 24: 4498-4509, 2004.**

Key Research Accomplishments

Our key research accomplishments lie in 2 areas. One is defining molecular mechanisms that regulate neuronal survival and death. These studies require the use of tissue culture model systems such as primary cultures of rat cerebellar neurons or rat ventral mesencephalic neurons, and cultured differentiated PC12 cells. Using these model systems, we have identified new cellular protein kinase pathways that suppress and activate neuronal apoptosis, and have identified a number of transcription factors and genes regulated by these protein kinase pathways. We predict that targeted delivery of specific protein kinase inhibitors and/or targeted expression of various transcription factors or genes will prove to be effective therapies for preventing neuronal cell death in the future. The other exciting area of accomplishment has been to link our *in vitro* findings with translational research. We have shown that treatment of dopamine neurons with either growth factors or inhibitors of p38 MAP kinase increases the survival of transplanted dopamine neurons. The advantages that the p38 MAP kinase inhibitors (pyridinyl compounds) have over growth factors and caspase inhibitors for preventing apoptosis include their small size, organic nature, and ability to cross the blood-brain barrier. These characteristics make the pyridinyl imidazole compounds promising candidate drugs for improving survival of dopamine neurons following transplantation into Parkinson's patients. We have also delineated the intrinsic and extrinsic death machinery in primary neurons in order to understand how proapoptotic and antiapoptotic protein kinases impact on the death process. Perhaps, the most exciting finding over the last year is the discovery that different types of neurons use distinct molecular mechanisms to die. While granule neurons die by a classic apoptotic pathway when deprived of trophic support, Purkinje neurons in the same cultures die by an autophagic pathway. Interestingly, the morphology of autophagic death seen in our cultures closely resembles the morphology of neurons seen in a variety of neurodegenerative diseases postautopsy.

Reportable Outcomes

Manuscripts

1. Pugazhenthi S, T Boras, MK Meintzer, **KA Heidenreich**, JE-B Reusch: Insulin-like growth factor I-mediated phosphorylation and activation of CREB in PC12 cells. Multiple signaling pathways are involved. J Biol Chem 274: 2829-2837, 1999.

2. Allen MP, C Zeng, K Schneider, MK Meintzer, C Basilico, B Varnum, **KA Heidenreich**, ME Wierman. Growth arrest specific gene (Gas 6)/adhesion related kinase (ARK) signaling promotes gonadotropin releasing hormone (GnRH) neuronal survival via ERK and Akt. Mol. Endocrinology 13: 191-201, 1999.

3. Pugazhenthi S, E Miller, C Sable, P Young, **KA Heidenreich**, LM Boxer, J E-B Reusch. Insulin-like growth factor-I induces bcl-2 promoter through the transcription factor cAMP response element binding protein. J. Biol. Chem. 274: 27529-27535, 1999.

4. Pugazhenthi S, A Nesterova, C Sable, **KA Heidenreich**, LM Boxer, LE Heasley, J E-B Reusch. Akt/ Protein kinase B mediated cell survival involves transcriptional upregulation of bcl-2. J. Biol. Chem. 275: 10761-10766, 2000.

5. Li MT, X Wang, MK Meintzer, and **KA Heidenreich**. CAMP protects neurons from apoptosis by inhibiting GSK-3B activity in rat cerebellar granule neurons. Mol. Cell Biol. 20: 9356-9363,2000.

6. Zawada WM, MK Meintzer, C Sable, CR Freed, and **KA Heidenreich**. Inhibitors of p38 MAP kinase increase the survival of transplanted dopamine neurons. Brain Res. 891:185-196, 2001.

7. Clarkson, ED, WM Zawada, KP Bell, JE Esplen, PK Choi, **KA Heidenreich**, and CR Freed. IGF-I and bFGF improve dopamine neuron survival and behavioral outcome in parkinsonian rats receiving cultured human fetal tissue strands. Exp. Neurology 168:183-191, 2001.

8. Linseman DA, **KA Heidenreich**, and SK Fisher. Fyn tyrosine kinase links muscarinic receptor stimulation to phosphorylation of the CdC42 effector ACK-1. J. Biol. Chem. 276: 5622-5628, 2001.

9. Li M, DA Linseman, MP Allen, MK Meintzer, X Wang, T Laessig, ME Wierman, and **KA Heidenreich**. MEFA and MEF2D undergo phosphorylation and caspase-mediated degradation during apoptosis of cultured rat cerebellar granule neurons. J. Neuroscience 21 (17): 6544-6552, 2001.

10. Linseman DA, TA Laessig, M McClure, MK Meintzer, H Barth, K Aktories, and **KA Heidenreich.** Inhibition of Rac/Cdc42 function induces apoptosis of cerebellar granule neurons via a c-jun signaling pathway. J. Biol. Chem. 276: 39123-39131, 2001.

11. Allen, MP, DA Linseman, H Udo, M Xu, B Varnum, ER Kandel, **KA Heidenreich**, and ME Wierman. A novel mechanism for GnRH neuron migration involving Gas6/Ark signaling to

p38 MAP kinase. Mol. Cell. Biol. 22 (2): 599-613, 2002.

12. Linseman, DA, ML McClure, RJ Bouchard, TA Laessig, D Brenner, and **KA Heidenreich**. Suppression of death receptor signaling in cerebellar Purkinje neurons protects neighboring granule neurons from apoptosis. J. Biol. Chem 277:24546-24553, 2002.

13. Linseman, DA, RA Phelps, RJ Bouchard, TA Laessig, SS Le, and **KA Heidenreich**. Insulin-like growth factor-I blocks Bim induction and intrinsic death signaling in cerebellar granule neurons. J. Neuroscience 22: 9287-9297, 2002.

14. Allen, MP, M Xu, DA Linseman, JE Pawlowski, GM Bokoch, **KA Heidenreich**, and ME Wierman Adhesion related kinase (ARK) repression of gonadotropin releasing hormone (GnRH) gene expression requires Rac activation of the extracellular signal-regulated kinase (ERK) pathway. J. Biol. Chem. 277: 38133-38140, 2002.

15. Wei S, F. Marches, B Daniel, S Sonda, **KA Heidenreich**, and T Curiel. Pyridinylimidazole p38 mitogen-activated protein kinase inhibitors block intracellular Toxoplasma gondii replication. .Int J Parasitol. 32(8):969-77, 2002.

16. Linseman, DA, BJ Cornejo, SS Le, MK Meintzer,, TA Laessig , RJ Bouchard, and **KA Heidenreich.** A novel mechanism for lithium neuroprotection involving suppression of myocyte enhancer factor 2D hyperphosphorylation and degradation. J.Neurochem.. 85: 1488-1499, 2003.

17. **Heidenreich KA**. Molecular Mechanisms of Neuronal Cell Death. In Parkinson's Disease, Annals of the New York Academy of Sciences, vol.991, 237-250, 2003.

18. Linseman, DA, CM Bartley, SS Le, TA Laessig , RJ Bouchard, MK Meintzer, M Li, and **KA Heidenreich.** Inactivation of the MEF2 repressor HDAC5 by endogenous CAMKII promotes depolarization-mediated neuronal survival. J. Biol. Chem. 278: 41472-41481, 2003.

19. Ahmadi F, DA Linseman , TN Grammatopoulos, RJ Bouchard, SM Jones, CR Freed, **KA Heidenreich,** and WM Zawada. The pesticide rotenone induces caspase-3 mediated apoptosis in ventral mesencephalic dopaminergic neurons. J. Neurochem. 86: 914-921, 2003.

20. Butts BD, DA Linseman, SS Le, TA Laessig , and **KA Heidenreich**. Insulin-like growth factor-I suppresses degradation of the pro-survival transcription factor myocyte enhancer factor 2D (MEF2D) during neuronal apoptosis. Horm. Metab. Res.35: 763-770, 2003.

21. **Heidenreich KA** and DA Linseman**.** Myocyte enhancer factor-2 (MEF2) transcription factors in neuronal differentiation and survival. Mol. Neurobiol. 29: 155-166, 2004.

22. McClure ML, DA Linseman, CT Chu, RJ Bouchard, TA Laessig, SS Le, and **KA Heidenreich**. Neurotrophins and death receptors regulate autophagic death in cerebellar Purkinje neurons. J. Neuroscience 24: 4498-4509, 2004.

Abstracts

1. Sable CL, MK Meintzer, **KA Heidenreich**: Regulation of apoptosis in rat cerebellar granule neurons. The Endocrine Society 1999.

2. Pugazhenthi S, E Miller, C Sable, **KA Heidenreich**, L Boxer, J E-B Reusch: Induction of the Bcl-2 promoter by p38 □ MAPK-mediated signaling pathway. The Endocrine Society 1999.

3. Zawada WM, MK Meintzer, C Sable, CR Freed, and **KA Heidenreich**. Pyridinyl imidazole compounds rescue dopaminergic neurons from apoptotic cell death. Soc. Neuroscience 1999.

4. Wierman ME, MP Allen, Z Fang, M Xu, C Zeng, **KA Heidenreich**, and S Tobet. Factors Regulating GnRH neurons. Invited speaker symposium, The Endocrine Society 2000

5. Zawada, WM, MK Meintzer, P Rao, J Marotti, X Wang, JE Esplen, ED Clark, CR Freed, and **KA Heidenreich**. Inhibitors of p38 MAP kinase increase survival of transplanted dopamine neurons. Soc. Neuroscience 2000.

6. Li, M, MP Allen, T Laessig, X Wang, ME Wierman, and **KA Heidenreich**. Myocyte enhancer factor-2 (MEF2) –A and –D regulate survival of rat cerebellar granule neurons. Soc. Neuroscience 2000.

7. Allen, MP, DA Linseman, **KA Heidenreich**, and ME Wierman, Growth arrest specific gene-6 (Gas6)/ adhesion related kinase (Ark) signaling meiates cytoskeletal remodeling and migration of gonadotropin releasing hormone (GnRH) neurons. Amer. Soc. Cell. Biol. 2000.

8. **Heidenreich KA.** Protein kinases that regulate neuronal survival and apoptosis. Joint meeting of Danish Soc. for Neurosci. and Soc. for Biochem and Mol. Biol. 2000.

9. McClure, ML and **KA Heidenreich**. The role of Fas signaling in neuronal apoptosis. UCHSC Research Forum, 2000.

10. Linseman, DA, M Li, MK Meintzer, T Laessig, and **KA Heidenreich**. IGF-I suppresses caspase activation and degradation of myocyte-enhancer factor-2D (MEF2-D) during apoptosis of cerebellar granule neurons. Endocrine Society 2001.

11. Allen, MP, DA Linseman, M Xu, **KA Heidenreich**, and ME Wierman. Cytoskeletal remodeling and migration of immortalized GnRH neurons is mediated by an adhesion related kinase (ARK)>RAC>p38 MAPK signaling pathway. Endocrine Society 2001.

12. Marches, F., **KA Heidenreich,** and T. Curiel. Pyridinylimidazoles inhibit intracellular T. gondii replication. International Congress on Toxoplasmosis. Freising, Germany, 2001.

13. Linseman, DA, T Laessig, MK Meintzer, M McClure, H, Barth, K Aktories, **KA Heidenreich.** Rac/Cdc42 function is required for cerebellar granule neuron survival. Gordon Conference, Oxford, UK

14. Allen, MP, DA Linseman, M Xu, **KA Heidenreich**, and ME Wierman. PI-3 kinase couples the adhesion related kinase (Ark) receptor to a Rac/p38 dependent migratory pathway in GnRH neurons. Society for Neuroscience, 2001.

15. Ahmadi, F, S Doolin, NR Zahniser, MP Grogan, **KA Heidenreich**, and WM Zawada. HNT- neurons are resistant to serum withdrawal and MPP+. Society for Neuroscience, 2001.

16. Linseman, DA, M Li, MK Meintzer, T Laessig, **KA Heidenreich**. Convergence of GSK-3 beta and c-jun signaling during apoptosis of cerebellar granule neurons. Society for Neuroscience, 2001.

17. McClure, ML, DA Linseman,, RJ Bouchard, TA Laessig, D Brenner, and **KA Heidenreich**. Suppression of death receptor signaling in cerebellar Purkinje neurons protects neighboring granule neurons form apoptosis. Society for Neuroscience, 2001.

18. McClure,ML.,DA Linseman, RJ Bouchard, TA Laessig, D Brenner, and **KA Heidenreich**. Suppression of death receptor signaling in cerebellar Purkinje neurons protects neighboring granule neurons form apoptosis. UCHSC Student Research Forum, October 12, 2001.

19. Linseman, DA, ML McClure, RA Phelps, RJ Bouchard, TA Laessig, SS Le, F Ahmadi, and **KA Heidenreich**. Extrinsic and intrinsic death signaling in cerebellar neuronal apoptosis: the IGF-I connection. 8th International Conference on Neural Transplantation and Repair, Keystone, CO 2002.

20. Jones, SM, MK Meintzer, CR Freed, **KA Heidenreich**, and Zawada, WM. SC68376, a novel inhibitor of p38 MAP kinase rescues rat and human dopaminergic neurons from apoptotic cell death. 8th International Conference on Neural Transplantation and Repair, Keystone, CO 2002

21. Ahmadi, F., S. Doolin, NR Zahniser, MP McGrogan**, KA Heidenreich**, and MW Zawada. Effects of serum withdrawal and MPP+ on the HNT-neurons. 8th International Conference on Neural Transplantation and Repair, Keystone, CO 2002.

22. Linseman, DA, RA Phelps, RJ Bouchard, TA Laessig, SS Le, F Ahmadi, and **KA Heidenreich.** IGF-I inhibits Bim induction and the intrinsic death signaling cascade in cerebellar granule neurons. Keystone Symposium, Mitochondria and Pathogenesis,

Copper, CO 2002.

23. McClure, ML, DA Linseman, RJ Bouchard, TA Laessig, FA Ahmadi, and **KA Heidenreich**, Suppression of death receptor signaling in cerebellar Purkinje neurons protects neighboring granule neurons from apoptosis via an IGF-I dependent mechanism. The Endocrine Society's 84th Annual Meeting, 2002.

24. Linseman, DA, RA Phelps, RJ Bouchard, TA Laessig, SS Le, and **KA Heidenreich**. Insulin-like growth factor-I rescues cerebellar granule cerebellar neurons from apoptosis by blocking Bim induction and mitochondrial death signaling. The Endocrine Society's 84th Annual Meeting, 2002.

25. McClure ML, D A Linseman, R Bouchard, T A Laessig, M K Meintzer, S S Le and **K A Heidenreich**. Identification of an autophagic death pathway in cerebellar Purkinje neurons downstream of death receptor signaling.. Society for Neuroscience 2002.

26. Ahmadi, F., DA Linseman, RJ Bouchard, S Jones, CR Freed, **KA Heidenreich**, and MW Zawada. Rotenone induces death of primary dopamine neurons by a caspase-dependent mechanism. Soc. for Neuroscience Annual meeting, 2002.

27. Linseman, DA, CM Bartley, MK Meintzer, SS Le, TA Laessig, RJ Bouchard, and **KA Heidenreich.** Ca2+/Calmodulin-dependent Protein kinase II Promotes Neuronal Survival by Inhibiting HDAC Repression of MED2D. The American Society for Cell Biology, 2002.

28. Linseman, DA, RA Phelps, TA Laessig, MK Meintzer, RJ Bouchard, SS Le, and **KA Heidenreich**. Bim induction and Bax translocation to mitochondria: key events in neuronal apoptosis that are targeted by neurotrophic factors. Keystone Symposium, Molecular mechanisms of Apoptosis, 2003.

29. Linseman DA, RA Phelps, TA Laessig, MK Meintzer, RJ Bouchard, SS Le, and **KA Heidenreich.** IGF-I blocks neuronal apoptosis by inhibiting Bim induction and Bax translocation to mitochondria. Gordon Research Conference, Insulin-like Growth Factors in Physiology and Disease, 2003.

30. Precht, TA, RA Phelps, DA Linseman, BD Butts, RJ Bouchard, SS Le, TA Laessig, and **KA Heidenreich**. Bax translocation to mitochondria is triggered by permeability transition pore opening in cerebellar granule neurons undergoing apoptosis. Society for Neuroscience 2003.

31. Le, SS, RJ Bouchard, TA Laessig, BD Butts, RA Phelps, **KA Heidenreich**, and DA Linseman. Inhibition of Rac GTPase induces Bim and activates a mitochondrial apoptotic casacade in cerebellar granule neurons. Society for Neuroscience 2003.

32. Butts, BD, DA Linseman, TA Precht, RA Phelps, TA Laessig, RJ Bouchard, SS Le, KL Tyler, **KA Heidenreich**. Glygogen synthase kinase –3□ promotes Bax translocation to

mitochondria during apoptosis of cerebellar granule neurons. Society for Neuroscience 2003.

33. Linseman, DA, CM Bartley, SS Le, TA Laessig, RJ Bouchard, and **KA Heidenreich**. CamKII promotes cerebellar granule cell survival by blocking HDAC repression of MEF2 transcriptional activity. Society for Neuroscience 2003.

34. McClure ML, DA Linseman, CT Chu, RJ Bouchard, TA Laessig, SS Le, and **KA Heidenreich**. Neurotrophins and death receptors regulate autophagic death in cerebellar Purkinje neurons. Society for Neuroscience 2003.

Invited talks

1999	Neuroscience Program, UCHSC, Denver, CO
1999	Plenary talk, American Federation for Medical Research, Carmel, CA
2000	Neuroscience Program, UCHSC, Denver, CO
2000	Division of Endocrinology, UCHSC, Denver, CO
2000	Program of Molecular and Cellular Pathology, University of Alabama, GA
2000	Joslin Diabetes Center and Harvard Medical School, Boston, MA
2000	Michael J. Fox Foundation for Parkinson's Research, Washington, D.C.
2001	Danish Society for Neuroscience and Danish Society for Biochemistry and Molecular Biology, Symposium on Molecular Mechanisms in Neuronal Degeneration, Copenhagen, Denmark
2001	Chairperson, Plenary Symposium on AKT and MAPK, The Endocrine Society
2002	Plenary talk, New York Academy of Science Symposium " PD: Life Cycle of the Dopamine Neuron", Princeton, N.J.
2003	Chairperson and Invited Speaker, Gordon Conference on Insulin-like Growth Factors, Ventura, CA
2003	Department of Pharmacology Retreat, Copper Mountain, CO, "Molecular Mechanisms of Neuronal Death"

List of personnel paid from research effort.
Dr. Kim Heidenreich
Mary Kay Meintzer
Kristine Himmerick
Dr. Mingtao Li
Brandon Cornejo
Dr. Brent Butts

Conclusions

The scope of research over the last 4 years has been to carry out Task#1, Task#2, and Task#3 of our original research proposal. Towards this goal, we have identified a number protein kinase cascades and some of the key effectors that regulate neuronal survival. In cultured rat cerebellar

granule neurons, a good model for studying apoptosis in primary differentiated neurons, we have studied 3 different pathways that regulate neuronal survival, a neurotrophic factor –regulated protein kinase pathway involving PI-3 kinase and Akt, a PKA pathway regulating GSK-3 β activity, and a Ca++ sensitive pathway regulating the activity of a family of transcription factors that signal survival. These studies have resulted in the publication of 19 articles in top tier journals, 1 chapter, and 1 invited review article. The PI and investigators in the lab have presented their research findings at numerous international and national meeting (34 abstracts). The PI has continued research in most of the areas described in the progress report with continued funding from the USAMRMC, the VA , and the NIH.

MOLECULAR AND CELLULAR BIOLOGY, Dec. 2000, p. 9356–9363 Vol. 20, No. 24
0270-7306/00/$04.00+0

Cyclic AMP Promotes Neuronal Survival by Phosphorylation of Glycogen Synthase Kinase 3β

MINGTAO LI,[1] XIAOMIN WANG,[1] MARY KAY MEINTZER,[1] TRACEY LAESSIG,[1] MORRIS J. BIRNBAUM,[2] AND KIM A. HEIDENREICH[1]*

Department of Pharmacology, University of Colorado Health Sciences Center, and The Denver Veterans Affairs Medical Center, Denver, Colorado,[1] and The Howard Hughes Medical Institute, University of Pennsylvania, Philadelphia, Pennsylvania[2]

Received 10 April 2000/Returned for modification 14 May 2000/Accepted 18 August 2000

Agents that elevate intracellular cyclic AMP (cAMP) levels promote neuronal survival in a manner independent of neurotrophic factors. Inhibitors of phosphatidylinositol 3 kinase and dominant-inactive mutants of the protein kinase Akt do not block the survival effects of cAMP, suggesting that another signaling pathway is involved. In this report, we demonstrate that elevation of intracellular cAMP levels in rat cerebellar granule neurons leads to phosphorylation and inhibition of glycogen synthase kinase 3β (GSK-3β). The increased phosphorylation of GSK-3β by protein kinase A (PKA) occurs at serine 9, the same site phosphorylated by Akt. Purified PKA is able to phosphorylate recombinant GSK-3β in vitro. Inhibitors of GSK-3 block apoptosis in these neurons, and transfection of neurons with a GSK-3β mutant that cannot be phosphorylated interferes with the prosurvival effects of cAMP. These data suggest that activated PKA directly phosphorylates GSK-3β and inhibits its apoptotic activity in neurons.

Neurons require continuous exposure to extracellular trophic factors for survival, and those that fail to receive sufficient trophic factor support undergo apoptotic cell death (34). Among the extracellular factors shown to influence neuronal survival are the neurotrophins, which include nerve growth factor, brain-derived neurotrophic factor, neurotrophin 3 and neurotrophin 4, the fibroblast growth factors, ciliary growth factor, insulin, and insulin-like growth factors (2, 31). Agents that elevate intracellular cyclic AMP (cAMP) also promote neuronal survival in a manner independent of neurotrophic factors (24, 38). Substantial progress has been made over the last several years in delineating signal transduction pathways that mediate trophic factor-induced cell survival. Less is known about the survival pathways activated by cAMP in neurons.

Recent reports have established a key role for phosphatidylinositol (PI)-3 kinase in regulating trophic factor-dependent survival of neurons (18, 22, 23). The Akt protein kinase (also termed proteins kinase B [PKB] and Rac) has been implicated as the transducer of PI-3 kinase-dependent survival signals generated by serum and certain growth factors (6, 22, 28). In response to PI-3 kinase activation, Akt binds to phosphorylated membrane lipids via its pleckstrin homology domain and is phosphorylated at threonine 308 and serine 473 (17). Phosphorylation of Akt at these two sites leads to its activation and the propagation of an antiapoptotic signal. Several downstream targets of Akt implicated in cell survival include the Bcl-2 family member BAD (13), caspase 9 (8), and FKHRL1, a member of the Forkhead family of transcription factors (5). Another Akt substrate recently implicated in cell fate decisions is glycogen synthase kinase 3 (GSK-3). Mammalian GSK-3 exists as two isoforms termed α (51 kDa) and β (47 kDa), each encoded by a distinct gene (45–47). The GSK-3 isoforms share 85% homology at the amino acid level and are ubiquitously expressed (45–47). Although GSK-3 was originally identified as a kinase that phosphorylates glycogen synthase, subsequent studies have revealed that GSK-3 has a broader role in the cell (11, 45–47). It phosphorylates a number of substrates not involved in glycogen metabolism, including the initiation factor eIF2B (44), the microtubule-associated protein tau (26), and the transcription factors CREB (21), c-myc (37), c-jun (4), and β-catenin (40). Recently, GSK-3β was shown by complementation to be the mammalian homologue of the *shaggy* gene from *Drosophila melanogaster*, which regulates cell fate decisions during axial patterning and neurogenesis (45). GSK-3β homologues in *Dictyostelium* (25) and *Xenopus* (27) also appear to regulate cell fate in development. The role of GSK-3β in mammalian cell development is less clear, although recent evidence suggests that it may be a downstream target of the PI-3 kinase-Akt antiapoptotic signaling pathway. Overexpression of a dominant-negative mutant of GSK-3β prevents apoptosis following inhibition of PI-3 kinase, whereas catalytically active GSK-3β induces apoptosis of both rat-1 and PC12 cells (36).

One possible mechanism by which cAMP could promote survival is by activating the PI-3 kinase-Akt pathway. Indeed, agents that elevate intracellular cAMP levels stimulate the activity of Akt when the enzyme is overexpressed in 292 cells (20, 39). The activation of Akt by cAMP is independent of PI-3 kinase activity, does not require the pleckstrin homology domain of Akt, and is dependent on T308 phosphorylation but not S473 phosphorylation. In cerebellar granule neurons, inhibition of PI-3 kinase completely blocked the survival effects of insulin-like growth factor I (IGF-I) but had no effect on cAMP-mediated survival (33). Likewise, in sympathetic ganglion neurons, expression of either a dominant-negative PI-3 kinase or a dominant-negative Akt blocked survival mediated by depolarization but not by cAMP (12). The inability of PI-3 kinase inhibitors or dominant-negative Akt mutants to block the prosurvival effects of cAMP in both neuronal types suggests that cAMP promotes neuronal survival by mechanism independent of PI-3 kinase-Akt activation. In this report, we show that elevation of intracellular cAMP levels in rat cerebellar granule neurons leads to phosphorylation and inhibition

* Corresponding author. Mailing address: Denver VAMC, 1055 Clermont St., Denver, CO 80220. Phone: (303) 399-8020, ext. 3891. Fax: (303) 393-5271. E-mail: kim.heidenreich@uchsc.edu.

of GSK-3β independent of Akt activation. The increased phosphorylation of GSK-3β by PKA occurs at serine 9, the site phosphorylated by Akt. Inhibitors of GSK-3 block apoptosis in these cells, and transfection of neurons with a GSK-3 mutant that cannot be phosphorylated interferes with the prosurvival effects of cAMP.

MATERIALS AND METHODS

Antibodies. The monoclonal anti-GSK-3β antibody was from Transduction Laboratories (Lexington, Ky.). The polyclonal phosphorus-specific GSK-3β (Ser9) antibody was obtained from Calbiochem (La Jolla, Calif.). The polyclonal phosphorus-specific antibodies for Akt (Ser473 and Thr308), p90 ribosomal S6 protein kinase (RSK) (Ser381), GSK-3α/β (Ser21 and Ser9), GSK-3β (Ser9), and mitogen-activated protein kinase (Thr202 and Tyr204), the polyclonal phosphorus-independent Akt antibody, the immobilized Akt antibody, and extracellular signal-regulated kinase (ERK) antibodies were from New England BioLabs (Beverly, Mass.). The polyclonal anti-β-galactosidase (β-Gal) antibody was purchased from 5′-3′ Inc. (Boulder, Colo.). Cy3-conjugated goat antibody to rabbit immunoglobulin G (IgG) and fluorescein-conjugated goat antibody to mouse IgG were purchased from Chemicon International, Inc. (Temecula, Calif.). The monoclonal antibody (clone 12CA5) against the hemagglutinin (HA) epitope was obtained from Boehringer Mannheim (Indianapolis, Ind.).

Materials. The PKA inhibitor H-89 dihydrochloride, the cell-permeative myristoylated PKI inhibitor, the cAMP-elevating agents forskolin and chlorophenylthiol (CPT)-cAMP, the PKC inhibitor bisindolylmaleimide, the PI-3 kinase inhibitor wortmannin, and the MEK inhibitor PD98059 were from Calbiochem. The recombinant GSK-3α and GSK-3β proteins were from New England BioLabs. The PKA catalytic subunit purified from bovine heart was from Promega (Madison, Wis.). Valproic acid and lithium chloride were purchased from Sigma (St. Louis, Mo.). Plasmid purification kits were from Qiagen (Valencia, Calif.), and calcium phosphate transfection kits were from Promega. The Akt kinase assay kit was from New England BioLabs. [γ-^{32}P]ATP (3,000 Ci/mmol) was purchased from Amersham Pharmacia Biotechnology and L-pyruvate kinase was purchased from Sigma. The phosphoglycogen synthase peptide 2 was obtained from Upstate Biotechnology.

Neuronal culture and induction of apoptosis. Rat cerebellar granule neurons were prepared from 7- to 8-day-old Sprague-Dawley rat pups (15 to 19 g) as described previously (35). Briefly, neurons were dissociated from freshly dissected cerebella by mechanical disruption in the presence of trypsin and DNase and were then plated on poly-L-lysine-coated Nunc culture plates (Fisher, Pittsburgh, Pa.). Cells were seeded at a density of 2.0×10^6/ml in basal modified Eagle medium (BME) containing 10% fetal bovine serum, 25 mM KCl, 2 mM glutamine, and penicillin (10 U/ml)-streptomycin (10 μg/ml). Cytosine arabinoside (10 μM) was added to the culture medium 24 h after plating to limit the growth of nonneuronal cells. With this protocol, 95 to 99% of the cultured cells were granule neurons. After 7 or 8 days in culture, apoptosis was induced by removing serum and reducing the extracellular potassium concentration from 25 to 5 mM. Neurons were rinsed two times in serum-free BME containing 5 mM KCl and then maintained in the same medium in the presence or absence of various drugs. Control cultures were treated identically but were maintained in serum-free medium supplemented with 25 mM KCl. When inhibitors were used for signaling assays, cells were treated with the inhibitor 30 min before the addition of the stimulus. Cells that did not receive drugs received a control vehicle (dimethyl sulfoxide [DMSO] for forskolin, H-89 dihydrochloride, wortmannin, and PD98059 and water for CPT-cAMP, valproic acid, and lithium chloride). The final concentration of DMSO was less than 0.1%.

Immunoblotting assay. Cerebellar granule neurons were cultured on poly-L-lysine-coated 35-mm plates for 7 or 8 days. After stimulation with drugs (the times are indicated in the figures), neurons were lysed by adding sodium dodecyl sulfate (SDS) sample buffer (62.5 mM Tris-HCl [pH 6.8], 2% [wt/vol] SDS, 10% glycerol, 50 mM dithiothreitol [DTT], 0.1% [wt/vol] bromphenol blue) and were immediately scraped off the plate. Samples were resolved by SDS–10% polyacrylamide gel electrophoresis and transferred to Hybond-P membranes (polyvinylidene difluoride; Amersham, Arlington Heights, Ill.). Membranes were incubated for an hour in a blocking buffer containing 5% (wt/vol) nonfat dry milk in TBST (10 mM Tris-HCl, 140 mM NaCl [pH 7.4], 0.1% Tween 20) and then incubated overnight at 4°C with appropriate primary antibody diluted (1:1,000) in TBST containing 5% bovine serum albumin (BSA). The membranes were washed for 15 min in TBST and then incubated at room temperature for 60 min with horseradish peroxidase-conjugated anti-rabbit or anti-mouse antibody diluted 1:2,000 in TBST containing 5% nonfat dry milk. After being washed extensively for 30 min in TBST, membranes were processed for 1 min using an ECL chemiluminescent substrate kit (Amersham) and exposed to autoradiographic film (Kodak, Rochester, N.Y.). Quantitation was performed using Bio-Rad Quantity One software.

Calcium phosphate transfection of neurons. Cerebellar granule neurons were transfected using a calcium phosphate coprecipitation method (34). All plasmids were prepared and purified with a Qiagen Plasmid Maxi kit (catalog no. 12163) according to the manufacturer's instructions. Briefly, neurons were cultured for 5 to 6 days in 24-well plates or 35-mm dishes. The DNA-calcium phosphate precipitate was prepared by mixing 1 volume of DNA in 250 mM $CaCl_2$ with an equal volume of 2× HBS (50 mM HEPES, 280 mM NaCl, 1.5 mM Na_2HPO_4 [pH 7.1]). Plasmid pcDNA3, pCMV5, pAkt (K179M), pcDNA3 GSK-3β (wt), pcDNA3 GSK-3β (S9A), or pcDNA GSK-3β (KI) contained in the precipitate was at a final concentration of 40 μg/ml together with 8 μg of an expression vector encoding β-Gal (pCMV-βgal) per ml to allow detection of the transfected cells. The calcium phosphate-DNA precipitate was incubated at room temperature for 30 min before it was added to the cultures. The conditioned culture medium was removed and saved. The cultures were washed two times with BME, and then 1.5 ml of transfection medium (BME, no addition of glutamine and antibiotics, 37°C, pH 7.4) was added to cultures, immediately followed by the addition of the calcium phosphate-DNA precipitate. Plasmids were added to the transfection medium at a final concentration of 4 to 5 μg/ml. Plates were incubated (37°C, 5% CO_2) for 30 min, and then the transfection medium was aspirated. After two washes with fresh transfection medium, the saved conditioned medium was added back to the cultures. Transfection efficiency was assessed by determining the percentage of cells expressing β-Gal by X-Gal (5-bromo-4-chloro-3-indolyl-β-D-galactopyranoside) staining or immunostaining (24 to 48 h later). Glycerol or DMSO shock did not increase transfection efficiency but did result in cell damage. Experimental treatments were initiated 24 h after transfection.

Immunostaining. Neurons were stained 2 days after transfection to identify cells expressing the proteins encoded by the transgenes. Cultures were fixed in 4% paraformaldehyde in phosphate-buffered saline (PBS) for 20 min at room temperature and permeabilized with 0.1% Triton X-100. The fixed cells were incubated at room temperature for 15 min in 5% goat serum in TBS-Triton (10 mM Tris-HCl, 140 mM NaCl [pH 7.4], 0.1% Triton X-100) to block nonspecific interactions of the antibodies and then incubated with the appropriate primary antibody diluted in 3% BSA in Tris-buffered saline overnight at 4°C. After being washed three times with TBS-Triton for 15 min, the cells were incubated at room temperature for 60 min with Cy3- or fluorescein-conjugated secondary antibodies in Tris-buffered saline containing 3% BSA. Expression of β-Gal was detected by immunostaining with a polyclonal antibody to β-Gal (1:500 dilution) followed by a Cy3-conjugated goat antibody to rabbit IgG (1:500). Neurons transfected with the HA epitope-tagged GSK-3β were immunostained with a monoclonal antibody to HA (1:500) followed by a fluorescein-conjugated goat antibody to mouse IgG (1:500). Stained cells were visualized by digital deconvolution fluorescence microscopy to confirm that β-Gal was coexpressed with wild-type (wt) GSK-3β, S9A GSK-3β, or kinase-inactive (KI) GSK-3β. To visualize the nuclei of transfected neurons, we included the DNA dye Hoechst 33258 (5.0 μg/ml) in the wash after the secondary antibody incubation.

In vitro phosphorylation of GSK-3 by PKA. The phosphorylation reaction was performed in 50 μl of kinase buffer (50 mM Tris [pH 7.2], 10 mM $MgCl_2$, 1 mM DTT) containing 4 U of PKA catalytic subunit (bovine heart; Promega), 0.3 μg of GSK-3β protein, and 100 μM ATP. Reactions were carried out in the absence and presence of the PKA inhibitor H-89 (5 μM) or the PKI inhibitor (2.5 μM). The phosphorylation reaction was allowed to proceed for 30 min at 30°C and was stopped by adding 3× SDS sample buffer. The phosphorylation of GSK-3β was measured by Western blotting using a GSK-3β (Ser9) antibody. In experiments where the K_m and V_{max} were determined, 50 μM [γ-^{32}P]ATP (5 μCi/nmol) was added to the kinase reaction mixture. At the end of the phosphorylation reactions, these samples were solubilized in Laemmli's sample buffer and analyzed by SDS-polyacrylamide gel electrophoresis. Gels were dried and subjected to autoradiography. The incorporation of phosphate into GSK-3β and L-pyruvate kinase (a known substrate of GSK-3) was determined by Cerenkov counting of excised SDS-polyacrylamide gel slices.

Assay of GSK-3β. After stimulation with forskolin or IGF-I, neurons were washed with cold PBS, and neuronal extracts were prepared in cell lysis buffer (20 mM Tris-HCl [pH 7.4], 150 mM NaCl, 1 mM EDTA, 1 mM EGTA, 1% Triton X-100, 2.5 mM sodium pyrophosphate, 5 mM β-glycerolphosphate, 1 mM Na_3VO_4, 1 μg of leupeptin per ml, 1 mM phenylmethylsulfonyl fluoride, 1 μM microcystin) for 15 min at 4°C. After brief sonication, the lysates were clarified by centrifugation at 15,000 × *g* for 10 min at 4°C, and GSK-3β from 200 μg of cell extract was immunoprecipitated with 1.0 μg of GSK-3β antibody for 2 h at 4°C with rotation. Protein G Plus/Protein A-agarose (20 μl of a 50% suspension) was then added, and the incubation was continued for 1 h at 4°C with rotation. Immune complexes were recovered by centrifugation at 4°C and were washed three times with extraction buffer and twice with kinase buffer. Kinase activity of the immunoprecipitated GSK-3 was assayed in a total volume of 40 μl containing 25 mM sodium glycerophosphate, 20 mM Tris-HCl [pH 7.4], 10 mM $MgCl_2$, 5 mM DTT, 20 μM phosphoglycogen synthase peptide 2, and 50 μM [γ-^{32}P]ATP (1 μCi). After 10 min of incubation at 30°C, reaction mixtures were centrifuged for 1 min, and 20 μl of the supernatant was spotted onto Whatman P81 phosphocellulose paper. Filters were washed in four changes of 175 mM phosphoric acid for a total of 20 min, rinsed in acetone, and dried, and the radioactivity was determined by Cerenkov counting. Background values obtained from reactions lacking cell lysate were subtracted from all values.

In vitro Akt kinase assay. After stimulation with the reagents indicated below, neuronal extracts were prepared by solubilizing the neurons in cell lysis buffer (20 mM Tris-HCl [pH 7.4], 150 mM NaCl, 1 mM EDTA, 1 mM EGTA, 1% Triton X-100, 2.5 mM sodium pyrophosphate, 5 mM β-glycerolphosphate, 1 mM Na_3VO_4, 1 μg of leupeptin per ml, 1 mM phenylmethylsulfonyl fluoride, 1 μM

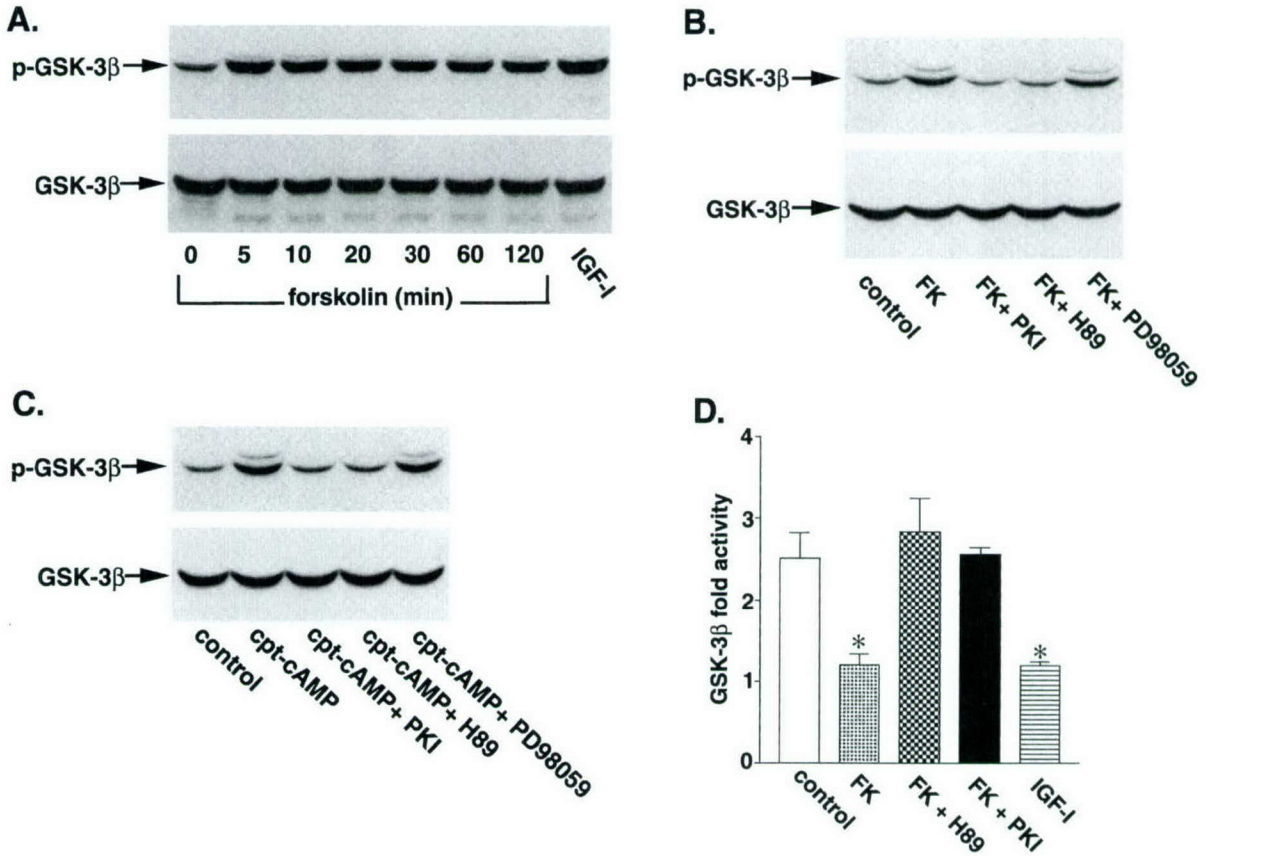

FIG. 1. Phosphorylation and inhibition of GSK-3β by forskolin and CPT-cAMP. (A) Cerebellar granule neurons were cultured for 7 days, washed twice with BME, and then placed in serum-free medium containing 5 mM KCl. Two hours later, the cells were either left untreated or treated with 10 μM forskolin for the indicated times. Some neurons were incubated with IGF-I (50 ng/ml) for 30 min as a positive control. Cell lysates were analyzed by immunoblotting with a phosphospecific GSK-3β (Ser9) antibody. (B) Neurons were pretreated for 30 min in the absence or presence of 25 μM cell-permeative PKI inhibitor, 10 μM H-89, or 30 μM PD98059 prior to incubation with 10 μM forskolin (FK) for 30 min. Cell lysates were immunoblotted with anti-GSK-3β (Ser9) antibody. (C) Neurons were pretreated for 30 min in the absence or presence of 25 μM cell-permeative PKI inhibitor, 10 μM H-89, or 30 μM PD98059 prior to incubation with 30 μM CPT-cAMP (cpt-cAMP) for 30 min. Results shown are representative of at least three experiments. (D) After serum and 25 mM KCl starvation in 5 mM KCl medium, neurons were incubated for 30 min with 10 μM forskolin in the presence or absence of 10 μM H-89, 25 μM PKI inhibitor, or IGF-I (50 ng/ml). After incubation, the neurons were lysed, GSK-3β was immunoprecipitated, and its activity was determined as described in Materials and Methods. Control neurons were washed similarly and then placed in serum-containing conditioned medium. The results are expressed as fold activity of control neurons and are mean values ± SEMs from three experiments. *, statistical significance according to Student's *t* test ($P < 0.05$ versus the value for 5 mM KCl).

microcystin) for 15 min at 4°C. After brief sonication, the lysates were clarified by centrifugation at 15,000 × *g* for 10 min at 4°C, and Akt from 200 μl of cell extract was immunoprecipitated with 20 μl of immobilized Akt antibody cross-linked to agarose hydrazide beads. After the beads were washed three times with cell lysis buffer and three times with kinase buffer (25 mM Tris-HCl, 10 mM $MgCl_2$, 1 mM DTT [pH 7.4]), kinase activity was assayed with GSK-3α fusion protein as a substrate (1 μg) in kinase buffer containing 100 μM ATP and 2.5 μM PKI inhibitor. The phosphorylation reaction was allowed to proceed for 30 min at 30°C and stopped by adding 3× SDS sample buffer. Phosphorylation of GSK-3α was measured by Western blotting using phospho-GSK-3α/β (Ser21 and Ser9) antibody.

Quantitation of apoptosis by nuclear morphological changes. Cerebellar granule neurons were cultured in 35-mm culture dishes and 24-well plates as described above. After removal of the medium, the neurons were rinsed once with cold PBS, pH 7.2, fixed for 10 min with 4% paraformaldehyde in PBS at 4°C, washed with distilled water, and dried at room temperature. Cells were stained with Hoechst 33258 (5 μg/ml) for 5 min, washed, and dried. Apoptosis was quantified by scoring the percentage of cells in the adherent cell population with condensed or fragmented nuclei. To obtain unbiased counting, cells were scored without knowledge of their prior treatment.

RESULTS

Forskolin and CPT-cAMP stimulate GSK-3β phosphorylation. Cultures of newborn rat cerebellar granule neurons, the interneurons of the cerebellum, provide a good model for investigating signaling pathways that regulate neuronal apoptosis because of the high degree of cellular homogeneity. These neurons survive and differentiate in vitro in the presence of serum and depolarizing concentrations of KCl (25 mM). If the medium is changed to serum-free medium containing 5 mM KCl, the neurons undergo apoptotic cell death. Previous studies have shown that apoptosis of cerebellar granule neurons is inhibited by a variety of molecules which raise cAMP levels (7, 15, 33, 42). To investigate the potential role of GSK-3β in mediating the protective effects of cAMP, we examined whether agents that elevate cAMP levels regulate the phosphorylation state of GSK-3β. After 7 days in culture, rat cerebellar granule neurons were incubated in serum-free medium containing 5 mM KCl for 4 h and then incubated with forskolin (10 μM), an activator of adenylate cyclase, to elevate intracellular cAMP levels. The neurons were then solubilized, and the phosphorylation state of GSK-3β was measured by Western blotting using phosphospecific GSK-3β (Ser9) antibodies. Forskolin rapidly increased the phosphorylation of GSK-3β (47 kDa) on serine 9 (Fig. 1A). The extent of GSK-3β phosphorylation by forskolin was similar to that obtained with a maximal concentration of IGF-I (50 ng/ml). The phosphor-

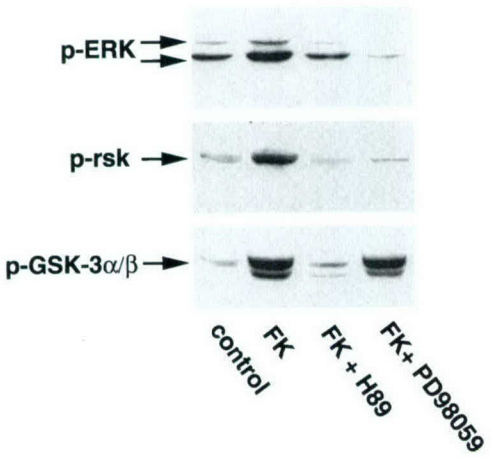

FIG. 2. Phosphorylation of GSK-3 by cAMP-PKA does not require activation of the ERK pathway. Neurons were treated as described for Fig. 1A and then pretreated for 30 min in the absence or presence of 10 μM H-89 or 30 μM PD98059 prior to incubation with 10 μM forskolin (FK) for 30 min. Cell lysates were immunoblotted with phosphospecific antibodies against ERK (Thr202 and Tyr204) (top), p90 RSK (Ser381) (middle), and GSK-3α/β (Ser21 and Ser9) (bottom). Results shown are representative of at least three experiments.

ylation of GSK-3β by forskolin was completely blocked when neurons were preincubated for 30 min with the cell-permeative myristoylated PKI inhibitor (25 μM) and with H-89 (10 μM), a selective inhibitor of PKA (Fig. 1B and C). Preincubation of neurons with PD98059, a MEK inhibitor that blocks the ERK pathway, had no significant effect on the phosphorylation of GSK-3β by forskolin. The ability of forskolin to stimulate phosphorylation of GSK-3β was mimicked by incubating the neurons with a cell permeative cAMP analog (CPT-cAMP) (Fig. 1C). As seen with forskolin, the phosphorylation of GSK-3β by CPT-cAMP was blocked by the PKI inhibitor and H-89 but not by PD98059 (Fig. 1C).

Phosphorylation of GSK-3β at serine 9 is known to inhibit enzyme activity. To confirm this, in vitro kinase assays were carried out following immunoprecipitation of GSK-3β using phosphoglycogen synthase peptide 2 as the substrate (Fig. 1D). Treatment of neurons with forskolin led to about a 50% decrease in GSK-3β activity, similar to the decrease in activity observed with IGF-I. The cell-permeative PKI inhibitor and H-89 blocked the forskolin-induced decrease in GSK-3β activity.

Phosphorylation of GSK-3β by forskolin is not mediated by the ERK pathway. The inability of the MEK inhibitor PD98059 to block phosphorylation of GSK-3β by forskolin suggested that the ERK pathway was not involved in the phosphorylation event. However, cAMP has been previously shown to activate the ERK pathway (19), and recent data have indicated that RSK can directly phosphorylate GSK-3β (41). To examine the potential relationship between activation of the ERK pathway and phosphorylation of GSK-3β by forskolin, we first determined whether forskolin activates the ERK pathway in rat cerebellar granule neurons. Incubation of neurons with forskolin (10 μM) for 30 min led to increased phosphorylation of ERK on threonine 202 and tyrosine 204 (Fig. 2, top panel) and RSK on serine 381 (Fig. 2, middle panel). The phosphorylation of ERK and RSK by forskolin was completely inhibited by the MEK inhibitor PD98059 (Fig. 2, top and middle panels). However, although PD98059 completely blocked the activation of ERK and RSK by forskolin, it had no effect on the phosphorylation of GSK-3β by forskolin (Fig. 2, bottom panel). As expected, H-89 inhibited the phosphorylation of ERK and GSK-3β by forskolin. Thus, although the activation of PKA stimulates the ERK pathway in neurons, this pathway does not lead to GSK-3β phosphorylation in cerebellar granule neurons.

Phosphorylation of GSK-3β by forskolin is not mediated by the Akt pathway. To investigate the potential role of the Akt pathway in the regulation of GSK-3β by forskolin, we examined whether forskolin could activate Akt in the cerebellar granule neurons. Neurons were incubated with forskolin, and the phosphorylation state of Akt was determined using phosphospecific (Ser473) antibodies (Fig. 3A). Forskolin had no effect on Akt phosphorylation at serine 473. In contrast, IGF-I (50 ng/ml) stimulated Akt phosphorylation at this site, and the increased phosphorylation of Akt by IGF-I was blocked by wortmannin. Similar results were obtained when phosphospecific (Ser308) antibodies were used (Fig. 3A), indicating that forskolin was unable to phosphorylate Akt at the two critical residues that activate the kinase. The activity of Akt was directly measured after immunoprecipitation with phosphorylation-independent Akt antibodies using a GSK-3α fusion protein as the substrate. Phosphorylation of GSK-3α was then detected by Western blotting using phosphospecific GSK-3α/β (Ser21 and Ser9) antibodies (Fig. 3B). Consistent with the data obtained with phosphospecific Akt antibodies, forskolin had no effect on Akt activity. However, in the control samples, IGF-I markedly increased the activity of Akt.

Additional experiments were done to examine whether a dominant-inactive Akt construct, pAkt (K179M), could block the protective effects of cAMP on cell survival (Fig. 3C). As previously reported, dominant-inactive Akt had no effect on the ability of forskolin or CPT-cAMP to protect rat cerebellar granule neurons from apoptosis induced by lowering extracellular potassium. On the other hand, dominant-inactive Akt significantly blocked the ability of IGF-I to protect these neurons from the same apoptotic stimulus.

Purified PKA can phosphorylate GSK-3β in vitro. Since forskolin did not appear to phosphorylate GSK-3β through the protein kinases known to directly phosphorylate GSK-3, we questioned whether PKA itself could directly phosphorylate GSK-3β. To address this question, an in vitro kinase assay was performed using purified PKA and recombinant GSK-3β. Phosphorylation of GSK-3β was detected by Western blotting with phosphospecific antibodies (Fig. 4). In the presence of ATP, the purified PKA catalytic subunit phosphorylated GSK-3β. The site phosphorylated by PKA in GSK-3β (Ser9) resides in the Akt (or PKB) consensus site. These data suggest that the Akt consensus site in GSK-3β (RTTSF) is similar enough to the PKA consensus site (RRXSF) for PKA phosphorylation. There was no detectable phosphorylation in the absence of purified PKA. The H-89 PKA inhibitor and the PKI inhibitor significantly blocked the in vitro phosphorylation of recombinant GSK-3β. Assays were carried out to determine the K_m and V_{max} for human recombinant GSK-3β and a known substrate, L-pyruvate kinase. The K_m and V_{max} values for GSK-3β and L-pyruvate kinase were 7.24 μM and 7.23 μM/min/mg of protein and 19.18 μM and 30.48 μM/min/mg of protein, respectively. These values were determined by nonlinear regression analysis of data plotted by Michaelis-Menton kinetics. The relatively low K_m for the in vitro phosphorylation of GSK-3β raises the possibility that PKA directly phosphorylates GSK-3β in vivo. To date, we have been unable to demonstrate a direct interaction between PKA and GSK-3β in neurons by coimmunoprecipitation (data not shown). This implies that the interaction between PKA and GSK-3β is not strong enough to detect by immunoprecipitation or that they do not interact in vivo because there is another kinase downstream of PKA that directly phosphorylates GSK-3β.

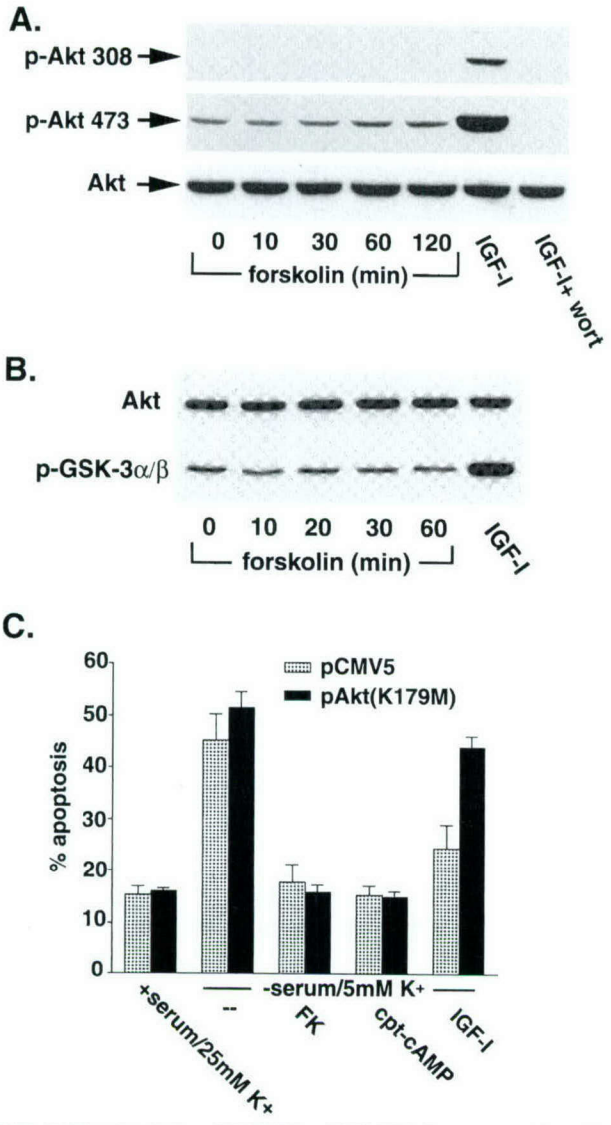

FIG. 3. Phosphorylation of GSK-3 by cAMP-PKA does not require activation of Akt. (A) Cerebellar granule neurons were cultured for 7 days, washed twice, and placed in serum-free medium containing 5 mM KCl. Two hours later, the cells were either left untreated or treated with 10 μM forskolin for the indicated times. Some neurons were incubated with IGF-I (50 ng/ml) in the absence or presence of wortmannin (wort) (100 nM) for 30 min as positive controls. Cell lysates were immunoblotted with antibodies to phospho-S473 Akt and phospho-T308 Akt. The membrane was then stripped and reprobed with antibodies to phosphorylation-independent Akt. (B) Neurons were treated as described for panel A. Akt was immunoprecipitated from cell lysates with an immobilized Akt antibody, and kinase activity was determined by an in vitro kinase assay using 1 μg of recombinant GSK-3α fusion protein as the substrate. Phosphorylation of GSK-3α was detected by immunoblotting with phosphospecific GSK-3α/β (Ser21 and Ser9) antibody (bottom). The membranes were stripped and reprobed with the antibody to phosphorylation-independent Akt (top). (C) Neurons were transfected with the indicated expression vectors (along with pCMV-β-Gal), and 24 h later they were placed in medium containing 25 mM KCl (K^+) plus serum or in deprivation medium (5 mM KCl, no serum) in the presence or absence of 10 μM forskolin (FK), 500 μM CPT-cAMP, or 50 ng/ml of IGF-I per ml. After 20 h, the neurons were fixed and costained with an antibody to β-Gal and Hoechst 33258. Apoptosis was quantified by scoring the percentage of transfected neurons in the adherent cell population with condensed or fragmented nuclei. Data are from three experiments and are the means ± SEMs.

Inhibitors of GSK-3β protect neurons from apoptosis. To determine the role of GSK-3β in the neuroprotective effects of cAMP we first examined the effects of various inhibitors of GSK-3β on apoptosis in rat cerebellar granule neurons. In

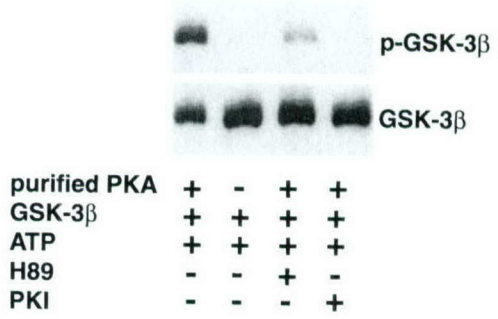

FIG. 4. In vitro phosphorylation of GSK-3 by purified PKA. The phosphorylation reaction mixture consisted of 4 U of purified PKA catalytic subunit, 1 μg of GSK-3β fusion protein, and 100 μM ATP. Reactions were carried out in the absence and presence of the PKA inhibitor H-89 (5 μM) and the PKI inhibitor (2.5 μM). The phosphorylation reaction was allowed to proceed for 30 min at 30°C and was stopped by adding 3× SDS sample buffer. The phosphorylation of GSK-3β (top) was measured by Western blotting with phospho-GSK-3β (Ser9) antibody. The membrane was stripped and reprobed with a monoclonal phosphorylation-independent antibody to GSK-3β (bottom).

agreement with previous studies, forskolin and CPT-cAMP markedly inhibited apoptosis induced by withdrawal of serum and lowering of the KCl concentration (Fig. 5). If cells are preincubated with PKA inhibitor H-89 prior to the addition of forskolin or CPT-cAMP, the protective effects are blocked. Consistent with results demonstrating that the ERK pathway does not mediate the phosphorylation of GSK-3β by forskolin or CPT-cAMP, the MEK inhibitor PD98059 did not influence the ability of forskolin and CPT-cAMP to protect neurons from apoptosis. Lithium and valproate, two direct inhibitors of

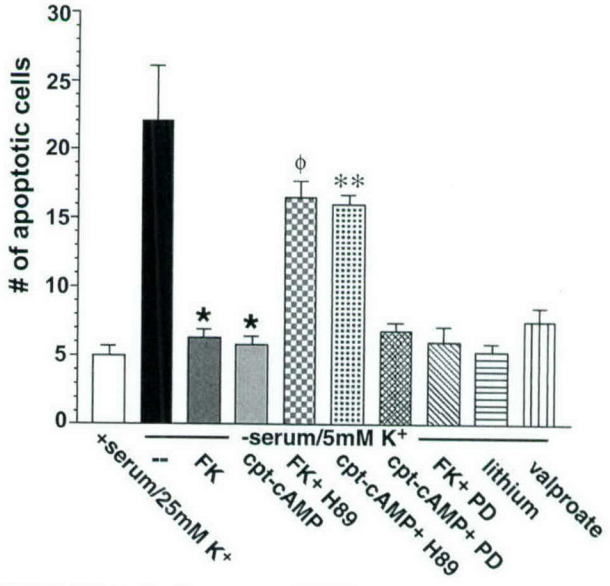

FIG. 5. Effects of various agents and inhibitors on apoptosis of rat cerebellar granule neurons. Cerebellar granule neurons were cultured for 7 days, washed twice with BME, and placed in serum-free medium containing 5 mM KCl in the absence or presence of forskolin (FK) (10 μM), CPT-cAMP (500 μM), forskolin plus H-89 (10 μM), CPT-cAMP plus H-89 (10 μM), CPT-cAMP plus PD98059 (PD) (30 μM), forskolin plus PD98059 (30 μM), lithium (15 mM), or valproate (15 mM). After 24 h neurons were stained with Hoechst 33258 (5 μg/ml) for 5 min, and apoptosis was quantified by scoring the percentage of neurons in the adherent cell population with condensed or fragmented nuclei. To obtain unbiased counting, cells were scored without knowledge of their prior treatment. Data are presented as means ± SEMs ($n = 4$). *, $P < 0.001$ versus apoptotic (serum-free, 5 mM KCl) medium; ϕ, $P < 0.001$ versus apoptotic medium plus forskolin; **, $P < 0.001$ versus apoptotic medium plus CPT-cAMP (Student's t test).

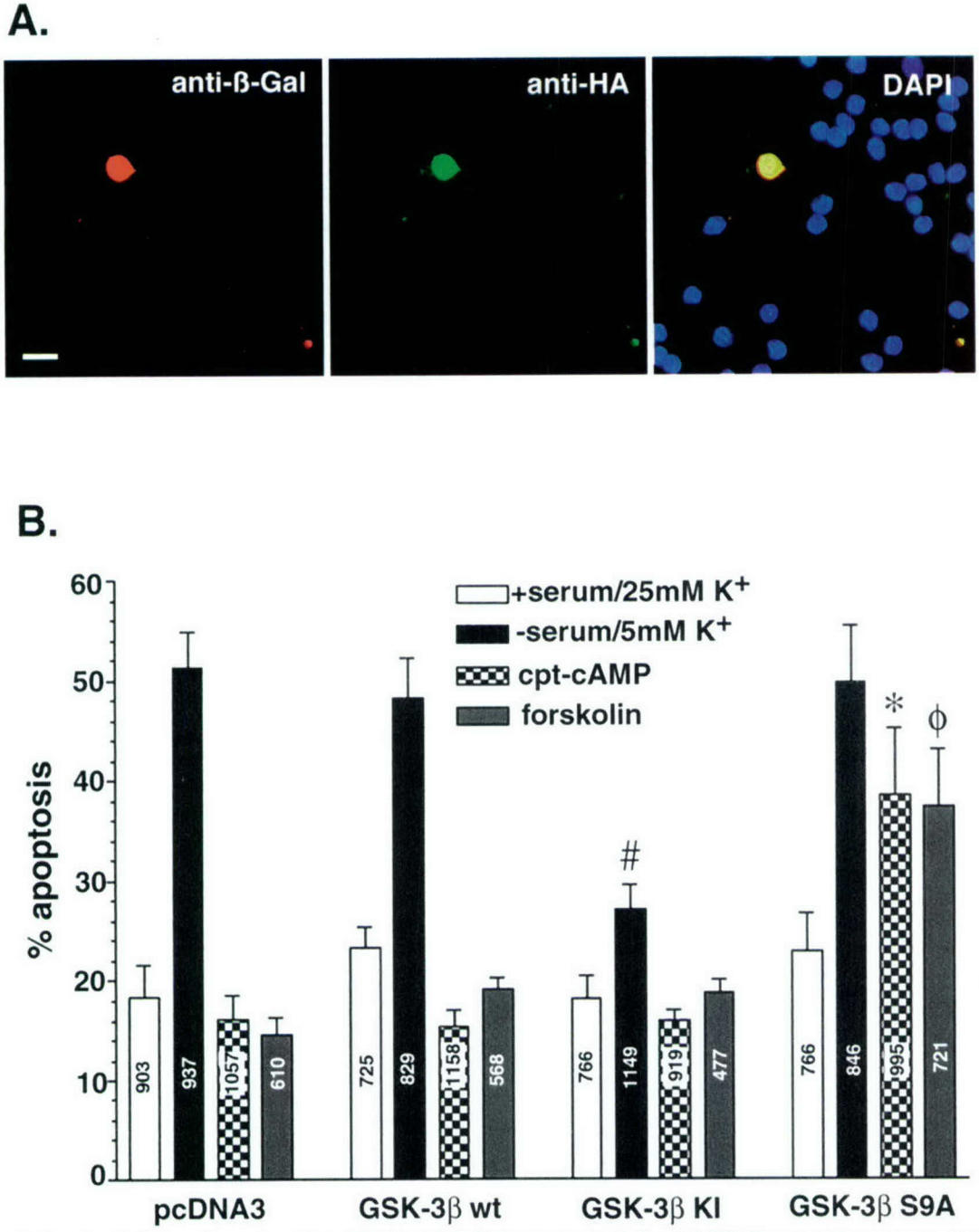

FIG. 6. Transfection of cerebellar granule neurons with wt-GSK-3β, a KI GSK-3β mutant, and a Ser9→Ala9 GSK-3β mutant. Neurons were cotransfected with the control vector, wt GSK-3β, (KI) GSK-3β, (S9A) GSK-3β along with pCMV-β-Gal. One day after transfection, the neurons were placed in complete medium (serum, 25 mM KCl) or switched to serum-free medium containing 5 mM KCl, with or without cAMP (500 μM) or forskolin (10 μM). After 24 h the transfected neurons were fixed and immunostained with an antibody to β-Gal (Cy3-coupled secondary antibody) and 12CA5 antibody to HA (fluorescein isothiocyanate-coupled secondary antibody). To reveal nuclear morphology, neurons were also stained with DAPI. (A) Demonstration of the triple-staining method in neurons grown in serum and 25 mM KCl. Bar, 10 μm. (B) Effects of GSK-3β constructs on neuronal survival. The β-Gal-positive neurons were scored as healthy or apoptotic as described for Fig. 3C. Data are presented as means ± SEMs ($n = 4$). #, $P < 0.001$ versus $pcFNA_3$ in pcDNA3 in apoptotic (serum-free, 5 mM KCl) medium; *, $P < 0.001$ versus pcDNA3 in apoptotic medium plus CPT-cAMP; ϕ, $P < 0.001$ versus $pcDNA_3$ in apoptotic medium plus forskolin (Student's t test). Numbers on the bars indicate the total number of neurons counted.

GSK-3β (41, 42), blocked apoptosis to the same extent as forskolin and CPT-cAMP. These data suggest that GSK-3β mediates the apoptotic effects induced by serum withdrawal and that inhibition of GSK-3β by phosphorylation protects neurons from apoptosis.

Transfection of cerebellar granule neurons with wt-GSK-3β, a KI GSK-3β mutant, and a Ser9→Ala9 GSK-3β mutant. To confirm the results from the inhibitor studies described above, neurons were transfected with GSK-3β plasmids to determine whether a kinase-dead mutant of GSK-3β would block

apoptosis induced in this model system. Transfections were also carried out with wt GSK-3β and a mutant of GSK-3β that cannot be phosphorylated at serine 9. In all of the transfection experiments, neurons were cotransfected with β-Gal as an indicator of transfection. The cultures were coimmunostained with rabbit antibodies against β-Gal (secondary antibody conjugated to Cy3) and mouse antibodies against HA, the epitope tag on the GSK constructs (secondary antibody conjugated to fluorescein isothiocyanate). DAPI (5′, 6′-diamidino-2-phenylindole) stain was included in the final wash of the cultures to determine nuclear morphology (Fig. 6A). Costained neurons were scored as apoptotic if they had one or more lobes of condensed chromatin. Seven hundred to 1,200 neurons were counted in each experimental group. The results from these experiments are shown in Fig. 6B. In cells transfected with the control vector, 18% ± 3% (mean ± standard error of the mean [SEM]) of the total neurons were apoptotic in the presence of serum. Serum withdrawal and lowering of the KCl concentration led to a threefold increase in the percentage of apoptotic neurons (51% ± 3%). Incubation of the neurons with CPT-cAMP or forskolin at the time of serum withdrawal prevented the increase in apoptosis. Similar data were obtained when neurons were transfected with wt GSK-3β. In contrast, transfection of neurons with KI GSK-3β blunted the increase in apoptosis induced by serum and KCl withdrawal (27% ± 4% versus 51% ± 3%) but had no effect on basal apoptosis or the ability of CPT-cAMP and forskolin to protect against apoptosis. On the other hand, transfection of neurons with a GSK-3β mutant that cannot be phosphorylated at serine 9 interfered with the ability of cAMP and forskolin to protect neurons from apoptosis but had little effect on basal apoptosis.

DISCUSSION

Agents that elevate intracellular cAMP levels, such as forskolin (a direct activator of adenylate cyclase), cholera toxin (an activator of G_s proteins), IBMX (a phosphodiesterase inhibitor), and pituitary adenylate cyclase-activating polypeptide (PACAP-38), protect neurons from a variety of apoptotic signals (7, 10, 12, 15, 19, 24, 29, 32, 33, 38, 42, 50). The antiapoptotic effects of cAMP are seen in many types of neuronal systems, including cerebellar granule neurons (7, 15, 24, 33, 38, 42), dopamine neurons (37), septal cholinergic neurons (29), and sympathetic and sensory neurons (1, 12, 43). The mechanisms underlying the antiapoptotic effects of cAMP are not well understood. In previous studies, two signaling pathways that could mediate the neuroprotective effect of cAMP have been explored: the ERK pathway and the PI-3 kinase-Akt pathway. The ERK pathway has been implicated in the survival of sympathetic neurons exposed to cytosine arabinoside (1) and in PC12 cells induced to undergo apoptosis by nerve growth factor withdrawal (49). However, other studies with sympathetic neurons (10, 43) indicate that cAMP promotes neuronal survival through an ERK-independent pathway. In our studies, cAMP stimulated phosphorylation of both ERK and RSK in the cerebellar granule neurons, but activation of this pathway did not lead to protection against apoptosis, since the MEK inhibitors blocked phosphorylation but not the ability of cAMP to protect the neurons from apoptosis. These results concur with the findings of Creedon et al. (10) and indicate that, in rat cerebellar granule neurons, the ERK pathway does not mediate the survival effects of cAMP. As previously discussed, most studies examining the role of PI-3 kinase-Akt in mediating the neuroprotective effects of cAMP have demonstrated that the Akt pathway is not involved. We reexamined the potential involvement of the Akt pathway, since GSK-3β is known to be downstream of Akt. The results from Western blotting with T308 and S473 phosphospecific Akt antibodies and direct Akt kinase assays showed that cAMP had no effect on Akt phosphorylation or activity in cerebellar granule neurons. Consistent with these findings, wortmannin and transfection of cerebellar granule neurons with a dominant-negative Akt mutant failed to diminish the protective effect of cAMP in our cells. Thus, Akt does not mediate the survival effects of cAMP in rat cerebellar granule neurons.

Our data suggest a novel signaling pathway by which cAMP promotes neuronal survival, which is a PKA pathway that leads to inhibition of GSK-3β. Forskolin and CPT-cAMP phosphorylate and inactivate GSK-3β in cerebellar granule neurons. As expected, the phosphorylation of GSK-3β by forskolin and CPT-cAMP is blocked by specific inhibitors of PKA. PKA phosphorylates GSK-3β in vitro at a site known to inhibit its activity, and indeed, forskolin inhibited the kinase activity of GSK-3β. If neurons are transfected with a GSK-3β mutant that cannot be phosphorylated, cAMP is unable to fully protect neurons from apoptosis. Furthermore, direct inhibitors of GSK-3β, valproate and lithium, and a dominant-negative mutant of GSK-3β protect cerebellar granule neurons from apoptosis. These data strongly support the hypothesis that cAMP activates PKA and leads to the phosphorylation and inactivation of GSK-3β, a proapoptotic kinase in cerebellar granule neurons.

The ability of PKA to phosphorylate GSK-3β in vitro supports the notion that PKA directly phosphorylates GSK-3β in vivo. These data suggest that PKA and Akt share a phosphorylation target in cells. Cell localization of PKA, Akt, and GSK-3β may be an important factor in determining which kinase has access to GSK-3β in response to a given stimulus. In addition to PKA and Akt, the protein kinases RSK and integrin-linked kinase also phosphorylate and inactivate GSK-3 (40, 50). Inactivation of GSK-3 by RSK is a proposed mechanism by which the *N*-methyl D-aspartate (NMDA)-activated ERK pathway opposes apoptosis. Inactivation of GSK-3 by integrin-linked kinase is thought to mediate the antiapoptotic effects of cell attachment (14). Thus, GSK-3β appears to represent a convergence site of multiple signaling pathways involved in cell fate decisions.

ACKNOWLEDGMENTS

We thank Paula Hoffman and Sanjiv Bhave for their assistance in establishing cultures of rat cerebellar granule neurons and Michael Browning for providing purified PKA. We also thank Jenifer Monks for her assistance with digital deconvolution fluorescent microscopy.

This research was supported by grants from the USAMRC (DAMD17-99-1-9481), NIH (NS38619-01A1), and VA (Merit Award and REAP Award).

REFERENCES

1. **Anderson, C. N. G., and A. M. Tolkovsky.** 1999. A role for MAPK/ERK in sympathetic neuron survival: protection against a p53-dependent, JNK-independent induction of apoptosis by cytosine arabinoside. J. Neurosci. **19:** 664–673.
2. **Barde, Y. A.** 1989. Trophic factors and neuronal survival. Neuron **2:**1525–1534.
3. **Beavo, J. A., P. J. Bechtel, and E. G. Krebs.** 1974. Preparation of homogeneous cyclic AMP-dependent protein kinase(s) and its subunits from rabbit skeletal muscle. Methods Enzymol. **38:**299–308.
4. **Boyle, W. J., T. Smeal, L. H. Defize, P. Angel, J. R. Woodgett, M. Karin, and T. Hunter.** 1991. Activation of protein kinase C decreases phosphorylation of c-Jun at sites that negatively regulate its DNA-binding activity. Cell **64:**573–584.
5. **Brunet, A., A. Bonni, M. J. Zigmond, M. Z. Lin, P. Juo, L. S. Hu, M. J. Anderson, K. C. Arden, J. Blenis, and M. E. Greenberg.** 1999. Akt promotes cell survival by phosphorylating and inhibiting a forkhead transcription factor. Cell **96:**857–868.

6. **Burgering, B. M. T., and P. J. Coffer.** 1995. Protein kinase B (cAkt) in phosphatidylinositol-3-OH kinase signal transduction. Nature **376:**599–602.
7. **Campard, P. K., C. Crochemore, F. Rene, D. Monnier, B. Koch, and J. P. Loeffler.** 1997. PACAP type I receptor activation promotes cerebellar neuron survival through the cAMP/PKA signaling pathway. DNA Cell Biol. **16:** 323–333.
8. **Cardone, M. H., M. Roy, H. R. Stennicke, G. S. Salvesen, T. F. Franke, E. Stanbridge, S. Frisch, and J. C. Reed.** 1998. Regulation of cell death protease caspase-9 by phosphorylation. Science **282:**1318–1321.
9. **Chen, G., L.-D. Huang, Y.-M. Jiang, and H. K. Manji.** 1999. The mood-stabilizing agent valproate inhibits the activity of glycogen synthase kinase-3. **72:**1327–1330.
10. **Creedon, D. J., E. M. Johnson, and J. C. Lawrence.** 1996. Mitogen-activated protein kinase-independent pathways mediate the effects of nerve growth factor and cAMP on neuronal survival. J. Biol. Chem. **271:**20713–20718.
11. **Cross, D. A. E., D. R. Alessi, P. Cohen, M. Andjelkovich, and B. A. Hemmings.** 1995. Inhibition of glycogen synthase kinase-3 by insulin mediated by protein kinase B. Nature **378:**785–789.
12. **Crowder, R. J., and R. S. Freeman.** 1999. The survival of sympathetic neurons promoted by potassium depolarization, but not cAMP, requires phosphatidylinositol 3-kinase and Akt. J. Neurochem. **73:**466–475.
13. **Datta, S. R., H. Dudek, X. Tao, S. Masters, H. Fu, Y. Gotoh, and M. E. Greenberg.** 1997. Akt phosphorylation of BAD couples survival signals to the cell-intrinsic death machinery. Cell **91:**231–241.
14. **Delcommenne, M., C. Tan, V. Gray, L. Rue, J. Woodgett, and S. Dedhar.** 1998. Phosphoinositide-3-OH kinase-dependent regulation of glycogen synthase kinase 3 and protein kinase B/Akt by integrin-linked kinase. Proc. Natl. Acad. Sci. USA **95:**11211–11216.
15. **D'Mello, S. R., C. Galli, T. Ciotti, and P. Calissano.** 1993. Induction of apoptosis in cerebellar granule neurons by low potassium: inhibition of death by insulin-like growth factor I and cAMP. Proc. Natl. Acad. Sci. USA **23:** 10989–10993.
16. **Dominguez, I., K. Itoh, and S. Y. Sokol.** 1995. Role of glycogen synthase kinase 3 β as a negative regulator of dorsoventral axis formation in Xenopus embryos. Proc. Natl. Acad. Sci. USA **92:**8498–8502.
17. **Downward, J.** 1998. Mechanisms and consequences of activation of protein kinase B/Akt. Curr. Opin. Cell Biol. **10:**262–267.
18. **Dudek, H., S. R. Datta, T. F. Franke, M. J. Birnbaum, R. Yao, G. M. Cooper, R. A. Segal, D. R. Kaplan, and M. E. Greenberg.** 1997. Regulation of neuronal survival by the serine-threonine protein kinase Akt. Science **275:** 661–665.
19. **Dugan, L. L., J. S. Kim, Y. Zhang, R. D. Bart, Y. Sun, D. M. Holtzman, and D. H. Gutmann.** 1999. Differential effects of cAMP in neurons and astrocytes. Role of B-raf. J. Biol. Chem. **36:**25842–25848.
20. **Filippa, M., C. L. Sable, C. Filloux, B. Hemmings, and E. V. Obberghen.** 1999. Mechanism of protein kinase B activation by cyclic AMP-dependent protein kinase. Mol. Cell. Biol. **19:**4989–5000.
21. **Foil, C. J., J. S. Williams, C.-H. Chou, Q. M. Wang, P. J. Roach, and O. M. Andrisani.** 1994. A secondary phosphorylation of $CREB^{341}$ at Ser^{129} is required for the cAMP-mediated control of gene expression. J. Biol. Chem. **269:**32187–32193.
22. **Franke, T. F., S. Yang, T. O. Chan, K. Datta, A. Kazlauskas, D. K. Morrison, D. R. Kaplan, and P. N. Tsichlis.** 1995. The protein kinase encoded by the Akt proto-oncogene is a target of the PDGF-activated phosphatidylinositol 3-kinase. Cell **81:**727–736.
23. **Fruman, D. A., R. E. Meyers, and C. C. Cantley.** 1998. Phosphoinositide kinases. Annu. Rev. Biochem. **67:**481–507.
24. **Hanson, M. G., Jr., S. Shen, A. P. Wiemelt, F. A. McMorris, and B. A. Barres.** 1998. Cyclic AMP elevation is sufficient to promote the survival of spinal motor neurons in vitro. J. Neurosci. **18:**7361–7371.
25. **Harwood, A. J., S. E. Plyte, J. Woodgett, H. Strutt, and R. R. Kay.** 1995. Glycogen synthase kinase 3 regulates cell fate in dictyostelium. Cell **80:**139–148.
26. **Hong, M., and V. M.-Y. Lee.** 1997. Insulin and insulin-like growth factor-1 regulate tau phosphorylation in cultured human neurons. J. Biol. Chem. **272:** 19547–19553.
27. **Itoh, K., T. L. Tang, B. G. Neel, and S. Y. Sokol.** 1995. Specific modulation of ectodermal cell fates in Xenopus embryos by glycogen synthase kinase. Development **121:**3979–3988.
28. **Jones, P. F., T. Jakubowicz, F. J. Pitossi, F. Maurer, and B. A. Hemmings.** 1991. Molecular cloning and identification of a serine threonine protein kinase of the second-messenger subfamily. Proc. Natl. Acad. Sci. USA **88:** 4171–4175.
29. **Kew, J. N., D. W. Smith, and M. V. Sofroniew.** 1996. Nerve growth factor withdrawal induces the apoptotic death of developing septal cholinergic neurons in vitro: protection by cyclic AMP analogue and high potassium. Neuroscience **70:**329–339.
30. **Klein, P. S., and D. A. Melton.** 1996. A molecular mechanism for the effect of lithium on development. Proc. Natl. Acad. Sci. USA **93:**8455–8459.
31. **Levi-Monalcini, R.** 1987. The nerve growth factor: thirty-five years later. EMBO J. **6:**1145–1154.
32. **Mena, M. A., M. J. Casarejos, A. Bonin, J. A. Ramos, and J. Garcia Yebenes.** 1995. Effects of dibutyryl cyclic AMP and retinoic acid on the differentiation of dopamine neurons: prevention of cell death by dibutyryl cyclic AMP. J. Neurochem. **65:**2612–2620.
33. **Miller, T. M., M. G. Tansey, E. M. Johnson, Jr., and D. J. Creedon.** 1997. Inhibition of phosphatidylinositol 3-kinase activity blocks depolarization and insulin-like growth factor I-mediated survival of cerebellar granule cells. J. Biol. Chem. **272:**9847–9853.
34. **Narayanan, V.** 1997. Apoptosis in development and disease of the nervous system. 1. Naturally occurring cell death in the developing nervous system. Pediatr. Neurol. **16:**9–13.
35. **Novelli, A., J. A. Reilly, P. G. Lysio, and R. C. Henneberry.** 1988. Glutamate becomes neurotoxic via the *N*-methyl-D-aspartate receptor when intracellular energy levels are reduced. Brain Res. **451:**205–212.
36. **Pap, M., and G. M. Cooper.** 1998. Role of glycogen synthase kinase-3 in the phosphatidylinositol 3-kinase/Akt cell survival pathway. J. Biol. Chem. **273:** 19929–19932.
37. **Plyte, S. E., K. Hughes, E. Nikolakaki, B. J. Pulverer, and J. R. Woodgett.** 1992. Glycogen synthase kinase-3: functions in oncogenesis and development. Biochim. Biophys. Acta **1114:**147–162.
38. **Rydel, R. E., and L. A. Greene.** 1988. cAMP analogs promote survival and neurite outgrowth in cultures of rat sympathetic and sensory neurons independently of nerve growth factor. Proc. Natl. Acad. Sci. USA **85:**1257–1261.
39. **Sable, C. L., N. Filippa, B. Hemmings, and E. Van Obberghen.** 1997. cAMP stimulates protein kinase B in a wortmannin-insensitive manner. FEBS Lett. **409:**253–257.
40. **Seeling, J. M., J. R. Miller, R. Gil, R. T. Moon, R. White, and D. M. Virshup.** 1999. Regulation of beta-catenin signaling by the B56 subunit of protein phosphatase 2A. Science **283:**2089–2091.
41. **Torres, M. A., H. Eldar-Finkelman, E. G. Krebs, and R. T. Moon.** 1999. Regulation of ribosomal S6 protein kinase-p90 (rsk), glycogen synthase kinase 3, and beta-catenin in early Xenopus development. Mol. Cell. Biol. **19:** 1427–1437.
42. **Villalba, M., J. Bockaert, and L. Journot.** 1997. Pituitary adenylate cyclase-activating polypeptide (PACAP-38) protects cerebellar granule neurons from apoptosis by activating the mitogen-activated protein kinase (MAP kinase) pathway. J. Neurosci. **17:**83–90.
43. **Virdee, K., and A. M. Tolkovsky.** 1995. Activation of p44 and p42 MAP kinases is not essential for the survival of rat sympathetic neurons. Eur. J. Neurosci. **7:**2159–2169.
44. **Welsh, G. I., and C. G. Proud.** 1993. Glycogen synthase kinase-3 is rapidly inactivated in response to insulin and phosphorylates eukaryotic initiation factor eIF-2B. Biochem. J. **294:**625–629.
45. **Welsh, G. I., C. Wilson, and C. G. Proud.** 1996. GSK3: a SHAGGY frog story. Trends Cell Biol. **6:**274–279.
46. **Woodgett, J. R.** 1991. A common denominator linking glycogen metabolism, nuclear oncogenes and development. Trends Biochem. Sci. **16:**177–181.
47. **Woodgett, J. R., S. E. Plyte, B. J. Pulverer, J. A. Mitchell, and K. Hughes.** 1993. Roles of glycogen synthase kinase-3 in signal transduction. Biochem. Soc. Trans. **21:**905–907.
48. **Xia, Z., H. Dudek, C. K. Miranti, and M. E. Greenberg.** 1996. Calcium influx via the NMDA receptor induces immediate early gene transcription by a MAP kinase/ERK-dependent mechanism. J. Neurosci. **16:**5425–5436.
49. **Xia, Z., M. Dickens, J. Raingeaud, R. J. Davis, and M. E. Greenberg.** 1995. Opposing effects of ERK and JNK-p38 MAP kinases on apoptosis. Science **270:**1326–1331.
50. **Yan, G. M., S. Z. Lin, R. P. Irwin, and S. M. Paul.** 1995. Activation of G proteins bidirectionally affects apoptosis of cultured cerebellar granule neurons. J. Neurochem. **65:**2425–2431.

THE JOURNAL OF BIOLOGICAL CHEMISTRY

Vol. 274, No. 39, Issue of September 24, pp. 27529–27535, 1999
Printed in U.S.A.

Insulin-like Growth Factor-I Induces *bcl-2* Promoter through the Transcription Factor cAMP-Response Element-binding Protein*

(Received for publication, May 21, 1999, and in revised form, June 23, 1999)

Subbiah Pugazhenthi‡§, Elisa Miller‡§, Carol Sable‡¶, Peter Young‖, Kim A. Heidenreich‡¶, Linda M. Boxer, and Jane E.-B. Reusch‡§ §§**

*From the Departments of §Endocrinology and ¶Pharmacology, University of Colorado Health Sciences Center, Denver, Colorado 80262, ‡Section of Endocrinology, Veterans Affairs Medical Center, Denver, Colorado 80220, ‖Molecular Immunology, SmithKline Beecham Pharmaceuticals, King of Prussia, Pennsylvania 19406, and the **Department of Medicine, Stanford University School of Medicine, Stanford, California 94305*

Insulin-like growth factor-I (IGF-I) is known to prevent apoptosis induced by diverse stimuli. The present study examined the effect of IGF-I on the promoter activity of *bcl-2*, a gene with antiapoptotic function. A luciferase reporter driven by the promoter region of *bcl-2* from −1640 to −1287 base pairs upstream of the translation start site containing a cAMP-response element was used in transient transfection assays. Treatment of PC12 cells with IGF-I enhanced the *bcl-2* promoter activity by 2.3-fold, which was inhibited significantly ($p < 0.01$) by SB203580, an inhibitor of p38 mitogen-activated protein kinase (MAPK). Cotransfection of the *bcl-2* promoter with MAPK kinase 6 and the β isozyme of p38 MAPK resulted in 2–3-fold increase in the reporter activity. The dominant negative form of MAPKAP-K3, a downstream kinase activated by p38 MAPK, and the dominant negative form of cAMP-response element-binding protein, inhibited the reporter gene activation by IGF-I and p38β MAPK significantly ($p < 0.01$). IGF-I increased the activity of p38β MAPK introduced into the cells by adenoviral infection. Thus, we have characterized a novel signaling pathway (MAPK kinase 6/p38β MAPK/MAPKAP-K3) that defines a transcriptional mechanism for the induction of the antiapoptotic protein Bcl-2 by IGF-I through the nuclear transcription factor cAMP-response element-binding protein in PC12 cells.

The products of the *bcl-2* gene belong to a growing family of proteins that are involved in the regulation of mammalian apoptosis. They include proapoptotic (Bax, Bad, Bid, and Bik) and antiapoptotic (Bcl-2, Bcl-x_L, and Brag-1) proteins (1). Complex interplay between these two groups of proteins seems to decide the fate of cells when exposed to apoptotic stimuli. In transgenic mice overexpressing the *bcl-2* gene, the loss of neuronal cells by natural cell death as well as experimental ischemia is significantly reduced (2). In *bcl-2* gene-ablated mice, loss of neurons and apoptosis in thymus and spleen has been observed (3). The expression pattern of Bcl-2 during murine embryogenesis by immunohistochemical analysis shows that this protein is restricted to zones of survival (4). Hence, expression of Bcl-2 appears to be a key regulatory step in promoting cell survival.

Insulin-like growth factor-I (IGF-I)[1] is known to exert antiapoptotic action in several cell types. One of the mechanisms by which IGF-I promotes cell survival is through down-regulation of the proapoptotic protein Bad. IGF-I stimulates the phosphorylation of Bad by activating phosphatidylinositol 3-kinase and Akt, leading to the sequestration of phospho-Bad in cytosol by the protein 14-3-3 (5). In addition to this cytosolic covalent modification, IGF-I-mediated expression of the antiapoptotic protein Bcl-x_L could play a role in the promotion of cell survival (6). This growth factor has been shown to inhibit the down-regulation of Bcl-2 protein induced by hypoxia in cultured rat cortical neurons and by interleukin-3 deprivation in murine myeloid progenitor cells (7, 8). The mechanism by which IGF-I sustains the expression of *bcl-2* has not been studied. IGF-I is likely to increase the *bcl-2* expression at the transcriptional level, since *bcl-2* promoter is positively regulated by the nuclear transcription factor CREB, and IGF-I can activate this transcription factor (9). The *bcl-2* gene consists of three exons with an untranslated first exon. It has a TATA-less GC-rich promoter with positive and negative regulatory elements (10–12). The presence of a CRE site in a region between −1526 and −1552 upstream of the translation start site has been reported (12). Phosphorylation of CREB by PKC in B lymphocytes leads to induction of the *bcl-2* gene in a CRE-dependent fashion and protection from apoptosis (12). In a recent study, we demonstrated that insulin-like growth factor-I-induced CREB activation involves p38 MAPK-mediated signaling pathway in PC12 cells (9). Hence, activation of p38 MAPK could stimulate the *bcl-2* promoter activity through CREB in these cells.

The p38 MAPK belongs to the MAPK superfamily, the other members being extracellular signal-regulated kinase 1/2 and stress-activated protein kinase/N-terminal Jun kinase. Activation of p38 MAPK has been observed during apoptosis mediated by diverse stimuli such as growth factor withdrawal and exposure to UV irradiation (13). p38 MAP kinase is important for programmed cell death, since its specific inhibitor SB203580 can prevent apoptosis (14). However, studies have demonstrated that p38 MAPK can be activated by growth factors, leading to induction of growth-promoting genes (9, 15). Differentiation of PC12 cells into a neuronal cell type and adipogenesis have been shown to require p38 MAPK (16, 17).

* This work was supported by Veterans Affairs (VA) Merit Review, Research Associate Career Development Award and NIDDK, National Institutes of Health, Grant KO8 DK02351 (to J. E.-B. R.) and a VA Research Enhancement Award Program grant (to J. E.-B. R. and K. A. H.). The costs of publication of this article were defrayed in part by the payment of page charges. This article must therefore be hereby marked "*advertisement*" in accordance with 18 U.S.C. Section 1734 solely to indicate this fact.

§§ To whom correspondence should be addressed: Section of Endocrinology (111H), Veterans Affairs Medical Center, 1055 Clermont St., Denver, CO 80220. Tel.: 303-399-8020 (ext. 2775); Fax: 303-393-5271; E-mail: ReuschJ@den-res.org.

[1] The abbreviations used are: IGF, insulin-like growth factor; CRE, cAMP-response element; CREB, cAMP-response element-binding protein; MAPK, mitogen-activated protein kinase; PBS, phosphate-buffered saline; WT, wild type; KCREB, dominant negative CREB.

The apparent discrepancy between these observations can probably be explained by the existence of several p38 MAPK isozymes with distinct functions. So far, four isozymes, α, β, γ, and δ, have been identified with several splice variants (18–21). In cardiomyocytes, β isozyme was shown to exert hypertrophic action, whereas p38α induces apoptosis (22). Identification of isoform specific regulation by trophic *versus* toxic factors should clarify this confusing scenario.

The objectives of the present investigation were (*a*) to examine the IGF-I mediated activation of *bcl-2* promoter in PC12 cells and characterize the signaling pathway involved in this activation and (*b*) to examine the isozyme specific role of p38 MAPK in the activation of *bcl-2* promoter. We demonstrate that IGF-I-induced *bcl-2* promoter activity proceeds in part through a novel signaling pathway involving MAPK kinase 6/p38β MAPK/MAPKAP-K3 and requires CREB.

EXPERIMENTAL PROCEDURES

Materials—Cell culture media and supplies were from Life Technologies, Inc. (Beverly, MA) and Gemini Bio Products, Inc. (Calabasas, CA). SB 203580 was obtained from Calbiochem. PD98059 was purchased from Biomol (Plymouth Meeting, PA). Different promoter regions of the *bcl-2* gene (full-length, −3934 to −1287; truncated with CRE site, −1640 to 1287; truncated without CRE −1526 to −1287; and the CRE mutated (−1640 to 1287)) were linked to luciferase reporter as described previously (12). The wild type and constitutively active forms of MAPK kinase 3 and MAPK kinase 6 were obtained from B. Derijard (CNRS, Nice, France) and Joel Raingeaud (Institut Curie, Orsay, France) respectively. The isozymes of p38 MAPK in pcDNA3 were provided by Jiahuai Han (San Diego, CA). The dominant negative triple mutant of MAPKAP-3 was obtained from Peter Young (SmithKline Beecham, King of Prussia, PA). The dominant negative CREB (pRS-VKCREB) was provided by Dr. Richard Goodman (Oregon Health Sciences University, Portland, OR). The luciferase assay kit was purchased from Analytical Luminescence Laboratory (San Diego, CA). Antibodies specific for CREB, phospho-CREB (Ser-133), p38 MAPK, phospho-p38 MAPK and phospho-ATF-2, and the ATF-2 fusion protein were obtained from New England Biolabs (Beverly, MA). Plasmids for transfection experiments were purified using Qiagen's (Valencia, CA) Maxi kit. Anti-FLAG antibody and other fine chemicals were purchased from Sigma.

Preparation of Recombinant Adenovirus—cDNA encoding full-length FLAG epitope-tagged p38β or MAPK kinase 6 (WT) were subcloned into *Hin*dIII and *Xba*I sites in the plasmid pACCMVpLpA, which includes the left end of the adenovirus chromosome with the *E1A* gene and the 5′-half of the *E1B* gene replaced by the cytomegalovirus major immediate early promoter, a multiple cloning site, and intron and polyadenylation sequences from SV40 (23). Recombinant adenovirus containing the various kinases were prepared using homologous recombination in HEK-293 cells (24). Plasmids containing the appropriate constructs in pACCMVpLpA were cotransfected into 293 cells by $Ca_3(PO_4)_2$ precipitation using 5 μg of the recombinant plasmid and approximately 0.2 μg of *Bst*BI-digested Ad5*dl*327$_{Bst}\beta$-gal-TP complex or with 1 μg of the recombinant plasmid and 5 μg of pJM17 (containing the chromosome of Ad5dl309 inserted into a bacterial plasmid vector) (25–27). Cells were grown until the positive cytopathic effect was evident (7–10 days). Medium from these cells was harvested and freeze-thawed to release virus, and serial dilutions were used to infect 293 cells for plaque purification. The cells were overlaid with 1% Noble agar containing medium and serum 18 h after infection and fed with fresh Noble agar/medium/serum after 4 days. On day 7, the cells were stained with neutral red, and 5-bromo-4-chloro-3-indolyl-b-D-galactopyranoside was added to Noble agar containing medium with serum. Clear plaques, which include viruses arising from homologous recombination between the recombinant plasmid and the right (large) arm of Ad5*dl*327$_{Bst}\beta$-gal-TP complex, were picked and grown in 293 cells, and positive recombinants were identified by Western analysis using the FLAG antibody. Virus was propagated and purified by CsCl gradient centrifugation (28).

Cell Culture—Rat pheochromocytoma (PC12) cells (provided by Dr. Gary Johnson, Denver, CO) were maintained in Dulbecco's modified Eagle's medium containing 10% fetal bovine serum, 5% heat-inactivated horse serum, 100 μg/ml streptomycin, and 100 microunits/ml penicillin at 37 °C in a humidified atmosphere at 8% CO_2. Cells were cultured in 6 × 35-mm wells for transfection studies. Medium was changed every second day. Confluent cell cultures were split 1:4 and used for the experiments 4 days later. The cells were fasted for five h by maintaining in the medium containing 0.1% fetal bovine serum and 0.05% heat-inactivated horse serum before treatment with growth factors and other agents in the experiments for measuring CREB phosphorylation. Stock solutions of the pharmacological inhibitor SB203580 and PD98059 were prepared in Me_2SO at a concentration of 1000-fold, so that when it was added to the culture medium, the concentration of Me_2SO was 0.1%.

Immunoblotting—Immunoblotting for phospho-CREB, dual phospho-p38 MAPK, and Bcl-2 was carried out as described previously (9). PC12 cells cultured in 60-mm dishes were incubated in serum-free medium before each experiment. After treatment with insulin-like growth factor-I for an appropriate duration, the cells were washed twice with ice-cold PBS, and total cell lysates were prepared by scraping the cells with 200 μl of 1× Laemmli sample buffer containing 100 mM dithiothreitol. The proteins were resolved on 12% SDS-polyacrylamide gels and transferred to polyvinylidene difluoride membranes. The blots were blocked with TBST (20 mM Tris-HCl, pH 7.9, 8.5% NaCl, and 0.1% Tween 20) containing 5% nonfat dry milk (blotting grade) at room temperature for 1 h. The blots were then treated with the primary antibody for phospho-p38 MAPK/phospho-CREB/Bcl-2 in TBST containing 5% bovine serum albumin at 4 °C overnight. After three washes with blocking buffer, the blots were incubated with anti-rabbit IgG conjugated to alkaline phosphatase for 1 h at room temperature. This was followed by three washes with blocking buffer, two washes with 10 mM Tris-HCl (pH 9.5), 10 mM NaCl, 1 mM $MgCl_2$, and a 5-min incubation with diluted CDP-Star reagent (New England Biolabs, Beverly, MA) and then exposed to x-ray film. The intensity of bands was quantitated by scanning.

p38 MAPK Assay—The PC12 cells were infected with adenoviral p38β linked to FLAG epitope and MAPK kinase 6 (WT) and exposed to IGF-I as described in the legend to Fig. 7. After washing the cells with PBS, 200 μl of ice-cold cell lysis buffer (20 mM Tris (pH 7.5), 150 mM NaCl, 1 mM EDTA, 1 mM EGTA, 1% Triton X-100, 2.5 mM sodium pyrophosphate, 1 mM β-glycerophosphate, 1 mM sodium orthovanadate, 10 μg/ml leupeptin, 500 nM okadaic acid, and 1 mM phenylmethylsulfonyl fluoride) was added. The cells were scraped, lysed by sonication, and centrifuged for 20 min. The supernatant (300 μg of protein) was mixed with 15 μg of FLAG antibody overnight at 4 °C. Protein A-Sepharose (20 μl) was added and gently rocked for 3 h at 4 °C. After centrifugation, the pellet was washed twice with cell lysis buffer and twice with kinase assay buffer (25 mM Tris (pH 7.5), 5 mM β-glycerophosphate, 2 mM dithiothreitol, 0.1 mM sodium orthovanadate, 10 mM $MgCl_2$). The pellet was suspended in 30 μl of kinase buffer with 200 μM ATP and 2 μg of ATF-2 fusion protein and incubated for 30 min at 30 °C. The reaction was terminated by the addition of 10 μl of 4× Laemmli sample buffer. These samples were electrophoresed and immunoblotted with antibody to phospho-ATF-2. The intensities of the bands were measured by scanning.

Transfection Procedure—Transient transfection was carried out using LipofectAMINE Plus reagent (Life Technologies, Inc.). PC12 cells were cultured to 60–80% confluence for transfection experiments in 6 × 35-mm plates. For each well, 1 μg of plasmids, 3 μl of Plus reagent, and 10 μg of LipofectAMINE reagent were used as per the manufacturer's instructions. The plasmid containing the β-galactosidase gene driven by the SV_{40} promoter was included to normalize the transfection efficiency. DNA and the LipofectAMINE reagent were diluted separately in 100 μl of serum-free medium without antibiotics, mixed together, and incubated at room temperature for 30 min. The culture plates were washed with PBS, and 800 μl of serum- and antibiotic-free medium was added. The 200 μl of the plasmid LipofectAMINE mixture was then added to each well, and the plates were incubated at 37 °C for 5 h. Then 1.0 ml of high serum medium (20% fetal bovine serum and 10% heat-inactivated horse serum) was added, and the cells were incubated for approximately 24 h before induction with growth factors for luciferase for 24 h. The cells were washed in PBS and lysed with 100 μl of reporter lysis buffer. The cells were lysed by freezing and thawing, and lysate was centrifuged at 14,000 RPM for 30 min. The supernatant was used for the assay of luciferase and β-galactosidase. Luciferase assays were carried out using the enhanced luciferase assay kit (Analytical Luminescence Laboratory, San Diego, CA) on a Monolight 2010 luminometer. The β-galactosidase assay was performed according to the method of Wadzinski *et al.* (29).

Statistical analysis was carried out by Student's *t* test.

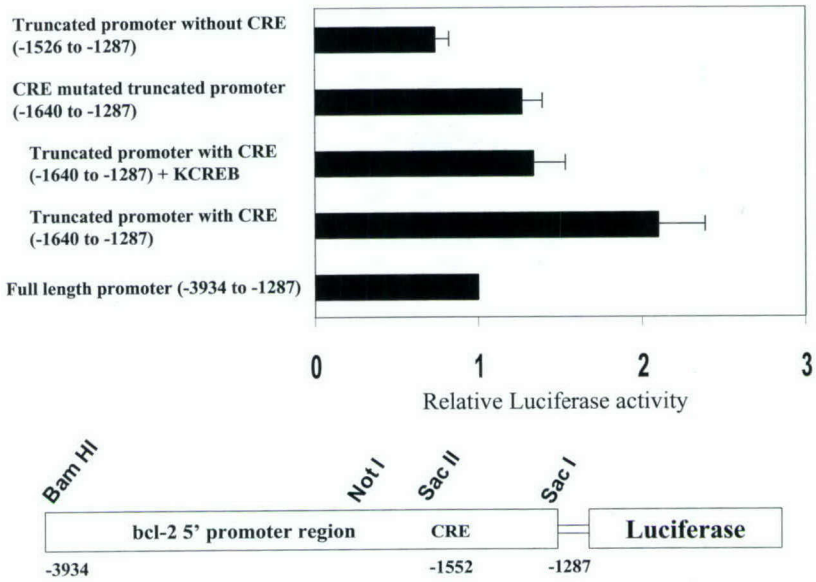

FIG. 1. **Basal activity of different promoter constructs of *bcl-2*.** PC12 cells were cultured in 6 × 35-mm wells to 60–75% confluence. The transfection was carried out in the medium without serum and antibiotics by the LipofectAMINE Plus method for 5 h with different *bcl-2* constructs as indicated. For each well, 1 μg of plasmid, 3 μl of Plus reagent, and 10 μg of LipofectAMINE reagent were used. To measure the efficiency of transfection, pRSV β-galactosidase was used. The cell lysates were prepared 48 h after the initiation of transfection. The activities of luciferase and β-galactosidase were measured by the procedures described under "Experimental Procedures." Results are means ± of four independent experiments, each carried out in duplicate.

RESULTS

Basal bcl-2 Promoter Activity Is Positively Regulated by CREB—Previous studies have shown the regulation of *bcl-2* promoter activity by positive and negative regulatory elements in the 5′ upstream region (10–12). To explore the importance of CRE in *bcl-2* expression, we first characterized these regulatory regions of *bcl-2* promoter in PC12 cells. The sequence from −3934 to −1287 was able to drive the expression of a luciferase gene from a promoterless reporter construct (Fig. 1). Truncation of the 5′-end from −3934 to −1640 led to a 2.5-fold increase in the promoter activity (Fig. 1). This increase seems to be due to the loss of negative regulatory regions identified by previous studies (10, 11). This truncated promoter region contains a CRE site between −1611 and −1526. Mutation of the CRE site decreased the luciferase activity by 50%. Additionally, cotransfection of the CRE-containing reporter construct with dominant negative CREB (KCREB) significantly ($p < 0.001$) decreased the luciferase induction. Progressive deletion from the 5′-end of the CRE site-containing region resulted in a 68% decrease of reporter activity. These experiments clearly demonstrate the positive regulation of basal *bcl-2* promoter activity by the nuclear transcription factor CREB.

IGF-I Stimulates the Expression of Bcl-2 by Inducing Its Promoter—IGF-I is known to up-regulate the expression of the pro-cell survival protein Bcl-x_L (30). We wanted to examine if this growth factor can increase the expression of Bcl-2. When PC12 cells were treated with 50 and 100 ng/ml concentrations of IGF-I, there was a significant ($p < 0.001$) increase in the expression of Bcl-2 as shown by the immunoblot (Fig. 2*A*). To understand the mechanism by which IGF-I stimulates the expression of Bcl-2, we examined the effect of this growth factor on the promoter activity of *bcl-2* gene. When PC12 cells were transiently transfected with a luciferase reporter driven by the CRE site containing truncated *bcl-2* promoter, IGF-I (100 ng/ml) was also able to increase its activity in a time-dependent manner (Fig. 2*B*). Treatment of the PC12 cells with this growth factor for 18 h led to a 2.3-fold increase in the *bcl-2* promoter activity over the untreated cells. When the promoter was cotransfected with dominant negative CREB, IGF-I stimulated reporter activity was decreased by 46% (Table I), indicating that this growth factor induces *bcl-2* promoter through activation of CREB.

IGF-I-mediated Induction of bcl-2 in PC12 Cells Involves p38 MAPK—Having shown the role of CREB in driving the *bcl-2* promoter and its induction by IGF-I, we then proceeded to examine the signaling pathways known to be stimulated by IGF-I that are involved in phosphorylation of CREB on serine 133. CREB has been shown to be phosphorylated and activated by signaling cascades mediated by protein kinase A, protein kinase C, Ca^{2+}, Ras, and phosphatidylinositol 3-kinase. In a recent study, we demonstrated that IGF-I-stimulated induction of chromogranin A, a neuroendocrine-specific gene responsive to CREB activation, involves the signaling mediated by MAPK kinase 6 and p38 MAPK (9). Hence, we examined the stimulation of *bcl-2* promoter activity by IGF-I in the presence

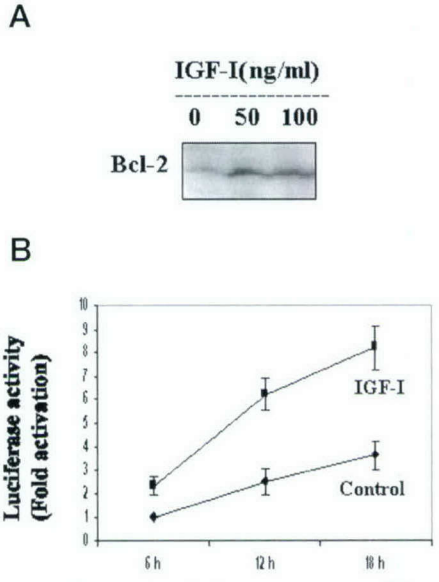

FIG. 2. **IGF-I induces the *bcl-2* promoter and increases the expression of Bcl-2 protein.** *A*, PC12 cells cultured in 6 × 35-mm plates to 80% confluence were treated in the absence and presence of IGF-I (50 and 100 ng/ml) for 24 h. After washing the cells in ice-cold PBS, 100 μl of Laemmli sample buffer was added, and the lysate was prepared by sonication. Protein samples were separated by SDS-PAGE and immunoblotted for Bcl-2. *B*, PC12 cells were transfected with the *bcl-2* promoter and pRSV β-galactosidase. After 24 h of transfection, the cells were exposed to IGF-I (100 ng/ml) for the indicated periods of time in the absence and presence of IGF-I (100 ng/ml). At the end of incubation period, cell lysates were prepared for the assay of luciferase and β-galactosidase. The values represent means ± S.E. of three observations, each being the average of duplicate measurements.

TABLE I
Effect of KCREB on IGF- and p38β MAPK-mediated activation of bcl-2 promoter

PC12 cells cultured in 6 × 35-mm wells to 60–75% confluence were transfected with CRE site-containing *bcl-2* promoter linked to luciferase reporter along with indicated plasmids in serum- and antibiotic-free medium. After 24 h of transfection, the cells were incubated in the absence and presence of IGF-I (100 ng/ml). Luciferase and β-galactosidase were assayed in the cell lysates. Control reporter activity in the absence of KCREB was taken as 100%. Values are mean ± S.E. of four independent experiments, each done in duplicate. *p* values relative to reporter activity in the absence of KCREB were obtained by Student's *t* test.

Cotransfection and treatment	Cotransfection of reporter with KCREB	
	Without KCREB	With KCREB
Control	100	51.0 ± 3.5[a]
IGF-I (100 ng/ml)	231.7 ± 25.3	124.3 ± 11.9[a]
MKK6 (Glu)	206.0 ± 13.6	101.0 ± 12.3[a]
p38β MAPK	224.7 ± 18.0	118.7 ± 16.8[a]
p38β MAPK + IGF-I	373.3 ± 52.5	182.0 ± 30.1[a]

[a] $p < 0.001$.

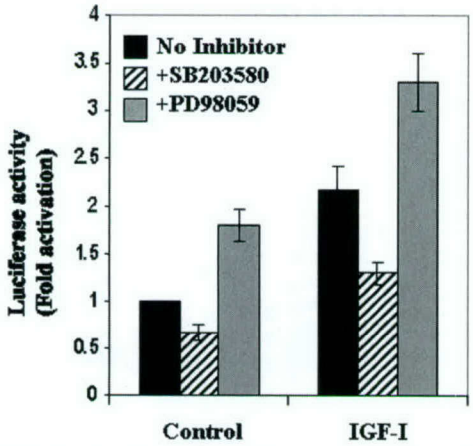

FIG. 3. **IGF-I activates the *bcl-2* promoter through the p38 MAPK-mediated signaling pathway.** PC12 cells cultured in 6 × 35-mm plates were transfected with CRE-containing *bcl-2* promoter construct along with pRSV β-galactosidase for 5 h by the LipofectAMINE Plus method. After 24 h of transfection, the cells were preincubated with PD98059 (40 μM) and SB203580 (10 μM) for 30 min and later exposed to IGF-I (100 ng/ml) for 24 h. The cells were lysed and assayed for luciferase. The efficiency of transfection was assessed by measuring the activity of β-galactosidase. The values are means ± S.E. of three observations, each done in duplicate.

of pharmacological inhibitors specific for different MAP kinases. The transfected cells were preincubated with PD98059 (40 μM), an inhibitor of MAPK kinase 1/2 (and therefore extracellular signal-regulated kinase 1/2) and SB203580 (10 μM), a specific inhibitor of p38 MAPK (Fig. 3). IGF-I-stimulated reporter activity was decreased (40%; $p < 0.01$) by SB203580 (Fig. 3). The MAPK kinase inhibitor (PD98059), on the other hand, increased the *bcl-2* promoter activity by 80% ($p < 0.001$) and 52% ($p < 0.01$) in the absence and presence of IGF-I (Fig. 3). The *bcl-2* gene has been shown to contain negative regulatory elements that respond to the Ets family of proteins, which are activated through the MAPK kinase/extracellular signal-regulated kinase pathway (11). Further studies are needed to examine this pathway. The results of the experiments with SB203580 demonstrate the involvement of p38 MAPK-mediated signaling pathway in the induction of *bcl-2* by IGF-I. We next examined the role of this pathway in the regulation of *bcl-2* expression in more detail.

MAPK Kinase 6-Mediated Activation of the bcl-2 Promoter—In the next series of experiments in PC12 cells, the *bcl-2*

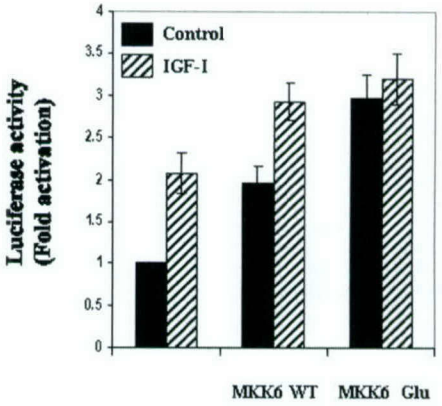

FIG. 4. **Activation of *bcl-2* promoter activity by MAPK kinase 6.** PC12 cells cultured to 60–75% confluence in 6 × 35-mm wells were transfected with CRE-containing *bcl-2* promoter construct and wild type and constitutively active forms (Glu) of MAPK kinase 6 in serum- and antibiotic-free medium. For each well, 1 μg of total plasmids, 3 μl of Plus reagent, and 10 μg LipofectAMINE reagent were used. After 24 h of transfection, the cells were incubated in the absence and presence of IGF-I for another 24 h, lysed, and assayed for luciferase and β-galactosidase. The values represent means ± S.E. of three observations, each carried out in duplicate.

reporter construct was cotransfected with wild type and dominant active forms of MAPK kinase 6, the upstream kinase known to activate p38 MAPK. The results of these studies indicated that MAPK kinase 6 is an activator of *bcl-2* promoter (Fig. 4). The wild type and constitutively active (Glu) forms of MAPK kinase 6 stimulated the luciferase activity by 2–3-fold ($p < 0.001$). MAPK kinase 6 (Glu)-mediated *bcl-2* promoter activity was decreased by 51% when the cells were cotransfected with KCREB (Table I). There were relatively smaller increases of 40 and 78% in promoter activity when cotransfected with wild type and constitutively active forms of MAPK kinase 3, respectively. This is likely to be due to differences observed in the activation pattern of p38 MAP kinases by MAPK kinase 3 and MAPK kinase 6. Among the isoforms of p38 MAPK, α, γ, and δ have been shown to be activated by both MAPK kinase 3 and MAPK kinase 6, whereas the β isoform is preferentially activated by MAPK kinase 6 (18, 20, 31).

p38β MAPK Activates the bcl-2 Promoter—In order to specifically understand the role of p38 MAP kinase isoforms in regulating the *bcl-2* promoter activity, we overexpressed them individually in PC12 cells. Among the various isozymes of p38 MAPK, β was found to stimulate *bcl-2* promoter activity in a dose-dependent manner (Fig. 5*A*). Coexpression of the reporter with 50–100 ng of p38β increased the activity by 2.1–2.8-fold. Although other isozymes of p38, α, γ, and δ, did show a small stimulation it was considerably less when compared with p38β. Optimal activation of p38 MAPK occurs when it is cotransfected with its upstream kinase, although previously it has been shown that p38 MAPK introduced alone is also activated by the endogenous pathway (18). We further confirmed the role of MAPK kinase 6 and p38β MAPK in *bcl-2* induction by using the specific inhibitor SB203580. This pyridinyl imadazole derivative has been shown to have an inhibitory effect in a highly specific manner toward p38 MAPK when compared with other MAPK family kinases such as extracellular signal-regulated kinase and N-terminal Jun kinase (32). There were decreases of 35–45% in promoter activity induced by p38β MAPK alone ($p < 0.01$) or in combination with MAPK kinase 6 ($p < 0.001$) when PC12 cells were preincubated for 30 min with 10 μM of SB203580 (Fig. 5*B*).

p38β MAPK-mediated Induction of bcl-2 Is Blocked by Dominant Negative MAPKAP-K3—Having demonstrated the induction of *bcl-2* promoter through the signaling pathway mediated

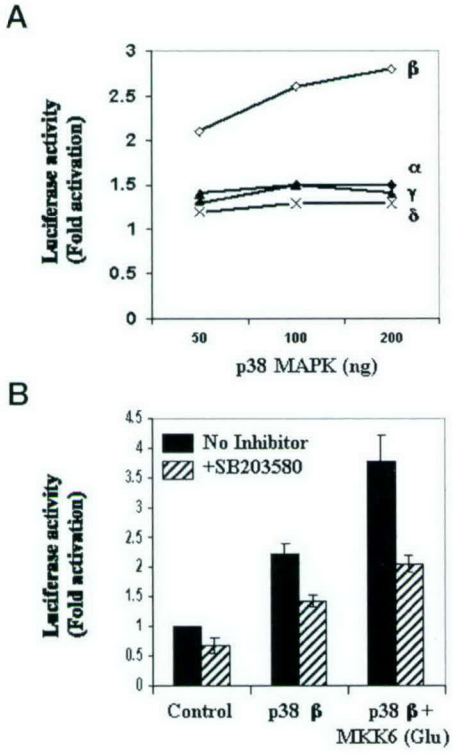

FIG. 5. **Activation of *bcl-2* promoter activity by p38β MAPK.** PC12 cells cultured in 6 × 35-mm wells were transfected with increasing amounts of various isozymes of p38 MAPK (*A*) or p38β and MAPK kinase 6 (Glu) (*B*). The transfection was carried out using LipofectAMINE Plus reagent in serum- and antibiotic-free medium (1 μg of total plasmids, 3 μl of Plus reagent, and 10 μg of LipofectAMINE reagent/well). After 24 h of transfection, the indicated sets of cells were treated with a 10 μM concentration of SB203580 for another 24 h (*B*). Luciferase and β-galactosidase were assayed in the cell lysates. The values represent means ± S.E. of three observations.

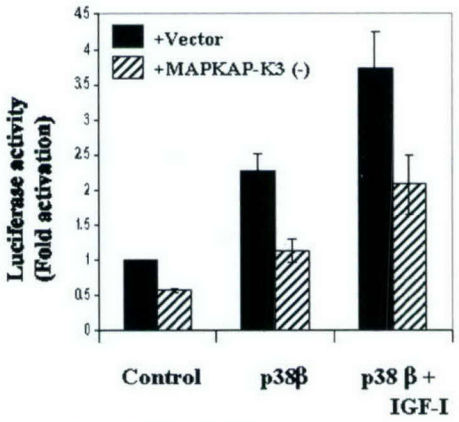

FIG. 6. **Inhibition of p38β MAPK-mediated activation of *bcl-2* by a dominant negative form of MAPKAP-K3.** PC12 cells cultured to 60–75% confluence were transfected with the CRE-site containing *bcl-2* promoter linked to the luciferase reporter and the indicated plasmids in serum- and antibiotic-free medium by the LipofectAMINE Plus method. After 24 h of transfection, the cells were treated in the absence and presence of IGF-I (100 ng/ml) for another 24 h. Luciferase and β-galactosidase were assayed in the cell lysates. Results are means ± S.E. of four independent experiments.

by MAPK kinase 6 and p38β MAPK, we further examined the mechanism by which this pathway can activate the transcription factor CREB through phosphorylation. A recently identified kinase, MAPKAP-K3, also known as 3pk, has been shown to be activated by p38 MAPK and extracellular signal-regulated kinase (33). When we cotransfected the reporter construct with triple mutant dominant negative form of MAPKAP-K3, 50 and 44% decreases ($p < 0.01$) in the p38β MAPK induced luciferase activity were observed in the absence and presence of IGF-I, respectively (Fig. 6). Further, when a dominant negative CREB (KCREB) was included in the transfection assay, induction by p38β MAPK decreased by 47–51% in the absence and presence of IGF-I (Table I). These experiments suggest the presence of a signaling pathway mediated by MAPK kinase 6/p38β MAPK/MAPKAP-K3, leading to the phosphorylation of CREB and subsequent induction of the CRE-containing *bcl-2* promoter.

Increased Expression of Bcl-2 Protein by p38β MAPK and MAPK Kinase 6—The experiments described so far clearly demonstrate the induction of *bcl-2* promoter by p38 MAPK. Next, we wanted to examine the effect of this signaling pathway on the expression of Bcl-2. Optimal transfection efficiency in PC12 cells is 10–15% with our current transfection strategies for reporter assays. Therefore, we introduced MAPK kinase 6 (WT) and p38β by adenoviral infection. We chose the wild type of MAPK kinase 6, since its effect can be further enhanced by IGF-I. Infection of the cells with increasing concentrations of adenoviral p38β and MAPK kinase 6 (WT) resulted in increased levels of phospho-p38, phospho-CREB, and Bcl-2 as shown by the immunoblots, the maximum increases being 2.2–3.4-fold (Fig. 7*A*). When PC12 cells infected with adenoviral p38β and MAPK kinase 6 (WT) were treated with IGF-I (100 ng/ml) for 10 min, p38 MAPK was activated by the growth factor as shown by a 64% increase in phosphorylation of p38 (Fig. 7*B*). We further confirmed IGF-I-mediated stimulation of p38 MAPK activity by immunoprecipitation kinase assay using ATF-2 as the substrate. As shown by the immunoblot for phospho-ATF-2, IGF-I was able to stimulate p38 MAPK activity significantly (47%; $p < 0.01$; Fig. 7*B*).

DISCUSSION

IGF-I has been shown to exert antiapoptotic action in several cell types. It stimulates the phosphorylation of the proapoptotic protein Bad though phosphatidylinositol 3-kinase and its downstream kinase Akt leading to its sequestration in cytosol by the protein 14-3-3 (5). Previous reports have demonstrated the ability of IGF-I to inhibit the down-regulation of Bcl-2 protein induced by hypoxia in cultured rat cortical neurons and by interleukin-3 deprivation in murine myeloid progenitor cells (7, 8). We now demonstrate that IGF-I induces promoter activity of the *bcl-2* gene through activation of CREB via a novel signaling pathway mediated by MAPK kinase 6/p38β MAPK/MAPKAP-K3 (Fig. 8).

CREB is phosphorylated on serine 133 by protein kinases belonging to several different families in addition to protein kinase A. Some of the kinases involved are RSK2, calmodulin-dependent protein kinase IV, and Akt (34–36). A number of growth factors activate CREB through a p38 MAPK-mediated signaling pathway (9, 15, 37). Downstream of p38 MAPK, many kinases capable of phosphorylating CREB have been identified. Fibroblast growth factor- and UV irradiation-mediated activation of p38 MAPK leads to the activation of CREB through MAPKAP-K2 (37, 38). A recently identified mitogen and stress-activated protein kinase, MSK1, phosphorylates CREB in response to the activation of extracellular signal-regulated kinase and p38 MAPK (39). Another kinase identified as MAPKAP-K3 and 3pk, capable of phosphorylating CREB, was examined in this study using a triple mutant dominant negative form (33, 40). When cotransfected with this mutant form of MAPKAP-K3, the induction of *bcl-2* by p38β MAPK is significantly impaired. This suggests that at least one of the targets of p38β MAPK important for CREB and *bcl-2* regulation is MAPKAP-K3. This may not be the only critical CREB kinase

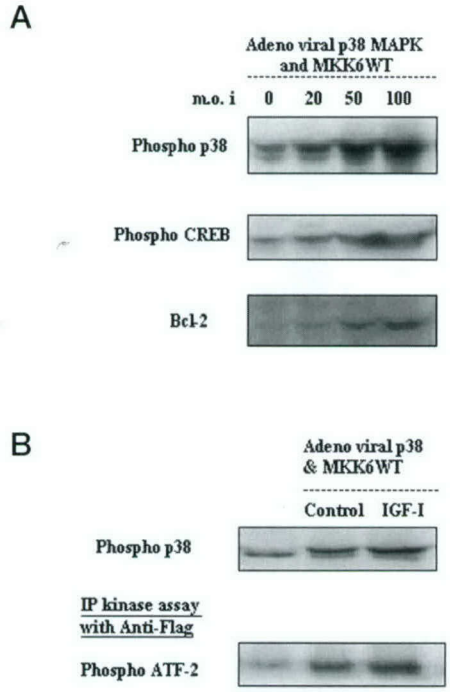

FIG. 7. **Increased expression of Bcl-2 protein by adenoviral p38β MAPK and MAPK kinase 6.** PC12 cells were cultured in 6 × 35-mm dishes to 60% confluence. *A*, the cells were infected with increasing (from 20 to 100) multiplicity of infection (*m.o.i.*) of adenoviral 38β MAPK and MAPK kinase 6 (WT). After 24 h of infection, the cells were washed with ice-cold PBS, and the cell lysates were prepared by the addition of 100 μl of 1× Laemmli sample buffer followed by sonication. The protein samples were electrophoresed and immunoblotted with the antibodies specific for phospho-p38 MAPK, phospho-CREB, and Bcl-2. *B*, the PC12 cells infected with adenoviral p38 β and MAPK kinase 6 (WT) at a multiplicity of infection of 50 for 24 h were incubated in the presence and absence of IGF-I (100 ng/ml) for 10 min. In one set of experiments, the cells were washed with ice-cold PBS, and the cell lysates were prepared by the addition of 100 μl of 1× Laemmli sample buffer. The samples were electrophoresed by SDS-PAGE and immunoblotted with antibody to phospho-p38 MAPK. In another set of experiments, cells were washed with ice-cold PBS and lysed with cell lysis buffer. The lysates were immunoprecipitated with anti-FLAG antibody, and the immune complex was pulled down with Protein A-Sepharose. Using recombinant ATF-2 as the substrate, a kinase reaction was carried, and the phospho-ATF-2 was detected by immunoblotting.

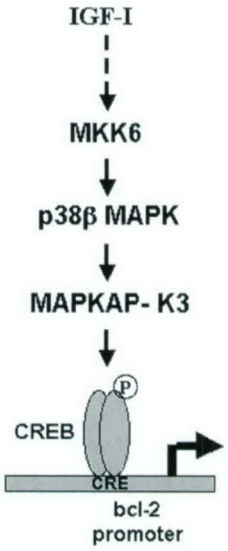

FIG. 8. **Proposed signaling pathway mediated by IGF-I leading to *bcl-2* induction.** IGF-I activates CREB through the signaling pathway involving MAPK kinase 6, p38β MAPK, and MAPKAP-K3, resulting in the induction of *bcl-2* promoter containing the cAMP-response element binding site.

activated by p38β MAPK in this system. Further studies to characterize the CREB kinase are limited by reagent availability.

The p38 MAPK family was initially identified as a stress response pathway and implicated in induction of apoptosis. More recently, several growth factors have been shown to activate p38 MAPK (9, 15, 41). The apparent discord in the results is probably due to the presence of multiple p38 MAPK isoforms with distinct functions. Isozyme-specific functional responses to p38 MAPK family members have been identified. Overexpression of constitutively active MAPK kinase 6 leads to protection of cardiomyocytes against different apoptotic stimuli in a p38 MAPK-dependent manner (42). p38 MAPK has been shown to exert distinct isozyme specific effects (22). The α isozyme induces apoptosis, whereas β isozyme mediates a hypertrophic protective response. In HeLa cells, apoptosis induced by Fas ligation and UV irradiation are blocked by p38β and augmented by p38α (43). Our observation that the β isoform of p38 MAPK can drive the *bcl-2* promoter in a CREB-dependent fashion, whereas the other isoforms do not have this effect, supports previous reports that specific isozymes of p38 MAPK play distinct roles. This does not appear to be an artifact of transient transfection strategies, as infection of PC12 cells with adenoviral p38 β MAPK and MAPK kinase 6 leads to increased phosphorylation of CREB and elevated expression of Bcl-2.

CREB has been shown to promote cell survival and prevent apoptosis against diverse stimuli. Expression of the dominant negative form of CREB in human melanoma cells leads to increased susceptibility to apoptosis (44, 45). Tissue-specific expression of the dominant negative form of CREB in transgenic mice leads to progressive cardiac disfunction, defective interleukin-2 production in thymocytes, and dwarfism resulting from somatotroph hypoplasia (46–48). Induction of the antiapoptotic protein Bcl-2 as shown by us in PC12 cells and by Wilson *et al.* (12) in B lymphocytes in a CREB-dependent manner provides a transcriptional mechanism by which this factor can promote cell survival. CREB is activated in the nervous system by numerous neurotrophic factors that promote survival and differentiation. These *in vivo* and *in vitro* studies clearly demonstrate the importance of CREB in cell survival. Our work on *bcl-2* provides insight as to the mechanism of the cytoprotection by CREB.

Acknowledgments—We thank Dr. Joel Raingeaud, Dr. B. Derijard, Dr. J. Schaack, Dr. Jiahuai Han, and Dr. Richard Goodman for providing valuable reagents. We acknowledge the excellent secretarial support of Gloria Smith. We thank Dr. Boris Draznin for critically reading the manuscript.

REFERENCES

1. Merry, D., and Korsmeyer, S. (1997) *Annu. Rev. Neurosci.* **20,** 245–267
2. Martinou, J.-C., Dubois-Dauphin, M., Staple, J. K., Rodriguez, I., Frankoowski, H., Missotten, M., Albertini, P., Talabot, D., Catsicas, S., Pietra, C., and Huarte, J. (1994) *Neuron* **13,** 1017–1030
3. Veis, D., Sorenson, C., Shutter, J., and Korsmeyer, S. (1993) *Cell* **75,** 229–40
4. Novack, D., and Korsmeyer, S. (1994) *Am. J. Pathol.* **145,** 61–73
5. Kulik, G., and Weber, M. (1998) *Mol. Cell. Biol.* **18,** 6711–6718
6. Párrizas, M., and LeRoith, D. (1997) *Endocrinology* **138,** 1355–1358
7. Tamatani, M., Ogawa, S., and Tohyama, M. (1998) *Brain Res. Mol. Brain Res.* **58,** 27–39
8. Minshall, C., Arkins, S., Straza, J., Conners, J., Dantzer, R., Freund, G., and Kelley, K. (1997) *J. Immunol.* **159,** 1225–1232
9. Pugazhenthi, S., Boras, T., O'Connor, D., Meintzer, M. K., Heidenreich, K. A., and Reusch, J. E.-B. (1999) *J. Biol. Chem.* **274,** 2829–2837
10. Young, R. L., and Korsmeyer, S. J. (1993) *Mol. Cell. Biol.* **13,** 3686–3697
11. Chen, H.-M., and Boxer, L. M. (1995) *Mol. Cell. Biol.* **15,** 3840–3847
12. Wilson, B. E., Mochon, E., and Boxer, L. M. (1996) *Mol. Cell. Biol.* **16,** 5546–5556
13. Xia, Z., Dickens, M., Raingeaud, J., Davis, R. J., and Greenberg, M. E. (1995) *Science* **270,** 1326–1331
14. Kummer, J. L., Rao, P. K., and Heidenreich, K. A. (1997) *J. Biol. Chem.* **272,**

20490–20494
15. Xing, J., Kornhauser, J. M., Xia, Z., Thiele, E. A., and Greenberg, M. E. (1998) *Mol. Cell. Biol.* **18,** 1946–1955
16. Engelman, J. A., Lisanti, M. P., and Scherer, P. E. (1998) *J. Biol. Chem.* **273,** 32111–32120
17. Morooka, T., and Nishida, E. (1998) *J. Biol. Chem.* **273,** 24285–24288
18. Jiang, Y., Chen, C., Li, Z., Guo, W., Gegner, J. A., Lin, S., and Han, J. (1996) *J. Biol. Chem.* **271,** 17920–17926
19. Li, Z., Jiang, Y., Ulevitch, R. J., and Han, J. (1996) *Biochem. Biophys. Res. Commun.* **228,** 334–340
20. Jiang, Y., Gram, H., Zhao, M., New, L., Gu, J., Feng, L., Di Padova, F., Ulevitch, R. J., and Han, J. (1997) *J. Biol. Chem.* **272,** 30122–30128
21. Wang, X. S., Diener, K., Manthey, C. L., Wang, S., Rosenzweig, B., Bray, J., Delaney, J., Cole, C. N., Chan-Hui, P.-Y., Mantlo, N., Lichenstein, H. S., Zukowski, M., and Yao, Z. (1997) *J. Biol. Chem.* **272,** 23668–23674
22. Wang, Y., Huang, S., Sah, V. P., Ross, J., Jr., Brown, J. H., Han, J., and Chien, K. R. (1998) *J. Biol. Chem.* **273,** 2161–2168
23. Gomez-Foix, A. M., Coats, W. S., Baque, S., Alam, T., Gerad, R. D., and Newgard, C. B. (1992) *J. Biol. Chem.* **267,** 25129–25134
24. Graham, F., Smiley, J., Russell, W., and Nairn, R. (1977) *J. Gen. Virol.* **36,** 59–74
25. Jordan, M., Schallhorn, A., and Wurm, F. (1996) *Nucleic Acids Res.* **24,** 596–601
26. McGrory, W., Bautista, D., and Graham, F. (1988) *Virology* **163,** 614–617
27. Schaack, J., Langer, S., and Guo, X. (1995) *J. Virol.* **69,** 3920–3923
28. Jones, N., and Shenk, T. (1978) *Cell* **13,** 181–188
29. Wadzinski, B., Wheat, W., Jaspers, S., Peruski, L., Lickteig, R., Johnson, G., and Klemm, D. (1993) *Mol. Cell. Biol.* **13,** 2822–2834
30. Parrizas, M., and LeRoith, D. (1997) *Endocrinology* **138,** 1355–1358
31. Enslen, H., Raingeaud, J., and Davis, R. J. (1998) *J. Biol. Chem.* **273,** 1741–1748
32. Cuenda, A., Rouse, J., Doza, Y. N., Meier, R., Cohen, P., Gallagher, T. F., Young, P. R., and Lee, J. C. (1995) *FEBS Lett.* **364,** 229–233
33. McLaughlin, M. M., Kumar, S., McDonnell, P. C., Van Horn, S., Lee, J. C., Livi, G. P., and Young, P. R. (1996) *J. Biol. Chem.* **271,** 8488–8492
34. Xing, J., Ginty, D. D., and Greenberg, M. E. (1996) *Science* **273,** 959–963
35. Sheng, M., Thompson, M. A., and Greenberg, M. E. (1991) *Science* **252,** 1427–1430
36. Du, K., and Montminy, M. (1998) *J. Biol. Chem.* **273,** 32377–32379
37. Tan, Y., Rouse, J., Zhang, A., Cariati, S., Cohen, P., and Comb, M. J. (1996) *EMBO J.* **15,** 4629–4642
38. Iordanov, M., Bender, K., Ade, T., Schmid, W., Sachsenmaier, C., Engel, K., Gaestel, M., Rahmsdorf, H. J., and Herrlich, P. (1997) *EMBO J.* **16,** 1009–1022
39. Deak, M., Clifton, A., Lucocq, L., and Alessi, D. (1998) *EMBO J.* **17,** 4426–4441
40. Sithanandam, G., Latif, F., Duh, F.-M., Bernal, R., Smola, U., Li, H., Kuzmin, I., Wixler, V., Geil, L., Shrestha, S., Lloyd, P. A., Bader, S., Sekido, Y., Tartof, K. D., Kashuba, V. I., Zabrovsky, E. R., Dean, M., Klein, G., Lerman, M. I., Minna, J. D., Rapp, U. R., and Allikmets, R. (1996) *Mol. Cell. Biol.* **16,** 868–876
41. Cheng, H.-L., and Feldman, E. L. (1998) *J. Biol. Chem.* **273,** 14560–14565
42. Zechner, D., Craig, R., Hanford, D. S., McDonough, P. M., Sabbadini, R. A., and Glembotski, C. C. (1998) *J. Biol. Chem.* **273,** 8232–8239
43. Nemoto, S., Xiang, J., Huang, S., and Lin, A. (1998) *J. Biol. Chem.* **273,** 16415–16420
44. Jean, D., Harbison, M., McConkey, D. J., Ronai, Z., and Bar-Eli, M. (1998) *J. Biol. Chem.* **273,** 24884–24890
45. Yang, Y. M., Dolan, L. R., and Ronai, Z. (1996) *Oncogene* **12,** 2223–2233
46. Fentzke, R. C., Korcarz, C. E., Lang, R. M., Lin, H., and Leiden, J. M. (1998) *J. Clin. Invest.* **101,** 2415–2426
47. Barton, K., Muthusamy, N., Chanyangam, M., Fischer, C., Clendenin, C., and Leiden, J. (1996) *Nature* **379,** 81–85
48. Struthers, R., Vale, W., Arias, C., Sawchenko, P., and Montminy, M. (1991) *Nature* **350,** 622–624

THE JOURNAL OF BIOLOGICAL CHEMISTRY Vol. 275, No. 15, Issue of April 14, pp. 10761–10766, 2000
Printed in U.S.A.

Akt/Protein Kinase B Up-regulates Bcl-2 Expression through cAMP-response Element-binding Protein*

(Received for publication, November 3, 1999, and in revised form, January 3, 2000)

Subbiah Pugazhenthi‡§, Albina Nesterova‡§, Carol Sable§¶, Kim A. Heidenreich§¶, Linda M. Boxer‖, Lynn E. Heasley, and Jane E.-B. Reusch‡§‡‡**

*From the Departments of ‡Endocrinology, ¶Pharmacology, and **Medicine, University of Colorado Health Sciences Center, Denver, Colorado 80262, the §Section of Endocrinology, Veterans Affairs Medical Center, Denver, Colorado 80220, and ‖Department of Medicine, Stanford University School of Medicine, Stanford, California 94305*

In our previous study we showed that insulin-like growth factor-I induces a cAMP-response element (CRE) site-containing Bcl-2 promoter through a novel signaling pathway involving mitogen-activated protein kinase kinase 6/p38β mitogen-activated protein kinase/MAP kinase-activated protein kinase-3/cAMP-response element-binding protein (CREB) (Pugazhenthi, S., Miller, E., Sable, C., Young, P., Heidenreich, K. A., Boxer, L. M., and Reusch, J. E.-B. (1999) *J. Biol. Chem.* 274, 27529–27535). In the present investigation, we define a second pathway contributing to CREB-dependent up-regulation of Bcl-2 expression as a novel anti-apoptotic function of Akt signaling. To examine the role of Akt on Bcl-2 expression, a series of transient transfections using a luciferase reporter gene driven by the promoter region of Bcl-2 containing a CRE were carried out. Pharmacological inhibition of phosphatidylinositol (PI) 3-kinase, the upstream kinase of Akt, with LY294002 led to a 45% decrease in Bcl-2 promoter activity. The reporter activity was enhanced 2.3-fold by overexpression of active p110 subunit of PI 3-kinase and inhibited 44% by the dominant negative p85 subunit of PI 3-kinase. Cotransfection with 3-phosphoinositide-dependent kinase (PDK1), which is required for the full activation of Akt, resulted in enhanced luciferase activity. Insulin-like growth factor-I-mediated induction of Bcl-2 promoter activity was decreased significantly ($p < 0.01$) by the dominant negative forms of p85 subunit of PI 3-kinase, PDK1, and Akt. These data indicate that regulation of Bcl-2 expression by IGF-I involves a signaling cascade mediated by PI 3-kinase/PDK1/Akt/CREB. Furthermore, we measured the Bcl-2 mRNA in PC12 cells overexpressing Akt by real-time quantitative reverse transcription-polymerase chain reaction using the TaqMan™ fluorogenic probe system. We observed a 2.1-fold increase in Bcl-2 mRNA levels in the Akt cell line compared with control PC12 cells, supporting the observation that enhanced CREB activity by Akt signaling leads to increased Bcl-2 promoter activity and cell survival.

The serine threonine kinase Akt/protein kinase B is an important mediator of metabolic as well as survival responses to insulin and growth factors (1). Akt is activated by translocation to plasma membrane when the PI 3-kinase-generated 3-phosphoinositides bind to its pleckstrin homology domain (2). For its full activation it needs to be further phosphorylated by 3-phosphoinositide-dependent kinase1 (PDK1)[1] at Thr-308 and by PDK2 at Ser-473. The metabolic actions of insulin mediated by Akt include stimulation of GLUT4 translocation and activation of glycogen synthase and the glycolytic enzyme 6-phosphofructose-2-kinase (1).

In addition to its metabolic actions, Akt/protein kinase B has been shown to promote cell survival by growth factors against several apoptotic stimuli (3, 4). The Bcl-2 family of proteins consisting of pro-apoptotic Bad, Bik, Bid. Etc. and anti-apoptotic Bcl-2 and Bcl-xL are important regulators of mammalian apoptosis (5). Bcl-2/Bcl-xL prevents the activation of caspase-9 by Apaf-1 and cytochrome *c* (6). Bcl-2 and Bad heterodimerize and neutralize each other's function. The fate of cells exposed to apoptotic signal is determined by the balance between pro- and anti-apoptotic proteins. One mechanism by which Akt prevents apoptosis is considered to proceed through phosphorylation of the pro-apoptotic protein Bad on Ser-136 (7). Phosphorylated Bad is sequestered by 14-3-3 protein, leading to its down-regulation. It has been also suggested that additional mechanisms might exist for the cell survival-promoting action of Akt (8, 9).

Up-regulation of Bcl-2 expression has been identified as a critical mechanism by which growth factors promote cell survival (10–13). The promoter region of Bcl-2 contains a cAMP-response element (CRE) site, and the transcription factor CREB has been identified as a positive regulator of Bcl-2 expression (13, 14). Akt, a target of IGF-I signaling, has been shown to activate CREB (15). Thus, it seemed possible that Akt activation through PI 3-kinase could mediate regulation of Bcl-2 expression by IGF-I.

In our previous studies in PC12 cells, we identified that three post-receptor pathways activated by IGF-I through extracellular-regulated kinase, p38β MAPK, and PI 3-kinase are capable of mediating Ser-133 phosphorylation of CREB (13, 16). However, in the context of CREB-driven Bcl-2 promoter, activation of the extracellular-regulated kinase pathway has been shown to have a negative regulatory effect through Ets domain transcription factors (14). We identified a novel IGF-I-mediated signaling cascade involving MAP kinase kinase 6/p38β MAPK/

* The work was supported by a Veterans Affairs Merit review grant and an American Diabetes Association research award and National Institute of Health Grant KO8 DK02351 (NIDDK) (to J. E.-B. R.) and a Veterans Affairs Research Enhancement Award Program grant (to J. E.-B. R. and K. A. H.). The costs of publication of this article were defrayed in part by the payment of page charges. This article must therefore be hereby marked "*advertisement*" in accordance with 18 U.S.C. Section 1734 solely to indicate this fact.

‡‡ To whom correspondence should be addressed: Section of Endocrinology (111H), Veterans Affairs Medical Center, 1055 Clermont St., Denver, CO 80220. Tel.: 303-399-8020 (ext. 2775); Fax: 303-393-5271; E-mail: ReuschJ@den-res.org.

[1] The abbreviations used are: PDK1, 3-phosphoinositide-dependent kinase 1; IGF, insulin-like growth factor; CRE, cAMP response element; CREB, CRE-binding protein; MAPK, mitogen-activated protein (MAP) kinase; PBS, phosphate-buffered saline; PI 3-kinase, phosphatidylinositol 3-kinase; RT-PCR, reverse transcription-polymerase chain reaction.

MAP kinase-activated protein kinase-3/CREB, leading to the induction of Bcl-2 promoter (13). However, SB203580, the p38 MAPK inhibitor blocked IGF-I-induced Bcl-2 promoter activity only partially. Earlier work in our laboratory demonstrated that IGF-I-mediated CREB phosphorylation and activation of CRE site-containing chromogranin A promoter requires PI 3-kinase (16). In that study, a dominant negative form of the regulatory subunit of PI 3-kinase was able to block IGF-I-mediated induction of a CRE site-containing promoter of chromogranin A, a neuro endocrine-specific gene. Du and Montminy (15) demonstrated recently that Akt stimulates the phosphorylation and the transcriptional activity of the CREB in HEK 293 cells. These reports clearly raise the possibility that Akt could mediate part of the IGF-I-induced increase in the expression of Bcl-2 at the transcriptional level. The objective of the present study was to examine whether IGF-I mediated signaling through PI 3-kinase and Akt leads to a CREB-dependent increase in Bcl-2 promoter activity.

EXPERIMENTAL PROCEDURES

Materials—The pharmacological inhibitors LY294002 and rapamycin were from Biomol (Plymouth Meeting, PA). Cell culture media and supplies were purchased from Gemini Bio Products, Inc (Calabasas, CA) and Life Technologies, Inc. The CRE site-containing promoter region of *bcl-2* gene was linked to a luciferase reporter as described previously (14). A luciferase reporter gene driven by TATA box joined to tandem repeats of CRE (4×) was purchased from Stratagene (La Jolla, CA). Plasmids for transfection experiments were purified using Qiagen's (Valencia, CA) maxi kit. Antibodies specific for Phospho (Ser-133) CREB and CREB were from New England Biolabs (Beverly, MA). The luciferase assay kit was purchased from Pharmingen (San Diego, CA).

Cell Culture—Rat pheochromocytoma (PC12) cells (provided by Dr. Derek LeRoith (NIDDK, National Institutes of Health, Bethesda, MD) were maintained in Dulbecco's modified Eagle's medium containing 10% fetal bovine serum, 5% heat-inactivated horse serum, 100 μg/ml streptomycin, and 100 microunits/ml penicillin at 37 °C in a humidified atmosphere at 8% CO_2. A cDNA encoding Akt with the Src myristoylation sequence at the N terminus (17) in the retroviral vector pLNCX (18) was packaged into replication-defective retrovirus using 293T cells along with the plasmids SV-ψ-A-MLV and SV-ψ-env$^-$-MLV by the procedure described previously (19, 20). Secreted retrovirus was supplemented with polybrene (8 μg/ml), filtered (0.45 μm), and incubated with PC12 cells for 24 h. Cells expressing Akt were selected by culturing them in medium containing G418. Apoptosis was induced in control PC12 (Neo-21) and the Akt clone by exposing them to serum-free medium for 72 h, and the viable cells were counted. Alternatively, the cells in regular medium were UV-irradiated (32 J/M^2), and 24 h later, the viable cells were counted. Cells were cultured in 6 × 35-mm wells coated with poly-L-lysine for transfection studies.

Isolation of Total RNA and Real-time Quantitative RT-PCR—Control and Akt-overexpressing PC12 cells were cultured in regular medium. Total RNA was isolated from these cells using TRIzol reagent (Life Technologies, Inc.) as per the manufacturer's protocol. RNA samples were further purified by DNase digestion and extraction with phenol and chloroform. The mRNA for Bcl-2 was measured by real-time quantitative RT-PCR using PE Applied Biosystems prism model 7700 sequence detection instrument. The sequences of forward and reverse primers as designed by Primer Express (PE ABI) were 5′-TGGGATGCCTTTGTGGAACT-3′ and 5′-GAGACAGCCAGGAGAAATCAAAC-3′, respectively. The TaqMan™ fluorogenic probe used was 5′-6FAM-TGGCCCCAGCATGCGACCTC-TAMRA-3′. During PCR amplification, 5′ nucleolytic activity of *Taq* polymerase cleaves the probe separating the 5′ reporter fluorescent dye from the 3′ quencher dye (21, 22). Threshold cycle, C_t, which correlates inversely with the target mRNA levels, was measured as the cycle number at which the reporter fluorescent emission increases above a threshold level. The Bcl-2 mRNA levels were corrected for 18 S ribosomal RNA, which was measured using a kit (PEABI, P/N 4308310) from Perkin-Elmer as per the manufacturer's protocol.

Immunoblotting—PC12 cells cultured in poly-L-lysine-coated 60-mm dishes under appropriate conditions were washed twice with ice-cold PBS, and the cell lysates were prepared. Protein content of lysates was measured (23), and appropriately diluted samples (containing equal amounts of protein) were mixed with 2× Laemmli sample buffer containing 100 mM dithiothreitol. The proteins resolved on a 12% SDS-polyacrylamide gels were transferred to polyvinylidene difluoride membranes. After blocking with Tris-buffered saline with Tween (20 mM Tris-HCl (pH 7.9), 8.5% NaCl, and 0.1% Tween 20) containing 5% non-fat dry milk at room temperature for 1 h, the blots were treated with the primary antibody in blocking buffer at 4 °C overnight. The blots were washed with blocking buffer and incubated with anti-rabbit IgG conjugated to alkaline phosphatase for 1 h at room temperature. After further washes with blocking buffer and with 10 mM Tris-HCl (pH 9.5), 10 mM NaCl, 1 mM $MgCl_2$, the blots were developed with CDP-Star reagent (New England Biolabs) and exposed to x-ray film.

Transfection Procedure—Transient transfections were carried out by the procedure described earlier using LipofectAMINE Plus reagent (Life Technologies, Inc.) (13). The cells were cultured to around 70% confluence in 6 × 35-mm plates. One μg of plasmid, 3 μl of Plus reagent, and 10 μg of LipofectAMINE reagent were used for each well. To normalize the transfection efficiency, the plasmid containing β-galactosidase gene driven by SV_{40} promoter was included. DNA and the LipofectAMINE reagent diluted in 100 μl of serum and antibiotic-free medium were mixed together and incubated at room temperature for 30 min. After washing the cells with PBS, 800 μl of serum and antibiotic-free medium was added. The plasmid and LipofectAMINE mixture was added to each well and incubated for 5 h. Then the cells were cultured in regular medium for 24 h before appropriate treatment. The cells were washed with cold PBS and lysed with 100 μl of reporter lysis buffer. After freezing and thawing, the lysate was centrifuged at 14,000 rpm for 30 min to collect the supernatant. Luciferase was assayed using the enhanced luciferase assay kit (Pharmingen) on a Monolight 2010 luminometer. The β-galactosidase assay was carried out as described earlier (13). Statistical analysis was performed by Student's *t* test.

RESULTS

Modulation of PI 3-Kinase Impacts Basal and IGF-I-stimulated Bcl-2 Promoter Activity—To investigate the role of PI 3-kinase in the regulation of Bcl-2 expression, PC12 cells transfected with a Bcl-2 promoter construct containing a CRE site were treated with the PI 3-kinase inhibitor LY294002. There was a 45% decrease ($p < 0.01$) in the reporter activity in the presence of the inhibitor (Fig. 1*A*), suggesting a positive role for PI 3-kinase. To confirm these observations, a series of transient transfections with constitutively active p110 subunit and the dominant negative p85 subunit of PI 3-kinase were carried out. Fig. 1*B* demonstrates the ability of PI 3 kinase activation to augment basal and IGF-I-stimulated Bcl-2 promoter activity. The basal activity increased by 2.3-fold in the presence of p110, whereas it was decreased to 56% of control by Δ p85. IGF-I-mediated regulation of Bcl-2 promoter activity was similarly affected. These observations indicate that IGF-I-induced Bcl-2 expression proceeds in part through activation of PI 3-kinase. Rapamycin did not inhibit the Bcl-2 promoter activity (Fig. 1*A*), suggesting a role for Akt rather than p70 s6 kinase in mediating PI 3-kinase action.

Full activation of Akt is known to require phosphorylation on Thr-308 by PDK-1, a kinase downstream of PI 3-kinase (1). We therefore examined the impact of PDK1 and dominant negative PDK1 on Bcl-2 promoter activity. Cotransfection of PC12 cells with PDK1 resulted in a 2.0-fold increase in reporter activity (Fig. 1*C*). The increase in reporter activity by PDK1 was further enhanced 66% by IGF-I, probably due to its induction through p38β MAPK mediated pathway (13). In contrast, kinase dead PDK1 decreased basal and IGF-I-mediated reporter activity by 37 and 62%, respectively. These data demonstrate important roles for PI 3-kinase and PDK1 in the transcriptional regulation of Bcl-2 expression.

Akt Regulation of Bcl-2 Expression Requires CREB—Akt is one of the downstream targets of PI 3-kinase signaling. Du and Montminy (15) recently reported the positive regulation of CREB activity by Akt. To explore whether Akt regulation of Bcl-2 required CREB, we examined the impact of dominant negative form of CREB, KCREB, on the Akt-stimulated Bcl-2 promoter activity. As shown in Fig. 2*A*, Akt-stimulated Bcl-2 reporter activity is decreased by KCREB. However, KCREB did

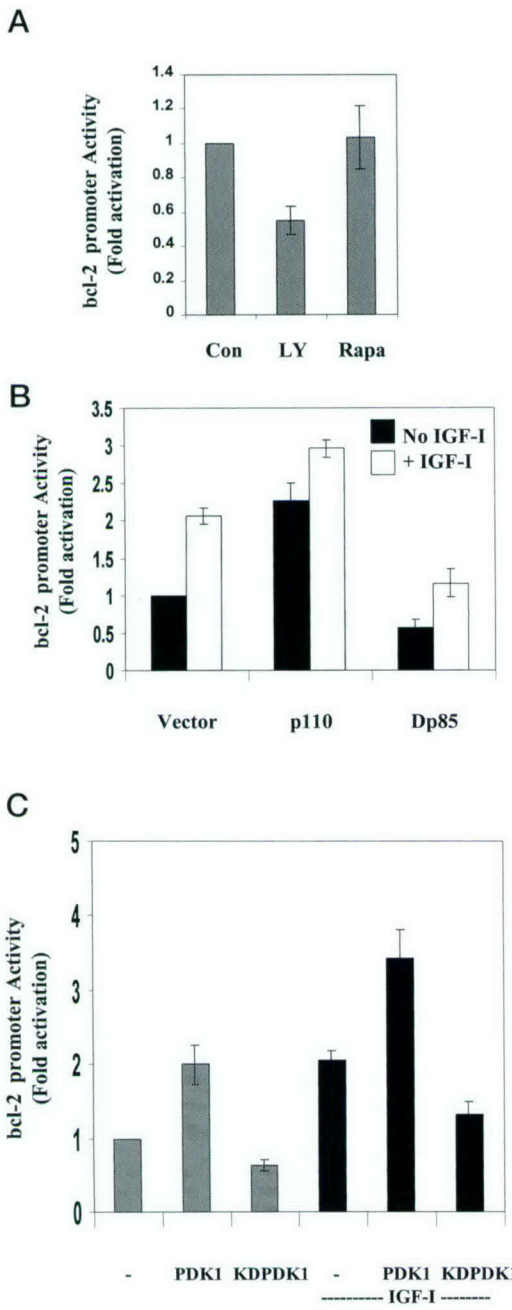

FIG. 1. **Activation of Bcl-2 promoter by PI 3-kinase signaling pathway.** PC12 cells cultured to 70% confluence in 6 × 35-mm wells were transfected with Bcl-2 reporter construct, pRSV β-galactosidase, and indicated plasmids (1 μg of total plasmids, 3 μl of plus reagent, and 10 μg of LipofectAMINE reagent/well). The reporter was cotransfected (*B* and *C*) with constitutively active catalytic subunit (*p110*) and dominant negative regulatory subunit (*Dp85*) of PI 3-kinase, wild type PDK1, and kinase dead PDK1 (*KDPDK1*). 24 h after transfection, the cells were treated with LY294002 (*LY*; 40 μM) and rapamycin (*Rapa*; 10 ng/ml) (*A*) and IGF-I (100 ng/ml; *B* and *C*) as indicated for another 24 h. The inhibitors were added to the culture medium the second time after 12 h. Cell lysates were prepared and assayed for luciferase and β-galactosidase. The values represent mean ± S.E. of observations from four independent experiments, each carried out in duplicate.

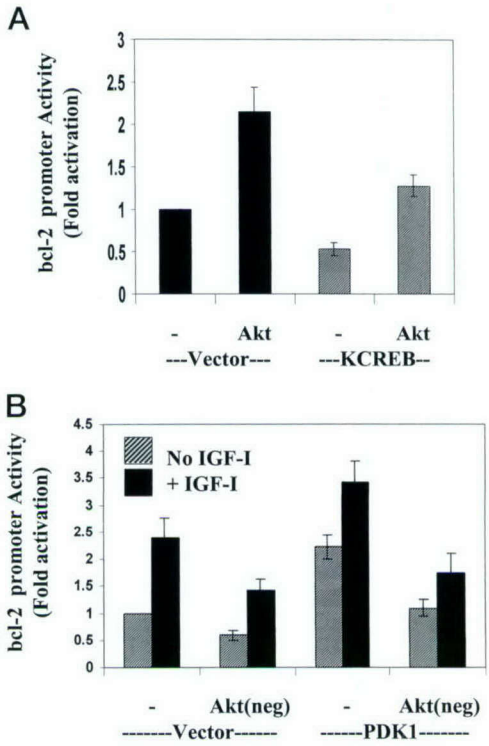

FIG. 2. **Modulation of Bcl-2 expression by Akt through CREB.** PC12 cells cultured to around 70% confluence were transfected with a CRE site-containing Bcl-2 reporter construct along with wild type Akt, dominant negative Akt (*Akt(neg)*; T308A; S473A), wild type PDK1, and KCREB as indicated for 5 h in serum and antibiotic-free medium followed by culturing in regular medium. One day later, the transfected cells were exposed to IGF-I (100 ng/ml) for another 24 h. Luciferase and β-galactosidase were assayed in the cell lysates. Values are means ± S.E. of four independent experiments.

not completely block Akt-mediated activation of the reporter. This could be due to the CREB-independent component in the activation of Bcl-2 promoter (14). In our previous study, we observed that the promoter retained modest activity after deletion or mutation of the CRE site (13). Furthermore cotransfection of the reporter with the dominant negative Akt (T308A; S473A) decreased basal and IGF-I-stimulated luciferase activity by 40% ($p < 0.01$) (Fig. 2*B*). These data support a role for the PI 3-kinase/PDK1/Akt/CREB pathway as a second signaling pathway important for IGF-I regulation of *bcl-2* gene expression. However PDK1 is known to have potential targets such as p90rsk and protein kinase C isoforms in addition to Akt that are capable of activating CREB. Hence we examined the effect of dominant negative Akt on PDK1-mediated induction. We did observe that PDK1 mediated stimulation of Bcl-2 promoter activity in the absence and presence of IGF-I to be decreased by 51 and 48%, respectively, when the dominant negative Akt was included in the cotransfection experiments. The possibility of PDK1 modestly activating Bcl-2 promoter through other pathways involving p90rsk and protein kinase C isoforms cannot be ruled out. Further studies are needed to explore these pathways in detail.

Increased CREB Activity and Bcl-2 Expression in PC12 Cell Line-expressing Akt—The results of previous experiments clearly demonstrated that Akt-mediated signaling activates Bcl-2 promoter through CREB, and this transcription factor needs to be phosphorylated for its activation. We therefore examined whether CREB phosphorylation on Ser-133 activation site is increased in PC12 cells expressing myristoylated Akt. We noted a significant (90%; $p < 0.01$) increase in CREB phosphorylation in these cells in the absence of IGF-I (Fig. 3, *A* and *B*). When these cells were treated with IGF-I (100 ng/ml) for 10 min, CREB phosphorylation increased from 2.2-fold in control cells to 2.9-fold in Akt-expressing cells. This enhanced PCREB formation could be due to growth factor action through p38β MAPK-mediated pathway as shown in our previous study (13). The CREB protein levels did not change significantly

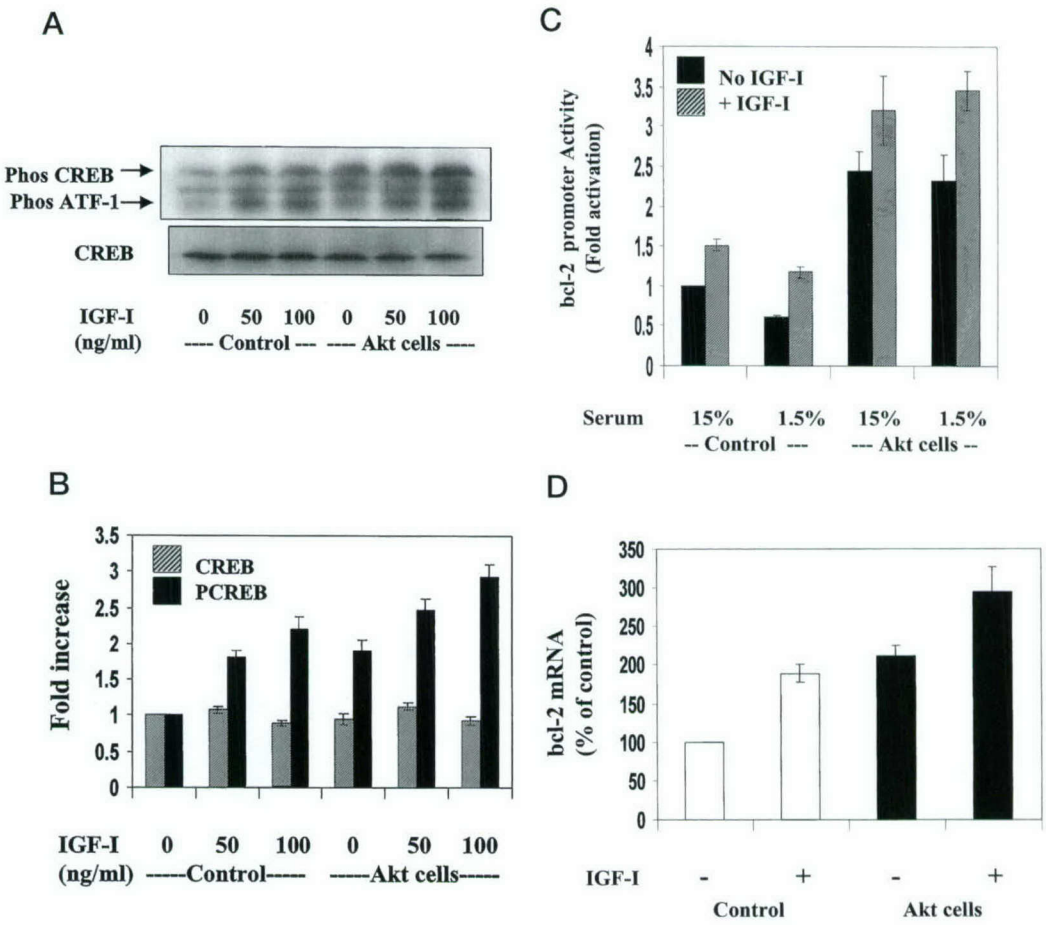

FIG. 3. **Increased CREB activity and Bcl-2 expression in PC12 cells expressing Akt.** *A* and *B*, control and Akt-expressing PC12 cells were cultured to 80% confluence in 60-mm dishes and then maintained in serum-free medium for 5 h. They were treated with the indicated concentrations of IGF-I for 10 min. The cells were washed with ice-cold PBS, and the cell lysates were prepared. Diluted cell lysates with equal protein content were mixed with 2× Laemmli sample buffer followed by sonication. The protein samples were electrophoresed and immunoblotted for phospho CREB (*PCREB*) and CREB. The blots were scanned, and the intensities of bands were quantitated using the Bio-Rad software Quantity One (*B*). *C*, control and Akt-expressing PC12 cells were transfected with a Bcl-2 reporter construct along with pRSV β-galactosidase for 5 h in serum and antibiotic-free medium. After 24 h of transfection, the transfected cells were exposed to media containing the indicated concentrations of serum in the absence and presence of IGF-I for another 24 h. A luciferase assay was carried out in the cell lysates and corrected for transfection efficiency by measuring the activity of β-galactosidase. The values are means ± S.E. of observations from four independent experiments. *D*, control and Akt-expressing PC12 cells cultured to 80% confluence were transferred to a low serum medium (0.1% fetal bovine serum and 0.05% heat-inactivated serum) in the absence and presence of IGF-I (100 ng/ml). After washing the cells with ice-cold PBS, TRIzol reagent was added to the cells, and total RNA was isolated. The Bcl-2 mRNA level was measured in these cells by real-time quantitative RT-PCR using the TaqMan™ fluorogenic probe system by PE Applied Biosystem.

under different experimental conditions (Fig. 3*B*). Hence Akt seems to activate CREB at the post-translational level. We next examined the CREB activity in the cells expressing Akt using a luciferase reporter driven by a CRE site-containing Bcl-2 promoter. The promoter activity was elevated in Akt cells both in the absence and presence of IGF-I (Fig. 3*C*), correlating with the increased CREB phosphorylation observed in the previous experiment (Fig. 3*A*). Interestingly, culturing transfected control cells in low serum medium resulted in a 40% decrease in promoter activity, whereas cells expressing Akt maintained its activation in the presence of low serum (Fig. 3*C*). Similar results were obtained with a luciferase reporter driven by four tandem repeats of CRE sites (results not shown). Furthermore, PC12 cells expressing Akt were found to have increased survival after serum withdrawal and exposure to UV (Table I). After 72 h of culture in serum-free medium, the survival rate was as high as 86% in the Akt clone as compared with 26% control cells. In addition, Akt increased survival in UV-exposed PC12 cells to 76% from 38% seen in control cells.

Data from the studies described above demonstrate the impact of PI 3-kinase/PDK1/Akt on the luciferase reporter construct driven by Bcl-2 promoter. To confirm the role of Akt in the up-regulation of endogenous Bcl-2 expression, we used the PC12 cell line overexpressing constitutively active myristoy-

TABLE I
Serum withdrawal-mediated and UV-induced apoptosis in PC12 cells expressing Akt

PC12 cells expressing the vector LNCX (Neo-21) or LNCX-Myr-Akt were cultured in Dulbecco's modified Eagle's medium without serum for 72 h, after which the viable cells were counted. The cell survival rate was expressed as percentage of viable cells that has been cultured in Dulbecco's modified Eagle's medium containing 1% horse serum. Furthermore, the above mentioned clones were UV-irradiated (32 J/m^2), and after 24 h, the viable cells were counted. The data are presented as percentage of viable cells in a control culture without radiation. The results are the mean ± S.E. of three independent experiments.

	Cell survival	
	Serum-free	UV
	% of control	
Neo-21	26.0 ± 9.9	37.9 ± 11.4
Akt	86.2 ± 14.5[a]	75.6 ± 14.2[a]

[a] < 0.01 *vs.* Neo-21.

lated Akt. We measured Bcl-2 mRNA levels in these cells by a sensitive real-time quantitative RT-PCR using the TaqMan™ fluorogenic probe system. Applied Biosystems prism model 7700 sequence detection instrument was used to measure the reporter fluorescence emission. As shown in Fig. 3*D*, there is a 2.1-fold increase in Bcl-2 mRNA level in Akt clone as compared with the control vector-only clone. Treatment of these cells with 100 ng/ml IGF-I increased the Bcl-2 mRNA level further to 3.0-fold, which could be due to IGF-I action through p38β MAPK (13). This experiment clearly provides a physiological relevance to the significance of Akt-mediated CREB activation.

DISCUSSION

Great insight has been gained over the recent few years regarding the mechanism of neuronal programmed cell death and the ability of growth factors to serve as anti-apoptotic agents. The majority of the data has suggested post-translational modification of the apoptotic machinery (7). The importance of PI 3-kinase and Akt for these effects has been reported by a number of groups (3, 4). The present study defines an additional critical regulatory function for Akt involving transcriptional regulation of the anti-apoptotic protein Bcl-2. We recently reported the induction of Bcl-2 by IGF-I through a novel signaling pathway mediated by MAP kinase kinase 6/p38β MAP kinase/MAP kinase-activated protein kinase-3 (13). Now we identify an additional pathway involving Akt for IGF-I-mediated activation of Bcl-2 promoter.

Regulation of neuronal survival by growth factors is known to proceed through the PI 3-kinase-mediated signaling (3). Low potassium-induced apoptosis in cerebellar granule neurons has been shown to be prevented by synthetic lipid products of PI 3-kinase when added to the culture medium (24). Downstream of this kinase, two signaling pathways involving Akt and p70 s6k have been identified. Dudek *et al.* (3) show that dominant negative Akt is able to induce apoptosis in rat cerebellar granular neurons, and rapamycin, an inhibitor of p70 s6 kinase, does not block insulin-mediated promotion of cell survival (3). Expression of a myristoylated Akt, the active form in immortalized rat hippocampal neuronal cells, leads to increased survival against apoptotic signal (25).

Akt-mediated phosphorylation of cytosolic proteins such as glycogen synthase kinase-3 and Bad is known to play a critical role in the regulation of metabolic pathways as well as prevention of cell death by insulin and growth factors (7). Recent studies indicate that Akt can regulate gene expression at the transcriptional level, suggesting a nuclear site of action. Akt increases the expression of GLUT1 in hepatoma cells (26) and leptin in adipocytes (27). Interleukin-2-mediated Akt activation in BAF/3 cells results in increased expression of Bcl-2. Furthermore, forkhead transcription factor has been identified as a nuclear target for Akt (28–32). It is known to induce insulin-like growth factor-binding protein-1 by stimulating its promoter activity. Akt has been shown to phosphorylate forkhead transcription factor at Thr-24, Ser-256, and Ser-319, the consensus phosphorylation sites both *in vitro* and *in vivo* (29). This covalent modification leads to the nuclear exclusion of forkhead transcription factor, leading to negative regulation of forkhead transcription factor -responsive genes by Akt (28).

Studies have indeed shown that this protein kinase can translocate to nucleus (33–35). Akt/protein kinase B is first translocated to the plasma membrane, where it is activated following phosphorylation on Thr-308 and Ser-473. Subsequently, Akt can be translocated to the nucleus. Meier *et al.* have demonstrated by confocal microscopy the nuclear translocation of Akt 20–30 min after mitogenic stimulation (34). Significant to our present study, it has been demonstrated that myristoylated Akt, which is membrane-directed, can also undergo partial nuclear localization (35), whereas Akt construct having both myristoylation and palmitoylation signals does not (34). The probable explanation for the difference seems to be that they anchor to the plasma membrane with different levels of affinity. We were able to observe increased CREB activity in PC12 cells expressing Akt with a myristoylation signal (Fig. 3*C*).

The transcription factor CREB has also been identified as a target for several signaling pathways mediated by growth factors. Nerve growth factor is known to increase CREB phosphorylation through Ras/MAP kinase kinase/extracellular-regulated kinase/Rsk2 (36). Fibroblast growth factor and IGF-I induce CRE site- containing promoters by activating p38 MAPK and MAPKAP-K2/3 (13, 37). IGF-I-stimulated CREB phosphorylation in PC12 cells is decreased by wortmannin, an inhibitor of PI 3-kinase, but not by rapamycin, an inhibitor of p70 s6k, suggesting that Akt is likely to be involved in CREB activation (16). In a recent study, Du and Montminy (15) demonstrated that Akt/protein kinase B stimulates the phosphorylation of CREB on serine 133 and promotes the recruitment of the coactivator CREB-binding protein (15). They also showed that Akt-mediated induction of CRE-driven gene expression is blocked by a serine to alanine mutation at position 133 using the Gal4 CREB system. In the present investigation, we further demonstrate the physiological importance of this signaling pathway in the activation of an endogenous CRE site-containing Bcl-2 promoter. When the luciferase reporter construct driven by Bcl-2 promoter was cotransfected with p110, PDK1, and Akt, there was significant stimulation of basal and IGF-I-induced luciferase activity. The dominant negative forms of the regulatory subunit of PI 3-kinase, Δp85, and Akt were able to decrease the promoter activity, suggesting that growth factor-mediated signaling through PI 3-kinase/PDK1/Akt could be involved in the induction of Bcl-2 expression. Hence Akt seems to promote cell survival through inactivation of Bad by phosphorylation and up-regulation of Bcl-2 by transcriptional activation.

Acknowledgments—We thank Dr. Nicholas Webster, Dr. Emmanuel Van Obberghen, and Dr. Richard Goodman for providing valuable reagents. We acknowledge the excellent secretarial support of Gloria Smith. We thank Dr. Boris Draznin for critically reading the manuscript. Quantitative RT-PCR was performed at the University of Colorado Cancer Center core facility.

REFERENCES

1. Coffer, P. J., Jin, J., and Woodgett, J. R. (1998) *Biochem. J.* **335,** 1–13
2. Downward, J. (1998) *Curr. Opin. Cell Biol.* **10,** 262–267
3. Dudek, H., Datta, S. R., Franke, T. F., Birnbaum, M. J., Yao, R., Cooper, G. M., Segal, R. A., Kaplan, D. R., and Greenberg, M. E. (1997) *Science* **275,** 661–664
4. Kulik, G., Klippel, A., and Weber, M. J. (1997) *Mol. Cell. Biol.* **17,** 1595–1606
5. Merry, D. E., and Korsmeyer, S. J. (1997) *Annu. Rev. Neurosci.* **20,** 245–267
6. Adams, J. M., and Cory, S. (1998) *Science* **281,** 1322–1326
7. Datta, S. R., Dudek, H., Tao, X., Masters, S., Fu, H., Gotoh, Y., and Greenberg, M. E. (1997) *Cell* **91,** 231–241
8. Hinton, H. J., and Welham, M. J. (1999) *J. Immunol.* **162,** 7002–7009
9. Scheid, M. P., and Duronio, V. (1998) *Proc. Natl. Acad. Sci. U. S. A.* **95,** 7439–7444
10. Singleton, J. R., Dixit, V. M., and Feldman, E. L. (1996) *J. Biol. Chem.* **271,** 31791–31794
11. Tamatani, M., Ogawa, S., and Tohyama, M. (1998) *Mol. Brain Res.* **58,** 27–39
12. Minshall, C., Arkins, S., Straza, J., Conners, J., Dantzer, R., Freund, G. G., and Kelley, K. W. (1997) *J. Immunol.* **159,** 1225–1232
13. Pugazhenthi, S., Miller, E., Sable, C., Young, P., Heidenreich, K. A., Boxer, L. M., and Reusch, J. E.-B. (1999) *J. Biol. Chem.* **274,** 27529–27535
14. Wilson, B. E., Mochon, E., and Boxer, L. M. (1996) *Mol. Cell. Biol.* **16,** 5546–5556
15. Du, K., and Montminy, M. (1998) *J. Biol. Chem.* **273,** 32377–32379
16. Pugazhenthi, S., Boras, T., O'Connor, D., Meintzer, M. K., Heidenreich, K. A., and Reusch, J. E.-B. (1999) *J. Biol. Chem.* **274,** 2829–2837
17. Ahmed, N. N., Grimes, H. L., Bellacosa, A., Chan, T. O., and Tsichlis, P. N. (1997) *Proc. Natl. Acad. Sci. U. S. A.* **94,** 3627–3632
18. Miller, A. D., and Rosman, G. J. (1989) *Biotechniques* **7,** 980–990
19. Landau, N. R., and Littman, D. R. (1992) *J. Virol.* **66,** 5110–5113
20. Pear, W. S., Nolan, G. P., Scott, M. L., and Baltimore, D. (1993) *Proc. Natl. Acad. Sci. U. S. A.* **90,** 8392–8396

21. Heid, C. A., Stevens, J., Livak, K. J., and Williams, P. M. (1996) *Genome Res.* **6,** 986–994
22. Gibson, U. E. M., Heid, C. A., and Williams, P. M. (1996) *Genome Res.* **6,** 995–1001
23. Bradford, M. M. (1976) *Anal. Biochem.* **72,** 248–254
24. Shimoke, K., Yamada, M., Ikeuchi, T., and Hatanaka, H. (1998) *FEBS Lett.* **437,** 221–224
25. Eves, E. M., Xiong, W., Bellacosa, A., Kennedy, S. G., Tsichlis, P. N., Rosner, M. R., and Hay, N. (1998) *Mol. Cell. Biol.* **18,** 2143–2152
26. Barthel, A., Okino, S. T., Liao, J., Nakatani, K., Li, J., Whitlock, J. P., Jr., and Roth, R. A. (1999) *J. Biol. Chem.* **274,** 20281–20286
27. Barthel, A., Kohn, A. D., Luo, Y., and Roth, R. A. (1997) *Endocrinology* **138,** 3559–3562
28. Tang, E. D., Nunez, G., Barr, F. G., and Guan, K.-L. (1999) *J. Biol. Chem.* **274,** 16741–16746
29. Rena, G., Guo, S., Cichy, S. C., Unterman, T. G., and Cohen, P. (1999) *J. Biol. Chem.* **274,** 17179–17183
30. Guo, S., Rena, G., Cichy, S., He, X., Cohen, P., and Unterman, T. (1999) *J. Biol. Chem.* **274,** 17184–17192
31. Biggs, W. H., Meisenhelder, J., Hunter, T., Cavenee, W. K., and Arden, K. C. (1999) *Proc. Natl. Acad. Sci. U. S. A.* **96,** 7421–7426
32. Brunet, A., Bonni, A., Zigmond, M. J., Lin, M. Z., Juo, P., Hu, L. S., Anderson, M. J., Arden, K. C., Blenis, J., and Greenberg, M. E. (1999) *Cell* **96,** 857–868
33. Andjelkovic, M., Alessi, D. R., Meier, R., Fernandez, A., Lamb, N. J. C., Frech, M., Cron, P., Cohen, P., Lucocq, J. M., and Hemmings, B. A. (1997) *J. Biol. Chem.* **272,** 31515–31524
34. Meier, R., Alessi, D. R., Cron, P., Andjelkovic, M., and Hemmings, B. A. (1997) *J. Biol. Chem.* **272,** 30491–30497
35. Ahmed, N. N., Franke, T. F., Bellacosa, A., Datta, K., Gonzalez-Portal, M.-E., Taguchi, T., Testa, J. R., and Tsichlis, P. N. (1993) *Oncogene* **8,** 1957–1963
36. Xing, J., Ginty, D. D., and Greenberg, M. E. (1996) *Science* **273,** 959–963
37. Tan, Y., Rouse, J., Zhang, A., Cariati, S., Cohen, P., and Comb, M. J. (1996) *EMBO J.* **15,** 4629–4642

The Journal of Neuroscience, September 1, 2001, 21(17):6544–6552

Myocyte Enhancer Factor 2A and 2D Undergo Phosphorylation and Caspase-Mediated Degradation during Apoptosis of Rat Cerebellar Granule Neurons

Mingtao Li,[1] Daniel A. Linseman,[1] Melissa P. Allen,[2] Mary Kay Meintzer,[1] Xiaomin Wang,[1] Tracey Laessig,[1] Margaret E. Wierman,[2] and Kim A. Heidenreich[1]

Departments of [1]Pharmacology and [2]Medicine, University of Colorado Health Sciences Center and the Denver Veterans Affairs Medical Center, Denver, Colorado 80262

Myocyte enhancer factor 2 (MEF2) proteins are important regulators of gene expression during the development of skeletal, cardiac, and smooth muscle. MEF2 proteins are also present in brain and recently have been implicated in neuronal survival and differentiation. In this study we examined the cellular mechanisms regulating the activity of MEF2s during apoptosis of cultured cerebellar granule neurons, an established *in vitro* model for studying depolarization-dependent neuronal survival. All four MEF2 isoforms (A, B, C, and D) were detected by immunoblot analysis in cerebellar granule neurons. Endogenous MEF2A and MEF2D, but not MEF2B or MEF2C, were phosphorylated with the induction of apoptosis. The putative sites that were phosphorylated during apoptosis are functionally distinct from those previously reported to enhance MEF2 transcription. The increased phosphorylation of MEF2A and MEF2D was followed by decreased DNA binding, reduced transcriptional activity, and caspase-dependent cleavage to fragments containing N-terminal DNA binding domains and C-terminal transactivation domains. Expression of the highly homologous N terminus of MEF2A (1–131 amino acids) antagonized the transcriptional activity and prosurvival effects of a constitutively active mutant of MEF2D (MEF2D-VP16). We conclude that MEF2A and MEF2D are prosurvival factors with high transcriptional activity in postmitotic cerebellar granule neurons. When these neurons are induced to undergo apoptosis by lowering extracellular potassium, MEF2A and MEF2D are phosphorylated, followed by decreased DNA binding and cleavage by a caspase-sensitive pathway to N-terminal fragments lacking the transactivation domains. The degradation of MEF2D and MEF2A and the generation of MEF2 fragments that have the potential to act as dominant-inactive transcription factors lead to apoptotic cell death.

Key words: MEF2; neurons; apoptosis; transcription; caspase; cerebellum

Myocyte enhancer factor 2 (MEF2) transcription factors are members of the MADS (MCM1-agamous-deficiens-serum response factor) family of transcription factors (Yu et al., 1992; Naya and Olson, 1999). A hallmark of MADS-box proteins is their combinational association with other MADS domain factors, as well as other heterologous classes of transcriptional regulators (Shore and Sharrocks, 1995). Mammalian MEF2 proteins are encoded by four genes (MEF2A, MEF2B, MEF2C, and MEF2D), each of which gives rise to alternatively spliced transcripts (Yu et al., 1992; Leifer et al., 1993; Martin et al., 1994). The MEF2 family of genes is highly expressed in cells of muscle lineage, where they have been shown to be important regulators of gene expression during the development of skeletal, cardiac, and smooth muscle (McDermott et al., 1993; Martin et al., 1994; Molkentin et al., 1996). In these tissues the MEF2 proteins interact with myogenic basic helix–loop–helix transcription factors such as MyoD to activate myogenesis (Molkentin and Olson, 1996; Ornatsky et al., 1997).

Received Feb. 9, 2001; revised June 15, 2001; accepted June 21, 2001.

This research was supported by United States Army Medical Research and Materiel Command Grant DAMD17-99-1-9481, by National Institutes of Health Grant NS38619-01A1, and by a Veterans Affairs Merit Award and Research Enhancement Award Program Award to K.A.H.

M.L. and D.A.L. contributed equally to this manuscript.

Correspondence should be addressed to Dr. Kim A. Heidenreich, Denver Veterans Affairs Medical Center-111H, 1055 Clermont Street, Denver, CO 80220. E-mail: kim.heidenreich@uchsc.edu.

All MEF2 family members also are highly expressed in neurons of the CNS (Leifer et al., 1993, 1994; McDermott et al., 1993; Ikeshima et al., 1995; Lyons et al., 1995; Mao et al., 1999). Recent *in vitro* findings support the hypothesis that MEF2 transcription factors regulate neuronal survival and development. In cultures of cerebral cortical neurons in which proliferating precursor cells and postmitotic differentiating neurons can be distinguished, MEF2C is expressed selectively in newly generated postmitotic neurons and is not detectable in BrdU-positive precursor cells (Mao et al., 1999). Transfection of postmitotic cortical neurons with different MEF2C mutants demonstrated that MEF2C is required for the survival of these neurons. In postnatal day 19 (P19) neuronal precursor cells, the expression of MEF2 induces a mixed neuronal/myogenic phenotype (Okamoto et al., 2000). During retinoic acid-induced neurogenesis of these cells, a dominant-negative form of MEF2C enhances apoptosis but does not affect cell division. On the other hand, P19 cells induced to undergo apoptosis can be rescued from cell death by the expression of constitutively active MEF2C. In addition, overexpression of MEF2C in P19 cells results in induction of neurofilament protein, the nuclear antigen NeuN, and MASH-1, a neural-specific transcription factor known to interact with MEF2s (Skerjanc and Wilton, 2000). These data suggest that MEF2 proteins regulate neuronal development by promoting survival and inducing differentiation.

In the present study we examined the mechanisms regulating the activity of MEF2 proteins during apoptosis of cultured rat

cerebellar granule neurons, a well established model of depolarization-dependent neuronal survival. We provide evidence that MEF2A and MEF2D are prosurvival factors with high DNA binding and transcriptional activity in postmitotic cerebellar granule neurons. When these neurons are induced to undergo apoptosis by lowering extracellular potassium, MEF2A and MEF2D are phosphorylated. The phosphorylation of MEF2D and MEF2A is followed by decreased DNA binding and cleavage by a caspase-sensitive pathway to N-terminal MEF2 fragments that lack the transactivation domain. The decreased DNA binding of MEF2s and the formation of MEF2 fragments that can act as dominant-inactive transcription factors are sufficient to block the prosurvival effects of MEF2s and induce apoptosis in mature cerebellar granule neurons.

MATERIALS AND METHODS

Materials. The MEF2A antibody is an affinity-purified rabbit polyclonal antibody that was raised to a peptide corresponding to codons 487–507 of human MEF2A purchased from Santa Cruz Biotechnology (Santa Cruz, CA). According to the manufacturer, this antibody may cross-react to a small extent with MEF2C. The affinity-purified rabbit polyclonal MEF2C antibody, a gift from John Schwarz (University of Texas Medical School, Houston, TX), was raised against an isoform-specific peptide representing codons 300–316 of human MEF2C and is specific for MEF2C (Firulli et al., 1996). The rabbit polyclonal antibody to MEF2B was raised against a polyhistidine fusion protein corresponding to codons 234–365 of human MEF2B and was kindly provided by Dr. Ron Prywes (Columbia University, NY). Antibody to MEF2D is a monoclonal antibody raised against a peptide corresponding to codons 346–511 of mouse MEF2D purchased from Transduction Laboratories (Lexington, KY). The dominant-inactive MEF2 mutant pcDNA3-MEF2A131 was kindly provided by Dr. Prywes. The dominant-active MEF2 mutant pCMV-MEF2D-VP16 was a gift from Dr. John C. McDermott (York University, Toronto, Ontario, Canada). The pGL2-MEF2-Luc reporter plasmid (Lemercier et al., 2000) was provided by Dr. Saadi Khochbin (INSERM, France). The caspase-3 antibody was purchased from Santa Cruz Biotechnology, and the polyclonal anti-β-galactosidase (β-gal) antibody was purchased from 5 Prime→3 Prime (Boulder, CO). Cy3-conjugated goat antibody to rabbit IgG was purchased from Chemicon (Temecula, CA). The caspase inhibitors YVAD-CHO, DEVD-FMK, and ZVAD-FMK were obtained from Calbiochem (La Jolla, CA). [α-^{32}P]CTP (3000 Ci/mmol) was purchased from Amersham Pharmacia Biotechnology (Piscataway, NJ).

Neuronal cell culture. Rat cerebellar granule neurons were prepared from 7- to 8-d-old Sprague Dawley rat pups (15–19 gm) as described previously (Li et al., 2000). Briefly, neurons were seeded at a density of 2.0×10^6 cells/ml in basal modified Eagle's (BME) medium containing 10% fetal bovine serum, 25 mM KCl, 2 mM glutamine, and penicillin (100 U/ml)/streptomycin (100 μg/ml). Cytosine arabinoside (10 μM) was added to the culture medium 24 hr after plating to limit the growth of non-neuronal cells. With the use of this protocol, 95–99% of the cultured cells were granule neurons. Transfections were performed at day 5–6 in culture, and experiments were performed after 7 d in culture. Apoptosis was induced by removing the serum and reducing the extracellular potassium concentration from 25 to 5 mM. Control cultures were treated identically but were maintained in serum-free medium supplemented with 25 mM KCl.

Western blot analysis. Western blot analysis was performed as described previously (Li et al., 2000). Briefly, neurons were lysed by adding SDS sample buffer [62.5 mM Tris-HCl, pH 6.8, 2% (w/v) SDS, 10% glycerol, 50 mM DTT, and 0.1% (w/v) bromphenol blue]. The samples were resolved by SDS-PAGE with the use of either 7.5 or 12% acrylamide gels, as indicated in the legends. Proteins were transferred to Hybond-P membranes (polyvinylidene difluoride). The membranes were incubated with anti-MEF2A (1:5000), anti-MEF2D (1:1000), anti-MEF2C (1:1000), and anti-MEF2B (1:500). After incubation with the primary antibodies the filters were washed and then incubated with the respective horseradish peroxidase (HRP)-conjugated anti-rabbit or anti-mouse antibody (Amersham Pharmacia Biotech). Then the blots were washed and subsequently were developed with an enhanced chemiluminescence system (Amersham Pharmacia Biotech) and exposed to Kodak autoradiographic film. Quantitation was performed with the Bio-Rad Quantity One software (Hercules, CA).

Preparation of nuclear extracts from cerebellar granule neurons. After 7 d in culture the cerebellar granule neurons were rinsed two times in serum-free BME containing 25 mM KCl and then maintained in 25 or 5 mM KCl medium in the absence or presence of caspase inhibitors. Neurons that did not receive inhibitors received the control vehicle dimethyl sulfoxide (DMSO). After the indicated times the neurons (100 mm dishes) were washed with ice-cold PBS and detached from culture dishes by a cell scraper in 0.5 ml of buffer A [0.25 M sucrose and (in mM) 15 Tris, pH 7.9, 60 KCl, 2 EDTA, pH 8.0, 0.5 EGTA, 15 NaCl, 1.0 Na_3VO_4, 50 NaF, 0.5 spermidine, 1 DTT, 1 benzamidine, and 0.5 PMSF plus 20 μg/ml leupeptin, 0.76 μg/ml pepstatin, and 2 μM aprotinin]. The cells were centrifuged at 250 × *g* for 5 min. The pellets were washed twice in buffer A and then homogenized with 15 strokes of a tight-fitting Dounce homogenizer to release the nuclei. Then the homogenate was centrifuged at 14,000 × *g* for 15 sec to pellet the nuclei. The supernatants were removed, and the pellets were resuspended in buffer C [(in mM) 20 HEPES, pH 7.9, 500 KCl, 1.5 $MgCl_2$, 1 EDTA, pH 8.0, 1.0 Na_3VO_4, 50 NaF, 1.0 DTT, 1 benzamidine, and 0.5 PMSF plus 20 μg/ml leupeptin, 0.76 μg/ml pepstatin, 25% glycerol, and 10 μM aprotinin]. Nuclear proteins were extracted at 4°C for 45 min, and insoluble nuclei were precipitated by centrifugation at 14000 × *g* for 15 min. Supernatants were dialyzed against a buffer containing 10% glycerol and (in mM) 10 Tris, pH 7.9, 5 $MgCl_2$, 50 KCl, 1 EDTA, pH 8.0, 1.0 Na_3VO_4, 50 NaF, 1 DTT, 1 PMSF, and 1 benzamidine for 3 hr at 4°C. The extracts were quantified for protein content by the BCA method (Pierce, Rockford, IL) and frozen in small aliquots at −70°C.

Electrophoretic mobility shift assays. Nuclear extracts from cerebellar granule neurons (10 μg) were incubated with double-stranded oligonucleotides corresponding to the muscle creatine kinase MEF2 site 5′-CGGATCGCTCTAAA*A*ATAACCCTGTCG-3′ (Amacher et al., 1993) or to a mutant oligonucleotide containing C→G and A→C substitutions at the two italicized residues. The oligomers were end-labeled with the Klenow fragment of DNA polymerase I (Life Technologies, Gaithersburg, MD) and [α-^{32}P]CTP to a specific activity of 10,000–30,000 cpm/ng. Binding reactions were performed for 20 min at 4°C in 1 mM dithiothreitol, 2.5 mM $MgCl_2$, 10% glycerol, 0.1 mg/ml bovine serum albumin, 30 ng/μl of poly(dI-dC), 20 mM HEPES, pH 7.9, and 50–100,000 cpm of oligomer in a total volume of 20 μl. For the supershift analysis, 1 μl of specific antisera or preimmune serum was added to the nuclear extracts for 20 min at 4°C, followed by another 20 min in the presence of labeled oligomers. The protein–DNA complexes were analyzed on 5% nondenaturing polyacrylamide gels containing 3% glycerol and 0.25× TBE (90 M Tris borate, 1 mM EDTA) in the cold room. After electrophoresis the gels were dried and exposed to film at −70°C.

Transfection assays and reporter gene expression. Cerebellar granule neurons were transfected by a calcium phosphate coprecipitation method described previously (Li et al., 2000). Neurons were transfected with 1 μg of MEF2-luciferase expression plasmids (pGL2-MEF2-luc) and/or 1–3 μg of MEF2D expression plasmids (pCMV-MEF2D-VP16, pcDNA3-MEF2A131) and 1 μg of pCMV-β-gal as an internal control for transfection efficiency. The total amount of DNA for each transfection was kept constant (7 μg/ml) by using the empty vector pcDNA3. Neurons were kept in conditioned medium after transfection for 2 hr; then the medium was replaced with BME containing 25 or 5 mM KCl. After 4 hr the cell extracts were prepared with reporter lysis buffer (Promega, Madison, WI), and the activities of luciferase and β-galactosidase were measured with the Luciferase Assay System (Promega) and the β-galactosidase Enzyme Assay System (Promega), respectively.

Quantitation of apoptosis in transfected neurons. Neurons were transfected as described previously (Li et al., 2000). Plasmids (pCMV-MEF2D-VP16, pCMV-MEF2D-VP16 plus pcDNA3-MEF2A131, and pCMV-LacZ) were added to the transfection media at a final concentration of 4–5 μg/ml. The total amount of DNA for each transfection was kept constant by using the empty vector pcDNA3. After transfection the neurons were switched to a medium containing 25 or 5 mM KCl. Then 16 hr later the cells were immunostained with a polyclonal antibody to β-galactosidase (1:500 dilution), followed by a Cy3-conjugated goat antibody to rabbit IgG (1:500) to identify cells expressing β-galactosidase. To visualize the nuclei of transfected neurons, we included the DNA dye Hoechst 33258 (5.0 μg/ml) in the wash after the secondary antibody incubation. Apoptosis was quantified by scoring the percentage of cells in the β-galactosidase-expressing cell population with condensed or fragmented nuclei. So that we could obtain unbiased counting, cells (~500)

were scored blindly without knowledge of their previous treatment. Experiments were performed in triplicate.

RESULTS

MEF2 protein expression and phosphorylation state in control and apoptotic cerebellar granule neurons

Primary cerebellar granule neurons represent a widely used *in vitro* model system that mimics the trophic action of neuronal activity that is seen in the developing nervous system (D'Mello et al., 1993; Miller et al., 1997). Thus, elevated levels of extracellular potassium promote neuronal survival by opening L-type voltage-sensitive calcium channels, leading to an influx of calcium into neurons. Lowering of extracellular potassium decreases calcium influx and promotes neuronal cell death by an apoptotic mechanism.

Western analysis indicated that all four members of the MEF2 superfamily of transcription factors were present in cerebellar granule cells (Fig. 1*A*). When neurons were induced to undergo apoptosis by lowering extracellular potassium, there were selective shifts in the mobility of MEF2A (Fig. 1*A*, *top*) and MEF2D (Fig. 1*A*, *bottom*) on SDS gels. The mobility shifts were detected in neuronal cell lysates as early as 30 min and sustained to 8 hr. The shifts in mobility of MEF2A and MEF2D were enhanced when the samples were electrophoresed for longer times through higher resolution gels (Fig. 1*B*). Treatment of neuronal protein extracts with calf intestinal alkaline phosphatase before electrophoresis reversed the mobility shift of MEF2A and MEF2D seen in the low potassium conditions, confirming that the shifts in mobility of MEF2A and MEF2D were attributable to enhanced serine/threonine phosphorylation (Fig. 1*C*). The phosphorylation sites responsible for the increase in phosphorylation seen on lowering intracellular calcium are functionally different from those previously reported to enhance transcription. Both a p38 inhibitor (10 μM SB203580) and a MEK inhibitor (10 μM PD98059) failed to block the increase in phosphorylation seen with the induction of apoptosis (data not shown). The relative intensities of the slower-migrating MEF2A and MEF2D proteins decreased after 4 and 8 hr in low potassium medium (Fig. 1*A*, *lanes 6, 8*), whereas the faster-migrating MEF2 proteins observed under depolarizing conditions remained constant, suggesting a link between MEF2 phosphorylation and degradation.

MEF2D transcriptional activity is regulated by extracellular potassium

The transcriptional activity of MEF2 proteins in cerebellar granule neurons was measured with a luciferase reporter plasmid that contains two MEF2 consensus sites, followed by the luciferase reporter gene (Lemercier et al., 2000). Cerebellar granule neurons grown in the presence of depolarizing potassium (25 mM) demonstrated high endogenous MEF2-driven luciferase activity (Fig. 2*A*). After the potassium was lowered to 5 mM for 4–8 hr, the transcriptional activity of the MEF2 reporter was decreased by ~90% ($p < 0.05$) (Figure 2*A*). Incubation in 5 mM potassium for 4 hr, followed by the readdition of 25 mM potassium for an additional 4 hr, restored ~50% of the MEF2 transcriptional activity (Fig. 2*A*). Similarly, the readdition of 25 mM potassium also reversed the mobility shift in MEF2D (Fig. 2*B*), suggesting that phosphorylation of MEF2D during apoptosis is associated with the observed decrease in MEF2 transcriptional activity. The fact that only a partial recovery of MEF2-driven luciferase activity was observed in the above experiment could be accounted for by the significant degradation of MEF2D that had occurred after

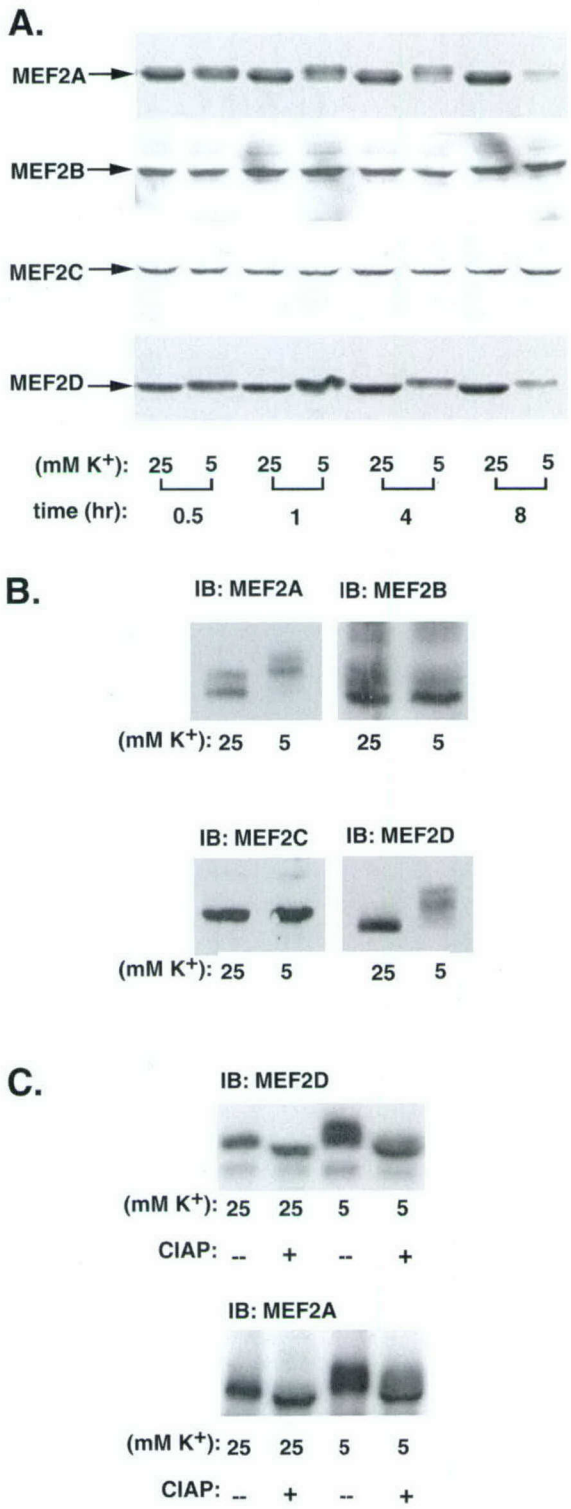

Figure 1. MEF2D and MEF2A, but not MEF2B and MEF2C, are phosphorylated and degraded during the apoptosis of cerebellar granule neurons. *A*, Cerebellar granule neurons (day 7) were placed in serum-free medium containing 25 or 5 mM KCl for the indicated times. Neuronal cell lysates were resolved on 7.5% SDS-acrylamide gels and subjected to Western analysis with the use of specific antibodies to MEF2A, MEF2B, MEF2C, and MEF2D. Data are representative of three separate experiments. *B*, Cell extracts were prepared as described above and analyzed on higher resolution gels. *C*, Cell extracts were incubated in the absence or presence of calf intestinal alkaline phosphatase (*CIAP*; 10 U/ml) before gel electrophoresis.

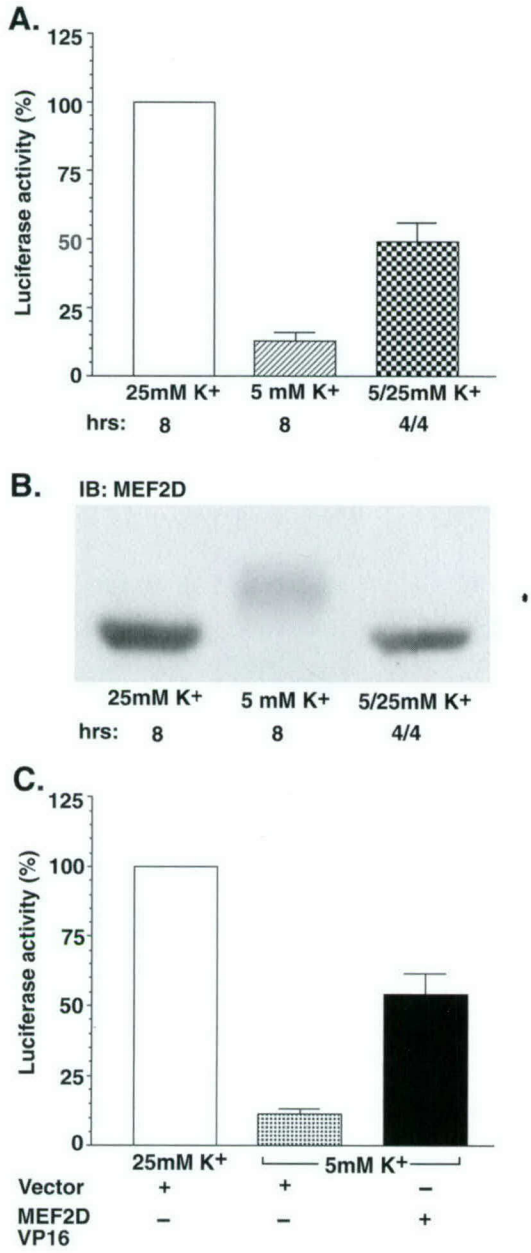

Figure 2. Neurons switched to 5 mM KCl show enhanced MEF2D phosphorylation and decreased MEF2 transcriptional activity; the readdition of 25 mM KCl promotes the dephosphorylation of MEF2D and the partial recovery of MEF2 transcriptional activity. *A*, Cerebellar granule neurons (day 6) were transfected with a MEF2-responsive luciferase reporter and pCMV-β-gal. After transfection (2 hr) the neurons were placed in serum-free medium containing either 25 or 5 mM KCl for 8 hr. In addition, some cells were incubated for 4 hr in 5 mM KCl, followed by the readdition of 25 mM KCl for an additional 4 hr. Then luciferase and β-galactosidase activities were determined as described in Materials and Methods. *B*, Cerebellar granule neurons were incubated as described in *A*, and the phosphorylation status and relative quantity of MEF2D were determined by immunoblot (*IB*) analysis. *C*, Cerebellar granule neurons were transfected with a MEF2-responsive luciferase reporter and pCMV-β-gal in the absence or presence of pCMV-MEF2D-VP16. After 4 hr the luciferase and β-galactosidase activities were determined. Data are expressed as a percentage of control neurons grown in 25 mM KCl and are the mean ± SEM ($n = 3$).

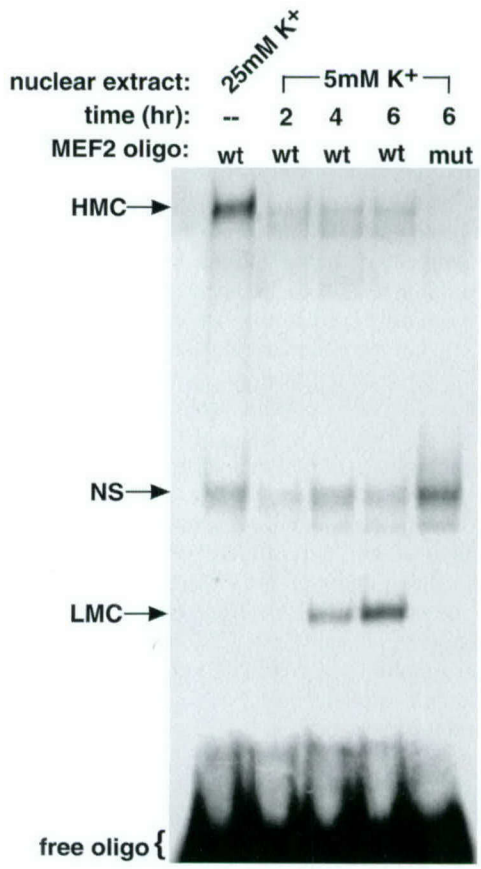

Figure 3. MEF2 DNA binding activity is decreased in apoptotic neurons. Cerebellar granule neurons (day 7) were placed in serum-free medium containing 25 or 5 mM KCl. After the indicated times, nuclear extracts were prepared, and gel mobility shift assays were performed with a double-stranded ^{32}P-labeled consensus (*wt*) or mutant (*mut*) MEF2 oligomer. *NS*, Nonspecific protein/DNA complex; *HMC*, high-mobility complex; *LMC*, low-mobility complex.

4 hr in 5 mM potassium (Fig. 2*B*, *lane 1* vs *lane 3*). Finally, transfection of neurons with MEF2D-VP16, a constitutively active mutant of MEF2D, attenuated the decline of MEF2 luciferase activity during potassium withdrawal (Fig. 2*C*). The decrease in MEF2 transcriptional activity was not attributable to a nonselective effect of cell death, because the transcriptional activity of AP-1 measured with an AP-1 luciferase reporter construct was increased by 30% under the same conditions by which the MEF2 transcriptional activity decreased (data not shown).

DNA binding of MEF2A and MEF2D is regulated by extracellular potassium

To determine whether the DNA binding activity of MEF2 proteins was regulated during induction of the apoptosis of cerebellar granule neurons, we performed electrophoretic mobility shift assays (EMSAs) by using wild-type and mutant MEF2 double-stranded oligonucleotides. Nuclear extracts from cerebellar granule neurons cultured in medium containing 25 mM KCl demonstrated one specific high-mobility protein–DNA complex, HMC (Fig. 3). Extracts from neurons cultured in 5 mM KCl revealed a decrease in the HMC that was detected as early as 2 hr after the potassium was lowered. In addition to the decrease in the HMC associated with the apoptotic response, a new lower-mobility MEF2–DNA binding complex, LMC, was detected in extracts

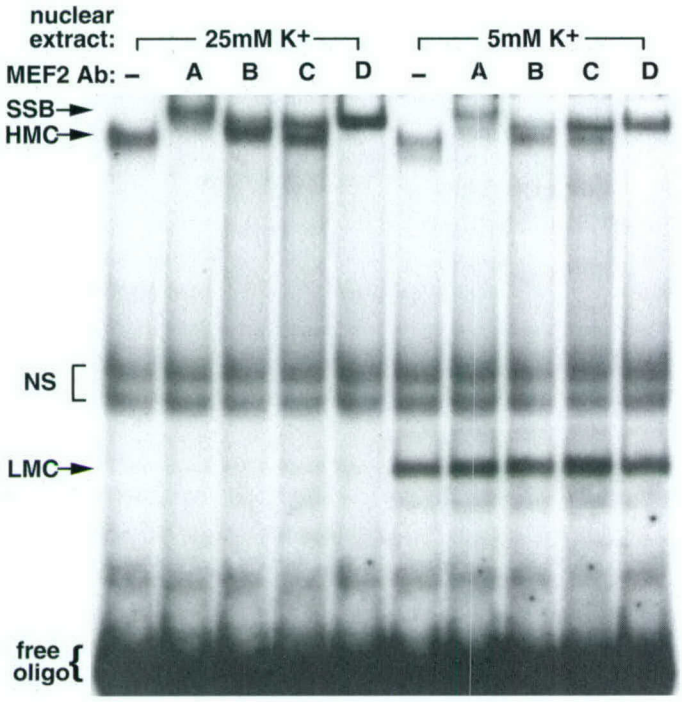

Figure 4. MEF2A and MEF2D are the major MEF2s in the high-molecular-weight DNA binding complex. Cerebellar granule neurons (day 7) were placed in serum-free medium containing 25 or 5 mM KCl. After 4 hr, nuclear extracts were prepared, and supershift gel mobility shift assays were performed with a double-stranded ^{32}P-labeled consensus MEF2 oligomer in the absence or presence of MEF2 antibodies. Note that the lower-molecular-weight complex did not shift with MEF2 antibodies. *SSB*, Supershifted band; *HMC*, high-mobility complex; *LMC*, low-mobility complex; *NS*, nonspecific protein/DNA complex.

isolated 4 and 6 hr after the media change. Neither the HMC nor the LMC was detected by using a mutant MEF2 oligonucleotide.

EMSAs that used antibodies against MEF2A, B, C, and D proteins were performed to determine which MEF2 proteins were bound to DNA under control and apoptotic conditions (Fig. 4). In control neurons, antibodies against MEF2A and MEF2D shifted the HMC to a slower migrating band (SSB), whereas antibodies against MEF2B and MEF2C had little effect on the MEF2–DNA complex. Similar results were obtained in apoptotic neurons, although the amount of high-mobility complex was significantly lower than that present in healthy neurons. Interestingly, the LMC was not shifted by any of the MEF2 antibodies. Because each of the antibodies was raised against the C terminus, but not the N terminus DNA binding domain of MEF2 proteins (Fig. 5*A*), we questioned whether MEF2A and MEF2D were degraded during apoptosis to yield MEF2 fragments that bound DNA but did not interact with the antibodies.

Degradation of MEF2A and MEF2D during apoptosis of cerebellar granule neurons

To test the hypothesis that MEF2 proteins were degraded during apoptosis, we performed Western analysis and exposed the transferred proteins to film for longer periods of time than in previous experiments. The results showed that, within 1 hr of inducing apoptosis, MEF2D was phosphorylated, as shown previously, and a smaller-molecular-weight MEF2D fragment appeared (Fig. 5*B*). The fragment, usually a broad band, had an apparent molecular weight of 40–45 kDa, ~15 kDa less than full-length MEF2D.

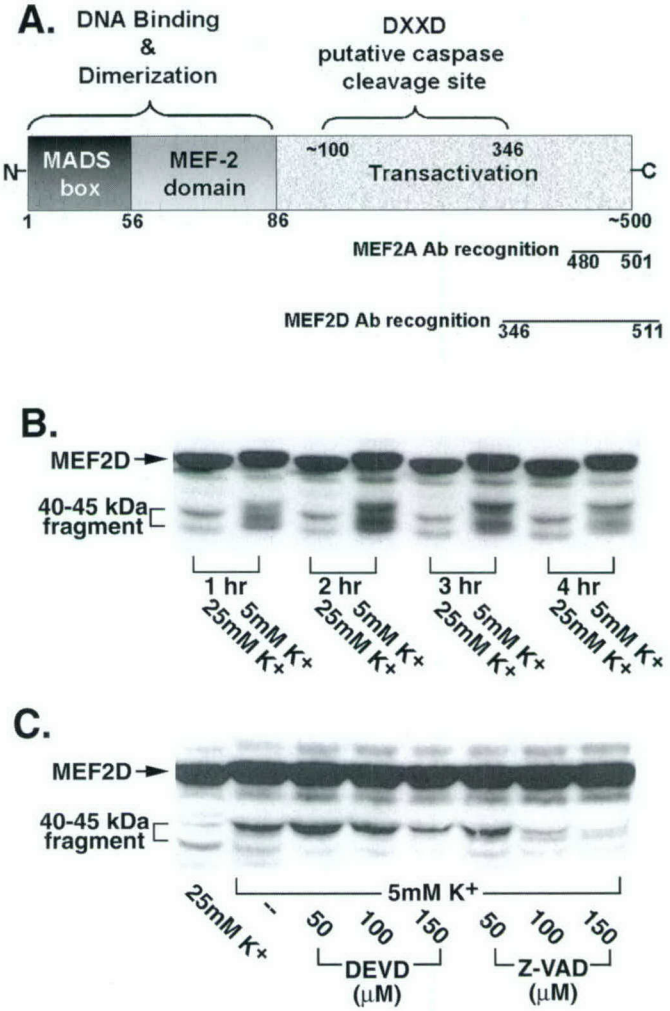

Figure 5. MEF2D is cleaved by a caspase-mediated pathway during apoptosis. *A*, Domain structure of the MEF2 proteins, including the MEF2A and MEF2D antibody recognition motifs and the putative caspase cleavage region. *B*, Cerebellar granule neurons (day 7) were placed in serum-free medium containing 25 or 5 mM KCl. At the indicated times, Western analysis was performed with 12% SDS-acrylamide gels and specific MEF2D antibodies. *C*, Neurons were placed in serum-free medium containing 25 or 5 mM KCl (4 hr) in the absence or presence of various concentrations of the caspase-3-specific inhibitor DEVD or the pan-caspase inhibitor Z-VAD. *Brackets* indicate a lower-molecular-weight cleavage product recognized by the C-terminal MEF2D antibody.

Analysis of various MEF2 sequences (rat MEF2D and mouse MEF2D1a and MEF2A) revealed several putative caspase cleavage sites (DXXD) between the DNA binding domain and the antibody recognition domain (amino acids 100–346) (Fig. 5*A*). To determine whether the MEF2 fragment that was generated during apoptosis resulted from caspase cleavage, we performed experiments to assess whether caspase inhibitors blocked formation of the MEF2D fragment. DEVD, a caspase-3-specific inhibitor, and Z-VAD, a nonselective caspase inhibitor, blocked the formation of the MEF2D fragment in a dose-dependent manner (Fig. 5*C*). Z-VAD was much more effective and potent than DEVD in preventing cleavage of MEF2D, suggesting that an upstream caspase rather than the downstream caspase-3 might be involved in cleaving MEF2D. Consistent with this idea was the finding that the cleavage of MEF2D occurred much earlier than the activation

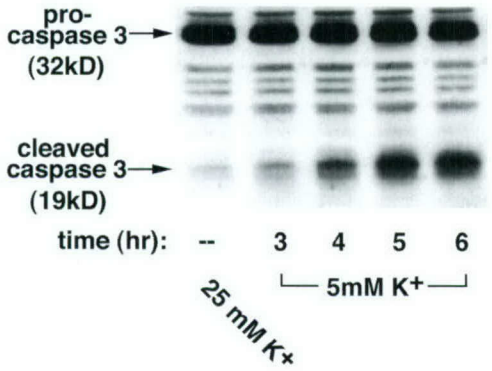

Figure 6. Caspase-3 activation in rat cerebellar granule neurons. Cerebellar granule neurons (day 7) were placed in serum-free medium containing 25 or 5 mM potassium. At the indicated times, Western analysis was performed with 15% SDS-acrylamide gels and an antibody that detects pro-caspase-3 and an active caspase-3 cleavage product.

of caspase-3, which was maximal at 5–6 hr after the induction of apoptosis (Fig. 6).

Caspase inhibitor blocks formation of the low-mobility protein–DNA complex

Blockade of MEF2D cleavage by caspase inhibitors supported the hypothesis that during apoptosis MEF2D is cleaved to generate a N-terminal DNA binding fragment, which is not recognized by antibodies directed against the regulatory domain, and a C-terminal fragment that is recognized by Western blotting. To test this hypothesis directly, we treated neurons with and without a caspase inhibitor before the EMSAs (Fig. 7). As shown previously in nuclear extracts from control neurons grown in 25 mM KCl, the LMC was very low (Fig. 7, *lane 1*). After 4 hr of apoptosis induced by lowering the extracellular potassium to 5 mM, the LMC was abundant (Fig. 7, *lane 2*). The caspase inhibitor Z-VAD, added at the time of the medium change, prevented the formation of the lower-molecular-weight complex (Fig. 7, *lane 3*). In addition, DVED and YVAD (a caspase-1-selective inhibitor) were only partially effective at inhibiting the formation of the low-molecular-weight complex (data not shown). Together, these data suggest that MEF2D and MEF2A are cleaved by a caspase-sensitive pathway to generate N-terminal fragments that bind to DNA but are not recognized by antibodies directed to the C terminus of each of these proteins.

The N-terminal MEF2 fragment can act as a dominant-negative transcription factor

Cleavage of MEF2 between the DNA binding domain and the antibody recognition domain would separate the DNA binding domain from the transactivation domain. To test the possibility that the N-terminal truncated fragment could act in a dominant-negative manner to block both the DNA binding and transcriptional activity of MEF2, we transfected neurons with MEF2D-VP16 in the absence or presence of increasing amounts of truncated MEF2A131. The expression plasmid MEF2D-VP16 encodes the DNA binding domain of mouse MEF2D (amino acids 1–92) fused to the transcriptional activation domain of VP16 (amino acids 412–490) under control of a CMV promoter. Its use as a constitutively active transcription factor has been reported previously (Han and Prywes, 1995). MEF2A131 encodes mouse MEF2A that is truncated at position 131, leaving the DNA binding domain intact, and is highly homologous to the corresponding region of MEF2D. After cotransfection of these

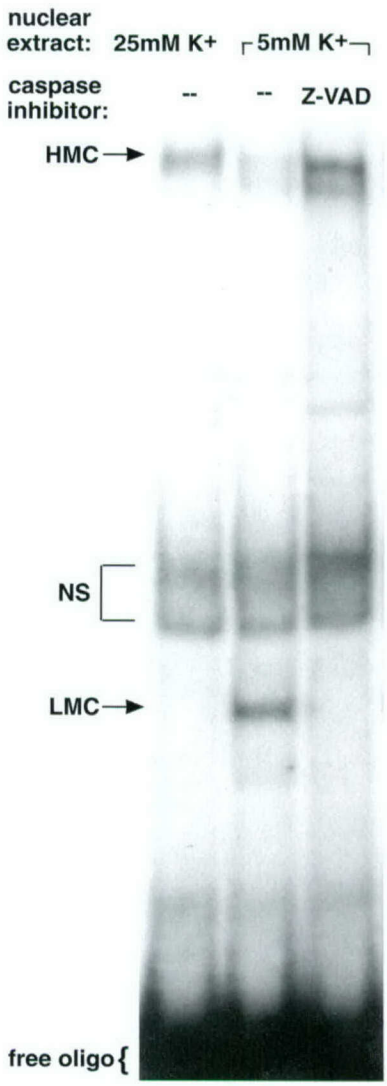

Figure 7. Formation of the lower-molecular-weight protein/DNA binding complex is prevented by caspase inhibition. Cerebellar granule neurons (day 7) were placed in serum-free medium containing 25 or 5 mM KCl in the absence or presence of 100 μM pan-caspase inhibitor (*Z-VAD*). After 4 hr, nuclear extracts were prepared, and gel mobility shift assays were performed with a double-stranded ^{32}P-labeled consensus MEF2 oligomer. *HMC*, High-mobility complex; *LMC*, low-mobility complex; *NS*, nonspecific protein/DNA complex.

two expression plasmids, transcriptional activity was determined with the MEF2 luciferase reporter plasmid (Fig. 8*A*). As observed previously, neurons incubated in 5 mM potassium had low MEF2 transcriptional activity. However, the expression of a constitutively active mutant of MEF2D (MEF2D-VP16) maintained high MEF2 transcriptional activity even in the presence of 5 mM potassium. When the VP16 mutant of MEF2D (1 μg) was expressed in the presence of increasing concentrations of truncated MEF2A131 (1–3 μg of DNA), the N-terminal MEF2 fragment blocked MEF2 luciferase activity in a dose-dependent manner (Fig. 8*A*). These data indicate that a truncated MEF2 can block the DNA binding and activity of MEF2 competitively. The consequence of the expression of truncated MEF2 on neuronal apoptosis is seen in Figure 8*B*. In these experiments, neurons were transfected with the control vector, MEF2D-VP16, or MEF2D-VP16 in the presence of increasing amounts of trun-

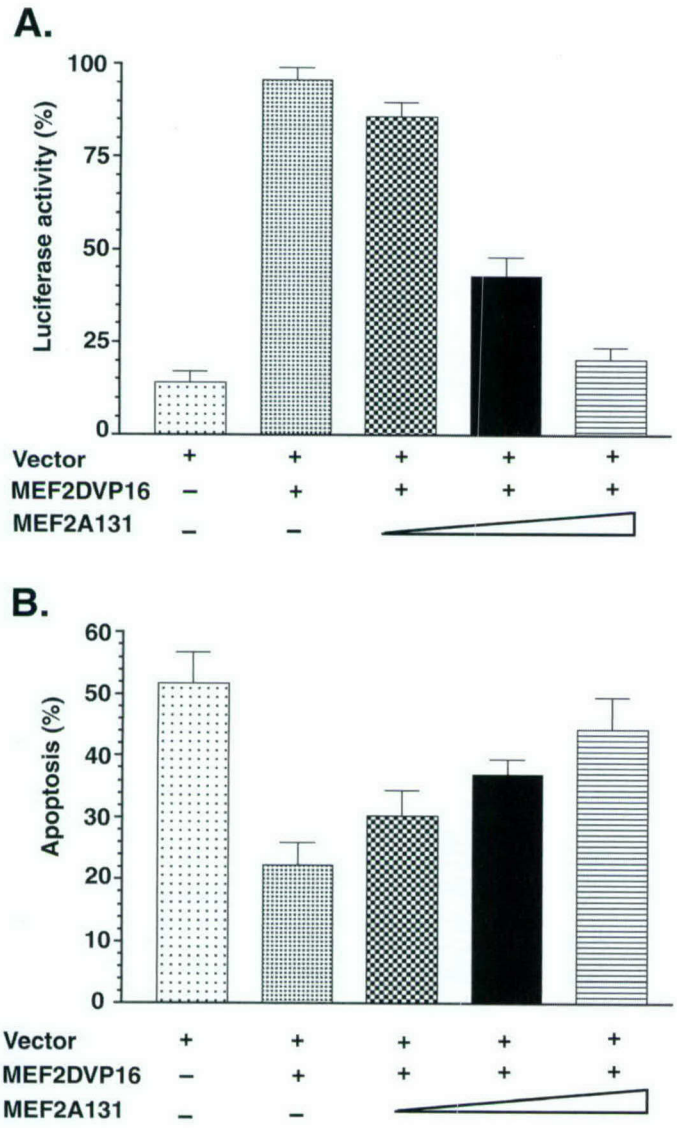

Figure 8. The N terminus of MEF2 antagonizes MEF2 activity and MEF2-mediated neuronal survival. *A*, Cerebellar granule neurons (day 6) were transfected with a MEF2-responsive luciferase reporter and pCMV-β-gal in the absence or presence of 1 μg of MEF2D-VP16 and MEF2A131 (1–3 μg). After transfection (2 hr) the neurons were placed in serum-free medium containing 5 mM KCl. After 4 hr, luciferase and β-galactosidase activities were determined. Luciferase activity was normalized with respect to that of β-galactosidase. Data are expressed as percentage of control neurons grown in 25 mM potassium. Data are the mean ± SEM ($n = 3$). *B*, Cerebellar granule neurons (day 5) were cotransfected with pCMV-β-gal and the indicated expression vector at the concentrations given in *A*. After transfection the neurons were placed in serum-free medium containing 5 mM KCl for 16 hr and then fixed and immunostained with a β-gal antibody. The neurons also were stained with Hoechst 33258. Apoptosis was quantified by scoring the percentage of transfected neurons with condensed or fragmented nuclei. Data are the mean ± SEM ($n = 3$). *Vector*, Empty pcDNA vector.

cated MEF2A131. In neurons maintained in 5 mM potassium for 16 hr the level of apoptosis was 56%. Transfection of the neurons with MEF2D-VP16 reduced the amount of apoptosis to ~22%. When the truncated MEF2A131 mutant (1–3 μg of DNA) was introduced with MEF2D-VP16 into neurons, the ability of MEF2D-VP16 to block apoptosis was attenuated in a dose-dependent manner. These data indicate that the MEF2 N-terminal fragment can act as a dominant-negative transcription factor and antagonize the prosurvival function of MEF2D.

DISCUSSION

Examination of the temporal and spatial localization of MEF2 proteins in brain has revealed that MEF2 expression coincides with the initiation of postmitotic neuronal maturation (Leifer et al., 1993, 1994; McDermott et al., 1993; Ikeshima et al., 1995; Lyons et al., 1995; Mao et al., 1999). For example, in the developing cerebral cortex, MEF2C immunoreactivity is present in the cortical plate and is not found in the intermediate zone or ventricular zone (Mao et al., 1999). At 14 weeks of gestation, MEF2C immunoreactivity is present in cell nuclei throughout the cortical plate. Subsequently, MEF2C immunoreactivity develops a bilaminate and then a trilaminate distribution and ultimately is expressed preferentially in layers II, IV, and VI of mature neocortex (Leifer et al., 1994). These findings suggest a role for MEF2C in postmitotic neuronal differentiation, in particular in the development of certain cortical layers.

In the cerebellum, MEF2A and MEF2D mRNA levels dramatically increase at ~P9, reach a peak at P15–P18, and stay high in adults (Leifer et al., 1994; Ikeshima et al., 1995; Lin et al., 1996; Mao and Wiedmann, 1999). This time course of MEF2 expression coincides with the expression of the $GABA_A$ receptor α6 subunit mRNA, a marker for the differentiation of mature cerebellar granule neurons. Immunohistochemical staining reveals that MEF2 protein expression occurs primarily in the internal granule cell layer of the cerebellum (Ikeshima et al., 1995). During postnatal development, differentiated granule neurons generated in the external germinal layer migrate to the internal granule layer where they are innervated by mossy fiber axons. There is considerable loss of granule neurons during this process and it is thought that the survival of granule neurons is regulated by depolarization-induced mechanisms during this time period.

Postmitotic granule neurons derived from neonatal rat can be maintained readily *in vitro* in their fully differentiated state if they are depolarized with a high extracellular concentration of potassium (D'Mello et al., 1993; Miller et al., 1997). If the extracellular potassium concentration is reduced, granule neurons undergo programmed cell death with classic morphological and biochemical features of apoptosis. These characteristics, along with the abundance and high degree of homogeneity, make cultured granule neurons an excellent model to examine the role of MEF2 proteins in depolarization-dependent neuronal survival.

In this report we have defined a novel mechanism by which the activity and levels of MEF2 proteins are regulated during apoptosis of cerebellar granule neurons. We also have shown that MEF2 proteins are regulated in an isotype-specific manner. All four MEF2 isoforms (A, B, C, and D) were detected by immunoblot analysis in rat cerebellar granule neurons. However, in agreement with results from immunocytochemistry and *in situ* hybridization (Ikeshima et al., 1995; Lyons et al., 1995), MEF2A and MEF2D were the most prominent MEF2 proteins detected in the cultured cerebellar granule neurons when equal amounts of total protein were analyzed by Westerns (data not shown). MEF2A and MEF2D appear to be responsible for most, if not all, of the MEF2 DNA binding activity in viable cerebellar granule neurons. When granule neurons are induced to undergo apoptosis by lowering potassium, endogenous MEF2A and MEF2D, but not MEF2B and MEF2C, are phosphorylated. Phosphorylation is accompanied by a decrease in MEF2 transcriptional activity, and both effects are reversed by the readdition of depolarizing potas-

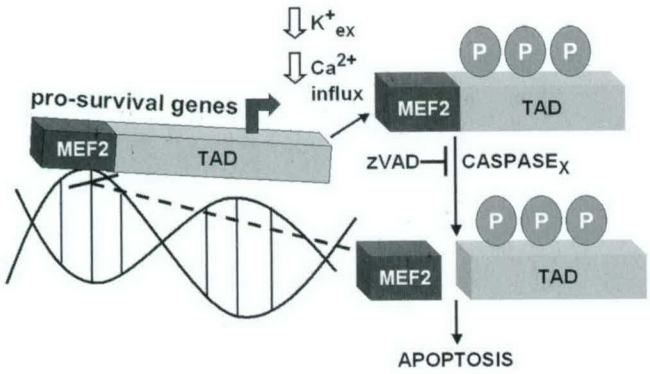

Figure 9. The regulation of MEF2 proteins during apoptosis of rat cerebellar granule neurons. When granule neurons are induced to undergo apoptosis by lowering extracellular potassium to 5 mM, endogenous MEF2D and MEF2A (data not shown) are phosphorylated. Phosphorylation of MEF2D induced by decreasing calcium influx not only leads to decreased DNA binding but also is associated with a caspase-dependent cleavage of MEF2D. The caspase involved in cleaving MEF2D remains to be identified. The cleavage of MEF2D results in an N-terminal fragment (~100 amino acids long) that retains its DNA binding capacity, is not recognized by C-terminal antibodies, and lacks the transactivation domain. The MEF2 N-terminal fragment is capable of blocking the activity of MEF2D, thus acting as a dominant-negative transcription factor. The decline in MEF2 activity because of decreased DNA binding and formation of a dominant-inactive MEF2 fragment leads to apoptosis.

sium. The most novel findings of the present study show that the phosphorylation of MEF2D that is induced by decreasing calcium influx not only correlates with decreased DNA binding but also is associated with a direct or indirect caspase-dependent cleavage of MEF2D (Fig. 9). The cleavage of MEF2D results in a N-terminal fragment (~100 amino acids long) that retains its DNA binding capacity, is not recognized by C-terminal antibodies, and lacks the transactivation domain. The MEF2 N-terminal fragment is capable of blocking the activity of MEF2D, thus acting as a dominant-negative transcription factor. The decline in MEF2 activity resulting from decreased DNA binding and formation of a dominant-inactive MEF2 fragment appears to be sufficient to mediate execution of the apoptotic process. Overexpression of a constitutively active MEF2D that does not get cleaved prevents the loss in MEF2 transcriptional activity during apoptosis and protects against apoptosis that is induced by lowering membrane depolarization and calcium influx.

The signaling pathways responsible for the changes in the phosphorylation state of MEF2 could involve an increase in the activity of a calcium-sensitive kinase, a decrease in the activity of a calcium-sensitive phosphatase, or both. Mao and Wiedman (1999) recently reported similar data that MEF2A is hyperphosphorylated when calcium influx is decreased or when the protein phosphatase calcineurin is inhibited in cerebellar granule neurons. Although other isoforms were not examined in the previous study, the data suggest that enhanced phosphorylation of MEF2A and MEF2D seen on lowering extracellular potassium is likely to be attributable to decreased activity of the calcium-dependent phosphatase calcineurin. Furthermore, because MEF2B and MEF2C did not undergo hyperphosphorylation in response to lowering extracellular potassium, the data indicate that MEF2A and MEF2D are regulated post-translationally in an isotype-specific manner in cerebellar granule neurons.

The putative phosphorylation sites described in this study are functionally distinct from the previously described phosphorylation sites that enhance MEF2 transcriptional activity. Some MEF2 isoforms directly interact with p38 MAP kinase and ERK5/BMK1 and are phosphorylated by both protein kinases (Kato et al., 1997; Yang et al., 1998; Ornatsky et al., 1999; Zhao et al., 1999). Phosphorylation of MEF2 proteins by p38 MAP kinase and ERK5 stimulates transcriptional activity. The increased transcriptional activity could involve changes in protein conformation that enhance interaction with the transcriptional machinery. Alternatively, phosphorylation might be required for the recruitment of an essential transcriptional cofactor or release of a repressor. In support of the latter mechanism, histone deacetylases (HDACs) have been shown to repress the transcriptional activity of MEF2s (Miska et al., 1999; Lemercier et al., 2000; Lu et al., 2000a,b; Youn et al., 2000). Phosphorylation of HDACs by the calcium-sensitive protein kinase CaMK results in the dissociation of HDACs and the unmasking of transcriptional activity.

Other studies in T-cells have mapped a calcineurin-dependent induction of the nur77 promoter to a putative MEF2 DNA binding site (Youn et al., 1999). Although the transcriptional activity of MEF2 in activated T-cells requires calcium signals, its DNA binding activity seems to be constitutive and insensitive to changes in calcium. Again, the data are in contrast to the results of this study in which decreases in intracellular calcium signaling resulted in decreased DNA binding and transcriptional activity. The antibodies used in T-cells examining nur77 promoter activity did not distinguish between MEF2 isoforms. This raises the possibility that the discrepancy may be attributable to differential regulation of the various MEF2 isoforms and/or the presence of cell type-specific accessory proteins.

In summary, the complexities in MEF2-regulated gene expression have been advanced primarily from studies in muscle and T-cells. In the present study we have delineated a novel phosphorylation signaling pathway associated with DNA binding, transcriptional activity, and degradation of neuronal MEF2 proteins. The data in this study also support the hypothesis that MEF2A and MEF2D regulate neuronal survival in the cerebellum, particularly in response to depolarization-induced signals that are important during development.

REFERENCES

Amacher SL, Buskin JN, Hauschka SD (1993) Multiple regulatory elements contribute differentially to muscle creatine kinase enhancer activity in skeletal and cardiac muscle. Mol Cell Biol 13:2753–2764.

D'Mello SR, Galli C, Ciotti T, Calissano P (1993) Induction of apoptosis in cerebellar granule neurons by low potassium: inhibition of death by insulin-like growth factor I and cAMP. Proc Natl Acad Sci USA 23:10989–10993.

Firulli AB, Miano JM, Bi W, Johnson AD, Casscells W, Olson EN, Schwarz JJ (1996) Myocyte enhancer binding factor-2 expression and activity in vascular smooth muscle cells. Association with the activated phenotype. Circ Res 78:196–204.

Han TH, Prywes R (1995) Regulatory role of MEF2D in serum induction of the c-*jun* promoter. Mol Cell Biol 15:2907–2915.

Ikeshima H, Imai S, Shimoda K, Hata J, Takano T (1995) Expression of a MADS-box gene, MEF2D, in neurons of the mouse central nervous system: implication of its binary function in myogenic and neurogenic cell lineages. Neurosci Lett 200:117–120.

Kato Y, Kravchenko VV, Tapping RI, Han J, Ulevitch RJ, Lee JD (1997) BMK1/ERK5 regulates serum-induced early gene expression through transcription factor MEF2C. EMBO J 16:7054–7066.

Leifer D, Krainc D, Yu YT, McDermott J, Breitbart RE, Heng J, Neve RL, Kosofsky B, Nadal-Ginard B, Lipton SA (1993) MEF2C, a MADS/MEF2-family transcription factor expressed in a laminar distribution in cerebral cortex. Proc Natl Acad Sci USA 90:1546–1550.

Leifer D, Golden J, Kowall NW (1994) Myocyte-specific enhancer binding factor 2C expression in human brain development. Neuroscience 63:1067–1079.

Lemercier C, Verdel A, Galloo B, Curtet S, Brocard MP, Khochbin S

(2000) mHDA1/HDAC5 histone deacetylase interacts with and represses MEF2A transcriptional activity. J Biol Chem 275:15594–15599.

Li M, Wang X, Meintzer MK, Laessig T, Birnbaum MJ, Heidenreich KA (2000) Cyclic AMP promotes neuronal survival by phosphorylation of glycogen synthase kinase 3β. Mol Cell Biol 20:9356–9363.

Lin X, Shah S, Bulleit RF (1996) The expression of MEF2 genes is implicated in CNS neuronal differentiation. Brain Res Mol Brain Res 42:307–316.

Lu J, McKinsey TA, Nicol RL, Olson EN (2000a) Signal-dependent activation of the MEF2 transcription factor by dissociation from histone deacetylases. Proc Natl Acad Sci USA 97:4070–4075.

Lu J, McKinsey TA, Zhang CL, Olson EN (2000b) Regulation of skeletal myogenesis by association of the MEF2 transcription factor with class II histone deacetylases. Mol Cell 6:233–244.

Lyons GE, Micales BK, Schwarz J, Martin JF, Olson EN (1995) Expression of *mef2* genes in the mouse central nervous system suggests a role in neuronal maturation. J Neurosci 15:5727–5738.

Mao Z, Wiedmann M (1999) Calcineurin enhances MEF2 DNA binding activity in calcium-dependent survival of cerebellar granule neurons. J Biol Chem 274:31102–31107.

Mao Z, Bonni A, Xia F, Nadal-Vicens M, Greenberg ME (1999) Neuronal activity-dependent cell survival mediated by transcription factor MEF2. Science 286:785–790.

Martin JF, Miano JM, Hustad CM, Copeland NG, Jenkins NA, Olson EN (1994) A MEF2 gene that generates a muscle-specific isoform via alternative mRNA splicing. Mol Cell Biol 14:1647–1656.

McDermott JC, Cardoso MC, Yu YT, Andres V, Leifer D, Krainc D, Lipton SA, Nadal-Ginard B (1993) hMEF2C gene encodes skeletal muscle- and brain-specific transcription factors. Mol Cell Biol 13:2564–2577.

Miller TM, Tansey MG, Johnson Jr EM, Creedon DJ (1997) Inhibition of phosphatidylinositol 3-kinase activity blocks depolarization and insulin-like growth factor I-mediated survival of cerebellar granule cells. J Biol Chem 272:9847–9853.

Miska EA, Karlsson C, Langley E, Nielsen SJ, Pines J, Kouzarides T (1999) HDAC4 deacetylase associates with and represses the MEF2 transcription factor. EMBO J 18:5099–5107.

Molkentin JD, Olson EN (1996) Combinatorial control of muscle development by basic helix–loop–helix and MADS-box transcription factors. Proc Natl Acad Sci USA 93:9366–9373.

Molkentin JD, Firulli AB, Black BL, Martin JF, Hustad CM, Copeland N, Jenkins N, Lyons G, Olson EN (1996) MEF2B is a potent transactivator expressed in early myogenic lineages. Mol Cell Biol 16:3814–3824.

Naya FS, Olson E (1999) MEF2: a transcriptional target for signaling pathways controlling skeletal muscle growth and differentiation. Curr Opin Cell Biol 11:683–688.

Okamoto S, Krainc D, Sherman K, Lipton SA (2000) Antiapoptotic role of the p38 mitogen-activated protein kinase–myocyte enhancer factor 2 transcription factor pathway during neuronal differentiation. Proc Natl Acad Sci USA 97:7561–7566.

Ornatsky OI, Andreucci JJ, McDermott JC (1997) A dominant-negative form of transcription factor MEF2 inhibits myogenesis. J Biol Chem 272:33271–33278.

Ornatsky OI, Cox DM, Tangirala P, Andreucci JJ, Quinn ZA, Wrana JL, Prywes R, Yu YT, McDermott JC (1999) Post-translational control of the MEF2A transcriptional regulatory protein. Nucleic Acids Res 27:2646–2654.

Shore P, Sharrocks AD (1995) The MADS-box family of transcription factors. Eur J Biochem 229:1–13.

Skerjanc IS, Wilton S (2000) Myocyte enhancer factor 2C upregulates MASH-1 expression and induces neurogenesis in P19 cells. FEBS Lett 472:53–56.

Yang CC, Ornatsky OI, McDermott JC, Cruz TF, Prody CA (1998) Interaction of myocyte enhancer factor 2 (MEF2) with a mitogen-activated protein kinase, ERK5/BMK1. Nucleic Acids Res 26:4771–4777.

Youn HD, Sun L, Prywes R, Liu JO (1999) Apoptosis of T-cells mediated by Ca^{2+}-induced release of the transcription factor MEF2. Science 286:790–793.

Youn HD, Grozinger CM, Liu JO (2000) Calcium regulates transcriptional repression of myocyte enhancer factor 2 by histone deacetylase 4. J Biol Chem 275:22563–22567.

Yu YT, Breitbart RE, Smoot LB, Lee Y, Mahdavi V, Nadal-Ginard B (1992) Human myocyte-specific enhancer factor 2 comprises a group of tissue-restricted MADS-box transcription factors. Genes Dev 6:1783–1798.

Zhao M, New L, Kravchenko VV, Kato Y, Gram H, di Padova F, Olson EN, Ulevitch RJ, Han J (1999) Regulation of the MEF2 family of transcription factors by p38. Mol Cell Biol 19:21–30.

Journal of Neurochemistry, 2003, **85**, 1488–1499 doi:10.1046/j.1471-4159.2003.01790.x

A myocyte enhancer factor 2D (MEF2D) kinase activated during neuronal apoptosis is a novel target inhibited by lithium

Daniel A. Linseman, Brandon J. Cornejo, Shoshona S. Le, Mary Kay Meintzer, Tracey A. Laessig, Ron J. Bouchard and Kim A. Heidenreich

Department of Pharmacology, University of Colorado Health Sciences Center and the Denver Veterans Affairs Medical Center, Denver, Colorado, USA

Abstract

Depolarization promotes the survival of cerebellar granule neurons via activation of the transcription factor myocyte enhancer factor 2D (MEF2D). Removal of depolarization induces hyperphosphorylation of MEF2D on serine/threonine residues, resulting in its decreased DNA binding and susceptibility to caspases. The subsequent loss of MEF2-dependent gene transcription contributes to the apoptosis of granule neurons. The kinase(s) that phosphorylates MEF2D during apoptosis is currently unknown. The serine/threonine kinase, glycogen synthase kinase-3β (GSK-3β), plays a pro-apoptotic role in granule neurons. To investigate a potential role for GSK-3β in MEF2D phosphorylation, we examined the effects of lithium, a non-competitive inhibitor of GSK-3β, on MEF2D activity in cultured cerebellar granule neurons. Lithium inhibited caspase-3 activation and chromatin condensation in granule neurons induced to undergo apoptosis by removal of depolarizing potassium and serum. Concurrently, lithium suppressed the hyperphosphorylation and caspase-mediated degradation of MEF2D. Moreover, lithium sustained MEF2 DNA binding and transcriptional activity in the absence of depolarization. Lithium also attenuated MEF2D hyperphosphorylation and apoptosis induced by calcineurin inhibition under depolarizing conditions, a GSK-3β-independent model of neuronal death. In contrast to lithium, MEF2D hyperphosphorylation was not inhibited by forskolin, insulin-like growth factor-I, or valproate, three mechanistically distinct inhibitors of GSK-3β. These results demonstrate that the kinase that phosphorylates and inhibits the pro-survival function of MEF2D in cerebellar granule neurons is a novel lithium target distinct from GSK-3β.

Keywords: apoptosis, cerebellar granule neuron, glycogen synthase kinase, lithium, MEF2 transcription factor, phosphorylation.

J. Neurochem. (2003) **85,** 1488–1499.

Apoptosis is a programmed form of cell death executed via the cleavage of critical cellular proteins by the caspase family of cysteine proteases (Shi 2002). Neuronal apoptosis is a highly regulated process that plays a key role in the normal development of the CNS (Nijhawan *et al.* 2000; Roth and D'Sa 2001). Aberrant neuronal apoptosis often occurs during adulthood and is thought to contribute to the development and progression of debilitating neurodegenerative diseases including Alzheimer's, Parkinson's, Huntington's, and Creutzfeldt–Jakob disease (Honig and Rosenberg 2000; Andersen 2001; Kawashima *et al.* 2001). In addition, significant apoptosis of transplanted neural tissue is one of the major impediments to neurotranplantation as a potential treatment for neurodegenerative disease (Schierle *et al.* 1999). Elucidation of the cellular signaling pathways that regulate neuronal survival and apoptosis is necessary to develop useful therapeutics to combat neurodegenerative disorders

Received January 22, 2003; revised manuscript received March 4, 2003; accepted March 5, 2003.

Address correspondence and reprint requests to Dr Kim A. Heidenreich, University of Colorado Health Sciences Center, Department of Pharmacology (C236), 4200 E. Ninth Ave., Denver, CO 80262, USA. E-mail: Kim.Heidenreich@UCHSC.edu

Abbreviations used: BSA, bovine serum albumin; CGN, cerebellar granule neuron; CK-2, casein kinase-2; CREB, cAMP response element binding protein; CyA, cyclosporin A; DAPI, 4,6-diamidino-2-phenylindole; EMSA, electrophoretic mobility shift assay; GSK-3β, glycogen synthase kinase-3β; HMC, high molecular weight protein–DNA complex; IGF-I, insulin-like growth factor-I; LMC, low molecular weight protein–DNA complex; MADS, MCM1-agamous-deficiens-serum response factor; MAPKAPK-2, mitogen-activated protein kinase-activated protein kinase-2; MEF2, myocyte enhancer factor 2; PBS, phosphate-buffered saline; PI3K, phosphatidylinositol 3-kinase; PKA, protein kinase A; PRAK, p38-regulated/activated protein kinase; SDS–PAGE, sodium dodecyl sulfate–polyacrylamide gel electrophoresis; VPA, sodium valproate.

and to enhance the survival of donor neurons following transplantation.

Primary cultures of cerebellar granule neurons (CGNs) isolated from early postnatal rats are a well-characterized *in vitro* model for investigating neuronal apoptosis. CGNs require both serum-derived growth factors and depolarization-mediated calcium influx for their survival and die by apoptosis when deprived of this trophic support (D'Mello *et al.* 1993; Atabay *et al.* 1996). Recently, a transcription-dependent mechanism was identified for the pro-survival effects of depolarization in CGNs. Depolarization activates a calcium-sensitive pathway that enhances the DNA binding and activity of the myocyte enhancer factor 2 (MEF2) transcription factors (Mao *et al.* 1999).

The mammalian MEF2 family is made up of four distinct isoforms (MEF2A, B, C and D) (McKinsey *et al.* 2002). The MEF2 proteins are members of the MADS (MCM1-agamous-deficiens-serum response factor) family of transcription factors (Shore and Sharrocks 1995). MEF2 genes were originally identified in cells of skeletal, cardiac, and smooth muscle lineages and play a key role in the myogenic differentiation of these tissues (Black and Olson 1998). In the CNS, the expression of MEF2 proteins is associated temporally and spatially with the initiation of post-mitotic neuronal maturation (Lyons *et al.* 1995). For example, the maturation of cerebral cortical neurons *in vivo* is associated with an enhanced expression of MEF2C (Leifer *et al.* 1993). Similarly, development and differentiation of the internal granule cell layer of the cerebellum involves the co-ordinated up-regulation of MEF2A and MEF2D (Lin *et al.* 1996). *In vitro* studies further support an essential role for MEF2 proteins in promoting neuronal survival. Transfection of primary cerebral cortical neurons with a dominant-interfering mutant of MEF2C induces apoptosis of these cells, whereas expression of a constitutively active MEF2 mutant significantly attenuates apoptosis of CGNs following removal of depolarizing potassium (Mao *et al.* 1999). Thus, MEF2 proteins are critical for the survival and differentiation of post-mitotic neurons *in vitro* and *in vivo*.

Recently, we identified two specific MEF2 isoforms, MEF2D and MEF2A, as substrates for caspase-dependent cleavage during the apoptosis of CGNs (Li *et al.* 2001). Following the removal of depolarizing potassium, MEF2D and MEF2A are rapidly hyperphosphorylated on serine/threonine residues. This hyperphosphorylation is followed by decreased DNA binding and cleavage by caspases to fragments that dissociate the NH_2-terminal DNA binding domain from the C-terminal transactivation domain. The NH_2-terminal MEF2 fragments in turn act as dominant-interfering transcription factors by inhibiting the DNA binding of full-length MEF2 proteins. The loss of MEF2 DNA binding, and the formation of truncated MEF2 fragments that have the potential to act as dominant-negative transcription factors, results in a marked decrease in MEF2-dependent transcription of putative pro-survival genes that contributes to neuronal apoptosis (Li *et al.* 2001; Okamoto *et al.* 2002).

In the above cascade of events, the initiating signal is the hyperphosphorylation of MEF2D and MEF2A on serine/threonine residues induced by removal of the depolarization stimulus. The phosphorylation that occurs on these proteins during apoptosis is functionally distinct from phosphorylation events that have previously been reported to enhance MEF2 transcriptional activity (e.g. via ERK5 or p38 MAP kinase) (Han *et al.* 1997; Kato *et al.* 1997). In fact, the hyperphosphorylation observed on MEF2D and MEF2A under non-depolarizing (apoptotic) conditions in CGNs results in a loss of MEF2 transcriptional activity (Li *et al.* 2001). Identification of the kinase(s) that phosphorylates MEF2 proteins during neuronal apoptosis is critical to understanding the regulation of these transcription factors.

Recently, we showed that the serine/threonine kinase, glycogen synthase kinase-3β (GSK-3β), is involved in the apoptotic death of CGNs (Li *et al.* 2000). In the current study, we found that lithium, a known inhibitor of GSK-3β (Klein and Melton 1996; Stambolic *et al.* 1996) that has previously been documented to protect CGNs from apoptosis (D'Mello *et al.* 1994; Grignon *et al.* 1996; Li *et al.* 2000; Mora *et al.* 2001), significantly attenuated the hyperphosphorylation of MEF2D and MEF2A. Lithium prevented the caspase-mediated degradation of MEF2D and sustained MEF2 DNA binding and transcriptional activity under non-depolarizing conditions. Surprisingly, the inhibitory effect of lithium on the hyperphosphorylation of MEF2D could be dissociated from inhibition of GSK-3β activity. These data suggest that lithium inhibits a distinct kinase that phosphorylates MEF2 proteins and blocks their pro-survival function during neuronal apoptosis.

Experimental procedures

Materials

Monoclonal antibody to MEF2D raised against a peptide corresponding to amino acids 346–511 of mouse MEF2D was purchased from Transduction Laboratories (Lexington, KY, USA). The MEF2A antibody is a rabbit polyclonal raised against a peptide corresponding to amino acids 487–507 of human MEF2A purchased from Santa Cruz Biotechnology (Santa Cruz, CA, USA). According to the manufacturer, this antibody may cross-react with MEF2D. Polyclonal antibody to Tau phosphorylated on Ser404 was also purchased from Santa Cruz Biotechnology. Polyclonal antibodies to total GSK-3β and GSK-3β phosphorylated on Ser9 and rabbit polyclonal antibody to active caspase-3 (for western blotting) were from Cell Signaling Technologies (Beverly, MA, USA). Rabbit polyclonal antibody to active caspase-3 (for immunocytochemistry) was from Promega Corporation (Madison, WI, USA). DAPI (4,6-diamidino-2-phenylindole), Hoechst dye 33258, lithium chloride, and valproic acid (2-propylpentanoic acid, sodium salt) were purchased from Sigma (St Louis, MO, USA). Wortmannin, H89,

cyclosporin A, and forskolin were obtained from Calbiochem (San Diego, CA, USA). Insulin-like growth factor-I (recombinant, human) was provided by Margarita Quiroga (Chiron Corporation, Emeryville, CA, USA). The pGL2-MEF2-luc reporter plasmid was provided by Dr Saadi Khochbin (INSERM, France). Both the β-galactosidase enzyme assay system and the luciferase assay system were purchased from Promega. FITC-conjugated anti-rabbit and Cy3-conjugated anti-mouse secondary antibodies were from Jackson Immunoresearch Laboratories (Westgrove, PA, USA). Horseradish peroxidase-conjugated secondary antibodies and reagents for enhanced chemiluminescence were from Amersham Pharmacia Biotech (Arlington Heights, IL, USA).

Neuronal cell culture

Rat CGNs were prepared from 7- to 8-day-old Sprague Dawley rat pups (15–19 g) as described previously (Li *et al.* 2000). Neurons were plated at a density of 2.0×10^6 cells/mL in Basal Modified Eagle's (BME) medium containing 10% fetal bovine serum, 25 mM KCl, 2 mM L-glutamine, and penicillin (100 U/mL)/streptomycin (100 μg/mL). Cytosine arabinoside (10 μM) was added to the culture medium 24 h after plating to limit the growth of non-neuronal cells. Using this protocol, greater than 95% of the cultured cells were CGNs. In general, transient transfections were performed on day 5 or 6 in culture and experiments were conducted after 7 days in culture. Apoptosis was induced by removing the serum and reducing the extracellular potassium from 25 mM to 5 mM. Control cultures were maintained in medium supplemented with serum and 25 mM KCl. Alternatively, apoptosis was induced by addition of the calcineurin protein phosphatase inhibitor, cyclosporin A, in serum-free medium containing depolarizing (25 mM) potassium.

Quantification of apoptosis

Following induction of apoptosis, cells were fixed with 4% paraformaldehyde and nuclei were stained with Hoechst dye. Cells were considered apoptotic if their nuclei were condensed and/or fragmented. In general, approximately 500 cells from two fields of a 35-mm well were counted. Data are presented as a percentage of cells in a given treatment group that were scored as apoptotic. Quantification of apoptosis was performed in triplicate.

Immunocytochemistry

Cerebellar cultures were plated on polyethyleneimine-coated glass cover slips at a density of $\sim 1.0 \times 10^5$ cells per cover slip. Seven days after plating, cells were induced to undergo apoptosis in low potassium, serum-free conditions in either the absence or presence of LiCl (20 mM). After treatment, cells were fixed with 4% paraformaldehyde and then permeabilized and blocked in phosphate-buffered saline (PBS, pH 7.4) containing 0.2% Triton-X-100 and 5% BSA. Cells were then incubated overnight at 4°C with mouse-anti-MEF2D (1 : 1000) and rabbit-anti-caspase-3 (active fragment, 1 : 250) diluted in PBS containing 0.2% Triton-X-100 and 2% BSA. The primary antibodies were aspirated and cells were washed five times with PBS. Cells were then incubated with the appropriate Cy3-conjugated and FITC-conjugated secondary antibodies (1 : 500) and DAPI for 1 h at room temperature (22°C). The cells were then washed five more times with PBS and coverslips were adhered to glass slides in mounting medium (0.1% *p*-phenylenediamine in 75% glycerol in PBS). Fluorescence imaging was performed on a Zeiss Axioplan 2 microscope equipped with a Cooke Sensicam deep-cooled CCD camera and images were analyzed and subjected to digital deconvolution using the Slidebook software program (Intelligent Imaging Innovations Inc., Denver, CO, USA).

Western blot analysis

Following incubation for the indicated times and with the reagents specified in the text, the culture medium was aspirated, cells were washed once with 2 mL of ice-cold PBS, placed on ice and scraped into lysis buffer (200 μL/35-mm well) containing 20 mM HEPES (pH 7.4), 1% Triton X-100, 50 mM NaCl, 1 mM EGTA, 5 mM β-glycerophosphate, 30 mM sodium pyrophosphate, 100 μM sodium orthovanadate, 1 mM phenylmethylsulfonyl fluoride, 10 μg/mL leupeptin, and 10 μg/mL aprotinin. Cell debris was removed by centrifugation at 6000 *g* for 3 min and the protein concentration of the supernatant was determined using a commercially available protein assay kit (Pierce Chemical Co., Rockford, IL, USA). Aliquots (~150 μg) of supernatant protein were diluted to a final concentration of 1 × sodium dodecyl sulfate-polyacrylamide gel electrophoresis sample buffer, boiled for 5 min, and electrophoresed through 7.5 or 15% polyacrylamide gels. Proteins were transferred to polyvinylidene difluoride membranes (Millipore Corp., Bedford, MA, USA) and processed for western blot analysis. Non-specific binding sites were blocked in PBS (pH 7.4) containing 0.1% Tween 20 (PBS-T) and 1% BSA for 1 h at room temperature. Primary antibodies were diluted in blocking solution and incubated with the membranes for 1 h. Excess primary antibody was removed by washing the membranes three times in PBS-T. The blots were then incubated with the appropriate horseradish peroxidase-conjugated secondary antibody diluted in PBS-T for 1 h and were subsequently washed three times in PBS-T. Immunoreactive proteins were detected by enhanced chemiluminescence. Autoluminograms shown are representative of from two to four independent experiments.

Preparation of nuclear extracts and electrophoretic mobility shift assays (EMSAs)

CGNs were detached from the dish by scraping into buffer and nuclei were released by Dounce homogenization. Nuclear proteins were extracted, dialyzed, and the protein content quantified exactly as described previously (Li *et al.* 2001). Nuclear extracts (10 μg) were incubated with double-stranded ^{32}P-end labeled oligonucleotides corresponding to the muscle creatine kinase MEF2 site or to a mutant oligonucleotide, as previously described (Li *et al.* 2001). Following incubation, the protein–DNA complexes were analyzed on 5% non-denaturing polyacrylamide gels containing 3% glycerol and 0.25 × TBE (90 M Tris borate, 1 mM EDTA). After electrophoresis, the gels were dried and exposed to film at −70°C.

Transfection assays and reporter gene expression

CGNs were transiently transfected using a calcium phosphate coprecipitation method described previously (Li *et al.* 2000). Cells were transfected with 1 μg of MEF2-luciferase expression plasmid (pGL2-MEF2-luc) and 1 μg of pCMV-β-gal as an internal control for transfection efficiency. The total amount of DNA for each transfection was kept constant. Following transfection, neurons were kept in conditioned medium for 2 h. The medium was then changed

to either high potassium, serum-containing medium or low potassium, serum-free medium, each in the absence or presence of LiCl (20 mM). Alternatively, cells were switched to serum-free depolarizing medium in the absence or presence of cyclosporin A. After an additional 2–4-h incubation, cell extracts were prepared using reporter lysis buffer and the activities of luciferase and β-galactosidase were measured with the respective enzyme assay system kits (Promega).

Data analysis

Results shown represent the means ± SEM for the number (n) of independent experiments performed. Statistical differences between the means of unpaired sets of data were evaluated using either a Student's t-test or one-way ANOVA followed by a *post-hoc* Dunnett's-test. A p-value of < 0.05 was considered statistically significant.

Results

Lithium rescues CGNs from apoptosis and inhibits the activation of caspase-3

CGNs maintained in the presence of serum and a depolarizing concentration of potassium (25 mM) contained nuclei that were large and intact, as demonstrated by DAPI staining (Fig. 1a). The acute removal of serum in combination with

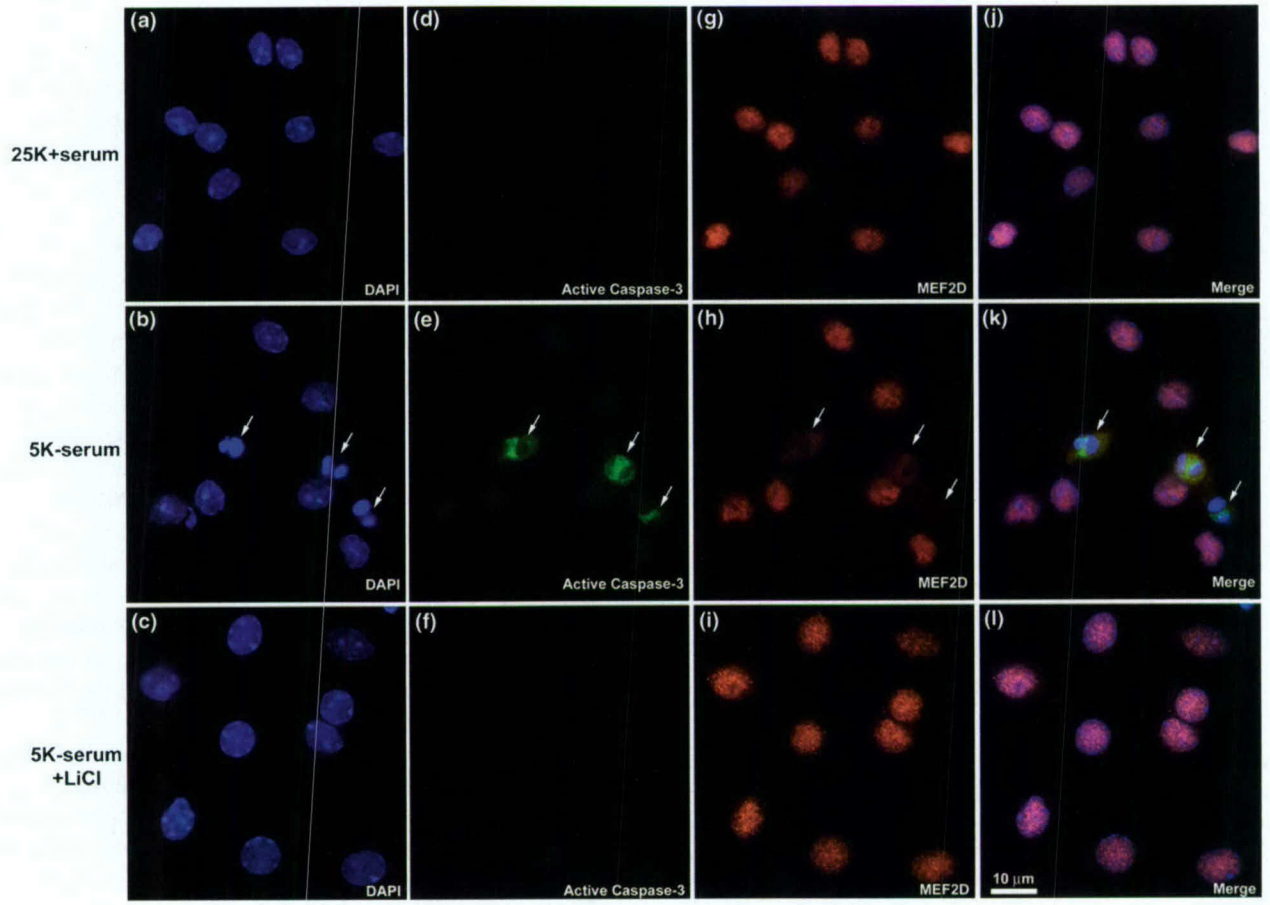

Fig. 1 Lithium inhibits CGN apoptosis and blocks caspase-3 activation and degradation of MEF2D. CGNs were incubated for 6 h in either control (25K + serum) or apoptotic (5K − serum) medium ± LiCl (20 mM). Following incubation, cells were fixed in 4% paraformaldehyde, permeabilized with 0.2% Triton-X-100 and blocked in 5% BSA. CGNs were incubated with primary antibodies to active caspase-3 (rabbit polyclonal) and MEF2D (mouse monoclonal). Following removal of excess primary antibodies, CGNs were then incubated with FITC-conjugated anti-rabbit and Cy3-conjugated anti-mouse secondary antibodies and DAPI. Fluorescent images were captured using a 63X oil objective. The images shown are representative of results obtained from two independent experiments. Scale bar = 10 μm. (a–c) DAPI staining of CGN nuclei with condensed and fragmented nuclei indicated by the arrows in (b). (d–f) Active caspase-3 was only detectable in CGNs incubated in apoptotic medium in the absence of LiCl. The most intense caspase-3 staining was observed in cells containing fragmented nuclei (see arrows in e). (g–i) MEF2D immunoreactivity was restricted to the nuclear compartment in CGNs maintained in either control medium or in apoptotic medium containing LiCl. In contrast, CGNs showing fragmented nuclei displayed MEF2D staining that was substantially decreased in intensity (compared with cells with intact nuclei) and was localized to the cytoplasm (see arrows in h). (j–l) Merged images showing the co-localization of active caspase-3 and MEF2D in CGNs containing fragmented nuclei (indicated by the arrows in k).

lowering of the extracellular potassium concentration to 5 mM (trophic factor withdrawal) for 6 h resulted in significant chromatin condensation and fragmentation in CGNs, consistent with induction of apoptosis (Fig. 1b). Addition of LiCl (20 mM) to trophic factor-deprived CGN cultures essentially abolished the induction of apoptosis (Fig. 1c). Quantification of the effects of increasing concentrations of LiCl on the formation of apoptotic nuclei observed at 24 h after trophic factor withdrawal, demonstrated a dose-dependent protective effect of lithium, with complete protection observed at a concentration of 20 mM (Fig. 2a). In agreement with numerous previous findings (D'Mello *et al.* 1994; Grignon *et al.* 1996; Li *et al.* 2000; Mora *et al.* 2001), these data confirm that lithium is effective at rescuing CGNs from apoptosis.

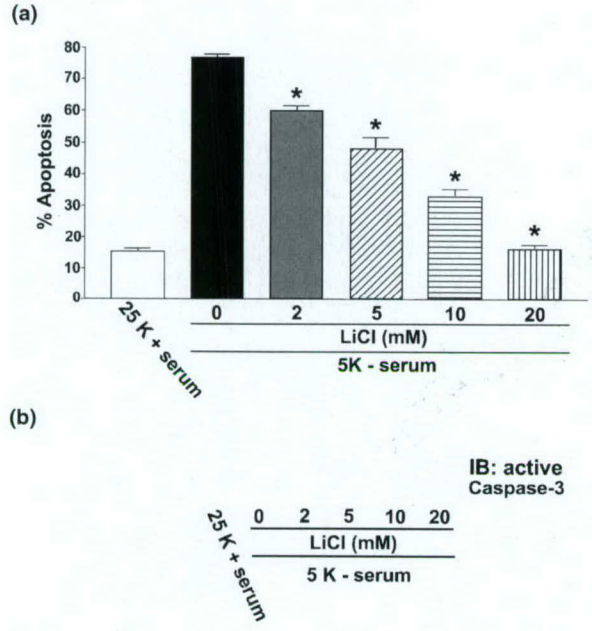

Fig. 2 Dose-dependence of lithium effects on CGN apoptosis and caspase-3 activation. (a) CGNs were incubated for 24 h in either control (25K + serum) or apoptotic (5K – serum) medium in the presence of increasing concentrations of LiCl. Following incubation, cells were fixed in 4% paraformaldehyde and nuclei were stained with Hoechst dye. Approximately 500 cells from at least two fields of a culture dish were scored for apoptosis from each condition. CGNs were considered apoptotic if their nuclei were condensed and/or fragmented. The data shown represent the means ± SEM for three independent experiments, each performed in triplicate. *Significantly different from the (5K – serum) condition in the absence of lithium ($p < 0.05$). (b) CGNs were incubated as described in (a) for 6 h and detergent-soluble cell lysates were electrophoresed on 15% polyacrylamide gels. Proteins were transferred to PVDF membranes and immunoblotted (IB) with a polyclonal antibody that specifically recognizes the active (cleaved) form of caspase-3, as described in Experimental procedures. The blot shown is representative of three separate experiments.

Apoptotic cell death is carried out by the caspase family of cysteine proteases (Shi 2002). Caspase-3 is an executioner caspase, activated following cleavage by initiator caspases (caspase-8 or −9), that has been implicated in the apoptosis of CGNs (Eldadah *et al.* 2000). CGNs maintained in medium containing serum and depolarizing potassium displayed very little active caspase-3 detectable by either immunocytochemistry (Fig. 1d) or immunoblotting (Fig. 2b, first lane) using antibodies that specifically recognize the cleaved form of the caspase. In contrast, trophic factor withdrawal for 6 h induced a marked activation of caspase-3 as shown immunocytochemically (Fig. 1e) and by western blotting (Fig. 2b, second lane). As previously reported (Mora *et al.* 2001), inclusion of LiCl during trophic factor withdrawal significantly attenuated the activation of caspase-3 (Fig. 1f) in a dose-dependent manner (Fig. 2b). Thus, consistent with its ability to decrease chromatin condensation and fragmentation, lithium concomitantly suppresses caspase activation in CGNs deprived of trophic support.

Lithium attenuates the hyperphosphorylation and degradation of MEF2D

Next, we examined the effects of LiCl on the hyperphosphorylation of MEF2D and MEF2A that occurs in CGNs undergoing apoptosis (Li *et al.* 2001). As shown in Fig. 3, immunoblotting CGN lysates revealed a marked upward shift in the electrophoretic mobility of MEF2D following the removal of trophic factors (Fig. 3a, compare the first and second lanes). We previously showed that this mobility shift is indicative of the hyperphosphorylation of MEF2D on serine/threonine residues, as it can be reversed by incubating the cell lysates with calf intestinal alkaline phosphatase (Li *et al.* 2001). Inclusion of LiCl at concentrations from 2 to 20 mM dose-dependently attenuated the hyperphosphorylation of MEF2D (Fig. 3a). In addition to the effect on MEF2D, LiCl (20 mM) also significantly blunted the hyperphosphorylation of MEF2A (Fig. 3b).

During neuronal apoptosis, MEF2D is a substrate for caspase-mediated cleavage (Li *et al.* 2001; Okamoto *et al.* 2002). Immunocytochemical analysis of CGNs demonstrated that MEF2D was localized exclusively to the nuclear compartment in cells maintained in the presence of serum and depolarization (Fig. 1g). Trophic factor withdrawal resulted in a decrease of MEF2D immunoreactivity in CGNs displaying active caspases and nuclear fragmentation (Fig. 1h). The reduction in the intensity of MEF2D staining was significantly blocked by lithium (Fig. 1i). Consistent with a caspase-dependent mechanism for MEF2D degradation, MEF2D appeared to colocalize with active caspases in trophic factor-deprived CGNs (Fig. 1k). Collectively, the above results demonstrate that lithium effectively inhibits both the hyperphosphorylation and caspase-mediated degradation of MEF2D that occur during CGN apoptosis.

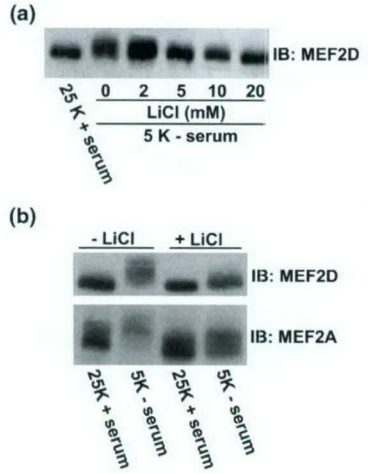

Fig. 3 Lithium attenuates the hyperphosphorylation of MEF2D and MEF2A induced following removal of depolarizing potassium and serum. (a) CGNs were incubated for 4 h in either control (25K + serum) or apoptotic (5K – serum) medium in the presence of increasing concentrations of LiCl. Following incubation, cell lysates were electrophoresed on 7.5% polyacrylamide gels and immunoblotted (IB) with a monoclonal antibody that specifically recognizes MEF2D, as described in Experimental procedures. (b) CGNs were incubated for 4 h in either control or apoptotic medium ± LiCl (20 mM). Cell lysates were subjected to sodium dodecyl sulfate – polyacrylamide gel electrophoresis (SDS–PAGE) and immunoblotted for either MEF2D or MEF2A. Note that the polyclonal antibody to MEF2A also cross-reacts with MEF2D, evident by the apparent doublet. The blots shown are each illustrative of three independent experiments.

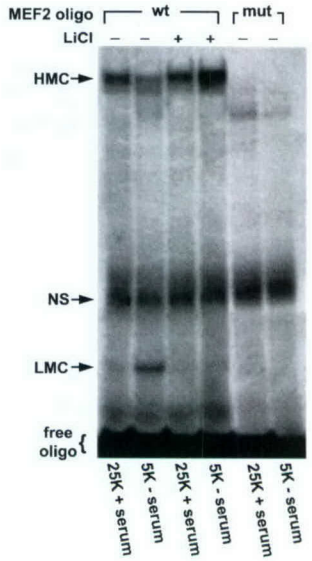

Fig. 4 Lithium prevents the loss of MEF2 DNA binding and blocks formation of truncated NH2-terminal MEF2 fragments in CGNs switched to medium lacking depolarizing potassium and serum. CGNs were incubated in either control (25K + serum) or apoptotic (5K – serum) medium ± LiCl (20 mM) for 4 h. Nuclear extracts were prepared and gel mobility shift assays were performed using either a double-stranded ^{32}P-labeled consensus (wild-type, wt) or mutant (mut) MEF2 oligonucleotide, as described in Experimental procedures. HMC, high molecular weight protein–DNA complex; LMC, low molecular weight protein–DNA complex; NS, non-specific protein–DNA complex. The HMC represents DNA binding by full length MEF2 proteins. The LMC represents DNA binding by truncated NH2-terminal MEF2 fragments (see Results). The gel shown is representative of two independent experiments that produced similar results.

Lithium sustains MEF2 DNA binding and inhibits formation of truncated NH_2-terminal MEF2 fragments

The hyperphosphorylation of MEF2 proteins results in decreased binding to DNA detectable by electrophoretic mobility shift assay (EMSA). As we previously reported (Li *et al.* 2001), nuclear extracts obtained from CGNs incubated in the presence of serum and depolarizing potassium contained a single specific high molecular weight protein–DNA complex (HMC) recognized by a wild-type MEF2 double-stranded oligonucleotide (Fig. 4, first lane). Removal of serum and depolarizing potassium for 4 h induced a decrease in the HMC, indicative of a relative loss of DNA binding by full-length MEF2 proteins (Fig. 4, second lane). Trophic factor withdrawal also promoted the appearance of a new low molecular weight protein–DNA complex (LMC) (Fig. 4, second lane) consisting of truncated MEF2 fragments that contain the NH_2-terminal DNA binding domain but lack the C-terminal transcriptional activation domain. We and others have previously shown that these NH2-terminal MEF2 fragments are generated via caspase-dependent cleavage of the full length MEF2 proteins, and have the potential to act as dominant-interfering transcription factors (Li *et al.* 2001; Okamoto *et al.* 2002). Inclusion of LiCl (20 mM) in apoptotic medium prevented both the decrease in DNA binding of full-length MEF2 proteins (i.e., loss of the HMC) and formation of the NH_2-terminal MEF2 fragments (i.e., appearance of the LMC) (Fig. 4, third and fourth lanes). Neither the HMC nor the LMC was detected using a mutant MEF2 oligonucleotide (Fig. 4, fifth and sixth lanes). These results show that lithium sustains MEF2 DNA binding and concurrently suppresses the formation of caspase-generated, dominant-negative MEF2 fragments in CGNs deprived of depolarization and serum.

Lithium preserves MEF2-dependent transcriptional activity in trophic factor-deprived CGNs

We utilized transient transfection of a luciferase reporter plasmid containing two MEF2 consensus sites followed by the luciferase reporter gene to measure the transcriptional activity of MEF2 proteins in CGNs. CGNs maintained in the presence of serum and depolarizing potassium exhibited high endogenous MEF2-dependent transcriptional activity. As shown in Fig. 5, trophic factor withdrawal for 2 h induced a marked (~60%) reduction in MEF2-driven luciferase activity. Consistent with the ability of lithium to attenuate the

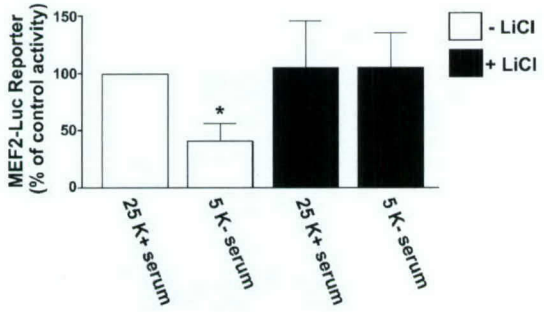

Fig. 5 Lithium sustains MEF2-dependent transcriptional activity in CGNs incubated in apoptotic medium. CGNs were transiently co-transfected with a MEF2-responsive luciferase reporter plasmid (pGL2-MEF2-Luc) and pCMV-β-gal. Two hours post-transfection, CGNs were incubated for a further 2 h in either control (25K + serum) or apoptotic (5K – serum) medium ± LiCl (20 mM). Following incubation, luciferase and β-galactosidase activities were assayed as described in Experimental procedures. Luciferase activity was normalized for transfection efficiency by dividing by the β-galactosidase activity. The normalized MEF2-Luc reporter activity obtained for CGNs incubated in control medium in the absence of lithium was set at 100% and all other values were calculated relative to the control. The data represent the means ± SEM. for three separate experiments, each performed in duplicate. *Significantly different from the (25K + serum) condition in the absence of lithium ($p < 0.05$).

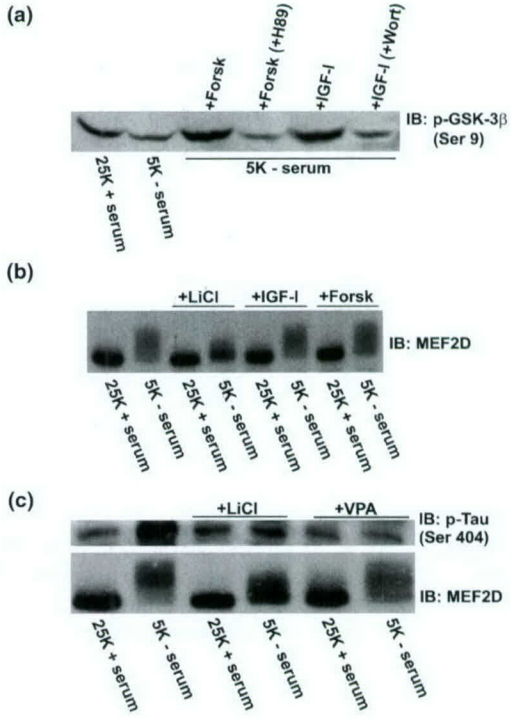

Fig. 6 Distinct inhibitors of GSK-3β do not mimic the inhibitory effects of lithium on MEF2D hyperphosphorylation. (a) CGNs were incubated for 4 h in either control (25K + serum) or apoptotic (5K – serum) medium alone or containing either forskolin (Forsk, 10 μM) ± H89 (10 μM) or insulin-like growth factor-I (IGF-I, 200 ng/mL) ± wortmannin (Wort, 100 nM). Following incubation, cell lysates from each treatment condition containing equal amounts of protein were subjected to SDS–PAGE on 10% polyacrylamide gels. Proteins were transferred to PVDF membranes and immunoblotted (IB) with a polyclonal antibody that specifically recognizes (*inactive*) GSK-3β phosphorylated on Ser9 (p-GSK-3β). (b) CGNs were incubated for 4 h in either control or apoptotic medium alone or containing either LiCl (20 mM), IGF-I (200 ng/mL), or Forsk (10 μM). Cell lysates were then western blotted for MEF2D, as described in Experimental procedures. (c) Cells were incubated for 4 h in either control or apoptotic medium alone or containing either LiCl (20 mM) or sodium valproate (VPA, 20 mM). Protein extracts were then immunoblotted for the GSK-3β substrate Tau phosphorylated on Ser404 (p-Tau, upper panel) and MEF2D (lower panel). The blots shown are each representative of results obtained in three separate experiments.

hyperphosphorylation and degradation of MEF2 proteins and to sustain MEF2 DNA binding, addition of LiCl (20 mM) prevented the loss of MEF2-dependent transcriptional activity in CGNs incubated in apoptotic medium. Thus, lithium sustains activity of the pro-survival MEF2 transcription factors in trophic factor-deprived CGNs.

The ability of lithium to block the hyperphosphorylation of MEF2D is not mimicked by distinct inhibitors of GSK-3β

One of the principal anti-apoptotic actions of lithium is inhibition of the serine/threonine kinase GSK-3β (Klein and Melton 1996; Stambolic *et al.* 1996), a protein that we previously implicated in the apoptosis of CGNs (Li *et al.* 2000). GSK-3β also plays a role in the apoptosis of primary cortical and sympathetic neurons (Crowder and Freeman 2000; Hetman *et al.* 2000). Moreover, in neuroblastoma cells GSK-3β translocates to the nucleus during apoptosis, consistent with a role for this kinase in the phosphorylation of nuclear substrates (Bijur and Jope 2001). To determine if the inhibitory effects of lithium on the hyperphosphorylation of MEF2D were mediated by its ability to blunt GSK-3β activity, we investigated the effects of three mechanistically distinct inhibitors of GSK-3β on MEF2D phosphorylation. We recently showed that activation of protein kinase A (PKA) is neuroprotective in CGNs through phosphorylation of an inhibitory serine residue (Ser9) on GSK-3β (Li *et al.* 2000). In agreement with this finding, forskolin, a direct activator of adenylyl cyclase, prevented the dephosphorylation (activation) of GSK-3β that occurs following trophic factor withdrawal in CGNs (Fig. 6a, first through third lanes). The phosphorylation of GSK-3β on Ser9 induced by forskolin was prevented by the PKA inhibitor H89 (Fig. 6a, fourth lane). Serine 9 on GSK-3β is also a consensus phosphorylation site for the antiapoptotic kinase AKT that is activated downstream of growth factor signaling in a phosphatidylinositol 3-kinase (PI3K)-dependent manner (van Weeren *et al.* 1998). Consistent with this, addition of insulin-like growth factor-I (IGF-I), a known survival factor

for CGNs (D'Mello *et al.* 1993; Linseman *et al.* 2002), induced phosphorylation (inactivation) of GSK-3β, an effect that was blocked by the PI3K inhibitor wortmannin (Fig. 6a, fifth and sixth lanes). Although both forskolin and IGF-I significantly induced phosphorylation of GSK-3β on Ser9, indicative of its inactivation, neither had any discernible effect on the hyperphosphorylation of MEF2D following trophic factor withdrawal from CGNs (Fig. 6b). Finally, incubation of CGNs with either lithium or sodium valproate (VPA, 20 mM), another recognized inhibitor of GSK-3β (Chen *et al.* 1999) that protects CGNs from apoptosis (Mora *et al.* 1999; Li *et al.* 2000), completely blocked phosphorylation of the GSK-3β substrate Tau (Utton *et al.* 1997) induced following trophic factor withdrawal (Fig. 6c, upper blot). However, VPA had no significant effect on the hyperphosphorylation of MEF2D observed under these conditions (Fig. 6c, lower blot). These results indicate that the inhibitory effects of lithium on MEF2D hyperphosphorylation can be dissociated from its ability to inhibit the pro-apoptotic kinase GSK-3β, suggesting the presence of an additional kinase target for lithium in CGNs.

Lithium blocks MEF2D hyperphosphorylation and apoptosis induced by calcineurin inhibition – a GSK-3β-independent model of CGN death

As trophic factor withdrawal results in both the activation of GSK-3β (Li *et al.* 2000) and the hyperphosphorylation of MEF2 proteins (Li *et al.* 2001) in CGNs, the relative contribution of lithium's effects on each of these signaling pathways to its pro-survival action is unclear. To strengthen the conclusion that inhibition of MEF2D hyperphosphorylation significantly contributes to lithium's neuroprotective action, we examined a different paradigm of CGN apoptosis. Previous work has shown that MEF2 DNA binding and transcriptional activity depend on depolarization-mediated activation of the calcium-regulated protein phosphatase calcineurin (Mao and Wiedmann 1999). In agreement with these findings, we observed that incubation of CGNs in depolarizing (25 mM KCl) medium containing the calcineurin inhibitor, cyclosporin A (CyA), resulted in the hyperphosphorylation of MEF2D (Fig. 7a, *compare first and fourth lanes*), loss of MEF2 transcriptional activity (Fig. 7b), and significant apoptosis (Fig. 7d, *open bars*). In contrast to trophic factor withdrawal (see Fig. 6a, *first and second lanes*), incubation with CyA under depolarizing conditions failed to activate GSK-3β (measured by dephosphorylation of the inhibitory residue Ser9, Fig. 7e, *compare first and second lanes*). This latter result was expected as GSK-3β has previously been shown to be regulated by a distinct protein phosphatase, PP2A (Mora *et al.* 2002). Thus, calcineurin inhibition in the presence of depolarizing potassium is a MEF2 phosphorylation-dependent, but GSK-3β-independent, model of CGN apoptosis. Lithium significantly blocked the hyperphosphorylation of MEF2D (Fig. 7a, *compare fourth and fifth lanes*), loss of MEF2 transcriptional activity (Fig. 7c), and apoptosis (Fig. 7d) induced by addition of CyA, strongly suggesting that inhibition of MEF2 hyperphosphorylation is a novel pro-survival action of lithium in CGNs.

Discussion

The effectiveness of lithium as a therapy for bipolar disorder is well documented (Muller-Oerlinghausen *et al.* 2002). However, the ability of lithium to act as a neuroprotective agent has only recently gained attention. Previous studies have demonstrated that lithium inhibits neuronal apoptosis *in vitro* induced by trophic factor withdrawal (D'Mello *et al.* 1994; Grignon *et al.* 1996; Li *et al.* 2000; Mora *et al.* 2001), excitotoxicity (Nonaka *et al.* 1998a; Chen and Chuang 1999), neurotoxin exposure (Nonaka *et al.* 1998b; Maggirwar *et al.* 1999), beta-amyloid (Alvarez *et al.* 1999), and ceramide (Centeno *et al.* 1998). Moreover, lithium inhibits hippocampal neuronal death induced by *in vivo* exposure to the neurotoxin aluminum (Ghribi *et al.* 2002). Lithium has also been shown to enhance the survival of chick ciliary ganglion neurons during embryonic development (Ikonomov *et al.* 2000). The above results demonstrate that lithium provides neuroprotection both *in vitro* and *in vivo*.

Although lithium is a known inhibitor of the pro-apoptotic serine/threonine kinase, GSK-3β (Klein and Melton 1996; Stambolic *et al.* 1996), relatively few studies have concluded that lithium provides neuroprotection via this mechanism (Maggirwar *et al.* 1999; Bijur *et al.* 2000; Li *et al.* 2000). Several alternative mechanisms have also been proposed. For example, lithium has recently been shown to inhibit a serine/threonine phosphatase that dephosphorylates (inactivates) the pro-survival kinase AKT (Mora *et al.* 2001, 2002). It is noteworthy however, that a principal target of AKT is GSK-3β (van Weeren *et al.* 1998), and therefore, the net result of this effect of lithium may inevitably involve inhibition of GSK-3β activity. In addition, lithium has been shown to up-regulate the expression of the anti-apoptotic Bcl-2 protein (Chen and Chuang 1999; Manji *et al.* 2000) and to decrease expression of the pro-apoptotic proteins, p53 and Bax (Chen and Chaung 1999). These latter effects are only observed after chronic (several days) treatment with lithium. In the current study, we investigated the neuroprotective mechanism of lithium in primary cultures of rat CGNs. Specifically, we analyzed the effects of lithium on the apoptotic processing of MEF2 proteins, transcription factors that are critical for CGN survival (Mao *et al.* 1999). In agreement with previous results showing that CGNs matured *in vitro* are protected from apoptosis by lithium (D'Mello *et al.* 1994; Grignon *et al.* 1996; Li *et al.* 2000; Mora *et al.* 2001), we found that acute addition of lithium effectively inhibits CGN apoptosis and caspase activation induced by removal of depolarizing potassium and serum. Moreover, our data reveal

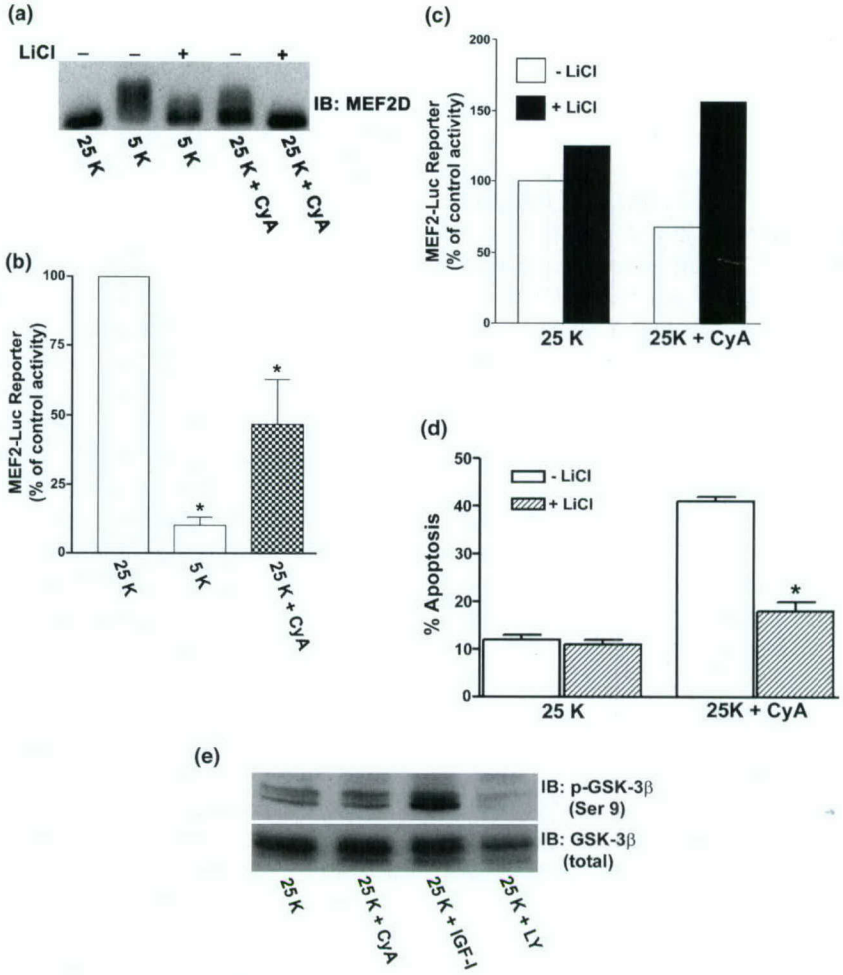

Fig. 7 Incubation with the calcineurin phosphatase inhibitor, cyclosporin A (CyA), under depolarizing conditions induces lithium-sensitive MEF2D hyperphosphorylation, loss of MEF2 transcriptional activity and apoptosis in the absence of GSK-3β activation. (a) CGNs were incubated for 4 h in serum-free medium containing either 25 mM KCl (25K), 5 mM KCl (5K), or 25 mM KCl + 10 μM CyA (25K + CyA) in the absence or presence of LiCl (20 mM). Following incubation, cell lysates were immunoblotted (IB) for MEF2D, as described in Experimental procedures. (b) CGNs were transiently co-transfected with a MEF2-responsive luciferase reporter plasmid (pGL2-MEF2-Luc) and pCMV-β-gal. Following transfection, cells were incubated for 4 h as described in (a) and luciferase and β-galactosidase activities were assayed and normalized as described in Experimental procedures. *Significantly different from the 25K control ($p < 0.05$). (c) Cells were transfected as described in (b) and were subsequently incubated in either 25K or 25K + CyA in the absence or presence of LiCl (20 mM). Luciferase and β-galactosidase activities were assayed and the results shown represent the mean values of triplicate samples from a single experiment. (d) CGNs were incubated for 24 h in either 25K medium alone or containing CyA (10 μM). Cells were stained with Hoechst dye and apoptosis was quantified as described in Experimental procedures. *Significantly different from 25K + CyA in the absence of lithium ($p < 0.05$). (e) CGNs were incubated for 4 h in the absence or presence of CyA. Cell lysates were probed for GSK-3β phosphorylated on Ser9 (upper panel) and total GSK-3β (lower panel). When the phospho-specific GSK-3β signal was normalized for the total GSK-3β, no significant change in phosphorylation state was observed with the addition of CyA. IGF-I and the PI3K inhibitor, LY294002 (LY), are included as positive and negative controls for GSK-3β phosphorylation on Ser9, respectively.

a novel mechanism for the pro-survival effects of lithium in CGNs that involves preservation of MEF2 transcriptional activity.

We show that lithium inhibits the hyperphosphorylation of MEF2D and MEF2A induced by trophic factor withdrawal in CGNs. Consistent with previous observations that hyperphosphorylation of MEF2 proteins leads to a decrease in their DNA binding (Mao and Wiedmann 1999; Li *et al.* 2001), we also show that lithium sustains MEF2 DNA binding and MEF2 transcriptional activity in trophic factor-deprived CGNs. In addition, lithium blocks the caspase-dependent formation of NH_2-terminal MEF2 fragments that have the potential to act as dominant-interfering transcription factors (Li *et al.* 2001; Okamoto *et al.* 2002). The relative contribution of MEF2 hyperphosphorylation versus MEF2 degradation to the induction of CGN apoptosis is presently

unclear. The ability of lithium to block the hyperphosphorylation of MEF2 proteins suggests that it acts very early in the apoptotic cascade as hyperphosphorylation of MEF2 precedes loss of DNA binding or transcriptional activity and caspase-mediated degradation of MEF2 proteins (Li *et al.* 2001). The latter likely leads to a more prolonged inhibition of MEF2 activity as the fragments formed have the potential to compete with newly synthesized full-length MEF2 proteins for DNA binding. However, it appears that hyperphosphorylation of MEF2 proteins may be the initiating event that ultimately leads to loss of MEF2 activity and apoptosis. This is the first report to demonstrate that lithium preserves the activity of MEF2 transcription factors in neurons subjected to an apoptotic stimulus. The fact that a constitutively active MEF2 mutant has previously been shown to protect CGNs from apoptosis (Mao *et al.* 1999) supports our conclusion that the effects of lithium on MEF2 proteins described above play an important role in the neuroprotective mechanism of this cation.

A likely target for the action of lithium in CGNs is the kinase that phosphorylates MEF2D and MEF2A during apoptosis. We initially examined the effects of lithium on phosphorylation of MEF2 proteins in CGNs because lithium is an established inhibitor of GSK-3β (Klein and Melton 1996; Stambolic *et al.* 1996), a serine/threonine kinase that is involved in the apoptosis of CGNs (Li *et al.* 2000). However, many of the results obtained in the present study argue against a role for GSK-3β in phosphorylating MEF2 proteins during CGN apoptosis. Firstly, forskolin and IGF-I, agents that promote the phosphorylation of GSK-3β on the inhibitory Ser9 via either PKA or AKT kinase activation, respectively (van Weeren *et al.* 1998; Li *et al.* 2000), had no significant effect on the hyperphosphorylation of MEF2D. Secondly, another compound known to inhibit GSK-3β, VPA (Chen *et al.* 1999), significantly blocked phosphorylation of the GSK-3β substrate Tau, but had no discernible effect on the hyperphosphorylation of MEF2D. Thirdly, MEF2D hyperphosphorylation was induced in depolarizing medium by addition of the calcineurin phosphatase inhibitor, CyA, conditions under which GSK-3β activity was not further stimulated. These results suggest that the kinase that phosphorylates MEF2D and inhibits DNA binding of MEF2 proteins during apoptosis of CGNs is a novel lithium target that is distinct from GSK-3β. This finding is in contrast to the ability of lithium to stimulate DNA binding of the transcription factor cAMP response element binding protein (CREB), an effect that is mediated via inhibition of GSK-3β (Grimes and Jope 2001). Collectively, these observations indicate that the potential for lithium to inhibit multiple pro-apoptotic signals, including GSK-3β and the kinase that phosphorylates MEF2 proteins, likely contributes to its effectiveness as a neuroprotective agent. In particular, the finding that lithium inhibits MEF2D hyperphosphorylation and apoptosis induced by calcineurin inhibition, a GSK-3β-independent model of CGN death, strongly supports the conclusion that inhibition of a MEF2 kinase is a novel anti-apoptotic action of lithium in neurons.

Finally, although lithium is commonly regarded as a highly selective inhibitor of GSK-3β (Klein and Melton 1996; Stambolic *et al.* 1996; Woodgett 2001), it is clear that it inhibits the function of other enzymes as well. For example, lithium is an established inhibitor of the inositol monophosphatase (Phiel and Klein 2001), and this effect may be involved in its efficacy in bipolar disorder (Atack *et al.* 1995). Recently, lithium has been suggested to inhibit activation of the protein serine/threonine phosphatase, PP2A, which is involved in the regulation of AKT activity (Mora *et al.* 2002). In regards to other potential kinases that may be inhibited by lithium, a recent screen against a relatively large panel of possible kinase targets showed that lithium (10 mM) inhibited GSK-3β most potently, but also decreased the activities of three other serine/threonine kinases tested, including casein kinase-2 (CK-2), mitogen-activated protein kinase-activated protein kinase-2 (MAPKAPK-2), and p38-regulated/activated protein kinase (PRAK) (Davies *et al.* 2000). Interestingly, CK-2 has previously been shown to phosphorylate MEF2C; however, this phosphorylation enhanced MEF2C binding to DNA (Molkentin *et al.* 1996). The potential of either MAPKAPK-2 or PRAK to phosphorylate the MEF2 proteins has not yet been examined. Thus, identification of the lithium-sensitive kinase that phosphorylates MEF2D and MEF2A in CGNs during apoptosis will require further investigation.

In conclusion, we have demonstrated that lithium inhibits the hyperphosphorylation and caspase-dependent degradation of MEF2 transcription factors and maintains their DNA binding and activity in CGNs deprived of depolarizing potassium and serum. These effects of lithium are mediated via the inhibition of a serine/threonine kinase, distinct from GSK-3β, that phosphorylates MEF2 proteins and inhibits their pro-survival function. These data identify the regulation of MEF2 transcriptional activity as a novel mechanism underlying the neuroprotective effects of lithium.

Acknowledgements

This work was supported by Department of Veterans Affairs Merit Awards (to KAH and DAL), a Department of Defense Grant DAMD17-99-1-9481 (to KAH), an NIH Grant NS38619–01A1 (to KAH), and a VA Research Enhancement Award Program (to KAH and DAL). The authors acknowledge Mingtao Li and Xiaomin Wang for technical support.

References

Alvarez G., Munoz-Montano J. R., Satrustegui J., Avila J., Bogonez E. and Diaz-Nido J. (1999) Lithium protects cultured neurons against beta-amyloid-induced neurodegeneration. *FEBS Lett.* **453**, 260–264.

Andersen J. K. (2001) Does neuronal loss in Parkinson's Disease involve programmed cell death? *Bioessays* **23**, 640–646.

Atabay C., Cagnoli C. M., Kharlamov E., Ikonomovic M. D. and Manev H. (1996) Removal of serum from primary cultures of cerebellar granule neurons induces oxidative stress and DNA fragmentation: protection with antioxidants and glutamate receptor antagonists. *J. Neurosci. Res.* **43**, 465–475.

Atack J. R., Broughton H. B. and Pollack S. J. (1995) Inositol monophosphatase – a putative target for Li^+ in the treatment of bipolar disorder. *Trends Neurosci.* **18**, 343–349.

Bijur G. N. and Jope R. S. (2001) Pro-apoptotic stimuli induce nuclear accumulation of glycogen synthase kinase-3 beta. *J. Biol. Chem.* **276**, 37436–37442.

Bijur G. N., De Sarno P. and Jope R. S. (2000) Glycogen synthase kinase-3beta facilitates staurosporine- and heat shock-induced apoptosis. Protection by lithium. *J. Biol. Chem.* **275**, 7583–7590.

Black B. L. and Olson E. N. (1998) Transcriptional control of muscle development by myocyte enhancer factor-2 (MEF2) proteins. *Annu. Rev. Cell Dev. Biol.* **14**, 167–196.

Centeno F., Mora A., Fuentes J. M., Soler G. and Claro E. (1998) Partial lithium-associated protection against apoptosis induced by C2-ceramide in cerebellar granule neurons. *Neuroreport* **9**, 4199–4203.

Chen G., Huang L. D., Jiang Y. M. and Manji H. K. (1999) The mood-stabilizing agent valproate inhibits the activity of glycogen synthase kinase-3. *J. Neurochem.* **72**, 1327–1330.

Chen R. W. and Chuang D. M. (1999) Long-term lithium treatment suppresses p53 and Bax expression but increases Bcl-2 expression. A prominent role in neuroprotection against excitotoxicity. *J. Biol. Chem.* **274**, 6039–6042.

Crowder R. J. and Freeman R. S. (2000) Glycogen synthase kinase-3 beta activity is critical for neuronal death caused by inhibiting phosphatidylinositol 3-kinase or Akt but not for death caused by nerve growth factor withdrawal. *J. Biol. Chem.* **275**, 34266–34271.

D'Mello S. R., Galli C., Ciotti T. and Calissano P. (1993) Induction of apoptosis in cerebellar granule neurons by low potassium: inhibition of death by insulin-like growth factor I and cAMP. *Proc. Natl Acad. Sci. USA* **90**, 10989–10993.

D'Mello S. R., Anelli R. and Calissano P. (1994) Lithium induces apoptosis in immature cerebellar granule cells but promotes survival of mature neurons. *Exp. Cell Res.* **211**, 332–338.

Davies S. P., Reddy H., Caivano M. and Cohen P. (2000) Specificity and mechanism of action of some commonly used protein kinase inhibitors. *Biochem. J.* **351**, 95–105.

Eldadah B. A., Ren R. F. and Faden A. I. (2000) Ribozyme-mediated inhibition of caspase-3 protects cerebellar granule cells from apoptosis induced by serum-potassium deprivation. *J. Neurosci.* **20**, 179–186.

Ghribi O., Herman M. M., Spaulding N. K. and Savory J. (2002) Lithium inhibits aluminum-induced apoptosis in rabbit hippocampus by preventing cytochrome c translocation, Bcl-2 decrease, Bax elevation and caspase-3 activation. *J. Neurochem.* **82**, 137–145.

Grignon S., Levy N., Couraud F. and Bruguerolle B. (1996) Tyrosine kinase inhibitors and cycloheximide inhibit Li+ protection of cerebellar granule neurons switched to non-depolarizing medium. *Eur. J. Pharmacol.* **315**, 111–114.

Grimes C. A. and Jope R. S. (2001) CREB DNA binding activity is inhibited by glycogen synthase kinase-3 beta and facilitated by lithium. *J. Neurochem.* **78**, 1219–1232.

Han J., Jiang Y., Li Z., Kravchenko V. V. and Ulevitch R. J. (1997) Activation of the transcription factor MEF2C by the MAP kinase p38 in inflammation. *Nature* **386**, 296–299.

Hetman M., Cavanaugh J. E., Kimelman D. and Xia Z. (2000) Role of glycogen synthase kinase-3 beta in neuronal apoptosis induced by trophic withdrawal. *J. Neurosci.* **20**, 2567–2574.

Honig L. S. and Rosenberg R. N. (2000) Apoptosis and neurologic disease. *Am. J. Med.* **108**, 317–330.

Ikonomov O. C., Petrov T., Soden K., Shisheva A. and Manji H. K. (2000) Lithium treatment in ovo: effects on embryonic heart rate, natural death of ciliary ganglion neurons, and brain expression of a highly conserved chicken homologue of human MTG8/ETO. *Brain Res. Dev. Brain Res.* **123**, 13–24.

Kato Y., Kravchenko V. V., Tapping R. I., Han J., Ulevitch R. J. and Lee J. D. (1997) BMK1/ERK5 regulates serum-induced early gene expression through transcription factor MEF2C. *EMBO J.* **16**, 7054–7066.

Kawashima T., Doh-ura K., Ogomori K. and Iwaki T. (2001) Apoptotic bodies in the cerebellum of Japanese patients with Creutzfeldt-Jakob disease. *Pathol. Int.* **51**, 140–144.

Klein P. S. and Melton D. A. (1996) A molecular mechanism for the effect of lithium on development. *Proc. Natl Acad. Sci. USA* **93**, 8455–8459.

Leifer D., Krainc D., Yu Y. T., McDermott J., Breitbart R. E., Heng J., Neve R. L., Kosofsky B., Nadal-Ginard B. and Lipton S. A. (1993) MEF2C, a MADS/MEF2-family transcription factor expressed in a laminar distribution in cerebral cortex. *Proc. Natl Acad. Sci. USA* **90**, 1546–1550.

Li M., Wang X., Meintzer M. K., Laessig T., Birnbaum M. J. and Heidenreich K. A. (2000) Cyclic AMP promotes neuronal survival by phosphorylation of glycogen synthase kinase 3 beta. *Mol. Cell Biol.* **20**, 9356–9363.

Li M., Linseman D. A., Allen M. P., Meintzer M. K., Wang X., Laessig T., Wierman M. E. and Heidenreich K. A. (2001) Myocyte enhancer factor 2A and 2D undergo phosphorylation and caspase-mediated degradation during apoptosis of rat cerebellar granule neurons. *J. Neurosci.* **21**, 6544–6552.

Lin X., Shah S. and Bulleit R. F. (1996) The expression of MEF2 genes is implicated in CNS neuronal differentiation. *Brain Res. Mol. Brain Res.* **42**, 307–316.

Linseman D. A., Phelps R. A., Bouchard R. J., Le S. S., Laessig T. A., McClure M. L. and Heidenreich K. A. (2002) Insulin-like growth factor-I blocks Bcl-2 interacting mediator of cell death (Bim) induction and intrinsic death signaling in cerebellar granule neurons. *J. Neurosci.* **22**, 9287–9297.

Lyons G. E., Micales B. K., Schwarz J., Martin J. F. and Olson E. N. (1995) Expression of MEF2 genes in the mouse central nervous system suggests a role in neuronal maturation. *J. Neurosci.* **15**, 5727–5738.

Maggirwar S. B., Tong N., Ramirez S., Gelbard H. A. and Dewhurst S. (1999) HIV-1 Tat-mediated activation of glycogen synthase kinase-3beta contributes to Tat-mediated neurotoxicity. *J. Neurochem.* **73**, 578–586.

Manji H. K., Moore G. J. and Chen G. (2000) Lithium up-regulates the cytoprotective protein Bcl-2 in the CNS *in vivo*: a role for neurotrophic and neuroprotective effects in manic-depressive illness. *J. Clin. Psychiatry* **61**, 82–96.

Mao Z. and Wiedmann M. (1999) Calcineurin enhances MEF2 DNA binding activity in calcium-dependent survival of cerebellar granular neurons. *J. Biol. Chem.* **274**, 31102–31107.

Mao Z., Bonni A., Xia F., Nadal-Vicens M. and Greenberg M. E. (1999) Neuronal activity-dependent cell survival mediated by transcription factor MEF2. *Science* **286**, 785–790.

McKinsey T. A., Zhang C. L. and Olson E. N. (2002) MEF2: a calcium-dependent regulator of cell division, differentiation and death. *Trends Biochem. Sci.* **27**, 40–47.

Molkentin J. D., Li L. and Olson E. N. (1996) Phosphorylation of the MADS-Box transcription factor MEF2C enhances its DNA binding activity. *J. Biol. Chem.* **271**, 17199–17204.

Mora A., Gonzalez-Polo R. A., Fuentes J. M., Soler G. and Centeno F. (1999) Different mechanisms of protection against apoptosis by valproate and Li+. *Eur. J. Biochem.* **266**, 886–891.

Mora A., Sabio G., Gonzalez-Polo R. A., Cuenda A., Alessi D. R., Alonso J. C., Fuentes J. M., Soler G. and Centeno F. (2001) Lithium inhibits caspase 3 activation and dephosphorylation of PKB and GSK3 induced by K^+ deprivation in cerebellar granule cells. *J. Neurochem.* **78**, 199–206.

Mora A., Sabio G., Risco A. M., Cuenda A., Alonso J. C., Soler G. and Centeno F. (2002) Lithium blocks the PKB and GSK3 dephosphorylation induced by ceramide through protein phosphatase-2A. *Cell Signal.* **14**, 557–562.

Muller-Oerlinghausen B., Berghofer A. and Bauer M. (2002) Bipolar disorder. *Lancet* **359**, 241–247.

Nijhawan D., Honarpour N. and Wang X. (2000) Apoptosis in neural development and disease. *Annu. Rev. Neurosci.* **23**, 73–87.

Nonaka S., Hough C. J. and Chuang D. M. (1998a) Chronic lithium treatment robustly protects neurons in the central nervous system against excitotoxicity by inhibiting N-methyl-D-aspartate receptor-mediated calcium influx. *Proc. Natl Acad. Sci. USA* **95**, 2642–2647.

Nonaka S., Katsube N. and Chuang D. M. (1998b) Lithium protects rat cerebellar granule cells against apoptosis induced by anticonvulsants, phenytoin and carbamazepine. *J. Pharmacol. Exp. Ther.* **286**, 539–547.

Okamoto S., Li Z., Ju C., Scholzke M. N., Mathews E., Cui J., Salvesen G. S., Bossy-Wetzel E. and Lipton S. A. (2002) Dominant-interfering forms of MEF2 generated by caspase cleavage contribute to NMDA-induced neuronal apoptosis. *Proc. Natl Acad. Sci. USA* **99**, 3974–3979.

Phiel C. J. and Klein P. S. (2001) Molecular targets of lithium action. *Annu. Rev. Pharmacol. Toxicol.* **41**, 789–813.

Roth K. A. and D'Sa C. (2001) Apoptosis and brain development. *Ment. Retard. Dev. Disabil. Res. Rev.* **7**, 261–266.

Schierle G. S., Hansson O., Leist M., Nicotera P., Widner H. and Brundin P. (1999) Caspase inhibition reduces apoptosis and increases survival of nigral transplants. *Nat. Med.* **5**, 97–100.

Shi Y. (2002) Mechanisms of caspase activation and inhibition during apoptosis. *Mol. Cell* **9**, 459–470.

Shore P. and Sharrocks A. D. (1995) The MADS-box family of transcription factors. *Eur. J. Biochem.* **229**, 1–13.

Stambolic V., Ruel L. and Woodgett J. R. (1996) Lithium inhibits glycogen synthase kinase-3 activity and mimics wingless signaling in intact cells. *Curr. Biol.* **6**, 1664–1668.

Utton M. A., Vandecandelaere A., Wagner U., Reynolds C. H., Gibb G. M., Miller C. C., Bayley P. M. and Anderton B. H. (1997) Phosphorylation of tau by glycogen synthase kinase 3beta affects the ability of tau to promote microtubule self-assembly. *Biochem. J.* **323**, 741–747.

van Weeren P. C., de Bruyn K. M., de Vries-Smits A. M., van Lint J. and Burgering B. M. (1998) Essential role for protein kinase B (PKB) in insulin-induced glycogen synthase kinase 3 inactivation. Characterization of dominant-negative mutant of PKB. *J. Biol. Chem.* **273**, 13150–13156.

Woodgett J. R. (2001) Judging a protein by more than its name: GSK-3. *Sci. STKE* **2001**, RE12.

THE JOURNAL OF BIOLOGICAL CHEMISTRY

Vol. 278, No. 42, Issue of October 17, pp. 41472–41481, 2003
Printed in U.S.A.

Inactivation of the Myocyte Enhancer Factor-2 Repressor Histone Deacetylase-5 by Endogenous Ca^{2+}/Calmodulin-dependent Kinase II Promotes Depolarization-mediated Cerebellar Granule Neuron Survival*

Received for publication, July 7, 2003, and in revised form, July 21, 2003
Published, JBC Papers in Press, August 1, 2003, DOI 10.1074/jbc.M307245200

Daniel A. Linseman, Christopher M. Bartley, Shoshona S. Le, Tracey A. Laessig, Ron J. Bouchard, Mary Kay Meintzer, Mingtao Li, and Kim A. Heidenreich‡

From the Department of Pharmacology, University of Colorado Health Sciences Center and the Denver Veterans Affairs Medical Center, Denver, Colorado 80262

Cerebellar granule neuron (CGN) survival depends on activity of the myocyte enhancer factor-2 (MEF2) transcription factors. Neuronal MEF2 activity is regulated by depolarization via a mechanism that is presently unclear. Here, we show that depolarization-mediated MEF2 activity and CGN survival are compromised by overexpression of the MEF2 repressor histone deacetylase-5 (HDAC5). Furthermore, removal of depolarization induced rapid cytoplasm-to-nuclear translocation of endogenous HDAC5. This effect was mimicked by addition of the calcium/calmodulin-dependent kinase (CaMK) inhibitor KN93 to depolarizing medium. Removal of depolarization or KN93 addition resulted in dephosphorylation of HDAC5 and its co-precipitation with MEF2D. HDAC5 nuclear translocation triggered by KN93 induced a marked loss of MEF2 activity and subsequent apoptosis. To selectively decrease CaMKII, CGNs were incubated with an antisense oligonucleotide to CaMKIIα. This antisense decreased CaMKIIα expression and induced nuclear shuttling of HDAC5 in CGNs maintained in depolarizing medium. Selectivity of the CaMKIIα antisense was demonstrated by its lack of effect on CaMKIV-mediated CREB phosphorylation. Finally, antisense to CaMKIIα induced caspase-3 activation and apoptosis, whereas a missense control oligonucleotide had no effect on CGN survival. These results indicate that depolarization-mediated calcium influx acts through CaMKII to inhibit HDAC5, thereby sustaining high MEF2 activity in CGNs maintained under depolarizing conditions.

Myocyte enhancer factor-2 (MEF2)[1] transcription factors were originally identified in cells of skeletal, cardiac, and smooth muscle lineages (1–4). In muscle, activity of MEF2 proteins is modulated by calcium-regulated signals that ultimately drive myogenic differentiation (5, 6). MEF2 proteins also play a critical role in the differentiation and survival of neurons in the developing central nervous system (CNS) (2, 7–11). In particular, MEF2 function is essential for activity-dependent neuronal survival mediated through the formation of proper synaptic contacts during CNS development (12).

In early postnatal cerebellum, transcripts for two mammalian MEF2 isoforms, MEF2A and MEF2D, are markedly increased in parallel with enhanced expression of the $GABA_A$ receptor α6 subunit, a marker for differentiation of mature cerebellar granule neurons (CGNs) (9). Similarly, primary cultures of CGNs, that require medium containing depolarizing extracellular potassium for their survival (13), demonstrate high levels of endogenous MEF2A and MEF2D proteins and MEF2 transcriptional activity. We have previously reported that MEF2A and MEF2D are phosphorylated and subsequently cleaved by caspases in CGNs that are deprived of depolarizing potassium (14). The resulting loss of MEF2 transcriptional activity contributes to CGN apoptosis under these conditions. Likewise, Gaudilliere *et al.* (15) recently showed that down-regulation of MEF2A using RNA interference significantly compromises depolarization-mediated survival of CGNs. Thus, MEF2 proteins transduce activity-dependent calcium signals into an essential pro-survival pathway in CGNs.

The precise mechanism(s) by which calcium influx regulates MEF2 activity in CGNs is presently unclear. Previous work in muscle indicates that activity of the calcium/calmodulin-dependent, serine/threonine phosphatase, calcineurin, is required for MEF2 function (16). Similarly, calcineurin positively regulates MEF2 DNA binding and transcriptional activity in CGNs (17). In muscle, calcineurin modulation of MEF2 activity is integrated with regulation by a pathway involving calcium/calmodulin-dependent protein kinase (CaMK) activity (5). Muscle MEF2 activity is repressed by interaction with class II histone deacetylases (HDACs) (18–20). Overexpression of constitutively-active CaMK isoforms I and IV in muscle and non-muscle cells (*e.g.* COS or NIH3T3 fibroblasts) promotes serine phosphorylation of HDACs. Phosphorylation of HDACs induces their nuclear export and promotes their association with cytosolic scaffolding proteins of the 14-3-3 family, ultimately resulting in derepression of MEF2 activity (21). Although these overexpression studies suggest a role for CaMK regulation of

* This work was supported by Department of Veterans Affairs Merit Awards (to K. A. H. and D. A. L.), a Department of Defense Grant DAMD17-99-1-9481 (to K. A. H.), a National Institutes of Health Grant NS38619-01A1 (to K. A. H.), and a Department of Veterans Affairs Research Enhancement Award Program (to K. A. H. and D. A. L.). The costs of publication of this article were defrayed in part by the payment of page charges. This article must therefore be hereby marked "*advertisement*" in accordance with 18 U.S.C. Section 1734 solely to indicate this fact.

‡ To whom correspondence should be addressed: University of Colorado, Health Sciences Center, Dept. of Pharmacology (C236), 4200 E. 9th Ave., Denver, CO 80262. Tel.: 303-399-8020 (ext. 3891); Fax: 303-393-5271; E-mail: Kim.Heidenreich@UCHSC.edu.

[1] The abbreviations used are: MEF2, myocyte enhancer factor-2; CGN, cerebellar granule neuron; FITC, fluorescein isothiocyanate; DAPI, 4′,6-diamidino-2-phenylindole; PBS, phosphate-buffered saline; BSA, bovine serum albumin; HA, hemagglutinin; CaMK, calcium/calmodulin-dependent protein kinase; HDAC, histone deacetylase; CREB, cAMP response element-binding protein; GFP, green fluorescent protein.

HDAC function in muscle, the endogenous CaMK isoform involved has yet to be identified. Moreover, a role for endogenous CaMK activity in modulating MEF2 function in neurons has not yet been investigated.

Here, we show that depolarization-mediated MEF2 activity and CGN survival are compromised by overexpression of the class II HDAC, HDAC5. Moreover, removal of depolarizing potassium or addition of a CaMK inhibitor induces nuclear translocation of endogenous HDAC5, loss of MEF2 activity, and CGN apoptosis. Finally, antisense-mediated down-regulation of CaMKIIα expression is sufficient to drive nuclear translocation of HDAC5 and induce CGN apoptosis under depolarizing conditions. These results demonstrate that CaMK-mediated inhibition of HDAC function plays a significant role in the calcium regulation of MEF2 activity and survival in CGNs. In addition, these data are the first to identify an endogenous CaMK isoform (CaMKII) that regulates HDAC function.

EXPERIMENTAL PROCEDURES

Materials—A truncated mutant of MEF2A lacking the C-terminal transcriptional activation domain, pcDNA3.1-MEF2A131, was kindly provided by Dr. Ron Prywes (Columbia University, New York). Empty pcDNA3.1 vector was obtained from Invitrogen (Grand Island, NY). Adenoviral green fluorescent protein (Ad-GFP) was a gift from Dr. Jerry Schaack (University of Colorado Health Sciences Center, Denver, CO). The pGL2-MEF2-luciferase reporter plasmid and HA-tagged HDAC5 and HDAC4 were provided by Dr. Saadi Khochbin (INSERM, France). Hoecsht dye number 33258, 4′,6-diamidino-2-phenylindole (DAPI), monoclonal antibody to the FLAG epitope, and monoclonal antibody to β-tubulin were from Sigma. Monoclonal antibody to the HA epitope and rabbit polyclonal antibodies to phospho-CREB (Ser-133), HDAC4, and HDAC5 for immunocytochemistry were obtained from Cell Signaling Technologies (Beverly, MA). Rabbit polyclonal antibody to active (cleaved) caspase-3 was from Promega (Madison, WI). Monoclonal antibody to MEF2D for immunocytochemistry and Western blotting was purchased from Transduction Laboratories (Lexington, KY). Monoclonal antibody to CaMKIIα for immunocytochemistry was from Chemicon (Temecula, CA). According to the manufacturer, this antibody may show some cross-reactivity with CaMKIIδ or γ subunits. FITC- and Cy3-conjugated secondary antibodies for immunofluorescence were from Jackson Immunoresearch Laboratories (West Grove, PA). Rabbit polyclonal antibody to MEF2 for immunoprecipitation, rabbit polyclonal antibody to HDAC5 for Western blotting, and protein A/G-agarose were obtained from Santa Cruz Biotechnology (Santa Cruz, CA). Horseradish peroxidase-linked secondary antibodies and reagents for enhanced chemiluminescence detection were purchased from Amersham Biosciences (Piscataway, NJ). KN93, KN62, phosphorothioate 18-mer antisense oligonucleotide complementary to CaMKIIα subunit mRNA nucleotides 33–50 (unlabeled and FITC-labeled), and an unlabeled, scrambled, missense control oligonucleotide were from Calbiochem (La Jolla, CA). According to the manufacturer, this antisense construct is highly specific for the α subunit of CaMKII and does not affect CaMKIIβ expression.

Cell Culture—Rat CGNs were isolated from 7-day-old Sprague-Dawley rat pups (15–19 g) as described previously (22). Briefly, neurons were plated on 35-mm diameter plastic dishes coated with poly-L-lysine at a density of 2.0×10^6 cells/ml in basal modified Eagle's medium containing 10% fetal bovine serum, 25 mM KCl, 2 mM L-glutamine, and penicillin (100 units/ml)/streptomycin (100 μg/ml) (Invitrogen). Cytosine arabinoside (10 μM) was added to the culture medium 24 h after plating to limit the growth of non-neuronal cells. Using this protocol, the cultures were ~95% pure for granule neurons. In general, experiments were performed after 7 days in culture.

Preparation of Adenoviral Dominant-negative MEF2 and Adenoviral Infection—pcDNA3.1-MEF2A131 was tagged on the C terminus with the FLAG epitope by polymerase chain reaction. The resulting FLAG-tagged construct was cloned into shuttle vector, and Ad-Flag-MEF2A131 was prepared using the Ad-Easy adenovirus expression kit according to the manufacturer's instructions (Quantum Biotechnologies Inc.). Recombinant adenoviruses were purified by cesium chloride gradient ultracentrifugation. The viral titer was determined by measuring the absorbance at 260 nm (where 1.0 absorbance units = 1×10^{12} particles/ml) and infectious particles were verified by plaque assay. Ad-GFP or Ad-FLAG-MEF2A131 was added to CGN cultures on day 4 at a multiplicity of infection (m.o.i.) of 100. On day 7 (72-h postinfection), CGN apoptosis was assessed in GFP-positive or FLAG-immunoreactive cells by DAPI staining.

Quantification of Apoptosis—Apoptosis was assessed by fixing CGNs in 4% paraformaldehyde and staining nuclei with either Hoechst dye (non-permeabilized cells) or DAPI (permeabilized cells for immunocytochemistry). Cells were considered apoptotic if their nuclei were either condensed or fragmented. In general, ~500 cells from at least two fields of a 35-mm well were counted. For immunocytochemical studies where cells were plated on glass coverslips, ~100–200 cells from 2–3 coverslips per treatment group were counted. Data are presented as the percentage of cells in a given treatment group which were scored as apoptotic. Experiments were performed on cells isolated from at least three independent preparations.

Immunocytochemistry—CGNs were cultured on polyethyleneimine-coated glass cover slips at a density of $\sim 2.5 \times 10^5$ cells per coverslip. Following incubation as described under "Results," cells were fixed in 4% paraformaldehyde and were then permeabilized and blocked in PBS (pH 7.4) containing 0.2% Triton X-100 and 5% BSA. Cells were then incubated for ~16 h at 4 °C with primary antibody diluted in PBS containing 0.2% Triton X-100 and 2% BSA. The primary antibody was aspirated and the cells were washed five times with PBS. The cells were then incubated with either Cy3-conjugated or FITC-conjugated secondary antibodies and DAPI for 1 h at room temperature. CGNs were then washed five more times with PBS and coverslips were adhered to glass slides in mounting medium (0.1% *p*-phenylenediamine in 75% glycerol in PBS). Fluorescent images were captured using a 63× oil immersion objective on a Zeiss Axioplan 2 microscope equipped with a Cooke Sensicam deep-cooled CCD camera and a Slidebook software analysis program for digital deconvolution (Intelligent Imaging Innovations Inc., Denver, CO).

Preparation of CGN Cell Extracts—After incubation for the indicated times and with the reagents specified in Results, the culture medium was aspirated; the cells were washed once with 2 ml of ice-cold PBS, pH 7.4, placed on ice, and scraped into lysis buffer (200 μl/35-mm well) containing 20 mM HEPES (pH 7.4), 1% Triton X-100, 50 mM NaCl, 1 mM EGTA, 5 mM β-glycerophosphate, 30 mM sodium pyrophosphate, 100 μM sodium orthovanadate, 1 mM phenylmethylsulfonyl fluoride, 10 μg/ml leupeptin, and 10 μg/ml aprotinin. Cell debris was removed by centrifugation at $6,000 \times g$ for 3 min and the protein concentration of the supernatant was determined using a commercially available protein assay kit (Pierce). Aliquots (~150 μg) of supernatant protein were diluted to a final concentration of 1× SDS- PAGE sample buffer, boiled for 5 min, and electrophoresed through 7.5% polyacrylamide gels. Proteins were transferred to polyvinylidene difluoride (PVDF) membranes (Millipore, Bedford, MA) and processed for immunoblot analysis.

Western Blot Analysis—Nonspecific binding sites were blocked in PBS (pH 7.4) containing 0.1% Tween 20 (PBS-T) and 1% BSA for 1 h at room temperature. Primary antibodies were diluted in blocking solution and incubated with the membranes for 1 h. Excess primary antibody was removed by washing the membranes three times in PBS-T. The blots were then incubated with the appropriate horseradish peroxidase-conjugated secondary antibody diluted in PBS-T for 1 h and were subsequently washed three times in PBS-T. Immunoreactive proteins were detected by enhanced chemiluminescence. Autoluminograms shown are representative of at least three independent experiments.

Immunoprecipitation of MEF2D—CGN lysates were prepared as described above, except in lysis buffer containing 0.1% Triton X-100. 4 μg of polyclonal antibody against MEF2D was added to 500 μl of lysate (~1 μg/μl CGN protein concentration), and samples were mixed for 16 h at 4 °C by continuous inversion. Agarose-conjugated protein A/G (40 μl) was added and samples were mixed for a further 4 h. Immune complexes were pelleted, washed three times with lysis buffer containing 0.1% Triton X-100, and boiled in 1× SDS-PAGE sample buffer. Immune complexes were resolved on 7.5% polyacrylamide gels, transferred to polyvinylidene difluoride, and immunoblotted for MEF2D and HDAC5.

CGN Transfection and Reporter Gene Expression—CGNs were transiently transfected using a calcium phosphate co-precipitation method described previously (14). Cells were co-transfected with 1 μg of MEF2-luciferase expression plasmid (pGL2-MEF2-luc), 1 μg of pCMV-β-gal as an internal control for transfection efficiency, and 2 μg of either pcDNA3.1, MEF2A131, or HA-tagged HDAC5. The total amount of DNA for each transfection was kept constant. Following transfection, neurons were placed in conditioned medium and the medium was subsequently changed to serum-free containing either 25 mM KCl or 5 mM KCl. After incubation, cell extracts were prepared using reporter lysis buffer and the activities of luciferase and β-galactosidase were measured with the respective enzyme assay system kits (Promega).

Incubation with Antisense Oligonucleotides to CaMKIIα—Phospho-

rothioate, FITC-labeled or unlabeled, antisense oligonucleotides to CaMKIIα, or a scrambled missense control oligonucleotide, were added directly to the culture medium (each at a final concentration of 1 μM), as was previously described for primary hippocampal neuronal cultures (23). Following incubation for 8–24 h, cells were processed for immunocytochemical analysis and/or quantification of apoptosis, as described under "Results."

Data Analysis—The results shown represent the means ± S.E. for the number (n) of independent experiments that were performed. Statistical differences between the means of unpaired sets of data were evaluated by one-way analysis of variance, followed by a post-hoc Dunnett's test. A p value of <0.01 was considered statistically significant.

RESULTS

Adenoviral Expression of a Dominant-negative MEF2 Mutant Blocks Depolarization-mediated Survival of CGNs—In CGNs co-transfected with a MEF2-luciferase reporter (24) and empty pcDNA3.1 vector, removal of the depolarization stimulus resulted in a dramatic loss of MEF2 activity (14 ± 2% of control, $p < 0.01$, Fig. 1*A*). This effect was mimicked under depolarizing conditions by co-transfection with a truncated, dominant-negative form of MEF2 (MEF2A131) that lacks the transcriptional activation domain. Expression of MEF2A131 decreased endogenous MEF2 activity in the presence of depolarization to 39 ± 6% ($p < 0.01$) of that observed in cells transfected with empty vector (Fig. 1*A*). Thus, dominant-negative MEF2 competes with endogenous MEF2 transcription factors for DNA binding, resulting in a loss of endogenous MEF2 activity.

Previous studies showing that MEF2 transcription factors are critical for CGN survival utilized either transient transfection protocols of MEF2 mutants (12, 14) or, more recently, RNA interference methodology to knock down expression of MEF2 proteins (15). One limitation of each of these approaches is that only a small percentage (usually <5%) of the CGNs are transfected. As a means of interfering with MEF2 activity in a larger, and possibly more representative, percentage of the CGN culture, we prepared a FLAG epitope-tagged MEF2A131 and expressed this construct in adenovirus. CGNs maintained in depolarizing medium were then infected with either adenovirus expressing green fluorescent protein (Ad-GFP, to serve as a control for adenoviral infection) or expressing the FLAG-tagged dominant-negative MEF2 (Ad-FLAG-MEF2A131). Each adenovirus was infected into the cells at an m.o.i. of 100 (equivalent to 10,000 infectious particles per cell). At this titer, the relative infection efficiency observed over three independent experiments was ~35% for Ad-FLAG-MEF2A131. Following infection, cells were incubated for 72 h and MEF2A131-expressing cells were identified by immunocytochemistry with a monoclonal anti-FLAG and a Cy3-conjugated secondary antibody. GFP-positive cells were detected by fluorescence under a FITC filter. Apoptosis was quantified by staining nuclei with DAPI and counting the percentage of GFP-positive or FLAG-MEF2A131-positive cells containing condensed and/or fragmented chromatin. As shown in Fig. 1*B*, infection with Ad-GFP did not result in significant CGN apoptosis (2 ± 1%), whereas cells expressing the FLAG-MEF2A131 demonstrated massive apoptosis (89 ± 7%), even in the presence of depolarization. In agreement with previous work (12, 14, 15), our results using an adenoviral dominant-negative MEF2 mutant demonstrate that MEF2 transcriptional activity is a critical component of depolarization-mediated survival signaling in CGNs.

Overexpression of the MEF2 Repressor HDAC5 Induces CGN Apoptosis in Depolarizing Medium—The activity of MEF2 transcription factors is repressed in skeletal, cardiac, and smooth muscle by members of the class II family of HDACs including HDAC4, 5, 7, and 9 (reviewed in Ref. 6). Consistent with a potential role for HDAC regulation of MEF2 activity in CGNs, overexpression of HA-tagged HDAC5 significantly decreased MEF2-driven luciferase activity (56 ± 6% of the empty vector control, $p < 0.01$) in cells cultured in the presence of depolarizing potassium (Fig. 2*A*). As a result of the loss in endogenous MEF2 activity, overexpression of HDAC5 induced significant CGN apoptosis (42 ± 1% compared with 17 ± 1% in cells transfected with empty vector, $p < 0.01$, Fig. 2*B*). Similar results were obtained following transfection with another class II family member, HDAC4 (data not shown). Thus, depolarization-mediated MEF2 activity and CGN survival are compromised by overexpression of HDAC transcriptional repressors.

Removal of Depolarizing Potassium or CaMK Inhibition

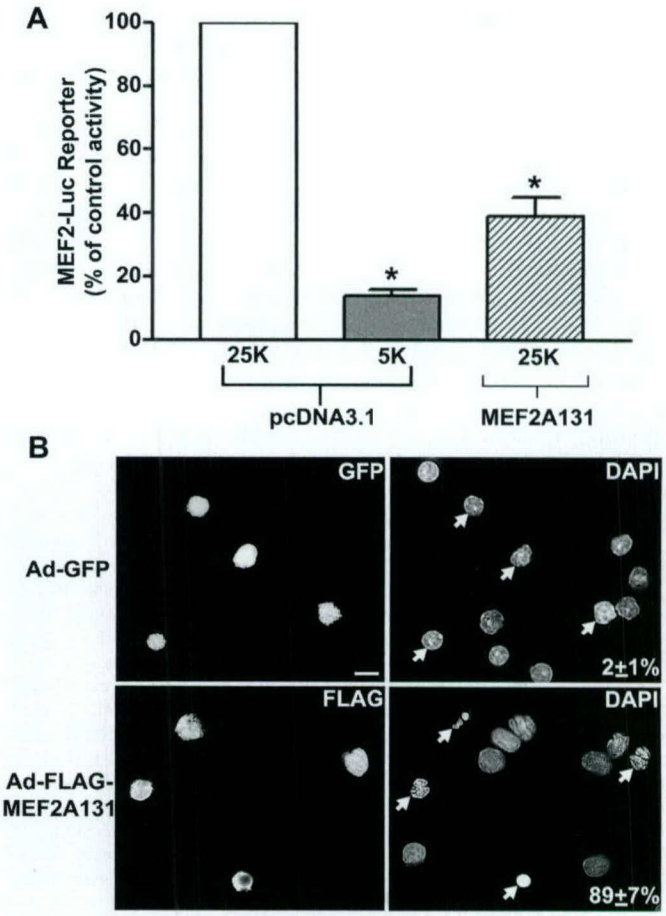

FIG. 1. **A truncated mutant of MEF2A acts as a dominant-negative transcription factor and inhibits depolarization-mediated survival of CGNs.** *A*, CGNs (day 7 *in vitro*) were transiently co-transfected with a MEF2-responsive luciferase reporter plasmid and pCMV-β-gal in the presence of either empty vector (pcDNA3.1) or a truncated mutant of MEF2A lacking the transcriptional activation domain (MEF2A131). After transfection, cells were placed in serum-free medium containing either 25 mM KCl (*25K*) or 5 mM KCl (*5K*). Luciferase and β-galactosidase activities were determined and luciferase activity was normalized with respect to that of β-galactosidase. Data are expressed as a percentage of the activity in control neurons transfected with empty vector. Results represent the mean ± S.E. for three independent experiments each performed in duplicate. *, significantly different from the empty vector control in 25K ($p < 0.01$). *B*, on day 4 *in vitro*, CGNs were placed in 25K medium and were infected with either adenovirus expressing green fluorescent protein (Ad-GFP) or expressing a FLAG-tagged truncated MEF2A (Ad-Flag-MEF2A131), each at a titer of 100 m.o.i. Cells were incubated for 72 h following infection and immunocytochemistry for the FLAG epitope was performed. GFP-positive cells were detected by fluorescence under a FITC filter. Nuclei were stained with DAPI and apoptosis was quantified by counting the percentage of either GFP-positive or FLAG-positive cells that had condensed and/or fragmented chromatin. The values shown represent the mean ± S.E. percent apoptosis for three experiments each performed in triplicate. *Arrows* in the DAPI (*right*) panels point to the corresponding GFP-positive or FLAG-positive cells shown in the *left* panels. *Scale bar*, 10 μm.

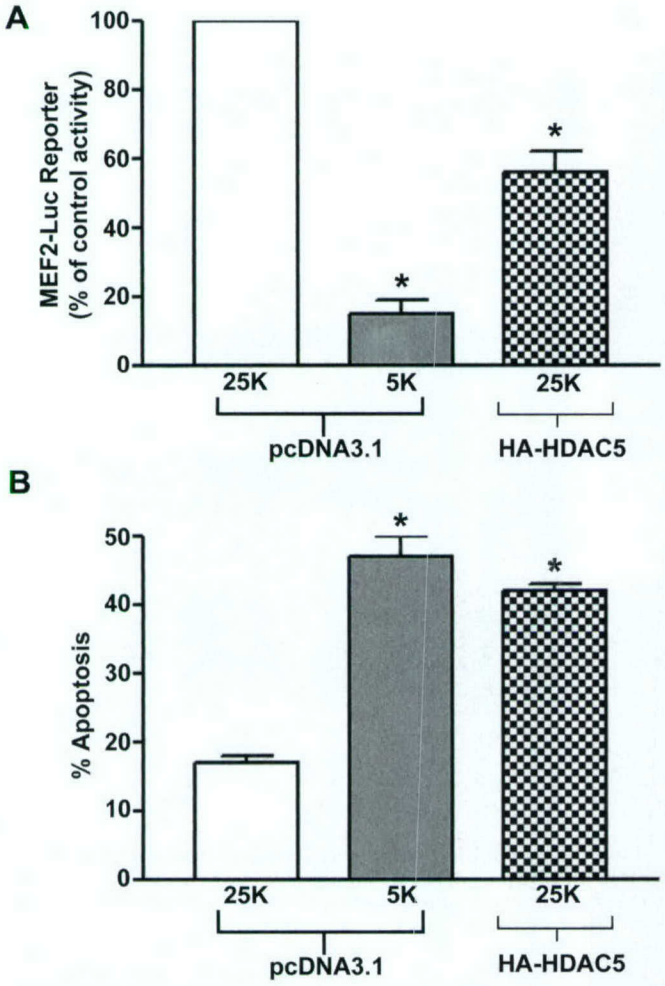

FIG. 2. **Overexpression of HDAC5 inhibits MEF2 activity and induces CGN apoptosis in depolarizing medium.** *A*, CGNs (day 7 *in vitro*) were transiently co-transfected with a MEF2-responsive luciferase reporter plasmid and pCMV-β-gal in the presence of either empty vector (pcDNA3.1) or HA-tagged HDAC5. After transfection, cells were placed in serum-free medium containing either 25 mM KCl (*25K*) or 5 mM KCl (*5K*). Luciferase and β-galactosidase activities were determined and luciferase activity was normalized with respect to that of β-galactosidase. Data are expressed as a percentage of the activity in control neurons transfected with empty vector. Results represent the mean ± S.E. for three independent experiments each performed in duplicate. *, significantly different from the empty vector control in 25K ($p < 0.01$). *B*, CGNs were transfected with either empty vector or HA-HDAC5 and then placed in either 25K or 5K medium for an additional 24 h. CGN apoptosis was quantified by DAPI staining of nuclei. HDAC5 expressing cells were identified by immunoreactivity for the HA epitope tag. The values shown represent the mean ± S.E. percent apoptosis for three experiments each performed in triplicate. *, significantly different from the empty vector control in 25K ($p < 0.01$).

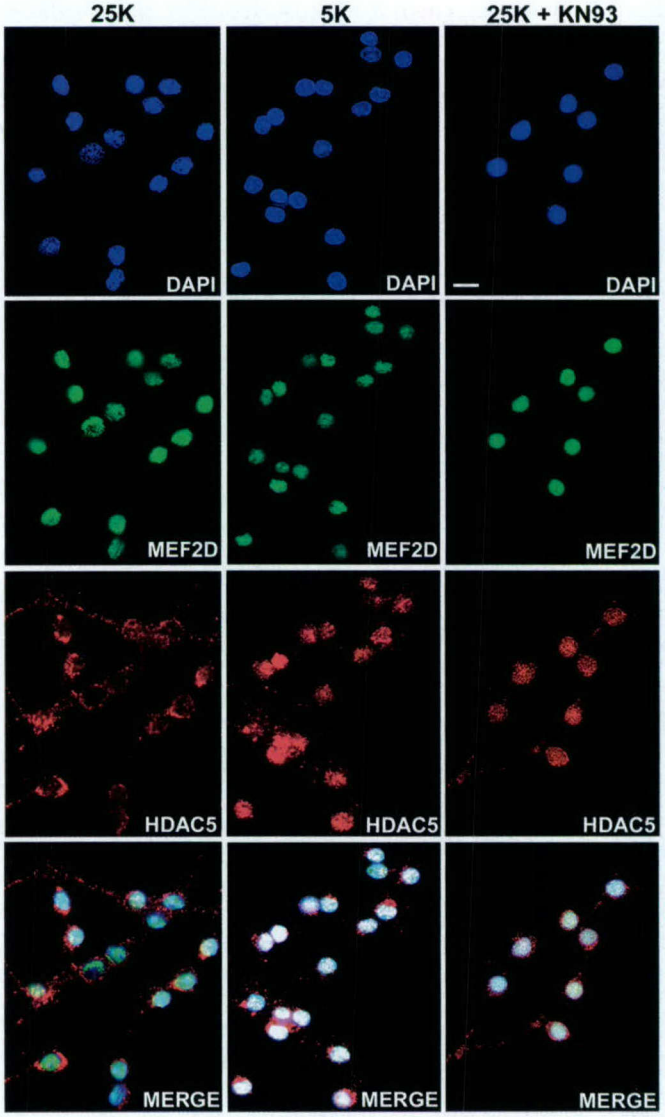

FIG. 3. **Cytoplasm-to-nuclear translocation of endogenous HDAC5 is induced in CGNs deprived of depolarizing potassium or incubated with the CaMK inhibitor KN93.** CGNs (day 7 *in vitro*) were incubated for 4 h in serum-free medium containing either 25 mM KCl (*25K*), 5 mM KCl (*5K*), or 25K+KN93 (5 μM). Following incubation, cells were fixed in 4% paraformaldehyde, permeabilized with 0.2% Triton X-100, and blocked in 5% BSA. HDAC5 and MEF2D were immunocytochemically localized by incubating the cells with a polyclonal antibody to HDAC5 and a monoclonal antibody to MEF2D followed by Cy3-conjugated and FITC-conjugated secondary antibodies, respectively. Nuclei were identified by DAPI staining. Digitally deconvolved images were captured using a 63× oil objective. The images shown are representative of results obtained in three independent experiments. The bottom row shows the merged images of the DAPI, FITC, and Cy3 channels. Note that MEF2D was exclusively nuclear under all conditions, whereas the localization of HDAC5 changed from cytoplasmic in 25K to nuclear in the 5K and 25K + KN93 conditions. The nuclear colocalization of HDAC5 with MEF2D and DAPI under the 5K and 25K+KN93 conditions is evident by the resultant white overlapping staining in the merged images. *Scale bar*, 10 μm.

Induces Cytoplasm-to-Nuclear Translocation of Endogenous HDAC5—We next examined the subcellular localization of endogenous HDAC5 and MEF2D in CGNs maintained in either depolarizing or non-depolarizing medium. Cells cultured in the presence of depolarizing extracellular potassium demonstrated immunocytochemical localization of HDAC5 in the cytoplasm with little to no immunoreactivity observed in nuclei. In contrast, MEF2D was localized exclusively to nuclei, and therefore, there was essentially no overlapping staining for MEF2D and HDAC5 in control CGNs (Fig. 3, *left panels*). Removal of depolarizing potassium for 4 h induced a dramatic cytoplasm-to-nuclear translocation of endogenous HDAC5, resulting in significant overlap of MEF2D and HDAC5 staining (Fig. 3, *middle panels*).

Previous work in skeletal and cardiac muscle has shown that the subcellular localization of class II HDACs during muscle differentiation can be regulated by CaMK activity (19, 20). Overexpression of either constitutively active CaMKI or CaMKIV induced phosphorylation of two serine residues (Ser-259 and Ser-498 in HDAC5) resulting in docking of HDACs to cytoplasmic scaffolding proteins of the 14-3-3 family (21). In this manner, CaMK-mediated phosphorylation of HDACs results in their nuclear exclusion, allowing for derepression of MEF2 activity that is required for muscle differentiation. To

examine if depolarization maintains HDAC5 in the cytoplasm of CGNs via endogenous CaMK activity, cells were incubated in depolarizing medium containing the CaMK inhibitor KN93. Inclusion of KN93 mimicked the effect of removing the depolarization stimulus, resulting in nuclear translocation of HDAC5 and its co-localization with MEF2D (Fig. 3, *right panels*). In a similar manner, either removal of the depolarization stimulus or addition of KN93 also induced the nuclear translocation of HDAC4 in CGNs (data not shown). These data suggest that depolarization promotes the nuclear exclusion of HDAC5 and 4 via the activity of an endogenous CaMK.

CaMK Inhibition Results in Dephosphorylation of HDAC5 and Its Association with MEF2D—To evaluate the phosphorylation status of endogenous HDAC5 in CGNs, we examined the electrophoretic mobility of HDAC5 on SDS-polyacrylamide gels. In cell lysates obtained from CGNs maintained in depolarizing medium, HDAC5 appeared as a broad band or doublet on Western blots (Fig. 4*A*, *first lane*). Removal of depolarizing potassium (Fig. 4*A*, *second lane*) or addition of the CaMK inhibitor, KN93 (Fig. 4*A*, *third lane*), increased the electrophoretic mobility of HDAC5 and resulted in the disappearance of the upper band of the doublet, indicative of a loss of the phosphorylated HDAC5 species. These results suggest that a CaMK activated by depolarization in CGNs regulates the phosphorylation status of HDAC5.

To determine if the dephosphorylation and nuclear translocation of HDAC5 induced by removal of the depolarization stimulus or CaMK inhibition permits its direct interaction with nuclear MEF2 proteins, we performed co-immunoprecipitation experiments. MEF2D immune complexes isolated from CGNs maintained in depolarizing medium did not contain any detectable HDAC5 (Fig. 4*B*, *first lane*). This finding is consistent with the immunocytochemical data shown in Fig. 3 that demonstrated little co-localization of MEF2D and HDAC5 under control conditions. In contrast, MEF2D isolated from cells incubated in either non-depolarizing medium or in the presence of KN93 co-precipitated with HDAC5 (Fig. 4*B*, *second* and *third lanes*). Note that the electrophoretic mobility of MEF2D was significantly retarded in cells cultured in non-depolarizing medium, consistent with its hyperphosphorylation under these conditions as we have previously reported (14, 25). Interestingly, CaMK inhibition also resulted in some decreased mobility of MEF2D, suggesting that HDAC5 association with MEF2D may alter the accessibility of MEF2D to phosphatases (*e.g.* calcineurin). Collectively, these data suggest that inhibition of CaMK activity in CGNs promotes the dephosphorylation and nuclear translocation of HDAC5, ultimately resulting in its co-association with MEF2 transcription factors.

CaMK Inhibition Blocks Depolarization-mediated MEF2 Activity and Survival of CGNs—To determine the functional consequences of HDAC5 nuclear translocation and its interaction with MEF2D, we next examined the effects of CaMK inhibition on MEF2 transcriptional activity and CGN survival. Incubation of CGNs with the CaMK inhibitors, KN93 or KN62, induced a marked decrease in endogenous MEF2 activity measured with a MEF2-driven luciferase reporter gene (Fig. 5*A*). Moreover, CaMK inhibition induced significant CGN apoptosis in the presence of depolarizing potassium (Fig. 5*B*). Apoptosis induced by KN93 was characterized morphologically by substantial chromatin fragmentation, microtubule disruption, and caspase-3 activation (Fig. 5*C*). These results demonstrate that inhibition of endogenous CaMK activity is sufficient to induce nuclear translocation of the MEF2 repressor, HDAC5, resulting in a loss of MEF2 activity and induction of CGN apoptosis.

Antisense to CaMKIIα Induces Nuclear Translocation of HDAC5—Previous work in skeletal muscle describing the regulation of HDAC localization by CaMK activity has relied on overexpression of various CaMK isoforms (19). To date, identification of the endogenous CaMK isozyme(s) involved in HDAC regulation has not been reported. The CaMK enzyme family is made up of several distinct isoforms, including CaMK I, II, and IV, with four distinct genes (α, β, δ, γ) coding for members of the CaMKII subfamily (26). Of the many CaMK isozymes identified, only CaMKIIα is exclusively expressed in the brain (27). The CaMK inhibitors, KN93 and KN62, lack isozyme specificity and have been shown to inhibit the activities of CaMKI, II and IV (28, 29). To selectively evaluate a role for CaMKII in regulating the subcellular localization of HDAC5 in CGNs, cells were incubated with a CaMKIIα-specific antisense oligonucleotide. This antisense construct has previously been reported to reduce CaMKIIα expression and induce epileptiform

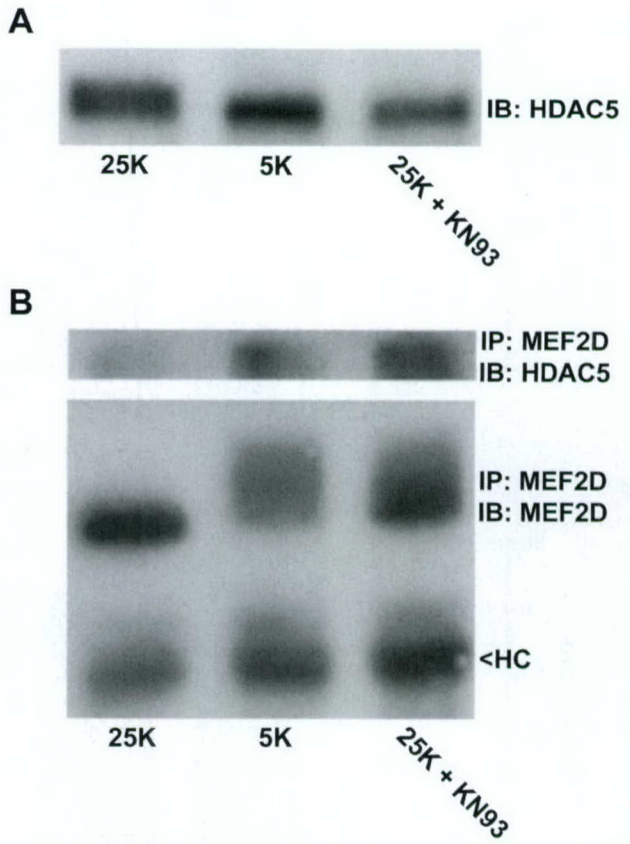

FIG. 4. **Removal of depolarizing potassium or addition of the CaMK inhibitor KN93 promotes an increased mobility of HDAC5 on polyacrylamide gels and association of HDAC5 with MEF2D.** *A*, CGNs (day 7 *in vitro*) were incubated for 4 h in serum-free medium containing either 25 mM KCl (*25K*), 5 mM KCl (*5K*), or 25K+KN93 (5 μM). Following incubation, detergent-soluble cell lysates were subjected to SDS-PAGE on 5% polyacrylamide gels and the proteins were subsequently transferred to polyvinylidene difluoride membranes. HDAC5 was detected by immunoblotting (*IB*) with a polyclonal antibody and a horseradish-peroxidase-conjugated secondary. Immunoreactive proteins were detected by enhanced chemiluminescence. The blot shown is representative of results obtained in three separate experiments. Note that HDAC5 runs as a broad apparent doublet in 25K, whereas under the 5K or 25K+KN93 conditions the upper band of the doublet disappears, indicative of an enhanced mobility of HDAC5 under these conditions. *B*, CGNs were incubated exactly as described in *A* and cell lysates were prepared. MEF2D was immunoprecipitated (*IP*) from the cell lysates using a polyclonal antibody and immune complexes were resolved on 7.5% gels. The membranes were cut at the 75 kDa standard and the upper portion of the blot was probed for HDAC5 while the lower portion was probed for MEF2D. The blots shown are indicative of data observed in two independent experiments. Note that HDAC5 was only detectable in MEF2D immune complexes obtained from CGNs incubated in either 5K or 25K+KN93 conditions. *HC*, immunoglobulin heavy chain from the precipitating antibody.

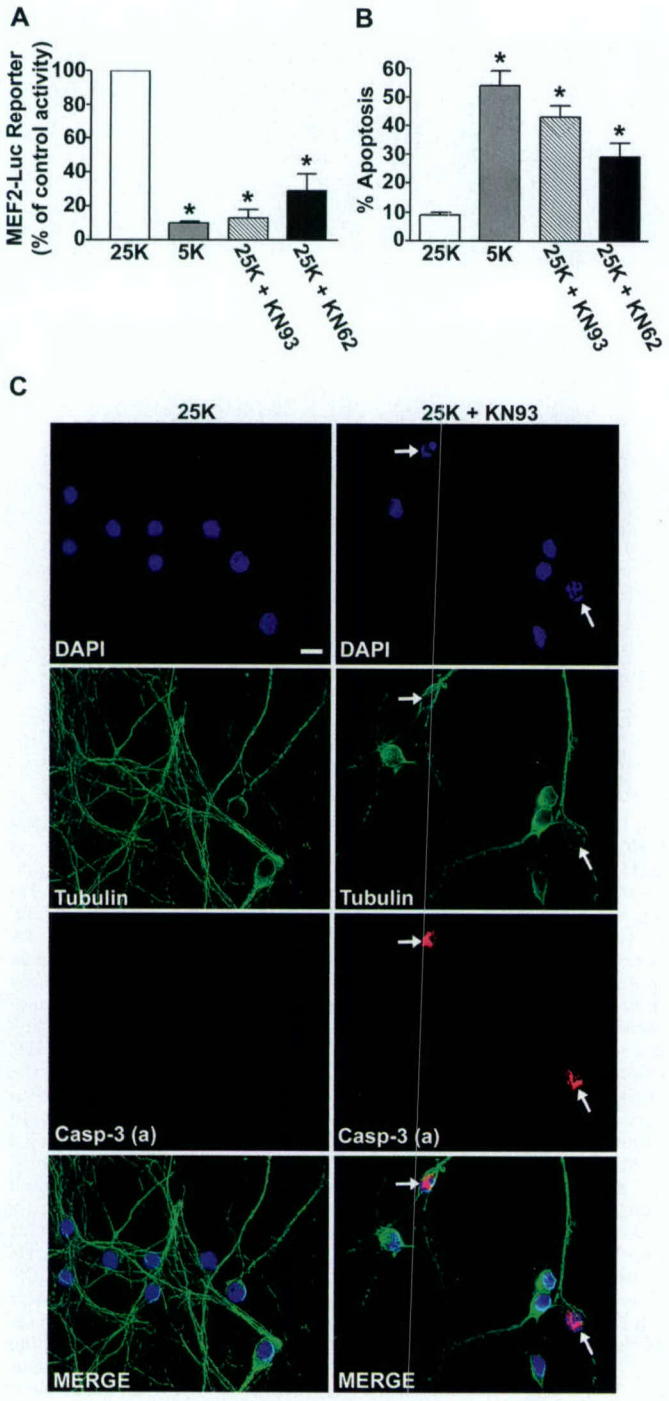

FIG. 5. **The CaMK inhibitors, KN93 and KN62, block depolarization-mediated MEF2 transcriptional activity and induce apoptosis of CGNs.** *A*, CGNs (day 7 *in vitro*) were transiently co-transfected with a MEF2-responsive luciferase reporter plasmid and pCMV-β-gal. After transfection for 2 h, cells were placed in serum-free medium containing either 25 mM KCl (*25K*) ± KN93 or KN62 (each at 5 μM) or 5 mM KCl (*5K*). Luciferase and β-galactosidase activities were determined 4 h later and luciferase activity was normalized with respect to that of β-galactosidase. Data are expressed as a percentage of the activity in control neurons transfected with empty vector. Results represent the mean ± S.E. for three independent experiments each performed in duplicate. *, significantly different from the 25K control ($p < 0.01$). *B*, CGNs (day 6 *in vitro*) were incubated in either 25K medium ± KN93 or KN62 or 5K medium for 24 h. CGN apoptosis was quantified by Hoechst staining of nuclei. The values shown represent the mean ± S.E. percent apoptosis for three experiments each performed in triplicate. *, significantly different from the 25K control ($p < 0.01$). *C*, CGNs incubated for 24 h in 25K medium alone (*left panels*) or containing KN93 (*right panels*) were fixed in 4% paraformaldehyde, permeabilized with 0.2% Triton X-100, and blocked in 5% BSA. β-tubulin and active (cleaved) caspase-3 [Casp-3 (a)] were immunostained by incubating the cells with a monoclonal antibody to tubulin and a polyclonal antibody that specifically recognizes the active fragment of caspase-3, followed by FITC-conjugated and Cy3-conjugated secondary antibodies, respectively. Nuclei were identified by DAPI staining. Digitally deconvolved images were captured using a 63× oil objective. The images shown are representative of results obtained in three independent experiments. The *bottom panels* show the merged images of the DAPI, FITC, and Cy3 channels. *Arrows* point to cells in the KN93 treated culture that demonstrate significant chromatin fragmentation and immunoreactivity for active caspase-3. Also, note the substantial loss of fine microtubule staining in the KN93-treated culture. *Scale bar*, 10 μm.

activity in primary cultured hippocampal neurons (23).

Addition of 1 μM FITC-labeled, phosphorothioate antisense oligonucleotide to CaMKIIα to CGN cultures for 8 h resulted in a marked reduction in CaMKIIα immunoreactivity in cells expressing the FITC-antisense when compared with cells in the same field that did not take up the antisense construct (Fig. 6*A*). In general, ~25% of the CGNs took up the FITC-labeled CaMKIIα antisense following 8–24 h of incubation at a concentration of 1 μM. Granule neurons expressing the FITC-CaMKIIα antisense demonstrated a dramatic redistribution of endogenous HDAC5 from the cytosol to the nucleus, even when maintained in depolarizing medium (Fig. 6*B*). In contrast, cells in the same field that did not express the antisense showed HDAC5 localization that was extensively cytoplasmic. These results indicate that the endogenous CaMKII isozyme regulates depolarization-mediated cytoplasmic localization of HDAC5 in CGNs.

Antisense to CaMKIIα Does Not Affect CaMKIV-dependent Phosphorylation of CREB—To confirm the selectivity of the CaMKIIα antisense, we examined its effects on phosphorylation of the CaMKIV substrate, cAMP-response element binding protein (CREB). A recent study demonstrated that CaMKIV activity promotes depolarization-mediated CGN survival via phosphorylation of CREB on the activating Ser-133 (30). As shown in Fig. 7*A* (*upper panels*), CREB phosphorylation on Ser-133 was high in CGNs maintained in depolarizing medium. Addition of the CaMK inhibitor, KN93, resulted in a complete loss of CREB phosphorylation (Fig. 7*A*, *lower panels*). This latter result is consistent with the relative non-selectivity of KN93 for the various isoforms of CaMK (28, 29). In contrast, the FITC-labeled antisense to CaMKIIα had no significant effect on CREB phosphorylation after 8 h of incubation (Fig. 7*B*, compare the CREB phosphorylation in FITC-positive cells to that in antisense-negative cells), a time point at which it caused significant nuclear translocation of HDAC5 (see Fig. 6*B*). These results demonstrate the selectivity of the CaMKIIα antisense. In addition, they suggest that CaMKII regulation of HDAC localization is an alternative calcium-dependent pathway to CaMKIV/CREB for mediating CGN survival.

Antisense to CaMKIIα Induces Caspase-3 Activation and Apoptosis of CGNs—To determine the extent of CGN apoptosis induced by antisense treatment, we quantified the number of cells with condensed and/or fragmented nuclei in cultures incubated with either the CaMKIIα antisense or a missense control oligonucleotide. Because the missense oligonucleotide was not fluorescently labeled, an unlabeled antisense was utilized in these experiments. The overall basal apoptosis of control CGN cultures maintained in depolarizing medium measured 9 ± 1% ($n = 3$ experiments, performed in triplicate) on day 8 *in vitro*. On day 7 *in vitro*, cells were exposed to either the CaMKIIα antisense or a control missense oligonucleotide for 24 h, each at a final concentration of 1 μM. CGN cultures incubated with the antisense to CaMKIIα demonstrated an overall apoptosis of 33 ± 11% ($n = 3$), whereas cells treated with the missense construct showed apoptosis comparable to

the untreated controls (8 ± 1%, $n = 3$). These results demonstrate that the scrambled missense had no discernible effect on CGN survival when added at the same concentration as the antisense construct.

As mentioned previously, in a given experiment ~25% of the entire culture took up the FITC-labeled antisense. Therefore, the overall apoptosis observed in CGN cultures incubated with the unlabeled antisense was consistent with near complete apoptosis of the antisense-positive cells. To verify this result, we quantitated the fraction of FITC-positive cells that were apoptotic following a 24-h incubation with 1 μM FITC-labeled CaMKIIα antisense. Greater than 95% of the FITC-positive (antisense-positive) CGNs were apoptotic under these conditions, as assessed by nuclear morphology. In agreement with these findings, essentially every cell that accumulated the FITC-labeled antisense to CaMKIIα for 24 h demonstrated substantial immunoreactivity for active (cleaved) caspase-3, whereas surrounding antisense-negative cells in the same field were devoid of active caspase-3 staining (Fig. 8). Thus, antisense-mediated depletion of CaMKIIα inhibits depolarization-dependent survival signaling and induces CGN apoptosis.

DISCUSSION

MEF2 proteins are members of the MADS (MCM1-agamous-deficiens-serum response factor) family of transcription factors (31–33). The mammalian MEF2 family consists of four distinct genes (A, B, C, D) that each code for multiple splice variants (31, 34). MEF2 proteins play a key role in the differentiation and survival of neurons during CNS development. The expression of MEF2 proteins in the developing CNS is regulated temporally and spatially in an isoform-specific manner, and coincides with neuronal maturation. For example, cerebral cortical neuron development is associated with changes in the expression of MEF2C (35–37), whereas CGN maturation is coupled to enhanced expression of MEF2A and MEF2D (9). Their differential tissue distribution suggests that MEF2 proteins may be regulated in an isoform-specific manner. Indeed this is the case in CGNs where MEF2A and MEF2D are phosphorylated and ultimately cleaved by caspases following removal of depolarizing potassium, whereas MEF2B and MEF2C are not modified in this manner (14). These findings indicate that signal transduction pathways which regulate MEF2 activity display both tissue-specific and isoform-specific properties.

To date, the modulation of MEF2 activity by calcium-regulated signals has largely been studied in muscle cells in which MEF2 proteins act as key regulators of myogenic differentiation (5, 6). Given that distinct MEF2 isoforms can be regulated differently, even within the same cell (14), it is unknown if signaling pathways that modulate MEF2 proteins in muscle will necessarily translate directly into neurons. Moreover, MEF2 regulation in muscle has been investigated during either myogenic differentiation (38–40) or hypertrophy (41–43). In contrast, a principal function of MEF2 proteins in neurons is to promote activity-dependent cell survival (12, 15). The signaling pathways that are invoked during muscle differentiation or hypertrophy may be different from those generated in neurons by activity-dependent calcium influx.

Despite these important differences, at least two signaling pathways have been implicated in MEF2 regulation in both muscle and neurons. First, the stress-activated protein kinase, p38 MAP kinase, stimulates MEF2 activity in hypertrophic muscle (41, 44) and in CGNs responding to depolarization (12). Second, the phosphatase, calcineurin, positively regulates MEF2 activity in both muscle cells (16, 45, 46) and CGNs (17). In muscle, p38 MAP kinase and calcineurin cooperate with CaMK to maximally activate MEF2 transcriptional activity (5, 47).

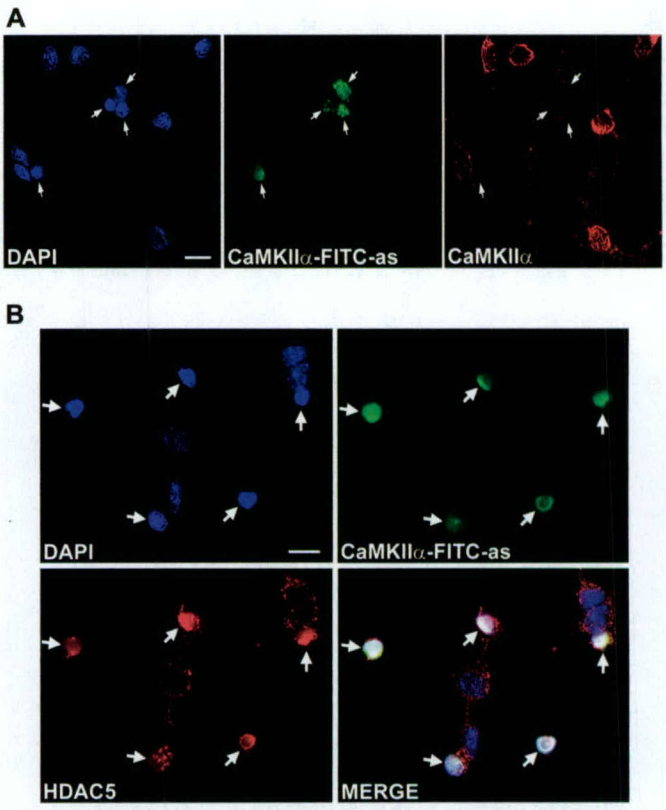

FIG. 6. **An antisense oligonucleotide to CaMKIIα decreases CaMKIIα expression and induces nuclear translocation of HDAC5.** *A*, CGNs (day 7 *in vitro*) were incubated in serum-free medium containing 25 mM KCl (*25K*) and a phosphorothioate, FITC-labeled antisense oligonucleotide to CaMKIIα (CaMKIIα-FITC-as, 1 μM final concentration). After incubation for 8 h, cells were fixed in 4% paraformaldehyde, permeabilized with 0.2% Triton X-100, and blocked in 5% BSA. Expression of endogenous CaMKIIα was then assessed by immunostaining with an isozyme-specific antibody and a Cy3-conjugated secondary. Nuclei were stained with DAPI and CGNs expressing the antisense construct were identified by positive staining in the FITC channel (indicated by the *arrows*). Note that cells positive for the antisense exhibited substantially less immunoreactivity for CaMKIIα than cells in the same field that did not take up the oligonucleotide. In general, ~25% of the entire CGN culture took up the FITC-labeled CaMKIIα antisense. The images shown are indicative of data obtained in two separate experiments. *Scale bar*, 10 μm. *B*, CGNs incubated exactly as described in *A* were immunostained for HDAC5 using a polyclonal antibody and a Cy3-conjugated secondary. The *arrows* point to cells that were positive for the CaMKIIα-FITC-as. Note that CGNs expressing the antisense demonstrated nuclear localization of HDAC5, whereas antisense-negative cells in the same field showed cytoplasmic localization of HDAC5. The *lower right panel* shows the merged image of the DAPI, FITC, and Cy3 channels; note the *white overlapping nuclear staining* in cells expressing the antisense and showing nuclear HDAC5. The results shown are representative of three independent experiments. *Scale bar*, 10 μm.

CaMK-mediated regulation of MEF2 activity in muscle has been proposed to occur primarily by an indirect mechanism. Class II HDAC proteins act as endogenous repressors of MEF2 transcriptional activity by directly interacting with MEF2 proteins in the nucleus (40). Overexpression of active CaMK I or IV derepresses MEF2 activity in muscle by phosphorylating HDACs and promoting their nuclear export (18, 19). CaMK-mediated phosphorylation of HDACs on specific serine residues promotes HDAC binding to cytosolic scaffolding proteins of the 14-3-3 family, resulting in sequestration of HDACs in the cytoplasm (21, 48). In the present study, we demonstrate that *endogenous* CaMKII plays a key role in CGNs to exclude HDACs from the nucleus, and in turn, to derepress MEF2 activity and promote cell survival.

We initially confirmed an essential role for MEF2 activity in

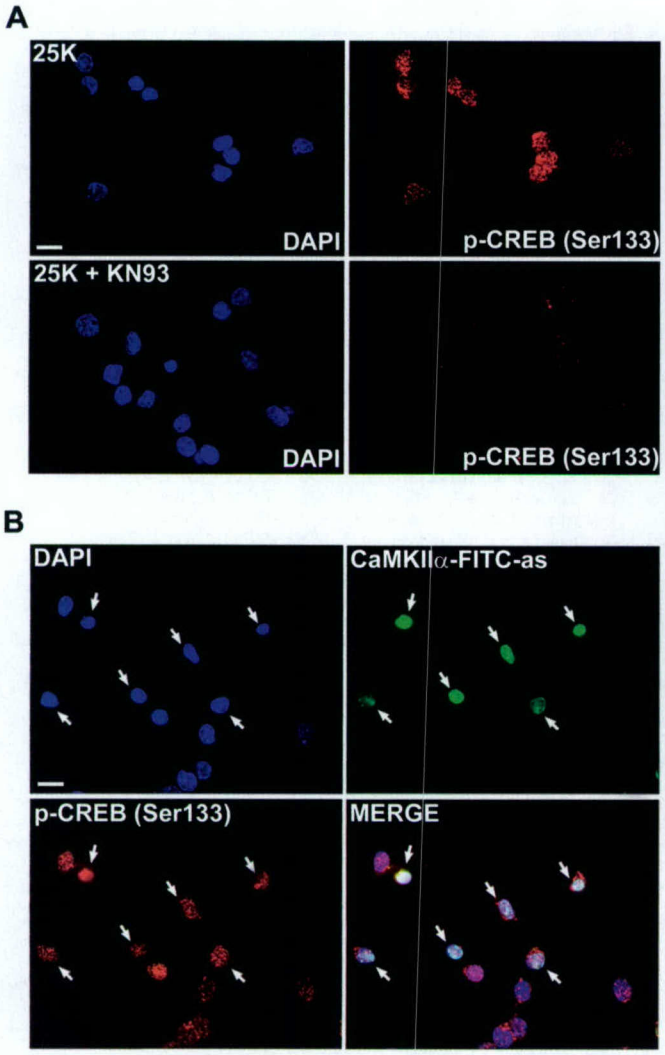

FIG. 7. **CREB phosphorylation in CGNs is not affected by a CaMKIIα antisense oligonucleotide.** *A*, CGNs (day 7 *in vitro*) were incubated for 4 h in serum-free medium containing 25 mM KCl (*25K*) in the absence or presence of KN93 (5 μM). Cells were fixed in paraformaldehyde and CREB phosphorylated on Ser-133 (p-CREB) was identified by staining with a phospho-specific polyclonal antibody and a Cy3-conjugated secondary. Each of the p-CREB images was captured with a 63× oil objective under a Cy3 filter using equal exposure times. Scale bar, 10 μm. *B*, cells were incubated for 8 h in 25K medium containing a FITC-labeled antisense oligonucleotide to CaMKIIα (CaMKIIα-FITC-as, 1 μM final concentration). Following incubation, cells were immunostained for p-CREB. *Arrows* point to CGNs that were positive for the FITC-labeled antisense. Note that all of the cells demonstrated similar immunoreactivity for p-CREB regardless of whether or not they expressed the CaMKIIα antisense. The images shown are indicative of three independent experiments. *Scale bar*, 10 μm.

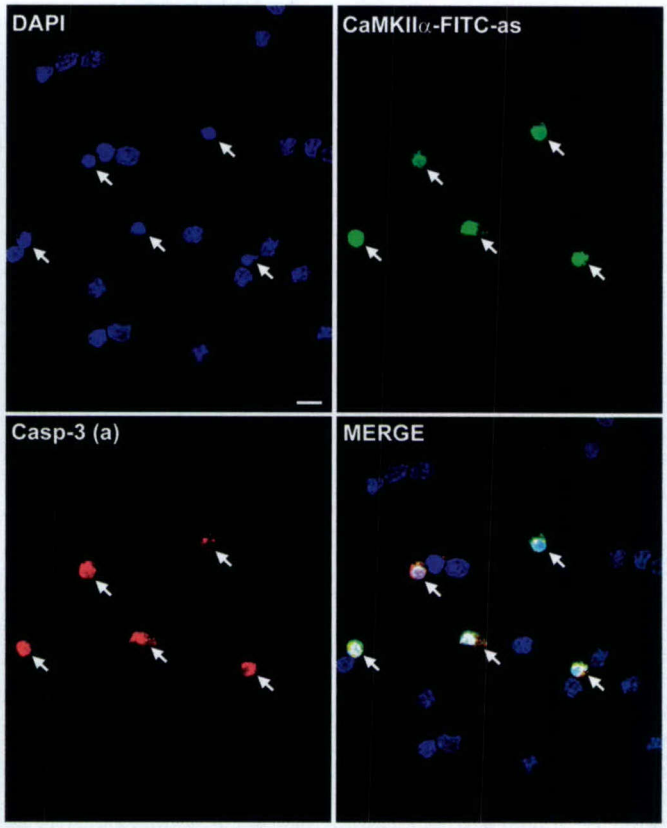

FIG. 8. **Antisense to CaMKIIα induces caspase-3 activation in CGNs maintained in depolarizing medium.** CGNs (day 7 *in vitro*) were incubated in serum-free medium containing 25 mM KCl (25K) and a phosphorothioate, FITC-labeled antisense oligonucleotide to CaMKIIα (CaMKIIα-FITC-as, 1 μM final concentration). After incubation for 24 h, cells were fixed in 4% paraformaldehyde, permeabilized with 0.2% Triton X-100, and blocked in 5% BSA. Activation of caspase-3 was assessed by immunostaining with a polyclonal antibody that specifically recognizes the active (cleaved) form of the caspase (Casp-3(a)), followed by a Cy3-conjugated secondary. Nuclei were stained with DAPI and CGNs expressing the antisense construct were identified by positive staining in the FITC channel (indicated by the *arrows*). Note that cells positive for the antisense exhibited high immunoreactivity for active caspase-3, whereas cells in the same field that did not take up the oligonucleotide showed no staining for active caspase. The images shown are representative of two independent experiments. *Scale bar*, 10 μm.

CGN survival by demonstrating that adenoviral infection of a truncated, dominant-interfering mutant of MEF2 (MEF2A131) is sufficient to induce apoptosis of CGNs that are maintained in depolarizing medium. To examine a potential role for HDACs in the regulation of MEF2 activity in CGNs, the effects of overexpressing the class II HDAC, HDAC5, on MEF2 activity and CGN survival were assessed. Transient transfection of CGNs with HDAC5 induced a significant loss of endogenous MEF2 transcriptional activity and substantial apoptosis under depolarizing conditions.

To directly investigate the involvement of endogenous HDAC5 in regulating MEF2 activity, we next analyzed the subcellular localization of MEF2D and HDAC5 in CGNs. As expected, the transcription factor MEF2D was exclusively nuclear under all conditions tested. In contrast, endogenous HDAC5 was extensively cytoplasmic in CGNs cultured in depolarizing medium. Either removal of the depolarization stimulus or addition of the CaMK inhibitor, KN93, induced a marked translocation of HDAC5 into the nucleus where it co-localized with MEF2D. While this article was in preparation, Chawla *et al.* (49) described a partial inhibition of HDAC5 nuclear export in hippocampal neurons following incubation with a similar CaMK inhibitor, KN62. However, these authors did not examine the effects of CaMK inhibition on MEF2 activity or neuronal survival downstream of HDAC shuttling. In the current study performed in CGNs, the nuclear translocation of HDAC5 was associated with its enhanced mobility on polyacrylamide gels (consistent with its dephosphorylation) and its co-precipitation with MEF2D. Collectively, these data indicate that depolarization-mediated calcium influx stimulates the activity of an endogenous CaMK that, in turn, phosphorylates HDAC5 and inhibits its nuclear localization.

The ultimate consequence of removing the depolarization stimulus from cerebellar cultures is the apoptotic death of CGNs (13, 50). Loss of MEF2 transcriptional activity precedes CGN death under non-depolarizing conditions and apoptosis can be attenuated by expression of a constitutively active

MEF2 mutant (12, 14). Previous work suggests a role for CaMK activity in depolarization-mediated survival of CGNs (51). In agreement with this, addition of the CaMK inhibitors, KN93 or KN62, to CGNs maintained in depolarizing medium mimicked the loss of MEF2 activity and induction of CGN apoptosis that normally occur under non-depolarizing conditions. The ability of CaMK inhibitors to induce the nuclear translocation of HDAC5 and the consequent loss of MEF2 activity suggests that an endogenous CaMK isozyme(s) actively derepresses MEF2-dependent transcription of putative pro-survival genes in CGNs maintained in depolarizing medium.

The regulation of HDAC localization by CaMK in muscle and other non-neuronal cells has been analyzed primarily by overexpression of various CaMK isoforms, including constitutively active mutants of CaMKI and IV (19, 48). Thus far, the endogenous CaMK isozyme(s) involved in HDAC regulation has not been identified. CaMKIIα is a brain-specific CaMK isozyme best known for its role in hippocampal long term potentiation, a cellular model of learning and memory (52). However, CaMKIIα is also expressed in cerebellum (53), where it has been implicated in CGN neurite outgrowth (51, 54). Since the CaMK inhibitors, KN93 and KN62, lack isozyme selectivity (28, 29), we utilized an antisense strategy to specifically interfere with CaMKII signaling in CGNs.

Recently, direct addition of a phosphorothioate antisense oligonucleotide to CaMKIIα to primary hippocampal neurons was shown to substantially decrease CaMKIIα expression *in vitro* (23). We found that addition of an identical FITC-labeled CaMKIIα antisense oligonucleotide to CGN cultures maintained in depolarizing medium resulted in a marked loss of CaMKIIα immunoreactivity and nuclear translocation of HDAC5. In contrast, this antisense construct had no discernible effect on phosphorylation of the CaMKIV substrate, CREB, demonstrating the specificity of the oligonucleotide for CaMKII. Finally, antisense to CaMKIIα induced caspase-3 activation and apoptosis, whereas a scrambled missense control oligonucleotide had no effect on CGN survival. Collectively, these results indicate that CaMKII is an important endogenous regulator of HDAC5 localization and MEF2-mediated survival of CGNs.

Our data implicating CaMKII in neuronal survival support previous findings suggesting that reductions in CaMKII activity contribute to neuronal death induced by excitotoxicity or ischemia *in vitro* and *in vivo* (55–58). Since loss of MEF2 activity has recently been implicated in excitotoxic and ischemic neuronal death (59), it will be interesting to determine if nuclear localization of HDAC5 (or other class II family members) is also detected in these conditions. One implication of this would be that HDAC repression may act in a coordinated manner with caspase-mediated degradation of MEF2 proteins to deplete MEF2 activity during neuronal apoptosis (14, 59).

In summary, data in the present study establish a principal role for endogenous CaMKII in the modulation of HDAC5 localization in CGNs. By phosphorylating HDAC5, CaMKII excludes this transcriptional repressor from the nucleus and prevents it from interacting with MEF2D. In this manner, CaMKII works in a coordinated fashion with other signaling molecules, such as calcineurin, to maximize MEF2-dependent transcription of putative pro-survival genes. These results add further insight into the complexities of MEF2 regulation in neurons and suggest that multiple calcium-regulated pathways act in concert to modulate the function of these important transcription factors during CNS development.

REFERENCES

1. Breitbart, R. E., Liang, C. S., Smoot, L. B., Laheru, D. A., Mahdavi, V., and Nadal-Ginard, B. (1993) *Development* **118,** 1095–1106
2. McDermott, J. C., Cardoso, M. C., Yu, Y. T., Andres, V., Leifer, D., Krainc, D., Lipton, S. A., and Nadal-Ginard, B. (1993) *Mol. Cell. Biol.* **13,** 2564–2577
3. Edmondson, D. G., Lyons, G. E., Martin, J. F., and Olson, E. N. (1994) *Development* **120,** 1251–1263
4. Firulli, A. B., Miano, J. M., Bi, W., Johnson, A. D., Casscells, W., Olson, E. N., and Schwarz, J. J. (1996) *Circ. Res.* **78,** 196–204
5. Wu, H., Naya, F. J., McKinsey, T. A., Mercer, B., Shelton, J. M., Chin, E. R., Simard, A. R., Michel, R. N., Bassel-Duby, R., Olson, E. N., and Williams, R. S. (2000) *EMBO J.* **19,** 1963–1973
6. McKinsey, T. A., Zhang, C. L., and Olson, E. N. (2002) *Trends Biochem. Sci.* **27,** 40–47
7. Ikeshima, H., Imai, S., Shimoda, K., Hata, J., and Takano, T. (1995) *Neurosci. Lett.* **200,** 117–120
8. Lyons, G. E., Micales, B. K., Schwarz, J., Martin, J. F., and Olson, E. N. (1995) *J. Neurosci.* **15,** 5727–5738
9. Lin, X., Shah, S., and Bulleit, R. F. (1996) *Brain Res. Mol. Brain Res.* **42,** 307–316
10. Krainc, D., Bai, G., Okamoto, S., Carles, M., Kusiak, J. W., Brent, R. N., and Lipton, S. A. (1998) *J. Biol. Chem.* **273,** 26218–26224
11. Okamoto, S., Krainc, D., Sherman, K., and Lipton, S. A. (2000) *Proc. Natl. Acad. Sci. U. S. A.* **97,** 7561–7566
12. Mao, Z., Bonni, A., Xia, F., Nadal-Vicens, M., and Greenberg, M. E. (1999) *Science* **286,** 785–790
13. D'Mello, S. R., Galli, C., Ciotti, T., and Calissano, P. (1993) *Proc. Natl. Acad. Sci. U. S. A.* **90,** 10989–10993
14. Li, M., Linseman, D. A., Allen, M. P., Meintzer, M. K., Wang, X., Laessig, T., Wierman, M. E., and Heidenreich, K. A. (2001) *J. Neurosci.* **21,** 6544–6552
15. Gaudilliere, B., Shi, Y., and Bonni, A. (2002) *J. Biol. Chem.* **277,** 46442–46446
16. Wu, H., Rothermel, B., Kanatous, S., Rosenberg, P., Naya, F. J., Shelton, J. M., Hutcheson, K. A., DiMaio, J. M., Olson, E. N., Bassel-Duby, R., and Williams, R. S. (2001) *EMBO J.* **20,** 6414–6423
17. Mao, Z., and Wiedmann, M. (1999) *J. Biol. Chem.* **274,** 31102–31107
18. Lu, J., McKinsey, T. A., Nicol, R. L., and Olson, E. N. (2000) *Proc. Natl. Acad. Sci. U. S. A.* **97,** 4070–4075
19. McKinsey, T. A., Zhang, C. L., Lu, J., and Olson, E. N. (2000) *Nature* **408,** 106–111
20. Dressel, U., Bailey, P. J., Wang, S. C., Downes, M., Evans, R. M., and Muscat, G. E. (2001) *J. Biol. Chem.* **276,** 17007–17013
21. McKinsey, T. A., Zhang, C. L., and Olson, E. N. (2000) *Proc. Natl. Acad. Sci. U. S. A.* **97,** 14400–14405
22. Li, M., Wang, X., Meintzer, M. K., Laessig, T., Birnbaum, M. J., and Heidenreich, K. A. (2000) *Mol. Cell. Biol.* **20,** 9356–9363
23. Churn, S. B., Sombati, S., Jakoi, E. R., Sievert, L., and DeLorenzo, R. J. (2000) *Proc. Natl. Acad. Sci. U. S. A.* **97,** 5604–5609
24. Lemercier, C., Verdel, A., Galloo, B., Curtet, S., Brocard, M. P., and Khochbin, S. (2000) *J. Biol. Chem.* **275,** 15594–15599
25. Linseman, D. A., Cornejo, B. J., Le, S. S., Meintzer, M. K., Laessig, T. A., Bouchard, R. J., and Heidenreich, K. A. (2003) *J. Neurochem.* **85,** 1488–1499
26. Soderling, T. R., Chang, B., and Brickey, D. (2001) *J. Biol. Chem.* **276,** 3719–3722
27. Burgin, K. E., Waxham, M. N., Rickling, S., Westgate, S. A., Mobley, W. C., and Kelly, P. T. (1990) *J. Neurosci.* **10,** 1788–1798
28. Kato, T., Sano, M., Miyoshi, S., Sato, T., Hakuno, D., Ishida, H., Kinoshita-Nakazawa, H., Fukuda, K., and Ogawa, S. (2000) *Circ. Res.* **87,** 937–945
29. Condon, J. C., Pezzi, V., Drummond, B. M., Yin, S., and Rainey, W. E. (2002) *Endocrinology* **143,** 3651–3657
30. See, V., Boutillier, A. L., Bito, H., and Loeffler, J. P. (2001) *FASEB J.* **15,** 134–144
31. Yu, Y. T., Breitbart, R. E., Smoot, L. B., Lee, Y., Mahdavi, V., and Nadal-Ginard, B. (1992) *Genes Dev.* **6,** 1783–1798
32. Shore, P., and Sharrocks, A. D. (1995) *Eur. J. Biochem.* **229,** 1–13
33. Molkentin, J. D., and Olson, E. N. (1996) *Proc. Natl. Acad. Sci. U. S. A.* **93,** 9366–9373
34. Martin, J. F., Miano, J. M., Hustad, C. M., Copeland, N. G., Jenkins, N. A., and Olson, E. N. (1994) *Mol. Cell. Biol.* **14,** 1647–1656
35. Leifer, D., Krainc, D., Yu, Y. T., McDermott, J., Breitbart, R. E., Heng, J., Neve, R. L., Kosofsky, B., Nadal-Ginard, B., and Lipton, S. A. (1993) *Proc. Natl. Acad. Sci. U. S. A.* **90,** 1546–1550
36. Leifer, D., Golden, J., and Kowall, N. W. (1994) *Neuroscience* **63,** 1067–1079
37. Leifer, D., Li, Y. L., and Wehr, K. (1997) *J. Mol. Neurosci.* **8,** 131–143
38. Black, B. L., and Olson, E. N. (1998) *Annu. Rev. Cell Dev. Biol.* **14,** 167–196
39. Puri, P. L., and Sartorelli, V. (2000) *J. Cell. Physiol.* **185,** 155–173
40. McKinsey, T. A., Zhang, C. L., and Olson, E. N. (2001) *Curr. Opin. Genet. Dev.* **11,** 497–504
41. Kolodziejczyk, S. M., Wang, L., Balazsi, K., DeRepentigny, Y., Kothary, R., and Megeney, L. A. (1999) *Curr. Biol.* **9,** 1203–1206
42. Passier, R., Zeng, H., Frey, N., Naya, F. J., Nicol, R. L., McKinsey, T. A., Overbeek, P., Richardson, J. A., Grant, S. R., and Olson, E. N. (2000) *J. Clin. Invest.* **105,** 1395–1406
43. Zhang, C. L., McKinsey, T. A., Chang, S., Antos, C. L., Hill, J. A., and Olson, E. N. (2002) *Cell* **110,** 479–488
44. Han, J., and Molkentin, J. D. (2000) *Trends Cardiovasc. Med.* **10,** 19–22
45. Chin, E. R., Olson, E. N., Richardson, J. A., Yang, Q., Humphries, C., Shelton, J. M., Wu, H., Zhu, W., Bassel-Duby, R., and Williams, R. S. (1998) *Genes Dev.* **12,** 2499–2509
46. Dunn, S. E., Simard, A. R., Bassel-Duby, R., Williams, R. S., and Michel, R. N. (2001) *J. Biol. Chem.* **276,** 45243–45254
47. Xu, Q., Yu, L., Liu, L., Cheung, C. F., Li, X., Yee, S. P., Yang, X. J., and Wu, Z. (2002) *Mol. Biol. Cell* **13,** 1940–1952
48. Kao, H. Y., Verdel, A., Tsai, C. C., Simon, C., Juguilon, H., and Khochbin, S. (2001) *J. Biol. Chem.* **276,** 47496–47507
49. Chawla, S., Vanhoutte, P., Arnold, F. J., Huang, C. L., and Bading, H. (2003)

J. Neurochem. **85,** 151–159
50. Linseman, D. A., Phelps, R. A., Bouchard, R. J., Le, S. S., Laessig, T. A., McClure, M. L., and Heidenreich, K. A. (2002) *J. Neurosci.* **22,** 9287–9297
51. Borodinsky, L. N., Coso, O. A., and Fiszman, M. L. (2002) *J. Neurochem.* **80,** 1062–1070
52. Silva, A. J., Stevens, C. F., Tonegawa, S., and Wang, Y. (1992) *Science* **257,** 201–206
53. Beaman-Hall, C. M., Hozza, M. J., and Vallano, M. L. (1992) *J. Neurochem.* **58,** 1259–1267
54. Borodinsky, L. N., O'Leary, D., Neale, J. H., Vicini, S., Coso, O. A., and Fiszman, M. L. (2003) *J. Neurochem.* **84,** 1411–1420
55. Shackelford, D. A., Yeh, R. Y., Hsu, M., Buzsaki, G., and Zivin, J. A. (1995) *J. Cereb. Blood Flow Metab.* **15,** 450–461
56. Churn, S. B., Limbrick, D., Sombati, S., and DeLorenzo, R. J. (1995) *J. Neurosci.* **15,** 3200–3214
57. Babcock, A. M., Liu, H., Paden, C. M., Churn, S. B., and Pittman, A. J. (1999) *J. Neurosci. Res.* **56,** 36–43
58. Babcock, A. M., Everingham, A., Paden, C. M., and Kimura, M. (2002) *J. Neurosci. Res.* **67,** 804–811
59. Okamoto, S., Li, Z., Ju, C., Scholzke, M. N., Mathews, E., Cui, J., Salvesen, G. S., Bossy-Wetzel, E., and Lipton, S. A. (2002) *Proc. Natl. Acad. Sci. U. S. A.* **99,** 3974–3979

Experimental Neurology **168,** 183–191 (2001)
doi:10.1006/exnr.2000.7593, available online at http://www.idealibrary.com on IDEAL®

IGF-I and bFGF Improve Dopamine Neuron Survival and Behavioral Outcome in Parkinsonian Rats Receiving Cultured Human Fetal Tissue Strands

Edward D. Clarkson,* W. Michael Zawada,†,‡,§ K. Pat Bell,‡ James E. Esplen,‡ Paul K. Choi,‡ Kim A. Heidenreich,§,¶,‖ and Curt R. Freed†,¶,‡,§,‖

*U.S. Army Medical Research Institute of Chemical Defense, 3100 Ricketts Point Road, MCMR-UV-DB, Aberdeen Proving Grounds, Maryland 21010-5400; †Department of Medicine, ¶Department of Pharmacology, ‡Division of Clinical Pharmacology, and §Neuroscience Program, University of Colorado School of Medicine, 4200 East Ninth Avenue, Denver, Colorado 80262; and ‖Denver Veterans Administration Medical Center, Denver, Colorado 80220

Received June 21, 1999; accepted October 13, 2000

To promote dopamine cell survival in human fetal tissue strands transplanted into immunosuppressed 6-OHDA-lesioned rats, we have preincubated tissue in insulin-like growth factor-I (IGF-I, 150 ng/ml) and basic fibroblast growth factor (bFGF, 15 ng/ml) *in vitro* for 2 weeks. Growth factor treatment did not affect the rate of homovanillic acid production *in vitro* but increased overall dopamine neuron survival in animals after transplant from 1240 ± 250 to 2380 ± 440 neurons ($P < 0.05$). Animals in the growth factor-treated group had a significantly greater reduction in methamphetamine-induced rotation (66%) compared to control transplants (30%, $P < 0.05$). We conclude that *in vitro* preincubation of human fetal tissue strands with IGF-I and bFGF improves dopamine cell survival and the behavioral outcome of transplants.

Key Words: **Parkinson's disease; human fetal tissue; 6-OHDA; transplantation; IGF-I; bFGF.**

INTRODUCTION

In Parkinson's disease, progressive deterioration of motor function results from the loss of nigrostriatal dopamine neurons and consequent dopamine depletion in the caudate and putamen (17). Among neurological disorders, Parkinson's disease is a prime candidate for a new strategy for treatment because drug therapy loses its effectiveness after 5 to 10 years. In 1979, Björklund and Stenevi (5) and Perlow *et al.* (43) demonstrated the potential benefits of mesencephalic grafts in parkinsonian rats. Since then, fetal tissue transplantation has been developed as a treatment for Parkinson's disease in humans (19–26, 32, 35, 59). Decisions about the appropriate age of human fetal donor tissue and its preparation have been based on extrapolation from the embryonic development of rodents as well as direct transplantation of human fetal tissue into parkinsonian rats (11, 26, 31, 49–52, 55–58).

A major problem with neurotransplantation is that up to 95% of embryonic dopamine neurons die after transplantation (7, 33). Since cells in transplants of embryonic mesencephalon have been shown to undergo apoptotic cell death *in vivo* (36, 62), we and others are examining possible uses of neurotrophic factors to reduce apoptosis (12, 13, 28, 37, 38, 47, 48, 61, 62). Two of the growth factors being examined are insulin-like growth factor-I (IGF-I) and basic fibroblast growth factor (bFGF) which improve dopamine neuron survival *in vitro* (30) and *in vivo* (53). We have recently shown that dopamine neuron survival can be improved by a 2-h preincubation of transplanted tissue with the growth factor combination of glial cell line-derived neurotrophic factor (GDNF), IGF-I and bFGF (62). We have also shown that a combination of IGF-I and bFGF reduces the rate at which dopamine neurons undergo apoptosis *in vitro* (61). The growth factors may be acting indirectly through stimulation of trophic factor production by astrocytes (18), since the neuroprotective effect can be blocked by inhibition of astrocyte proliferation with cytosine arabinoside (61). We have found that most dopamine cell death occurs in the first day to the first week after transplant (62). This result indicates that short-term induction of astrocytes by IGF-I and bFGF *in vivo* may be sufficient to protect transplanted dopamine neurons from programmed cell death.

To provide time for quality control of tissue prior to transplantation, we have developed methods for maintaining human embryonic cells in culture for extended periods of 1 to 4 weeks prior to transplant (20, 21). In a further effort to improve survival of cells after transplant, we have now tested whether long-term (14 day)

0014-4886/01 $35.00

in vitro incubation of human fetal tissue with the combination of IGF-I and bFGF will promote the subsequent survival of these cells after transplantation into hemiparkinsonian rats.

Currently in our laboratory, strands of human fetal tissue placed in tissue culture are tested for dopamine production by measuring the concentration of the dopamine metabolite homovanillic acid (HVA) in tissue culture supernatant. The *in vitro* storage method is also critical for accumulating a sufficient quantity of tissue for transplantation and for demonstrating that the tissue is not infected with bacteria, viruses, or fungi. The *in vitro* environment provides an opportunity to treat tissue with trophic factors in an effort to improve survival of cells following transplantation.

MATERIALS AND METHODS

Preparation of Fetal Tissue

Postmitotic embryonic dopamine cells from early in development, 13 to 15 days after conception in the rat and 45 to 55 days after conception in the human (40), are able to survive and develop when implanted in the adult Parkinsonian brain (9, 10, 33, 50). Only tissue from human embryos in this developmental range was used in this study.

Fetal tissue was obtained after elective abortion by standard clinical methods and with the use of sterile collection apparatus. Women donating tissue signed specific informed consent for experimental use of tissue. The consent and all collection methods complied with state and federal laws and were approved by the Colorado Combined Institutional Review Board. The rostral half of ventral mesencephalon containing dopamine cells was dissected as a block about 2 by 4 by 1 mm. This block was then cut in half down the midline to generate two identical pieces of mesencephalon. These pieces are referred to subsequently as a "matched pair." The tissue was washed in three petri dishes each containing ~20 ml of cold calcium- and magnesium-free Hanks' balanced salt solution (HBSS).

Tissues strands were created by extruding one half of a mesencephalon through a glass cannula with a luer adaptor at one end and a taper to a 0.2-mm bore at the other (14, 20, 21). These extruders were made by heating and drawing a commercially available blank (Kimble Kontes, Cat. No. 663500-0444, Vineland, NJ). Mesencephalic tissue was aspirated into the hub of a 1 ml tuberculin syringe in HBSS and then slowly ejected through the buffer-filled glass extruder. Care was taken to avoid excess pressure during extrusion, which could cause compression/decompression damage to the tissue. Strands were extruded into 4 ml culture medium in one well of a six-well plastic tissue culture plate (Corning Inc., Corning, NY). Medium was F12 containing 5% dialyzed human placental serum (heat inactivated at 55°C for 30 min), heparin (1 μg ml^{-1}) to bind bFGF (63), 2.2 μg ml^{-1} ascorbic acid, 10 μg ml^{-1} vancomycin (Eli Lilly & Co., Indianapolis, IN), 2 μg ml^{-1} gentamicin (Elkins-Sinn Inc., Cherry Hill, NJ), and 2 mM L-glutamine (Sigma, St. Louis, MO).

Human recombinant IGF-I (150 ng/ml; Cephalon Inc., Philadelphia, PA) and human recombinant bFGF (15 ng/ml; Scios Inc., Mountain View, CA) were added to the medium immediately after strands were placed in culture. Medium was changed at 3, 6, 9, 12, and 14 days after strands were placed in culture. This was done by removing and freezing 2 ml of medium for later HVA analysis and then adding 2 ml of fresh medium together with fresh IGF-I and bFGF.

High-Performance Liquid Chromatography (HPLC) Analysis

Testing for the content of HVA in tissue culture extracts used HPLC with electrochemical detection (Bioanalytical Systems) as previously described (3, 29). Separation was achieved on a Spherisorb ODSA microbore column (1 × 100 mm, Keystone Scientific) using a mobile phase containing, per liter, 13.7 ml phosphoric acid, 4.1 g trichloroacetic acid, 0.5 g sodium EDTA, 0.4 g octyl sodium sulfate, and 8% methanol (pH 3.0). Any detectable HVA in the medium blank was subtracted from each sample.

Unilateral 6-OHDA Injections

Male Sprague–Dawley rats (250–350 g) were anesthetized with equithesin (4 ml/kg) and placed in a stereotaxic frame. A 30-gauge cannula was then lowered into the medial forebrain bundle at the following coordinates: AP, −4.3 mm posterior to bregma; L, 1.5 mm from the midline; VD, −7.5 mm from the dura (42). Ten micrograms of 6-OHDA HBr (RBI, Natick, MA), dissolved in 5 μl sterile saline containing 0.2% ascorbate, was infused at 1 μl/min over 5 min (55). The cannula was left in place an additional 2 min with no infusion. Then the pump was started and the cannula was withdrawn while infusing saline. Lesions were tested behaviorally as noted below and confirmed histologically postmortem by the unilateral loss of TH-immunoreactive dopamine neurons in the substantia nigra.

Methamphetamine and Apomorphine-Induced Rotation

Two weeks after surgery, the completeness of the lesion was assessed by measuring turning behavior in response to methamphetamine HCl (5.0 mg/kg, ip, Sigma) and apomorphine (0.05 mg/kg, sc, Sigma) in a flat-bottomed rotometer. Methamphetamine circling was selected as the primary behavioral variable. Briefly, the rotometer consisted of a plexiglass cylinder

20 cm in diameter. The rat was tethered to a counter with a harness fastened around its chest. Rats that circled ipsilateral to the lesion more than 3.0 rpm during the period of 30 to 120 min after methamphetamine injection were used for transplantation and further rotational testing. Average ipsilateral rotation of animals chosen for the experiments was 8.3 rpm for controls and 7.2 rpm for IGF-I/bFGF-treated group. We have previously demonstrated (45) that in our methamphetamine-induced circling test performed in flat-bottomed Plexiglas cylinders, circling above 2 rpm correlates with >95% dopamine depletion. In contrast, Ungerstedt and Arbuthnott demonstrated that when methamphetamine-induced circling test is performed in hemispherical bowls instead of cylinders, higher circling rates (4–6 rpm) predict >95% dopamine depletion (55).

Circling after apomorphine was also addressed. Rats that showed apomorphine-induced turning contralateral to the lesion of greater than 3.0 rpm during the period of 0 to 30 min after injection were considered to be positive for an apomorphine effect and had apomorphine data collected. Average apomorphine-induced rotation of animals chosen for the experiments was 8.1 rpm for controls and 6.1 rpm for IGF-I/bFGF-treated group. Of the six pairs of rats that were positive for methamphetamine-induced rotation, only five pairs were positive for apomorphine-induced rotation. Methamphetamine- and apomorphine-induced turning was measured 4, 8, and 10.5 weeks after transplantation to test the behavioral effect of developing neural grafts. To prevent possible confounding of drug test effects, methamphetamine-induced turning was measured 48 h after apomorphine testing.

Transplantation of Embryonic Tissue

Recipient animals were anesthetized with equithesin (4 ml/kg). Three burr holes were made through the skull and a 20-gauge guide cannula supported by a motorized stereotaxic arm (Narishige, Tokyo) was used for transplantation. The cannula was lowered into the brain to 3.0 or 3.5 mm below the dura. Three transplant sites were required to accommodate all of the tissue present in one-half of a human mesencephalon. Transplant coordinates were: (i) AP 0.0 mm from bregma, L 2.0 mm from midline, VD −7.0 to −3.0 mm below dura; (ii) AP 0.0 mm from bregma, L 3.5 mm from midline, VD −7.5 to −3.5 mm below dura; and (iii) AP 1.0 mm anterior to bregma, L 3.5 mm from midline, VD −7.0 to −3.0 mm below dura. Animals were paired based on whether they received growth-factor-treated or nontreated tissue from the same human mesencephalon.

Matched pair tissue strands representing half-mesencephalons were removed from tissue culture, reextruded as described above, and then drawn up into a 24-gauge Stainless-steel transplantation cannula in a volume between 4 and 8 μl. The transplantation cannula (which protruded 4 mm beyond the guide) was then inserted through the guide cannula to a final depth of 7 or 7.5 mm below the dura. The tissue was ejected with the aid of a syringe pump over 4 min. For each transplant, the pump was switched on and allowed to run for 15 s and then the cannula was withdrawn at a rate of 1 mm/min with the pump running. At the top of the tract (after 4 min) the pump and guide cannula were stopped for 2 min to allow the pressure to equilibrate. Afterward, withdrawal was continued while about 4 μl of HBSS was pumped through the cannula. No sham transplants were done since in our previous work we found that shams had no improvement in amphetamine- (44) and methamphetamine-induced rotation (15, 60). All transplanted rats were immunosuppressed 24 h prior to transplantation with cyclosporine A (Sandimmune; 10 mg/kg; sc; Sandoz) and daily thereafter for the duration of the experiment.

Tyrosine Hydroxylase Immunohistochemistry

At 10.5 weeks after transplant, following behavioral testing, animals were killed by chloral hydrate overdose (2 g/kg, ip) and intracardially perfused with heparinized saline (30 units/ml) followed by 4% phosphate-buffered paraformaldehyde. The brains were postfixed for 2 days in the same fixative and cryoprotected in 30% sucrose. Forty-micrometer sections were cut on a freezing microtome, and each section was processed for TH immunohistochemistry.

The staining procedure supplied by the manufacturer was used. After blocking for 1 h with 10% goat serum, 1% BSA, and 0.3% Triton-X at 37°C, the slices were incubated in polyclonal, affinity-purified rabbit anti-rat TH antibody 1:200 (Pel-Freez, Rogers, AR) for 16 h at 37°C. Sections were then incubated with a secondary biotinylated, affinity-purified, goat anti-rabbit IgG antibody and subsequently with avidin/biotinylated horseradish peroxidase complex, each for 4 h at room temperature (Vector Lab, Burlingame, CA). The peroxidase was visualized with diaminobenzidine dissolved in PBS and 0.03% hydrogen peroxide.

Anatomical Analysis

The total number of dopamine neurons within the transplant tracts was estimated by counting all TH-positive cells in every third section from the area of the striatum-containing transplant. Sequential section stereological counting (16) was not possible since the 40-μm sections were collected six sections per single well of a 24-well plate and were thus randomized per well. For each animal, sections were collected in multiple wells and at least 16 sections from each transplant were examined for the presence of dopamine neurons. Abercrombie's correction (1) with an assumed

cell diameter of 20 μm was used to generate the final estimate of the number of surviving dopamine neurons in each animal. Work previously done in our laboratory has shown that treatment with a combination of IGF-I and bFGF does not affect transplanted dopamine neuron size (14). To assure that treatment with IGF-I and bFGF did not alter dopamine neuron cell size, which would render use of Abercrombie's correction inappropriate, one rat was selected from each transplant group for detailed neuron size analysis. The rat selected had closest to the median value of surviving dopamine neurons for each group. In each selected rat, images of all sections containing grafted cells were captured at $\times$400 magnification into SlideBook digital deconvolution software (Intelligent Imaging Innovations). The size of the soma for all dopamine neurons was determined using SlideBook's analysis tools. The total number of TH^+ somas measured was 197 for the control and 408 for the animal receiving IGF-I/bFGF treatment.

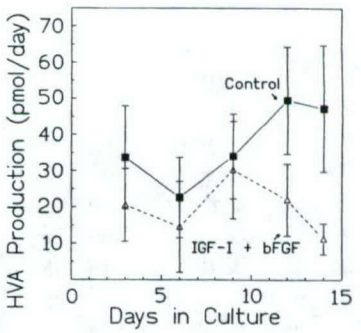

FIG. 1. Effects of growth factor treatment on HVA production in human fetal tissue. Matched pairs of mesencephalon strands were made by bisecting fragments of human fetal ventral mesencephalon, extruding through a 0.2-mm-diameter cannula, and treating for 2 weeks either with IGF-I (150 ng/ml) + bFGF (15 ng/ml) in F12 medium supplemented with 5% human placental serum (open triangles) or with F12 supplemented with serum alone (solid squares). Testing for the content of HVA in tissue culture extracts was done by HPLC with electrochemical detection (2, 32). All data represent the mean $\pm$ SEM (n = 6 pairs).

Statistical Analysis

The behavioral data were analyzed via SAS Procedures GLM and Mixed (SAS Institute, Cary, NC) using a mixed effects model appropriate for repeated measures data (34). This method accounts for variability between rats as well as between multiple measurements on the same rat. The TH^+ neuron survival and TH^+ neuron soma size data were analyzed using Student's t test and InStat statistical software (GraphPad, San Diego, CA).

RESULTS

Measurement of the stable dopamine metabolite HVA in the medium of cultured fetal strands provides evidence for ongoing production of dopamine in the tissue culture (Fig. 1). Levels of HVA production per day appeared to be lower in fetal strands treated with the combination of IGF-I and bFGF, though these differences did not reach statistical significance (n = 6, $P > 0.2$). The same trend was seen in cumulative HVA levels, with IGF-I/bFGF-treated strands producing a total of 320 $\pm$ 130 pmol after 14 days *in vitro* and untreated control strands producing 490 $\pm$ 130 pmol after 14 days *in vitro* (data not shown). This difference was not statistically significant.

Figure 2 shows that animals receiving growth-factor-treated human fetal mesencephalon had a significantly greater behavioral improvement than animals transplanted with human mesencephalon not treated with growth factors. Transplants of growth-factor-treated strands led to a significant reduction in methamphetamine-induced rotation at 10.5 weeks post-transplant when compared to control strands ($P <$ 0.05; Fig. 2A). Growth-factor-treated strands appeared to cause a more rapid improvement in apomorphine circling when compared to control strands (Fig. 2B). However, these apparent differences did not reach statistical significance ($P > 0.05$). By 10.5 weeks, both groups had nearly stopped circling to apomorphine, indicating that enough human dopamine cells survived to eliminate apomorphine circling.

The number of surviving dopamine neurons in grafts of animals sacrificed 10.5 weeks after transplant is shown in Fig. 3A. Transplants of fetal tissue strands treated with the combination of IGF-I/bFGF had better dopamine neuron survival than untreated control grafts. In animals receiving one-half a human mesencephalon treated with growth factors, a total of 2380 $\pm$ 440 dopamine neurons survived (Fig. 3A). By contrast, animals receiving the non-growth-factor-treated half mesencephalon had only 1240 $\pm$ 250 surviving dopamine neurons ($P < 0.05$; Fig. 3A). Photomicrographs of representative sections from untreated and growth-factor-treated grafts are shown in Figs. 3B and 3C.

To assure that growth factor treatment did not alter dopamine neuron cell size, which would render use of Abercrombie's correction inappropriate, one rat was selected from each transplant group for detailed neuron size analysis. The rat selected had closest to the median value of surviving dopamine neurons for each group. Measurement of soma size of TH^+ neurons from images captured at $\times$400 magnification into SlideBook digital deconvolution software revealed that average area of TH^+ cell soma was not changed by the *ex vivo* growth factor treatment (Fig. 4A). Specifically, average area of TH^+ cell soma of control cells was 193 $\pm$ 3 μm^2 and 187 $\pm$ 2 μm^2 in tissue treated with IGF-I and bFGF. Photomicrographs of representative TH^+ cells in untreated and growth-factor-treated grafts are shown in Figs. 4B and 4C.

DISCUSSION

Our study demonstrates that treating individual fragments of human fetal ventral mesencephalon with a combination of IGF-I/bFGF for 2 weeks in tissue culture leads to better survival of dopamine neurons after transplant into immunosuppressed hemiparkinsonian rats. Previous work in our laboratory has shown that combinations of IGF-I and bFGF reduce the rate of apoptotic death in rat dopamine neurons *in vitro* (61), and pretreatment with a combination of GDNF, IGF-I, and bFGF improves cell survival after transplant (62). Cotransplantation of bFGF-expressing fibroblasts with rat mesencephalic dopamine neurons greatly enhanced survival of transplanted cells and accelerated behavioral recovery (53). We hypothesize that treatment of human fetal tissue with IGF-I/bFGF reduces the rate of apoptotic death that occurs while the strands are in culture. Because these growth factors appear to work indirectly by stimulating astrocyte proliferation and neurotrophic factor production (18, 53, 61), the ben-

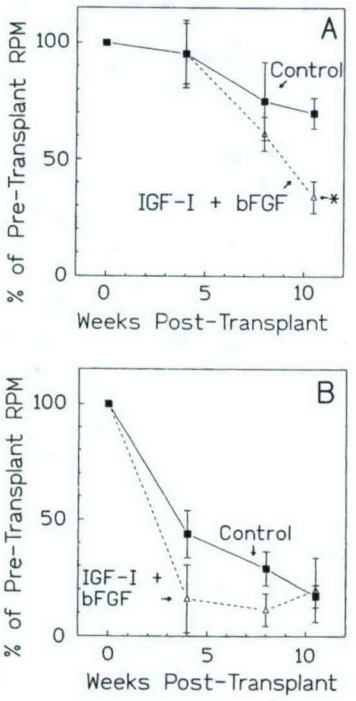

FIG. 2. Effects of transplanted human fetal tissue on behavioral deficits in 6-OHDA-lesioned rats. Matched pairs of mesencephalon strands were treated either with IGF-I + bFGF (open triangles) or with no growth factors (control, solid squares). Tissue was transplanted into striatum of 6-OHDA-lesioned rats. (A) rotational rate induced by methamphetamine (5 mg/kg, ip). Animals receiving growth-factor-treated strands had an improvement at 10.5 weeks posttransplant compared to controls. Asterisk represents statistical significance at $P < 0.05$ compared to controls using a mixed effects analyses of variance (29) ($n = 6$ pairs) and (B) rotational rate induced by apomorphine (0.05 mg/kg, sc). Animals receiving growth-factor-treated strands had their rotational rate induced by apomorphine measured at 4, 8, and 10.5 weeks after transplantation. Although the growth-factor-treated animals had a greater reduction in apomorphine-induced circling, this rate of reduction was not significantly greater when compared to controls.

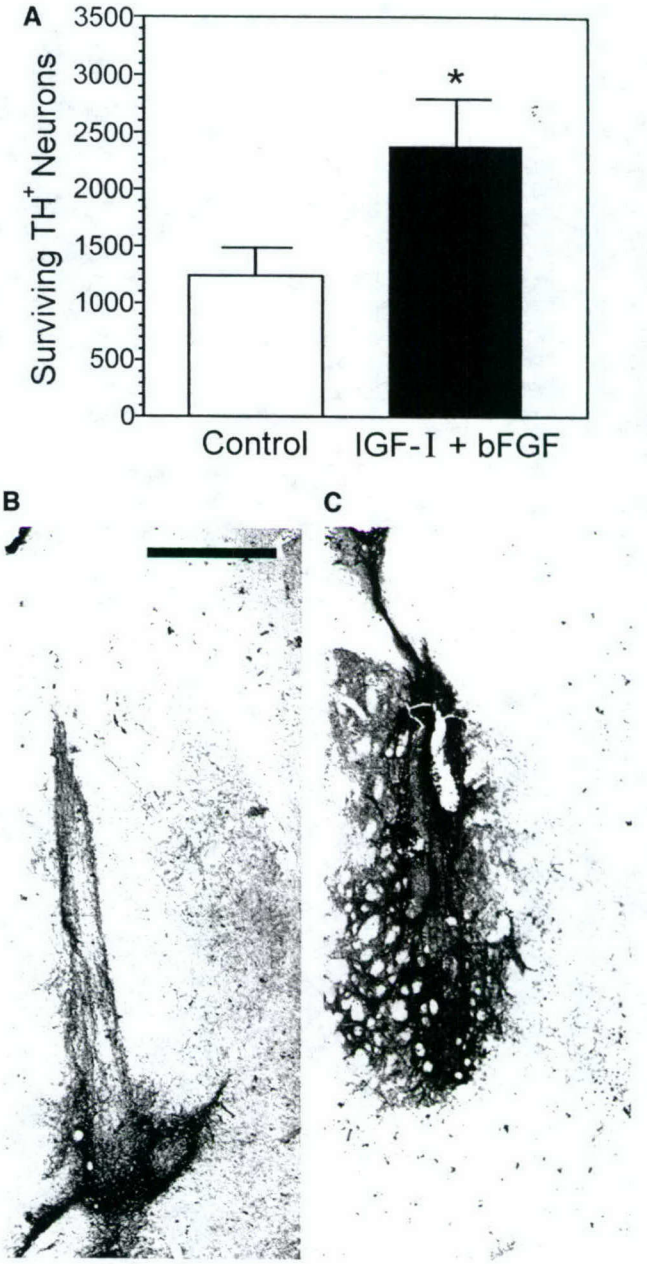

FIG. 3. Effects of treatment with IGF-I + bFGF on human dopamine neurons transplanted into 6-OHDA-lesioned rats. (A) Matched pairs of mesencephalon strands treated with IGF-I + bFGF (solid bar) and control tissue (open bar) were transplanted into 6-OHDA-lesioned rats. At 10.5 weeks posttransplant the rats were sacrificed, brain sections made at 40 μm, sections were stained for TH immunoreactivity, and all TH^+ neurons were counted. Estimates are for the whole brain using Abercrombie's correction (1). Data are presented as the mean $\pm$ SEM. Significance was shown by the Student's t test. Dopamine neuron survival was significantly enhanced by IGF-I and bFGF ($^*P < 0.05$, $n = 6$). (B) Micrograph showing TH^+ neurons in a representative control graft. (C) Micrograph showing TH^+ neurons in a representative graft treated with a combination of IGF-I and bFGF. Bar in B and C, 500 μm.

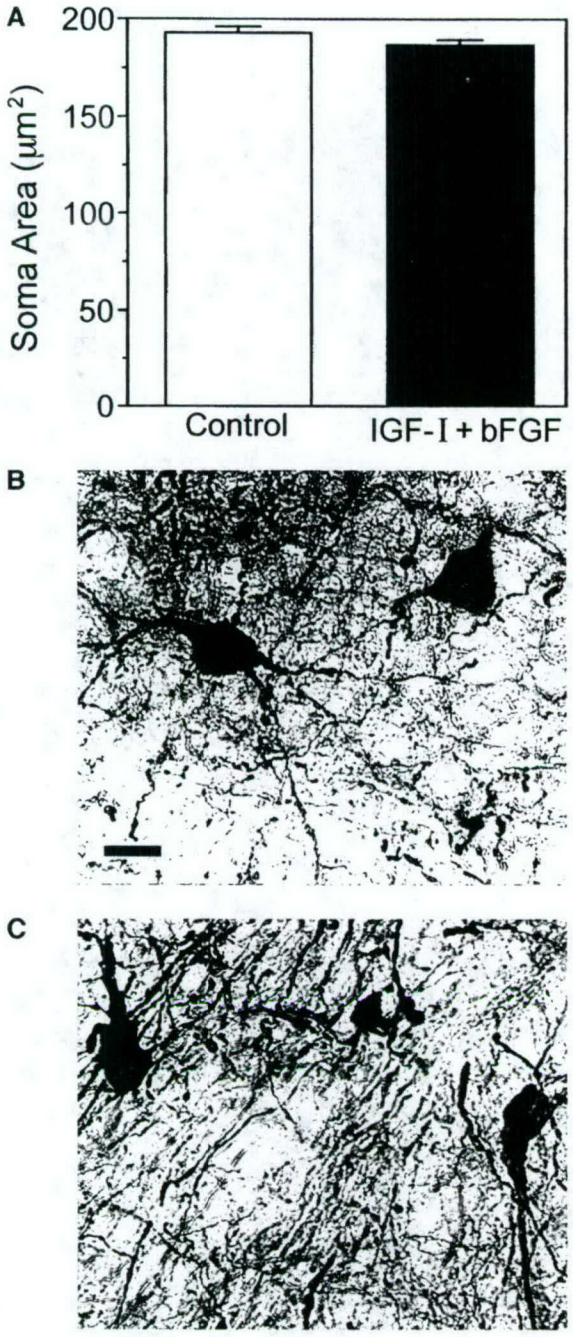

FIG. 4. Dopamine neuron cell size analysis. (A) Mean soma area of TH^+ neurons found in two different experimental groups 10.5 weeks after grafting. Student's *t* test confirmed that the IGF-I and bFGF treatment had no significant effect on the mean soma area of transplanted dopamine neurons. (B) Transplant of control ventral mesencephalic tissue showing TH^+ neurons. (C) Transplant of growth factor combination-treated tissue. Bar for B and C, 20 μm.

eficial effect of growth factor treatment may also carry over for a few days after transplantation.

In addition to antiapoptotic properties of some growth factors, treatment with inhibitors of specific proapoptotic pathways has proven to be neuroprotective (8). Specifically, 2-h preincubation of rat ventral mesencephalic cell suspension with a caspase inhibitor, Ac-YVAD-cmk, tripled survival of transplanted dopamine neurons (47). By contrast, transplantation of mouse ventral mesencephalon overexpressing the antiapoptotic protein Bcl-2 did not affect dopamine neuron survival, although fiber outgrowth was improved in such grafts (48). Other neuroprotective treatments attempt to reduce free radical damage to transplanted cells. An approach that has shown promise in protecting transplanted dopamine neurons has treated cell suspensions with antioxidants such as lazaroids (37, 41). The lazaroid trilazad mesylate improves survival of cultured human embryonic dopamine neurons (41). Another effective strategy is transplantation of mesencephalic tissue overexpressing Cu/Zn superoxide dismutase (38).

Storing dopamine neurons prior to transplantation is critically important for accumulation of enough specimens for a transplant operation and to test tissue for infection. To store dopamine neurons prior to transplantation, freshly dissected ventral mesencephalon can be placed in hibernation medium at 10°C for up to several days (46, 54). In our study, human embryonic brain tissue was stored at 10°C for up to several hours prior to dissection and was then placed in tissue culture for 2 weeks. We have found that dopamine cells in culture medium containing 5% human placental serum and a combination of IGF-I and bFGF have nearly 100% increased survival in transplants compared to cells cultured without growth factors. Others have shown that supplementation of hibernating cells with a combination of 8% human placental cord serum, GDNF and brain-derived neurotrophic factor improved TH-immunoreactive cell survival by 40% (54). Rat ventral mesencephalic tissue hibernated for 6 days in GDNF-containing medium enhanced 6-week survival of transplanted dopamine neurons by 30% (2). Cryopreservation would be desirable for long-term storage of cells. Unfortunately, cryopreservation methods lead to unacceptable losses of rat and human mesencephalic cells, regardless if the cells are cryopreserved as tissue fragments or cell suspension (46). Transplantation of cryopreserved human embryonic dopamine neurons reduced survival of dopamine neurons to only 9% of fresh tissue control grafts (27).

Since bFGF can expand the progenitor population for dopamine neurons in embryonic rat cultures (6), it is possible that the IGF-I/bFGF combination may lead to more surviving dopamine neurons by promoting progenitor cell division in human fetal tissue strands. The observed increase in dopamine neuron survival in animals receiving IGF-I/bFGF-treated fetal tissue correlates with the greater improvement in behavioral deficits seen in animals receiving growth-factor-treated fetal tissue compared to control tissue. Although treatment with the IGF-I/bFGF combination led to faster

recovery of methamphetamine-induced circling, complete behavioral recovery was not achieved due to the slow maturation of human dopamine grafts in the rat host (4, 50).

For the past 10 years, we have prepared embryonic tissue as strands for transplantation into patients with Parkinson's disease (20, 21). Since we have shown that treatment of these strands with the combination of IGF-I and bFGF can nearly double the survival of dopamine neurons in transplants as well as significantly improve behavioral effects of transplants, growth factor pretreatment may prove useful for improving dopamine neuron survival after transplantation in Parkinson's disease patients.

ACKNOWLEDGMENTS

The authors thank Dr. J. A. Abraham from Scios Inc., Mountain View, California, for providing bFGF and Dr. J. M. Farah from Cephalon Inc., West Chester, Pennsylvania, for providing IGF-I for these studies. This work was supported by USPHS R01 NS29982 and R01 NS18639; the General Clinical Research Centers Program National Centers for Research Resources, NIH (M01 RR00069); and The Program to End Parkinson's Disease (C.R.F.) and R01 NS38619 (K.A.H. and W.M.Z.).

REFERENCES

1. Abercrombie, M. 1946. Estimation of nuclear population from microtome sections. *Anat. Rec.* **94:** 239–247.
2. Apostolides, C., E. Sanford, M. Hong, and I. Mendez. 1998. Glial cell line-derived neurotrophic factor improves intrastriatal graft survival of stored dopaminergic cells. *Neuroscience* **83:** 363–372.
3. Amus, P. A., and C. R. Freed. 1979. Reversed-phase high-performance liquid chromatography of catecholamines and their congeners with simple acids as ion-pairing reagents. *J. Chromatogr.* **169:** 303–311.
4. Belkadi, A. M., C. Gény, S. Naimi, R. Jeny, M. Peschanki, and D. Riche. 1997. Maturation of fetal human neural xenografts in the adult rat brain. *Exp. Neurol.* **144:** 369–380.
5. Björklund, A., and U. Stenevi. 1979. Reconstruction of the nigrostriatal dopamine pathway by intracerebral nigral transplants. *Brain Res.* **177:** 555–560.
6. Bouvier, M. M., and C. Mytilineou. 1995. Basic fibroblast growth factor increases division and delays differentiation of dopamine precursors in vitro. *J. Neurosci.* **15:** 7141–7149.
7. Brundin, P., O. Isacson, and A. Björklund. 1985. Monitoring of cell viability in suspensions of embryonic CNS tissue and its use as a criterion for intracerebral graft survival. *Brain Res.* **331:** 251–259.
8. Brundin, P., J. Karlsson, M. Emgrad, G. S. Schierle, O. Hansson, A. Petersen, and R. F. Castilho. 2000. Improving the survival of grafted dopaminergic neurons: A review over current approaches. *Cell Transplant.* **9:** 179–195.
9. Brundin, P., O. G. Nilsson, R. E. Strecker, O. Lindvall, B. Asted, and A. Björklund. 1986. Behavioral effects of human fetal dopamine neurons grafted in a rat model of Parkinson's disease. *Exp. Brain Res.* **65:** 235–240.
10. Brundin, P., R. E. Strecker, H. Widner, D. J. Clarke, O. G. Nilsson, B. Astedt, O. Lindvall, and A. Björklund. 1988. Human fetal dopamine neurons grafted in a rat model of Parkinson's disease: Immunological aspects, spontaneous and drug-induced behavior, and dopamine release. *Exp. Brain Res.* **70:** 192–208.
11. Clarke, D. J., P. Brundin, R. E. Strecker, O. G. Nilsson, A. Björklund, and O. Lindvall. 1998. Human fetal dopamine neurons grafted in a rat model of Parkinson's disease: Ultrastructural evidence for synapse formation using tyrosine hydroxylase immunocytochemistry. *Exp. Brain Res.* **73:** 115–126.
12. Clarkson, E. D., W. M. Zawada, and C. R. Freed. 1995. GDNF reduces apoptosis in dopaminergic neurons *in vitro*. *NeuroReport* **7:** 145–149.
13. Clarkson, E. D., W. M. Zawada, and C. R. Freed. 1997. GDNF improves survival and reduces apoptotic cell death in human embryonic dopaminergic neurons *in vitro*. *Cell Tissue Res.* **289:** 207–210.
14. Clarkson, E. D., W. M. Zawada, F. S. Adams, P. K. Bell, and C. R. Freed. 1998. Embryonic mesencephalic tissue strands show greater dopamine neuron survival and better behavioral outcome than cell suspensions after transplantation in parkinsonian rats. *Brain Res.* **806:** 60–68.
15. Clarkson, E. D., F. G. La Rosa, J. Edwards-Prasad, D. A. Weiland, S. W. Witta, C. R. Freed, and K. N. Prasad. 1998. Improvement of neurological deficits in 6-hydroxydopamine-lesioned rats after transplantation with allogeneic simian virus 40 large tumor antigen gene-induced immortalized dopamine cells. *Proc. Natl. Acad. Sci. USA* **95:** 1265–1270.
16. Coggeshall, R. E., and H. A. Lekan. 1996. Methods for determining numbers of cells and synapses: A case for more uniform standards of review. *J. Comp. Neurol.* **364:** 6–15.
17. Ehringer, H., and O. Hornykiewicz. 1960. Verteilung von noradrenalin and dopamin (3-hydroxytyramin) im gehirn des menschen und ihr verhalten bei erkrankungen des extrapyramidalen systems. *Klin. Wochenschr.* **38:** 1236–1239.
18. Engele, J., and M. C. Bohn. 1991. The neurotrophic effects of fibroblast growth factors on dopaminergic neurons *in vitro* are mediated by mesencephalic glia. *J. Neurosci.* **11:** 3070–3078.
19. Freed, C. R., R. E. Breeze, N. L. Rosenberg, S. A. Schneck, T. H. Wells, J. N. Barrett, S. T. Grafton, S. C. Huang, D. Eidelberg, and D. A. Rotenberg. 1990. Transplantation of human fetal dopamine cells for Parkinson's disease: Results at 1 year. *Arch. Neurol.* **47:** 505–512.
20. Freed, C. R., R. E. Breeze, N. L. Rosenberg, S. A. Schneck, *et al.* 1991. Fetal neural implants for Parkinson's disease: Results at 15 months. In *Restorative Neurology, Intracerebral Transplantation in Movement Disorders,* Vol. 4, pp. 69–77. Elsevier, Amsterdam.
21. Freed, C. R., R. E. Breeze, N. L. Rosenberg, S. A. Schneck, E. Kriek, J. X. Qi, T. Lone, Y. B. Zhang, J. A. Snyder, T. H. Wells, L. O. Ramig, L. Thompson, J. C. Mazziotta, S. C. Huang, S. T. Grafton, D. Brooks, G. Sawle, G. Schroter, and A. A. Ansari. 1992. Survival of implanted fetal dopamine cells and neurologic improvement 12 to 46 months after transplant for Parkinson's disease. *N. Engl. J. Med.* **327:** 1549–1555.
22. Freed, C. R., R. E. Breeze, N. L. Rosenberg, and S. A. Schneck. 1992. Embryonic dopamine cell implants as a treatment for the second phase of Parkinson's disease: Replacing failed nerve terminals. In *Advances in Neurology* (H. Narabayashi, T. Nagatsu, N. Yanagisawa, and Y. Mizuno, Eds.), Vol. 60, pp. 721–728. Raven Press, New York.
23. Freed, C. R., R. E. Breeze, S. A. Schneck, R. A. E. Bakay, and A. A. Ansari. 1995. Fetal neural transplantation for Parkinson disease. In *Clinical Immunology: Principles and Practice* (R. R. Rich, Eds.), pp. 1677–1687. Mosby–Year Book, St. Louis, MO.
24. Freeman, T. B., M. S. Spence, B. D. Boss, D. H. Spector, R. E. Strecker, C. W. Olanow, and J. H. Kordower. 1991. Development of dopaminergic neurons in the human substantia nigra. *Exp. Neurol.* **113:** 344–353.

25. Freeman, T. B., C. W. Olanow, R. A. Hauser, G. M. Nauert, D. A. Smith, C. V. Borlongan, P. R. Sanberg, D. A. Holt, J. H. Kordower, F. J. G. Vingerhoets, B. J. Snow, D. Calne, and L. Gauger. 1995. Bilateral fetal nigral transplantation into the postcommissural putamen in Parkinson's disease. *Ann. Neurol.* **38:** 379–388.
26. Freeman, T. B., P. R. Sanberg, G. M. Nauert, C. V. Borlongan, E.-Z. Liu, B. D. Boss, D. Spector, C. W. Olanow, and J. H. Kordower. 1995. The influence of donor age on the survival of solid and suspension intraparenchymal human embryonic nigral grafts. *Cell Transplant.* **4:** 141–154.
27. Frodl, E. M., W. M. Duan, H. Sauer, A. Kupsch, and P. Brundin. 1994. Human embryonic neurons xenografted to the rat: Effects of cryopreservation and varying regional source of donor cells on transplant survival, morphology and function. *Brain Res.* **647:** 286–298.
28. Hefti, F. 1997. Neurotrophic factor therapy—Keeping score. *Nature Med.* **3:** 497–498.
29. Herregodts, P., and Y. Michotte. 1987. Combined ion-pair extraction and high-performance liquid chromatography for the determination of the biogenic amines and their major metabolites in single brain tissue samples. *J. Chromatogr.* **421:** 51–60.
30. Knusel, B., P. P. Michel, J. S. Schwaber, and F. Hefti. 1990. Selective and nonselective stimulation of central cholinergic and dopaminergic development *in vitro* by nerve growth factor, basic fibroblast growth factor, epidermal growth factor, insulin and insulin-like growth factors I and II. *J. Neurosci.* **10:** 558–570.
31. Kondoh, T., L. L. Pundt, and W. C. Low. 1995. Development of human fetal ventral mesencephalic grafts in rats with 6-OHDA lesions of the nigrostriatal pathway. *Neurosci. Res.* **21:** 223–233.
32. Kopyov, O. V., D. Jacques, A. Lieberman, C. M. Duma, and R. L. Rogers. 1996. Clinical study of fetal mesencephalic intracerebral transplants for the treatment of Parkinson's disease. *Cell Transplant.* **5:** 327–337.
33. Kordower, J. H., T. B. Freeman, B. J. Snow, F. J. G. Vingerhoets, E. J. Mufson, P. R. Sanberg, R. A. Hauser, D. A. Smith, M. Nauert, D. P. Perl, and C. W. Olanow. 1995. Neuropathological evidence of graft survival and striatal reinnervation after the transplantation of fetal mesencephalic tissue in a patient with Parkinson's disease. *N. Engl. J. Med.* **322:** 1118–1124.
34. Laird, N. M., and J. H. Ware. 1982. Random effects for longitudinal data. *Biometrics* **38:** 963–974.
35. Lindvall, O., P. Brundin, H. Widner, S. Rehncrona, B. Gustavii, R. Frackowiak, K. L. Leenders, G. Sawle, J. C. Rothwell, C. D. Marsden, and A. Björklund. 1990. Grafts of fetal dopamine neurons survive and improve motor function in Parkinson's disease. *Science* **247:** 574–577.
36. Mahalik, T. J., W. E. Hahn, G. H. Clayton, and G. P. Owens. 1994. Programmed cell death in developing grafts of fetal substantia nigra. *Exp. Neurol.* **129:** 27–36.
37. Nakao, N., E. M. Frodl, W.-M. Duan, H. Widner, and P. Brundin. 1994. Lazaroids improve the survival of grafted rat embryonic dopamine neurons. *Proc. Natl. Acad. Sci. USA* **91:** 12408–12412.
38. Nakao, N., E. M. Frodl, H. Widner, E. Carlson, F. A. Eggerding, C. J. Epstein, and P. Brundin. 1995. Overexpressing Cu/Zu superoxide dismutase enhances survival of transplanted neurons in a rat model of Parkinson's disease. *Nature Med.* **1:** 226–231.
39. Olanow, C. W., J. H. Kordower, and T. B. Freeman. 1996. Fetal nigral transplantation as a therapy for Parkinson's disease. *Trends Neurosci.* **19:** 102–109.
40. O'Rahilly, R., and F. Muller. 1987. *Developmental Stages in Human Embryos,* Carnegie Institution of Washington publication 637. Meriden-Stinehour Press, Meriden, CT.
41. Othberg, A., M. Keep, P. Brundin, and O. Lindvall. 1997. Trilazad mesylate improves survival of rat and human embryonic mesencephalic neurons *in vitro. Exp. Neurol.* **147:** 498–502.
42. Paxinos, G., and C. Watson. 1986. *The Rat Brain in Stereotaxic Coordinates.* Academic Press, New York.
43. Perlow, M. J., W. J. Freed, B. J. Hoffer, A. Seiger, L. Olson, and R. J. Wyatt. 1979. Brain grafts reduce motor abnormalities produced by destruction of nigrostriatal dopamine system. *Science* **204:** 643–647.
44. Richards, J. B., K. E. Sabol, and C. R. Freed. 1990 Unilateral dopamine depletion causes bilateral deficits in conditioned rotation in rats. *Pharmacol. Biochem. Behav.* **36:** 217–223.
45. Richards, J. B., K. E. Sabol, E. H. Kriek, and C. R. Freed. 1993. Trained and amphetamine-induced circling behavior in lesioned, transplanted rats. *J. Neural Transm. Plast.* **4:** 157–166.
46. Sauer, H. 2000. Pregraft tissue storage methods for intracerebral transplantation. In *Neuromethods: Neural Transplantation Methods* (S. B. Dunnet, A. A. Boulton, and G. B. Baker, Eds.), Vol. 36, pp. 27–40. Humana Press, Totowa, NJ.
47. Schierle, G. S., O. Hansson, M. Leist, P. Nicotera, H. Widner, and P. Brundin. 1999. Caspase inhibition reduces apoptosis and increases survival of nigral transplants. *Nature Med.* **5:** 97–100.
48. Schierle, G. S., M. Leist, J. C. Martinou, H. Widner, P. Nicotera, and P. Brundin. 1999. Differential effects of Bcl-2 overexpression on fibre outgrowth and survival of embryonic dopaminergic neurons in intracerebral transplants. *Eur. J. Neurosci.* **11:** 3073–3081.
49. Spenger, C., N. S. Haque, L. Studer, L. Evtouchenko, B. Wagner, B. Buhler, U. Lendahl, and R. W. Seiler. 1996. Fetal ventral mesencephalon of human and rat origin maintained in vitro and transplanted to 6-hydroxydopamine-lesioned rats gives raise to grafts rich in dopaminergic neurons. *Exp. Brain Res.* **112:** 47–57.
50. Strömberg, I., M. Bygdeman, M. Goldstein, A. Seiger, and L. Olson. 1986. Human fetal substantia nigra grafted to the dopamine-denervated striatum of immunosuppressed rats: Evidence for functional reinnervation. *Neurosci. Lett.* **71:** 271–276.
51. Strömberg, I., P. Almqvist, M. Bygdeman, T. E. Finger, G. Gerhardt, A. C. Granholm, T. J. Mahalik, A. Seiger, B. Hoffer, and L. Olson. 1988. Intracerebral xenografts of human mesencephalic tissue into athymic rats: Immunochemical and *in vivo* electrochemical studies. *Proc. Natl. Acad. Sci. USA* **85:** 8331–8334.
52. Strömberg, I., M. Bygdeman, M. Goldstein, A. Seiger, and L. Olson. 1988. Human fetal substantia nigra grafted to the dopamine-denervated striatum of immunosuppressed rats: Evidence for functional reinnervation. *Neurosci. Lett.* **71:** 271–276.
53. Takayama, H., J. Ray, H. K. Raymon, A. Baird, L. J. Fisher, and F. H. Gage. 1995. Basic fibroblast growth factor increases dopaminergic graft survival and function in a rat model of Parkinson's disease. *Nature Med.* **1:** 53–58.
54. Thajeb, P., Z. D. Ling, E. D. Potter, and P. M. Carvey. 1997. The effects of storage conditions and trophic supplementation on the survival of fetal mesencephalic cells. *Cell Transplant.* **6:** 297–307.
55. Ungerstedt, U., and G. W. Arbuthnott. 1970 Quantitative recording of rotational behavior in rats after 6-hydroxydopamine lesions of the nigrostriatal dopamine system. *Brain Res.* **24:** 485–490.

56. Van Horne, C. G., T. Mahalik, B. Hoffer, M. Bygdeman, P. Almqvist, P. Stieg, A. Seiger, L. Olson, and I. Strömberg. 1990 Behavioral and electrophysiological correlates of human mesencephalic dopaminergic xenograft function in the rat striatum. *Brain Res. Bull.* **25:** 325–334.

57. Walters, A. M., D. J. Clarke, H. F. Bradford, and G. H. Stern. 1992. The properties of cultured fetal human and rat brain tissue and its use as grafts for the relief of the parkinsonian syndrome. *Neurochem. Res.* **17:** 893–900.

58. Wang, Y., J. C. Lin, A. L. Chiou, J. Y. Liu, and F. C. Zhou. 1995. Human ventromesencephalic grafts restore dopamine release and clearance in hemiparkinsonian rats. *Exp. Neurol.* **136:** 98–106.

59. Widner, H., J. Tetrud, S. Rehncrona, B. Snow, P. Brundin, B. Gustavii, and J. W. Langston. 1992. Bilateral fetal mesencephalic grafting in two patients with Parkinsonism induced by 1-methyl-4-phenyl-1,2,3,6-tetrahydropyridine (MPTP). *N. Engl. J. Med.* **327:** 1556–1563.

60. Zawada, W. M., J. B. Cibelli, P. K. Choi, E. D. Clarkson, P. J. Golueke, S. E. Witta, K. P. Bell, J. Kane, A. P. Ponce de Leon, D. J. Jerry, J. M. Robl, C. R. Freed, and S. L. Stice. 1998. Somatic cell cloned transgenic bovine neurons for transplantation in parkinsonian rats. *Nature Med.* **4:** 569–574.

61. Zawada, W. M., D. L. Kirschman, J. J. Cohen, K. A. Heidenreich, and C. R. Freed. 1996. Growth factors rescue embryonic dopamine neurons from programmed cell death. *Exp. Neurol.* **140:** 60–67.

62. Zawada, W. M., D. J. Zastrow, E. D. Clarkson, F. S. Adams, K. P. Bell, and C. R. Freed. 1998. Growth factors improve immediate survival of embryonic dopamine neurons after transplantation into rats. *Brain Res.* **786:** 96–103.

63. Yayon, A., M. Klagsbrun, J. D. Esko, P. Leder, and D. M. Ornitz. 1991. Cell surface, heparin-like molecules are required for binding of basic fibroblast growth factor to its affinity receptor. *Cell* **64:** 841–848.

The Journal of Neuroscience, November 1, 2002, 22(21):9287–9297

Insulin-Like Growth Factor-I Blocks Bcl-2 Interacting Mediator of Cell Death (Bim) Induction and Intrinsic Death Signaling in Cerebellar Granule Neurons

Daniel A. Linseman, Reid A. Phelps, Ron J. Bouchard, Shoshona S. Le, Tracey A. Laessig, Maria L. McClure, and Kim A. Heidenreich

Department of Pharmacology, University of Colorado Health Sciences Center and the Denver Veterans Affairs Medical Center, Denver, Colorado 80262

Cerebellar granule neurons depend on insulin-like growth factor-I (IGF-I) for their survival. However, the mechanism underlying the neuroprotective effects of IGF-I is presently unclear. Here we show that IGF-I protects granule neurons by suppressing key elements of the intrinsic (mitochondrial) death pathway. IGF-I blocked activation of the executioner caspase-3 and the intrinsic initiator caspase-9 in primary cerebellar granule neurons deprived of serum and depolarizing potassium. IGF-I inhibited cytochrome *c* release from mitochondria and prevented its redistribution to neuronal processes. The effects of IGF-I on cytochrome *c* release were not mediated by blockade of the mitochondrial permeability transition pore, because IGF-I failed to inhibit mitochondrial swelling or depolarization. In contrast, IGF-I blocked induction of the BH3-only Bcl-2 family member, Bim (Bcl-2 interacting mediator of cell death), a mediator of Bax-dependent cytochrome *c* release. The suppression of Bim expression by IGF-I did not involve inhibition of the c-Jun transcription factor. Instead, IGF-I prevented activation of the forkhead family member, FKHRL1, another transcriptional regulator of Bim. Finally, adenoviral-mediated expression of dominant-negative AKT activated FKHRL1 and induced expression of Bim. These data suggest that IGF-I signaling via AKT promotes survival of cerebellar granule neurons by blocking the FKHRL1-dependent transcription of Bim, a principal effector of the intrinsic death-signaling cascade.

Key words: insulin-like growth factor; cerebellar granule neuron; apoptosis; mitochondria; Bim; forkhead transcription factor

Insulin-like growth factor-I (IGF-I) has significant neurotrophic and neuroprotective effects. IGF-I expression is regulated differentially in various brain regions and is associated temporally with critical stages of CNS development (Rotwein et al., 1988; Bach et al., 1991). Deficits in IGF-I are observed in Alzheimer's disease (Mustafa et al., 1999) and degenerative cerebellar ataxias (Torres-Aleman et al., 1996), and recombinant IGF-I slows disease progression in sporadic amyotrophic lateral sclerosis (Lai et al., 1997). IGF-I decreases neuronal apoptosis and enhances functional recovery in animal models of neurodegeneration including toxin exposure (Fernandez et al., 1998), transient ischemia (Liu et al., 2001), and neurotransplantation (Clarkson et al., 2001). Similarly, IGF-I rescues primary neurons from apoptosis induced by trophic factor withdrawal (Russell et al., 1998), excitotoxicity (Tagami et al., 1997), and oxidative stress (Heck et al., 1999). Thus IGF-I is essential for the survival of CNS neurons *in vivo* and *in vitro*.

Cerebellar granule neurons (CGNs) are critically dependent on IGF-I for their survival (Lin and Bulleit, 1997). In hereditary models of cerebellar Purkinje cell degeneration (pcd; *lurcher*), the primary death of Purkinje neurons induces the subsequent apoptosis of CGNs because of the loss of Purkinje-derived IGF-I (Bartlett et al., 1991; Zhang et al., 1997; Selimi et al., 2000a). Transgenic mice overexpressing IGF-I exhibit a remarkable doubling of CGN number (Ye et al., 1996) and show decreased expression of caspase-3 in cerebellum (Chrysis et al., 2001). These observations illustrate that IGF-I protects CGNs from apoptosis *in vivo*.

Similarly, IGF-I rescues primary CGNs from apoptosis induced by removal of depolarizing potassium and serum (trophic factor withdrawal), an established *in vitro* model of neuronal apoptosis (D'Mello et al., 1993; Galli et al., 1995; Miller et al., 1997a). CGN apoptosis involves activation of the intrinsic (mitochondrial) death pathway (Green, 1998). For example, trophic factor-deprived CGNs demonstrate Bax-dependent cytochrome *c* release from mitochondria (Desagher et al., 1999), and CGNs isolated from Bax knock-out mice are less sensitive to trophic factor withdrawal (Miller et al., 1997b). Moreover, the BH3-only proapoptotic Bcl-2 family member, Bim (Bcl-2 interacting mediator of cell death), is induced in CGNs undergoing apoptosis (Harris and Johnson, 2001; Putcha et al., 2001). BH3-only proteins facilitate intrinsic death signaling in a Bax-dependent manner (Desagher et al., 1999; Zong et al., 2001). Although it is recognized that IGF-I rescues CGNs via phosphatidylinositol 3 kinase (PI3K) and AKT (Dudek et al., 1997; Miller et al., 1997a), the effects of IGF-I on components of the intrinsic death pathway have not been examined.

Here we found that IGF-I suppresses induction of Bim, cytochrome *c* release from mitochondria, and activation of the intrinsic initiator caspase-9 and the executioner caspase-3 in trophic factor-deprived CGNs. Although c-Jun N-terminal protein kinase

Received March 22, 2002; revised Aug. 5, 2002; accepted June 24, 2002.

This work was supported by a Department of Veterans Affairs Merit Award (K.A.H.), Department of Defense Grant DAMD17-99-1-9481 (K.A.H.), National Institutes of Health Grant NS38619-01A1 (K.A.H.), and a Department of Veterans Affairs Research Enhancement Award Program (K.A.H. and D.A.L.). We thank Mary Kay Meintzer for her help with preparation of this manuscript.

Correspondence should be addressed to Dr. Kim A. Heidenreich, Department of Pharmacology (C236), University of Colorado Health Sciences Center, 4200 East Ninth Avenue, Denver, CO 80262. E-mail: Kim.Heidenreich@UCHSC.edu.

(JNK)/c-Jun signaling has been implicated in the induction of Bim during neuronal apoptosis (Harris and Johnson, 2001; Whitfield et al., 2001), our data suggest that IGF-I suppresses Bim expression via a distinct mechanism involving inhibition of the forkhead transcription factor FKHRL1. These results indicate that the intrinsic death pathway is a principal target of IGF-I in neurons.

MATERIALS AND METHODS

Materials. Recombinant human IGF-I was provided by Margarita Quiroga (Chiron, Emeryville, CA). Polyclonal antibodies to Bim, Bcl-X_L, caspase-3, caspase-9, cytochrome *c*, and c-Jun were from Santa Cruz Biotechnology (Santa Cruz, CA). Polyclonal antibodies to phospho-c-Jun (Ser^{63}), phospho-AKT (Ser^{473}), and AKT were from Cell Signaling Technologies (Beverly, MA). Polyclonal antibodies to phospho-FKHRL1 (Ser^{253}) and FKHRL1 were from Upstate Biotechnology (Lake Placid, NY). Cy3-conjugated secondary antibodies for immunocytochemistry were purchased from Jackson ImmunoResearch Laboratories (West Grove, PA). Horseradish peroxidase-linked secondary antibodies and reagents for enhanced chemiluminescence detection were obtained from Amersham Biosciences (Piscataway, NJ). JC1, tetramethylrhodamine ethyl ester (TMRE), and MitoTracker Green were from Molecular Probes (Eugene, OR). Wortmannin, Hoechst dye number 33258, and 4′,6-diamidino-2-phenylindole (DAPI) were from Sigma (St. Louis, MO). Adenoviral cytokine response modifier A (CrmA) was obtained from Dr. James DeGregori [University of Colorado Health Sciences Center (UCHSC), Denver, CO]. Adenoviral CMV (negative control adenovirus) was from Dr. Jerry Schaack (UCHSC). Adenoviral kinase-dead K179M mutant (dominant-negative) AKT was obtained from Drs. Prem Sharma and Jerry Olefsky (University of California, San Diego, CA).

Cell culture. Rat CGNs were isolated from 7-d-old Sprague Dawley rat pups (15–19 gm) as described previously (Li et al., 2000). Briefly, neurons were plated on 35-mm-diameter plastic dishes coated with poly-L-lysine at a density of 2.0×10^6 cells/ml in basal modified Eagle's medium containing 10% fetal bovine serum, 25 mM KCl, 2 mM L-glutamine, and 100 U/ml penicillin/100 μg/ml streptomycin (Invitrogen, Grand Island, NY). Cytosine arabinoside (10 μM) was added to the culture medium 24 hr after plating to limit the growth of non-neuronal cells. With the use of this protocol the cultures were ~95–99% pure for granule neurons. In general, experiments were performed after 7 d in culture.

Quantification of apoptosis. Apoptosis was induced by removing serum and decreasing the extracellular potassium concentration from 25 to 5 mM. After 24 hr the CGNs were fixed with 4% paraformaldehyde, and the nuclei were stained with either Hoechst dye or DAPI. Cells were considered apoptotic if their nuclei either were condensed or were fragmented. In general, ~500 cells from at least two fields of a 35 mm well were counted. Data are presented as the percentage of cells in a given treatment group that were scored as apoptotic. Experiments were performed at least in triplicate.

Preparation of CGN cell extracts. After incubation for the indicated times and with the reagents specified in Results, the culture medium was aspirated; the cells were washed once with 2 ml of ice-cold PBS, pH 7.4, placed on ice, and scraped into lysis buffer (200 μl/35 mm well) containing (in mM): 20 HEPES, pH 7.4, 50 NaCl, 1 EGTA, 5 β-glycerophosphate, 30 sodium pyrophosphate, and 1 phenylmethylsulfonyl fluoride plus 1% Triton X-100, 100 μM sodium orthovanadate, 10 μg/ml leupeptin, and 10 μg/ml aprotinin. Cell debris was removed by centrifugation at $6000 \times g$ for 3 min, and the protein concentration of the supernatant was determined by a commercially available protein assay kit (Pierce, Rockford, IL). Aliquots (~150 μg) of supernatant protein were diluted to a final concentration of 1× SDS-PAGE sample buffer, boiled for 5 min, and electrophoresed through 10–15% polyacrylamide gels. Proteins were transferred to polyvinylidene difluoride (PVDF) membranes (Millipore, Bedford, MA) and processed for immunoblot analysis.

Immunoblot analysis. Nonspecific binding sites were blocked in PBS, pH 7.4, containing 0.1% Tween 20 (PBS-T) and 1% BSA for 1 hr at room temperature. Primary antibodies were diluted in blocking solution and incubated with the membranes for 1 hr. Excess primary antibody was removed by washing the membranes three times in PBS-T. Then the blots were incubated with the appropriate horseradish peroxidase-conjugated secondary antibody diluted in PBS-T for 1 hr and subsequently were washed three times in PBS-T. Immunoreactive proteins were detected by enhanced chemiluminescence. In some experiments the membranes were reprobed after stripping in 0.1 M Tris-HCl, pH 8.0, 2% SDS, and 100 mM β-mercaptoethanol for 30 min at 52°C. The blots were rinsed twice in PBS-T and processed as above with a different primary antibody. Autoluminograms shown are representative of at least three independent experiments.

Immunocytochemistry. CGNs were cultured on polyethyleneimine-coated glass coverslips at a density of $\sim 2.5 \times 10^5$ cells per coverslip. After incubation as described in Results, the cells were fixed in 4% paraformaldehyde and were permeabilized and blocked in PBS, pH 7.4, containing 0.2% Triton X-100 and 5% BSA. Cells then were incubated for ~16 hr at 4°C with primary antibody diluted in PBS containing 0.2% Triton X-100 and 2% BSA. The primary antibody was aspirated, and the cells were washed five times with PBS. Then the cells were incubated with a Cy3-conjugated secondary antibody and DAPI for 1 hr at room temperature. CGNs were washed five more times with PBS, and coverslips were adhered to glass slides in mounting medium (0.1% *p*-phenylenediamine in 75% glycerol in PBS). Fluorescent images were captured by using either 63× or 100× oil immersion objectives on a Zeiss Axioplan 2 microscope equipped with a Cooke Sensicam deep-cooled CCD camera and a Slidebook software analysis program for digital deconvolution (Intelligent Imaging Innovations, Denver, CO).

Measurement of mitochondrial swelling. CGNs were incubated as described in Results, and JC1 (final concentration, 2 μg/ml) was added to the cultures 30 min before fixation to stain mitochondria. JC1 fluorescence was captured in paraformaldehyde-fixed cells by using a Cy3 filter under a 100× oil objective. Then the diameters of ~150 mitochondria per treatment condition were measured from digitally deconvolved images obtained from a total of 15–20 CGNs (randomly pooled from four independent experiments).

Assessment of mitochondrial membrane potential. CGNs grown on glass coverslips were incubated as described in Results, and TMRE (500 nM) was added directly to the cells 30 min before the end of the incubation period. After incubation the coverslips were inverted onto slides into a small volume of phenol red-free medium containing TMRE (500 nM). Living cells then were imaged with a Cy3 filter to detect TMRE fluorescence under a 100× oil objective. All images were acquired at equal exposure times for TMRE fluorescence to assess the relative mitochondrial membrane potentials.

Adenoviral infection. Recombinant adenoviruses were purified by cesium chloride gradient ultracentrifugation. The viral titer (multiplicity of infection) was determined by measuring the absorbance at 260 nm (where 1.0 absorbance unit = 1×10^{12} particles/ml), and infectious particles were verified by plaque assay. Adenoviral (Ad)-CMV, Ad-CrmA, or Ad-dominant-negative (DN)-AKT was added to CGN cultures on day 5 at a multiplicity of infection of 50. At 48 hr after infection either CGN apoptosis was induced by removal of serum and depolarizing potassium for 24 hr (for Ad-CMV and Ad-CrmA) or cell lysates were prepared directly for Western blotting for phospho-FKHRL1 and Bim (for Ad-CMV and Ad-DN-AKT).

Data analysis. The results that are shown represent the means ± SEM for the number (*n*) of independent experiments that were performed. Statistical differences between the means of unpaired sets of data were evaluated by one-way ANOVA, followed by a *post hoc* Dunnett's test. A p value of <0.01 was considered statistically significant.

RESULTS

IGF-I suppresses CGN apoptosis and activation of caspase-3 and caspase-9

Primary CGNs are dependent on depolarization-mediated calcium influx and serum-derived growth factors for their survival *in vitro* (D'Mello et al., 1993; Galli et al., 1995). The removal of serum and depolarizing potassium induced marked apoptosis of CGNs, characterized morphologically by chromatin condensation and fragmentation (Fig. 1*A*). Quantification of CGN apoptosis was performed by counting the number of cells with condensed and/or fragmented nuclei from several representative fields for each incubation condition. Basal CGN apoptosis was ~10% and increased to ~60% after 24 hr of trophic factor withdrawal (Fig. 1*B*). We used this cell system to investigate the mechanism of IGF-I neuroprotection. As described previously (D'Mello et al., 1993; Galli et al., 1995; Miller et al., 1997a), the addition of IGF-I

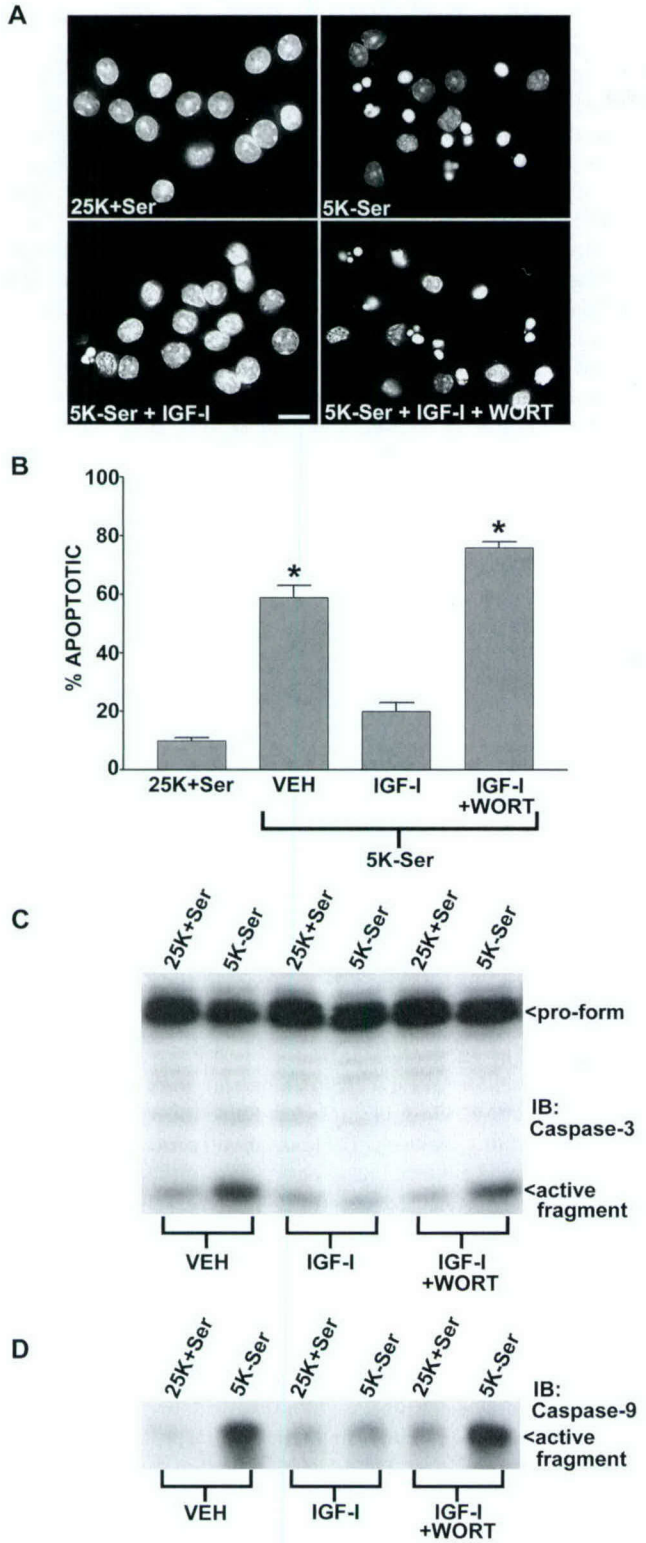

Figure 1. IGF-I inhibits apoptosis and activation of the executioner caspase-3 and the intrinsic initiator caspase-9 in CGNs subjected to trophic factor withdrawal. *A*, CGNs were incubated for 24 hr in either control (*25K+Ser*) or apoptotic (*5K-Ser*) medium containing either PBS vehicle (*VEH*) or IGF-I (200 ng/ml) in the absence or presence of wortmannin (*WORT*; 100 nM). After incubation the CGNs were fixed, and the nuclei were stained with DAPI. Scale bar, 10 μm. *B*, The percentages of apoptotic CGNs observed under the conditions described in *A* were quantified by counting ~500 CGNs per field in two fields per condition. Values represent the means ± SEM for three independent experiments, each performed in triplicate. *Significantly different from the 25K+Ser control ($p < 0.01$). *C*, CGNs were incubated as described in *A*, but for only 6 hr. Detergent-soluble cell lysates were subjected to SDS-PAGE on 15% polyacrylamide gels, and the proteins were transferred to PVDF membranes. Activation of caspase-3 was assessed by immunoblotting (*IB*) with a polyclonal antibody that recognizes both the proform (~32 kDa) and the cleaved form (~19 kDa active fragment) of the enzyme. The blot shown is representative of results obtained in three separate experiments. *D*, CGNs were incubated exactly as described in *C*, and the cell lysates were electrophoresed as described in *C*. Activation of caspase-9 was assessed by Western blotting with a polyclonal antibody that specifically recognizes the cleaved form (active fragment) of the caspase. The blot shown is representative of three independent experiments.

to cerebellar cultures immediately after trophic factor withdrawal resulted in an ~80% reduction in CGN apoptosis (Fig. 1*A*,*B*). The ability of IGF-I to rescue CGNs from apoptosis required the activation of PI3K, as demonstrated by the loss of protection observed in the presence of wortmannin (Fig. 1*A*,*B*). Activation of the executioner caspase-3 has been implicated in the apoptotic death of CGNs (Eldadah et al., 2000). Consistent with this, we observed cleavage of caspase-3 from the proform to an active fragment within 6 hr of serum and potassium deprivation (Fig. 1*C*). Like the results obtained for nuclear condensation and fragmentation, IGF-I inhibited caspase-3 activation in a PI3K-dependent manner (Fig. 1*C*). This latter result suggested that IGF-I blocks proapoptotic signaling events early in the apoptotic cascade, because caspase-3 cleavage commonly is thought to signify commitment to apoptosis.

To identify potential targets of IGF-I action upstream of the executioner caspase-3 in the apoptotic cascade, we focused on components of the intrinsic (mitochondrial) death pathway (Green, 1998). Recent data indicate that the intrinsic death pathway plays a significant role in CGN apoptosis evoked by trophic factor withdrawal (Miller et al., 1997b; Desagher et al., 1999). Immediately upstream of caspase-3 cleavage, activation of the initiator caspase-9 is the most distal event in the intrinsic pathway (Kuida et al., 1998). Recently, caspase-9 activation was shown to be required for caspase-3 cleavage in CGNs deprived of serum and depolarizing potassium (Gerhardt et al., 2001). Consistent with the involvement of caspase-9 in CGN apoptosis, we found that infection of CGNs with adenoviral CrmA, an inhibitor of Group III caspases (including caspase-9), but not Group II caspases (such as caspase-3) (Garcia-Calvo et al., 1998), significantly decreased apoptosis from 72 ± 8% ($n = 3$) to 29 ± 3% ($n = 3$; $p < 0.01$). In contrast, a negative control adenovirus (Ad-CMV) had no effect on CGN apoptosis (70 ± 8%; $n = 3$). After acute serum and potassium deprivation, we observed marked cleavage of caspase-9 consistent with its activation (Fig. 1*D*). As was observed for caspase-3 cleavage, activation of caspase-9 was inhibited significantly by IGF-I in a PI3K-dependent manner (Fig. 1*D*), demonstrating that IGF-I suppresses a key component of the intrinsic death pathway in CGNs.

IGF-I inhibits release of cytochrome *c* from mitochondria and its redistribution to neuronal processes

Caspase-9 is activated after its association with Apaf-1 and cytochrome *c*, which assemble into a large oligomeric complex known as the apoptosome (Zou et al., 1999). Formation of the apoptosome occurs after release of the mitochondrial protein, cytochrome *c*, into the cytoplasm. In CGNs maintained in the pres-

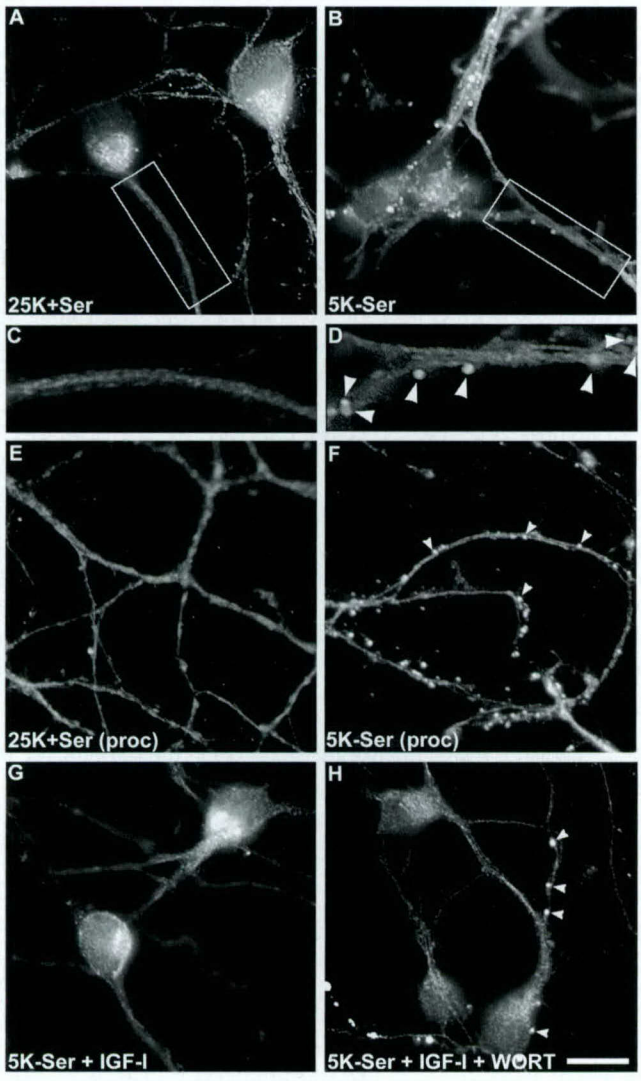

Figure 2. IGF-I blocks cytochrome *c* release from mitochondria and prevents its redistribution to focal complexes localized in neuronal processes. CGNs were incubated for 4 hr in control (*25K+Ser*) or apoptotic (*5K-Ser*) medium containing either PBS vehicle or IGF-I (200 ng/ml) in the absence or presence of wortmannin (*WORT*; 100 nM). After incubation the CGNs were fixed in 4% paraformaldehyde, permeabilized with 0.2% Triton X-100, and blocked with 5% BSA. Cytochrome *c* was localized by incubating the cells with a polyclonal antibody to cytochrome *c* and a Cy3-conjugated secondary antibody. Digitally deconvolved images were captured by using a 63× oil objective. The images shown are representative of results obtained in three separate experiments. Scale bar, 10 μm. *A*, CGNs incubated in control medium demonstrated intense cytochrome *c* staining in the perinuclear region consistent with localization to mitochondria. Very diffuse staining was observed in neuronal processes. *B*, CGNs incubated in apoptotic medium for 4 hr showed a marked redistribution of cytochrome *c*. Note the overall diffuse staining throughout the cytoplasm accompanied by the formation of distinct, brightly fluorescent focal complexes on the cell bodies and processes. *C*, The area demarcated by the *box* in *A* is enlarged to show the diffuse cytochrome *c* staining in a control neuronal process. *D*, The area demarcated by the *box* in *B* is enlarged to show the intense cytochrome *c* staining localized to discrete focal complexes (indicated by the *arrowheads*) in neuronal processes of CGNs deprived of serum and depolarizing potassium. *E*, A region containing multiple processes (*proc*) from control CGNs is shown. Note the overall diffuse cytochrome *c* staining. *F*, A region containing multiple processes from CGNs incubated in apoptotic medium for 4 hr is shown. Note the presence of many distinct focal areas of intense cytochrome *c* staining (indicated by the *arrowheads*). *G*, CGNs incubated in apoptotic medium containing exogenous IGF-I displayed cytochrome *c* localization to mitochondria similar to control CGNs (see *A* for comparison). *H*, CGNs incubated in apoptotic medium containing both IGF-I and wortmannin showed cytochrome *c* staining similar to CGNs incubated in apoptotic medium alone (see *B* for comparison). Focal complexes of cytochrome *c* staining are indicated by the *arrowheads*.

ence of serum and depolarizing potassium, cytochrome *c* was localized predominantly in mitochondria (Fig. 2*A*), with only diffuse staining observed in neuronal processes (Fig. 2*C*,*E*). Removal of serum and depolarizing potassium for 4 hr resulted in a rapid redistribution of cytochrome *c* from mitochondria to a diffuse staining throughout the cytoplasm. This redistribution was accompanied by the formation of many pronounced punctate areas of cytochrome *c* staining (Fig. 2*B*). The latter were observed primarily, although not exclusively, in distinct focal complexes localized to neuronal processes (Fig. 2*D*,*F*). In contrast to cytochrome *c* staining, no detectable redistribution of the mitochondrial marker MitoTracker Green was observed in neuronal processes under apoptotic conditions, indicating that the punctate areas of cytochrome *c* staining were not associated with intact mitochondria (data not shown). Inclusion of IGF-I during trophic factor withdrawal prevented the release and redistribution of cytochrome *c* from mitochondria (Fig. 2*G*). However, the addition of wortmannin in combination with IGF-I restored the release of cytochrome *c* from mitochondria and its redistribution to focal complexes in neuronal processes (Fig. 2*H*), indicating that the effects of IGF-I on cytochrome *c* release were PI3K-dependent. Thus, IGF-I inhibits the release of cytochrome *c* from mitochondria and, in this manner, blocks the subsequent activation of the intrinsic initiator caspase-9.

Mitochondrial swelling and mitochondrial membrane depolarization are not prevented by IGF-I

There are two potential mechanisms underlying cytochrome *c* release from mitochondria that have received considerable attention. The first involves opening of the permeability transition pore (PTP). The PTP is a heteromeric protein complex that includes the voltage-dependent anion channel, the adenine nucleotide translocator, and cyclophilin D as well as several other proteins (for review, see Martinou and Green, 2001). The PTP is localized at contact sites between the inner and outer mitochondrial membranes. Some apoptotic stimuli are capable of opening the PTP, resulting in disruption of the mitochondrial membrane potential (depolarization), a decline in ATP production, and entry of solutes and water into the mitochondrial matrix. Ultimately, mitochondrial swelling and rupture of the outer mitochondrial membrane occur, allowing the leakage of proteins (e.g., cytochrome *c*) from the intermembrane space into the cytoplasm. We used the mitochondrial dye JC1 to visualize mitochondria in CGNs undergoing apoptosis. Although the absolute amount of JC1 accumulated in mitochondria varies with membrane potential, JC1 is extremely photostable and labels all mitochondria to some extent (White and Reynolds, 1996). After incubation with JC1 the CGNs were fixed, and the diameters of labeled mitochondria were measured after digital deconvolution imaging. As shown in Figure 3, serum and potassium deprivation for 4 hr resulted in dramatic swelling of mitochondria in CGNs (Fig. 3*A*, *top panels*). This effect was reversible if serum and depolarizing potassium were restored within the first 2 hr after trophic factor withdrawal (Fig. 3*A*, *bottom right panel*). Inclusion of IGF-I during the apoptotic stimulus did not prevent the swelling of CGN

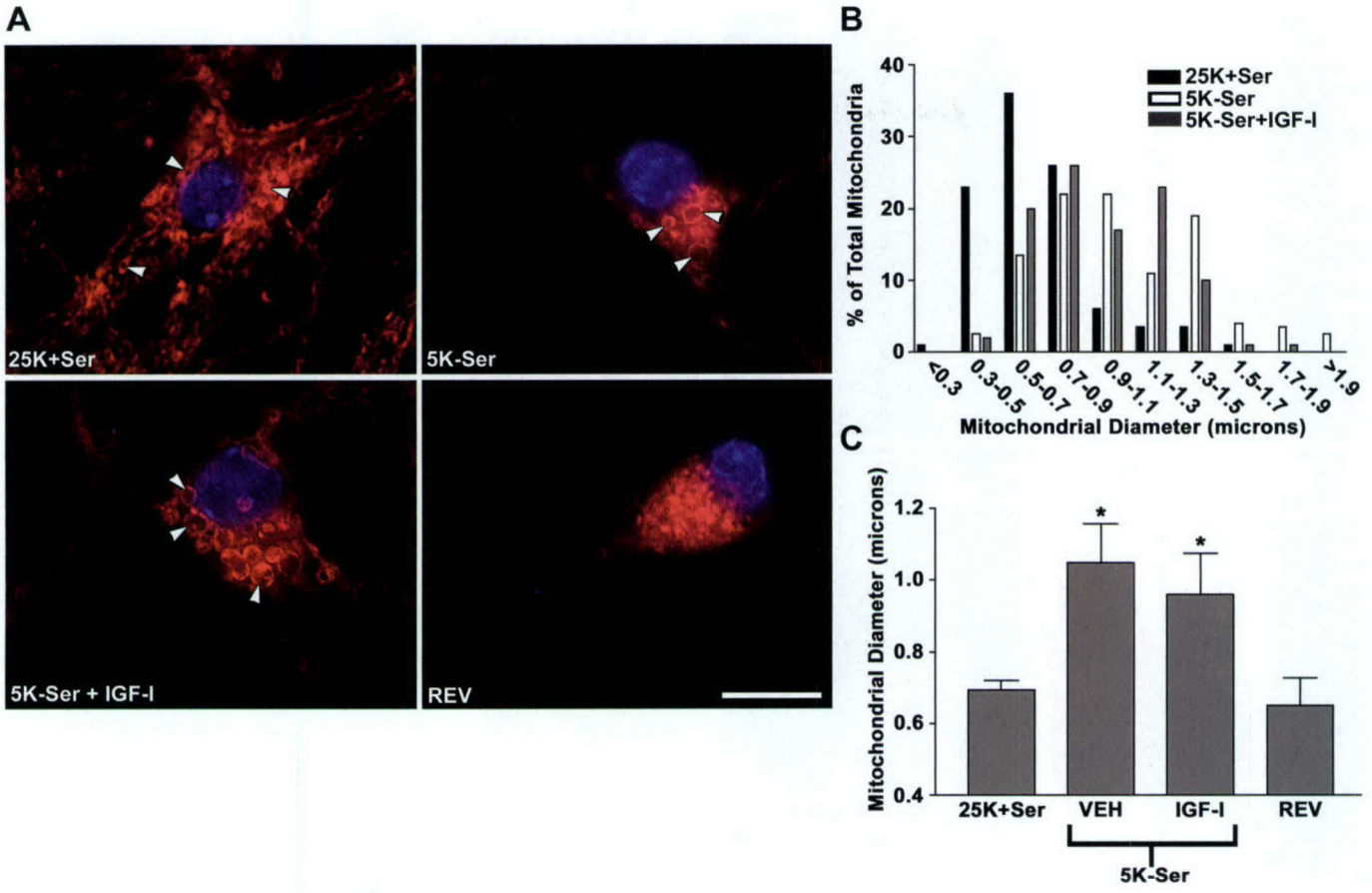

Figure 3. Mitochondrial swelling induced by trophic factor withdrawal is not inhibited by IGF-I. CGNs were incubated for 4 hr in either control (*25K+Ser*) or apoptotic (*5K-Ser*) medium containing either PBS vehicle (*VEH*) or IGF-I (200 ng/ml). To test for reversibility of mitochondrial swelling, we first incubated CGNs for 2 hr in apoptotic medium and then returned them to control medium for an additional 2 hr before staining (*REV*). In preliminary time course experiments a 2 hr incubation in apoptotic medium was found to be sufficient to induce marked mitochondrial swelling (data not shown). At 30 min before fixation, JC1 (final concentration, 2 μg/ml) and Hoechst dye were added to the cultures to stain mitochondria and nuclei, respectively. JC1 fluorescence was captured by using a Cy3 filter under a 100× oil objective. *A*, Representative images of CGNs incubated as described above and stained with Hoechst and JC1. Mitochondria are indicated by the *arrowheads*. Note the dramatic swelling of mitochondria in CGNs incubated in apoptotic medium in either the absence or presence of IGF-I. Mitochondrial swelling was completely reversible if control medium was replaced within 2 hr (*REV*). The images shown are representative of CGNs from four separate experiments. Scale bar, 10 μm. *B*, Distribution of mitochondrial diameters from CGNs observed under the conditions described in *A*. The diameters of ~150 mitochondria per treatment condition were measured from digitally deconvolved images obtained from a total of 15–20 CGNs (randomly pooled from 4 independent experiments). The mitochondrial diameters were categorized into the indicated size groups and graphed as a percentage of the total mitochondria with a given diameter *C*, Quantification of the mean mitochondrial diameters for CGNs observed under the conditions described in *A*. Values represent the means ± SEM mitochondrial diameters obtained from the mitochondria measured in *B*. *Significantly different from the 25K+Ser control; $p < 0.01$.

mitochondria (Fig. 3*A*, *bottom left panel*). The distribution of mitochondrial diameters under control, apoptotic, and apoptotic plus IGF-I conditions is shown in Figure 3*B*, and the mean diameters are shown in Figure 3*C*. Serum and potassium deprivation resulted in a significant 50% increase in the mean mitochondrial diameter in CGNs (0.69 ± 0.03 μm in control vs 1.05 ± 0.11 μm in apoptotic; $p < 0.01$), an effect that was unaltered by IGF-I (0.96 ± 0.12 μm) (Fig. 3*C*). Interestingly, inclusion of IGF-I in trophic factor-deprived CGNs failed to reverse the mitochondrial swelling even after 48 hr of incubation, although apoptosis was still blocked at this time point. However, the readdition of depolarizing potassium for the latter 24 hr of the incubation period did reverse the mitochondrial swelling, indicating that it is a depolarization-sensitive event that is unaffected by IGF-I (data not shown).

Next we analyzed the mitochondrial membrane potential by incubating living CGNs with the membrane potential-sensitive dye TMRE. TMRE is accumulated actively in mitochondria possessing an intact membrane potential but is excluded or lost from mitochondria that are depolarized (Krohn et al., 1999). CGNs maintained in the presence of serum and depolarizing potassium displayed mitochondria that were stained brightly with TMRE, indicative of an intact membrane potential (Fig. 4, *top left panel*). Because these experiments were conducted in living CGNs, we showed that the mitochondrial membrane potential of control CGNs was maintained throughout the duration required to capture all of the images described below (Fig. 4, *bottom right panel*). Serum and potassium deprivation for 4 hr resulted in a marked loss of mitochondrial TMRE staining, consistent with mitochondrial membrane depolarization (Fig. 4, *top right panel*). As was observed for mitochondrial swelling, the addition of IGF-I to trophic factor-deprived CGNs did not prevent the loss of mitochondrial membrane potential (Fig. 4, *bottom left panel*). The above results demonstrate that IGF-I does not block cytochrome

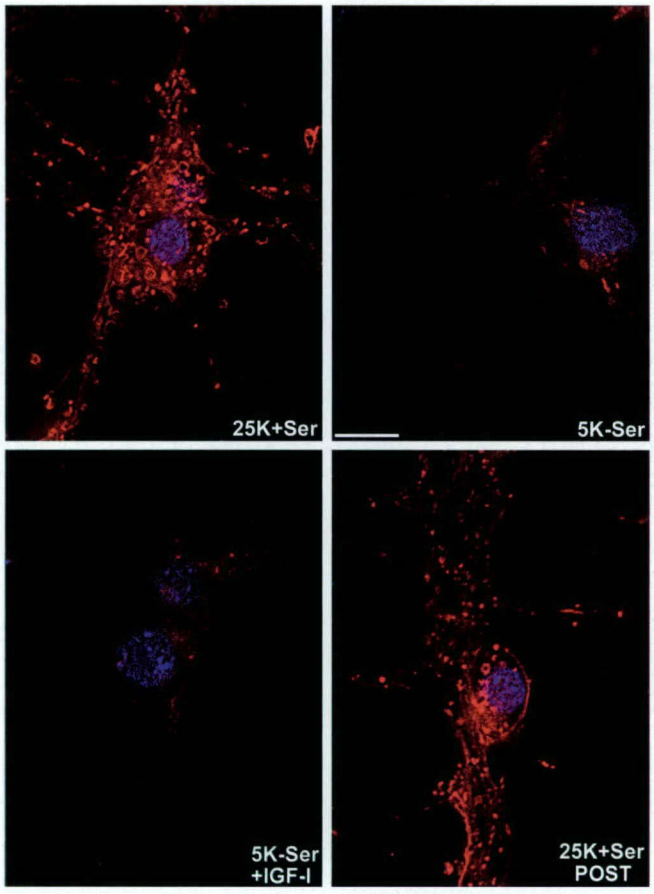

Figure 4. Mitochondrial membrane depolarization elicited by trophic factor withdrawal is not prevented by IGF-I. CGNs grown on glass coverslips were incubated for 4 hr in either control (*25K+Ser*) or apoptotic (*5K-Ser*) medium alone or containing IGF-I (200 ng/ml). At 30 min before the end of the incubation period TMRE and Hoechst were added directly to the cells. After incubation the coverslips were inverted onto slides into a small volume of phenol red-free medium lacking serum or depolarizing potassium but containing TMRE (500 nM). Living cells then were imaged under a 100× oil objective. Nuclear staining with Hoechst is shown in *blue*; TMRE is shown in *red*. Scale bar, 10 μm. CGNs maintained in control medium during the 4 hr incubation period displayed many mitochondria that were stained intensely with TMRE, indicative of an intact membrane potential (*top left panel*). In contrast, CGNs incubated in apoptotic medium in either the absence (*top right panel*) or presence (*bottom left panel*) of IGF-I expressed very little detectable mitochondrial TMRE staining, characteristic of a loss of mitochondrial membrane potential or depolarization. Approximately 5–10 min was required to capture the images described above. Therefore, at the end of the capture duration a final image was acquired of another control CGN to show that the mitochondrial membrane potential was not compromised during the time required to capture the images (*25K+Ser POST*). All of the images shown were acquired at equal exposure times for TMRE fluorescence and are representative of results obtained from three independent experiments, each performed in duplicate.

c release from CGN mitochondria by the inhibition of mitochondrial swelling or depolarization, suggesting that opening of the PTP does not play a significant role in cytochrome *c* release during apoptosis of CGNs.

IGF-I blocks induction of the BH3-only Bcl-2 family member Bim

The second potential mechanism by which cytochrome *c* release is regulated involves the formation of a Bax- or Bak-containing

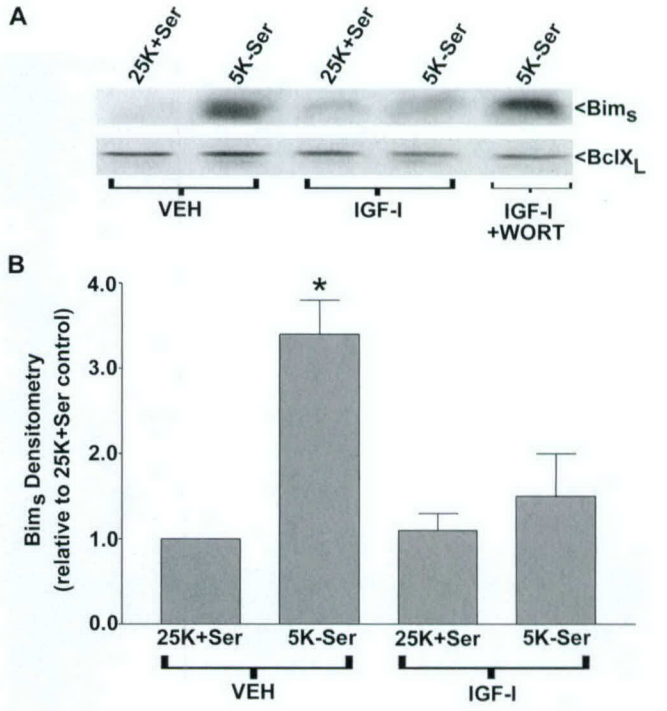

Figure 5. IGF-I inhibits induction of the BH3-only Bcl-2 family member Bim in a PI3K-dependent manner. *A*, CGNs were incubated for 6 hr in either control (*25K+Ser*) or apoptotic (*5K-Ser*) medium containing either PBS vehicle (*VEH*) or IGF-I (200 ng/ml) ± wortmannin (*WORT*; 100 nM). After incubation the cell lysates were subjected to SDS-PAGE on 15% polyacrylamide gels, and the proteins were transferred to PVDF membranes. Bim expression was assessed by immunoblotting with a polyclonal antibody to Bim that specifically recognized an ~15 kDa protein, consistent with the apparent molecular weight of Bim short (*Bim$_S$*). To affirm equal protein loading, we then stripped the blot and reprobed it for the anti-apoptotic Bcl-2 family member Bcl-X_L, which did not demonstrate any significant change in expression under the conditions of this experiment. The blots shown are representative of three separate experiments. *B*, Quantification of Bim$_S$ expression observed under the conditions described in *A* was performed by computer-assisted imaging densitometry. Values represent the means ± SEM for three independent experiments and are expressed relative to the densitometry of Bim$_S$ observed in control CGNs (set to 1.0). *Significantly different from the 25K+Ser control ($p < 0.01$).

"pore" in the outer mitochondrial membrane that permits the passage of proteins (Korsmeyer et al., 2000). Bax and Bak are proapoptotic members of the Bcl-2 family that appear to serve a redundant function in making the mitochondrial membrane permeable to cytochrome *c* (Wei et al., 2001). The BH3-only Bcl-2 family members, including Bad, Bid, Dp5/Hrk, and Bim, have been shown to promote the proapoptotic effects of Bax and Bak while concomitantly suppressing the prosurvival function of Bcl-2 (Desagher et al., 1999; Zong et al., 2001). Recently, Bim was shown to be upregulated after either nerve growth factor (NGF) withdrawal from primary sympathetic neurons or serum and potassium withdrawal from CGNs (Putcha et al., 2001; Whitfield et al., 2001). Moreover, overexpression of Bim or related BH3-only family members promotes apoptosis of CGNs in a Bax-dependent manner (Harris and Johnson, 2001). Immunoblotting for Bim after acute trophic factor withdrawal in CGNs demonstrated a marked increase in the expression of Bim short (Bim$_S$, ~15 kDa) (Fig. 5*A*), the most proapoptotic splice variant of this protein family (O'Connor et al., 1998). Quantification of the change in protein expression by densitometry revealed that serum

and potassium deprivation for 6 hr induced a significant 3.4 ± 0.4-fold increase ($n = 3$; $p < 0.01$) in Bim_s (Fig. 5*B*). Inclusion of IGF-I completely blunted the induction of Bim_s (1.5 ± 0.5-fold increase; $n = 3$) in a PI3K-dependent manner (Fig. 5*A*,*B*). In contrast, the expression of the prosurvival Bcl-2 family member Bcl-X_L was unaffected by either trophic factor withdrawal or IGF-I (Fig. 5*A*). These data indicate that the suppression of Bim is one mechanism by which IGF-I inhibits cytochrome *c* release in CGNs deprived of serum and depolarizing potassium.

IGF-I does not suppress Bim expression by inhibiting c-Jun

Activation of the transcription factor c-Jun is required for apoptosis of primary sympathetic neurons subjected to NGF withdrawal (Eilers et al., 1998) and CGNs undergoing serum and potassium deprivation (Watson et al., 1998). The ability of a dominant-negative mutant of c-Jun to rescue sympathetic neurons from apoptosis recently has been attributed, in part, to its ability to block the induction of Bim (Whitfield et al., 2001). The transcriptional activity of c-Jun is stimulated after its phosphorylation on multiple serine residues (including Ser^{63} and Ser^{73}) by upstream kinases of the JNK family (Minden et al., 1994). Chemical inhibitors of JNK have been shown to inhibit apoptosis of CGNs (Harada and Sugimoto, 1999; Coffey et al., 2002) and to attenuate Bim mRNA expression in CGNs subjected to trophic factor withdrawal (Harris and Johnson, 2001). In the present study we observed that incubation of trophic factor-deprived CGNs with the pyridinyl imidazole JNK/p38 inhibitor SB203580 (Harada and Sugimoto, 1999; Coffey et al., 2002) blunted the phosphorylation of c-Jun on Ser^{63} (Fig. 6*A*) and prevented the increased expression of c-Jun detected by immunoblotting (Fig. 6*B*). Moreover, SB203580 significantly attenuated the induction of Bim_s, consistent with a role for c-Jun in the regulation of Bim expression in CGNs (Fig. 6*C*,*D*). To determine whether IGF-I blocks Bim induction via an inhibition of c-Jun, we analyzed the effects of IGF-I on c-Jun phosphorylation and expression. The addition of IGF-I to CGNs deprived of serum and depolarizing potassium failed to attenuate either the phosphorylation of c-Jun on Ser^{63} (Fig. 6*E*) or the increased expression of c-Jun observed by Western blot (Fig. 6*F*). Thus IGF-I suppresses the induction of Bim in apoptotic CGNs via a mechanism that is independent of the transcription factor c-Jun.

IGF-I prevents dephosphorylation and nuclear translocation of the forkhead transcription factor FKHRL1

Recently, a member of the forkhead family of transcription factors, FKHRL1, was shown to regulate the induction of Bim in lymphocytes undergoing apoptosis in response to cytokine withdrawal (Dijkers et al., 2000). Furthermore, overexpression of a constitutively active mutant of FKHRL1 was sufficient to increase Bim expression in B-cells (Dijkers et al., 2000). The actions of forkhead family members are regulated by phosphorylation on serine and threonine residues. The prosurvival kinase AKT is the main effector of IGF-I that is activated downstream of PI3K, and FKHRL1 has been identified as a principal substrate of AKT in neuronal cells (Brunet et al., 1999; Zheng et al., 2000). Therefore, we first assessed the phosphorylation status of AKT and FKHRL1 in CGNs by immunoblotting with phospho-site-specific antibodies. CGNs cultured in the presence of serum and depolarizing potassium showed marked phosphorylation of AKT on Ser^{473}, indicative of high AKT activity (Fig. 7*A*, *first lane*). In parallel, control CGNs also exhibited high phosphorylation of FKHRL1 on Ser^{253}, one of the sites targeted by AKT (Fig. 7*B*, *first lane*). Removal of serum and depolarizing potassium resulted in a pronounced dephosphorylation (inactivation) of AKT (Fig. 7*A*, *second lane*) and a corresponding loss of FKHRL1 phosphorylation (Fig. 7*B*, *second lane*). The addition of IGF-I to CGNs deprived of serum and depolarizing potassium maintained the phosphorylation of both AKT (Fig. 7*A*) and FKHRL1 (Fig. 7*B*), effects that were blocked by the PI3K inhibitor wortmannin.

Phosphorylation of FKHRL1 on Thr^{32} and Ser^{253} by AKT results in the translocation of FKHRL1 from the nucleus to the cytoplasm where it subsequently is sequestered by 14-3-3 proteins (Brunet et al., 1999). Thus IGF-I signaling via AKT has the potential to regulate negatively the transcriptional activity of FKHRL1 by excluding it from the nucleus. We next examined the cellular localization of FKHRL1 in CGNs. FKHRL1 was localized predominantly to the cytoplasm in CGNs maintained in the presence of trophic factors (Fig. 7*C*, *top left panel*). After acute trophic factor withdrawal FKHRL1 underwent a dramatic translocation to the nucleus (Fig. 7*C*, *top right panel*). The nuclear translocation of FKHRL1 was prevented completely by IGF-I (Fig. 7*C*, *bottom left panel*) in a PI3K-dependent manner (Fig. 7*C*, *bottom right panel*). Collectively, these results demonstrate that, under conditions in which IGF-I blocks Bim induction (Fig. 5), it concurrently sustains high AKT activity, robust FKHRL1 phosphorylation, and the exclusion of FKHRL1 from the nucleus. These findings are consistent with a role for FKHRL1 in the regulation of Bim expression in CGNs. Moreover, these data suggest a novel mechanism by which IGF-I suppresses Bim induction in trophic factor-deprived CGNs by blocking the actions of FKHRL1.

Adenoviral-mediated expression of dominant-negative AKT results in dephosphorylation of FKHRL1 and induction of Bim

To assess more directly the role of AKT in the regulation of FKHRL1 activity and Bim expression, we infected CGNs with an adenovirus expressing a kinase-dead dominant-negative mutant of AKT (Ad-DN-AKT). As described above, CGNs cultured in the presence of serum and depolarizing potassium showed marked phosphorylation of AKT on Ser^{473}, indicative of high endogenous AKT activity (Fig. 7*A*, *first lane*). Under these conditions the adenoviral-mediated expression of DN-AKT resulted in a marked dephosphorylation of FKHRL1 on the AKT target site Ser^{253} (Fig. 8*A*) when compared with CGNs infected with a negative control adenovirus (Ad-CMV). Moreover, the dephosphorylation of FKHRL1 induced by DN-AKT was associated with a coordinated increase in the expression of Bim_s (Fig. 8*B*). These data further support a mechanism by which IGF-I/AKT signaling blocks Bim induction at the level of the FKHRL1 transcription factor.

DISCUSSION

IGF-I promotes the survival of CGNs both *in vitro* and *in vivo* (Ye et al., 1996; Lin and Bulleit, 1997). In the current study we have investigated the neuroprotective mechanism of IGF-I in CGNs by systematically analyzing its effects on components of the intrinsic death-signaling cascade. First we found that IGF-I suppressed activation of the executioner caspase-3 in CGNs subjected to trophic factor withdrawal. This effect was blocked by the PI3K inhibitor wortmannin, consistent with a role for PI3K/AKT signaling in the IGF-I-mediated survival of CGNs. Previously, ribozyme-mediated downregulation of caspase-3 was shown to

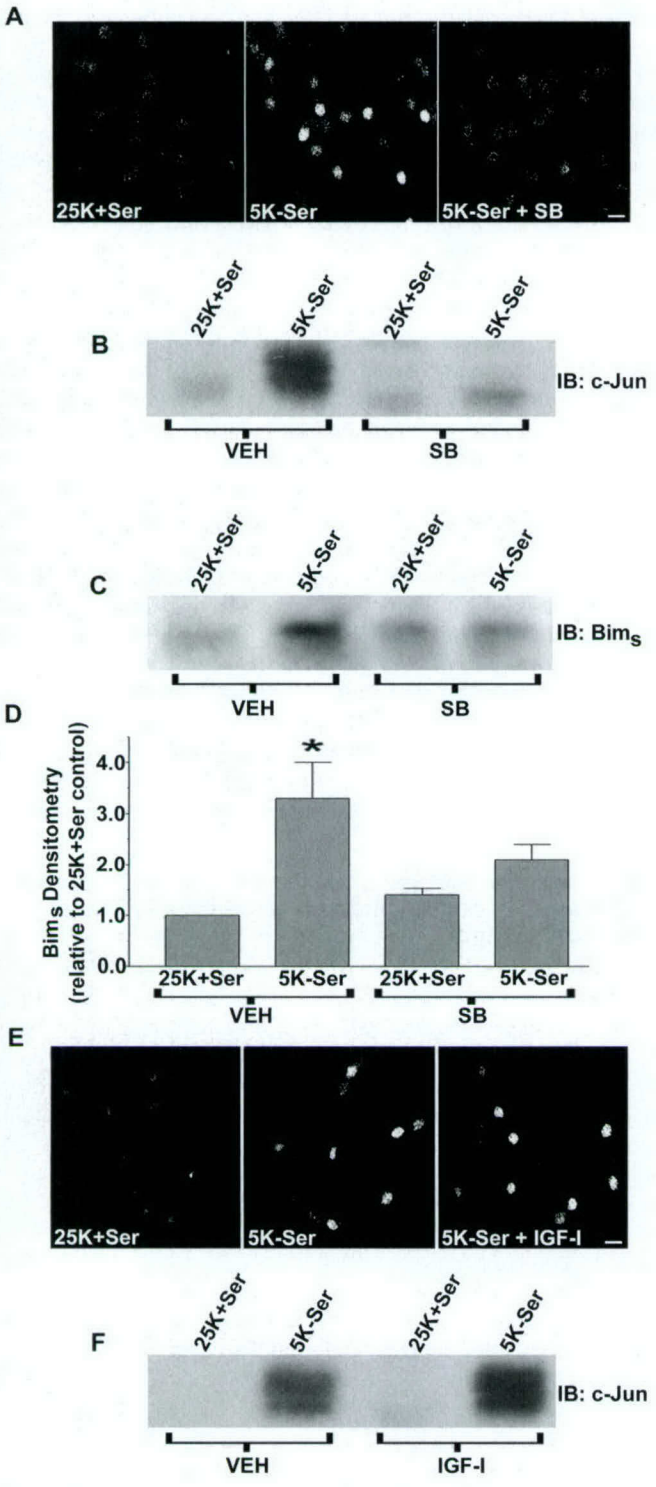

Figure 6. Inhibition of c-Jun signaling attenuates the induction of Bim. IGF-I does not block c-Jun activation in trophic factor-deprived CGNs. *A*, CGNs were incubated for 4 hr in either control (*25K+Ser*) or apoptotic (*5K-Ser*) medium in the absence or presence of the JNK/p38 inhibitor SB203580 (*SB*; 20 μM). After incubation the cells were fixed, and c-Jun phosphorylated on Ser[63] was detected exclusively in the nuclear compartment by using a phospho-specific polyclonal antibody. The images shown are representative of results obtained in three independent experiments. Scale bar, 10 μm. *B*, CGNs were incubated for 4 hr in either control (*25K+Ser*) or apoptotic (*5K-Ser*) medium in the presence of either DMSO vehicle (*VEH*; 0.2%) or SB (20 μM), and cell lysates were subjected to SDS-PAGE on 10% polyacrylamide gels. Proteins were transferred to PVDF membranes and immunoblotted (*IB*) with a polyclonal antibody to c-Jun. The blot shown is representative of three separate experiments. *C*, CGNs were incubated as described in *B*, but for 6 hr, and the cell lysates were electrophoresed on 15% polyacrylamide gels and probed for Bim$_S$. *D*, Densitometric analysis of Bim$_S$ from three independent experiments performed as described in *C*. The densitometry of Bim$_S$ detected in control (*25K+Ser*) CGNs was set at 1.0, and all other values were calculated relative to the control. *Significantly different from the 25K+Ser control ($p < 0.01$). *E*, CGNs were incubated for 4 hr in either control (*25K+Ser*) or apoptotic (*5K-Ser*) medium in the presence of either PBS vehicle (*VEH*) or IGF-I (200 ng/ml). After incubation the nuclear c-Jun phosphorylated on Ser[63] was detected by using a phospho-specific polyclonal antibody. The images shown are representative of three experiments. Scale bar, 10 μm. *F*, CGNs incubated as described in *E* were lysed, and extracted proteins were immunoblotted for c-Jun. The blot shown is illustrative of results obtained from three separate experiments.

inhibit CGN apoptosis (Eldadah et al., 2000), supporting involvement of this executioner caspase in the mechanism of cell death. Comparable with our results, IGF-I has been shown to attenuate caspase-3 activation in other models of neuronal apoptosis via a PI3K/AKT-dependent mechanism (Van Golen and Feldman, 2000; Barber et al., 2001). We also found that IGF-I blocked activation of the intrinsic initiator caspase-9 in a PI3K-dependent manner. Recently, selective peptide inhibitors of caspase-9 were shown to prevent caspase-3 activation in CGNs, demonstrating that caspase-9 activation occurs upstream of the executioner during CGN apoptosis (Gerhardt et al., 2001). Moreover, we found that adenoviral CrmA, an inhibitor of caspase-9, protected CGNs from apoptosis. Similar to our data, IGF-I has been shown to prevent caspase-9 activation in rat retinal ganglion cells after optic nerve transection (Kermer et al., 2000). Collectively, these data suggest a common mechanism by which IGF-I blocks activation of the executioner caspase-3 in neurons via inhibition of the upstream intrinsic initiator caspase-9.

Because caspase-9 is activated after its recruitment into the apoptosome, we analyzed the effects of IGF-I on cytochrome *c* release from mitochondria. Acute trophic factor withdrawal from CGNs induced a rapid redistribution of cytochrome *c* from mitochondria to focal complexes localized in neuronal processes. The precise nature of these complexes is currently under investigation, but it is possible that these cytochrome *c*-rich structures represent large aggregates of apoptosomes. This would allow for a localized activation of caspases in neuronal processes where many structural targets of these proteases exist (e.g., cytoskeletal proteins). We currently are attempting to colocalize Apaf-1 and caspase-9 by immunocytochemical methods to these cytochrome *c*-containing complexes. Regardless of their exact content, IGF-I essentially abolished the formation of these complexes and maintained cytochrome *c* in mitochondria. The effects of IGF-I on cytochrome *c* redistribution were prevented by wortmannin, consistent with a previously recognized role for PI3K/AKT in the inhibition of cytochrome *c* release (Kennedy et al., 1999). The above results suggest that IGF-I inhibits the activation of caspase-9 by preventing the release of cytochrome *c* and the subsequent formation of apoptosomes.

We next examined the role of the mitochondrial PTP in mediating the release of cytochrome *c* during CGN apoptosis. In trophic factor-deprived CGNs marked mitochondrial swelling and depolarization were observed, indicative of PTP opening. Although IGF-I has been shown to prevent mitochondrial depolarization in neuroblastoma cells exposed to hyperosmotic conditions (Van Golen and Feldman, 2000), we did not observe any

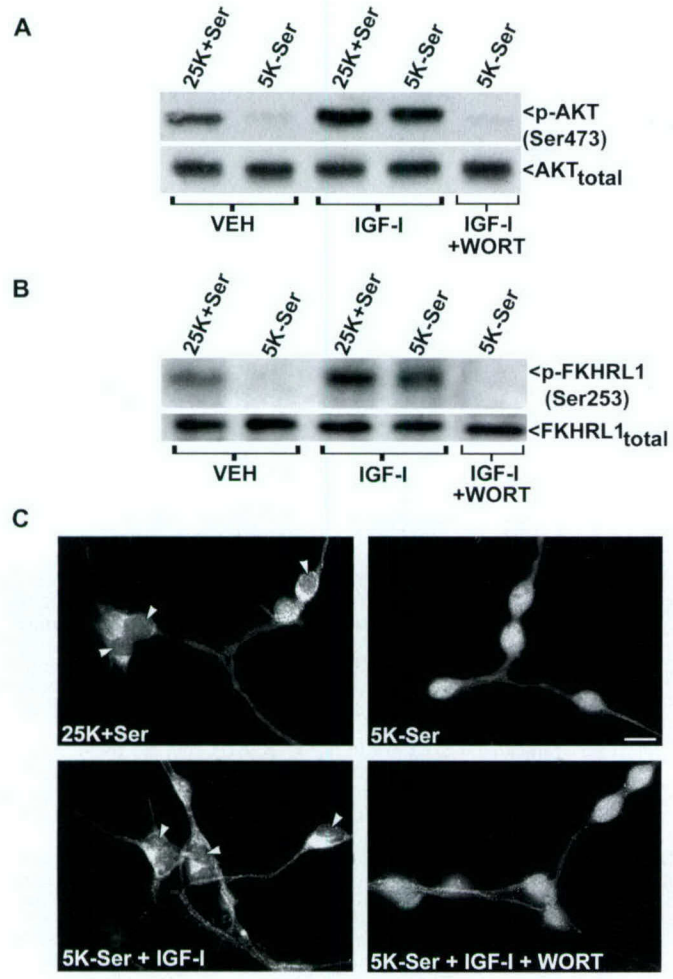

Figure 7. IGF-I sustains the phosphorylation of AKT and FKHRL1 and prevents the nuclear localization of FKHRL1 in CGNs deprived of trophic support. *A*, CGNs were incubated for 4 hr in either control (*25K+Ser*) or apoptotic (*5K-Ser*) medium containing either PBS vehicle (*VEH*) or IGF-I (200 ng/ml) ± wortmannin (*WORT*; 100 nM). After incubation the cell lysates were subjected to SDS-PAGE on 10% polyacrylamide gels, and the proteins were transferred to PVDF membranes. Membranes were probed with a phospho-specific antibody that detects *active* AKT that was phosphorylated on Ser^{473} (*p-AKT*). Then the blots were stripped and reprobed for total AKT to demonstrate equal loading. The blots shown are typical of results obtained in three separate experiments. *B*, CGNs were treated exactly as described in *A*, and the cell lysates were immunoblotted for *inactive* FKHRL1 that was phosphorylated on Ser^{253} (p-FKHRL1) by using a phospho-specific antibody. Then the membranes were stripped and reprobed for total FKHRL1 to verify equal loading. The blots shown are illustrative of three independent experiments. *C*, CGNs incubated as described in *A* were fixed and then incubated with a polyclonal antibody to FKHRL1, followed by a Cy3-conjugated secondary antibody. Fluorescent digitally deconvolved images were acquired by using a 63× oil objective. The *arrowheads* indicate nuclei that are relatively devoid of FKHRL1 immunoreactivity. The images shown are representative of three separate experiments. Scale bar, 10 μm.

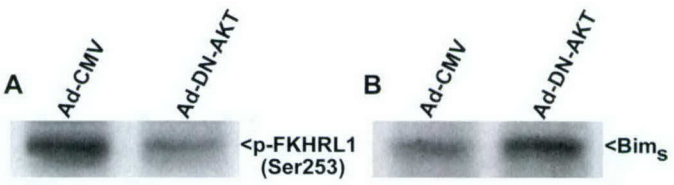

Figure 8. Adenoviral dominant-negative AKT induces dephosphorylation of FKHRL1 and increases Bim expression. On day 5 in culture the CGNs were infected with either a negative control adenovirus (*Ad-CMV*) or adenovirus expressing kinase-dead (dominant-negative) AKT (*Ad-DN-AKT*), each at a multiplicity of infection of 50. At 48 hr after infection the cell lysates were subjected to SDS-PAGE on either 7.5% (*p-FKHRL1*) or 15% (Bim_s) polyacrylamide gels, and the proteins were transferred to PVDF membranes. *A*, The membrane was probed with a phospho-specific antibody to *inactive* FKHRL1 phosphorylated on Ser^{253} (*p-FKHRL1*). *B*, The blot was probed with a polyclonal antibody that detects the short isoform of Bim (Bim_s).

effect of IGF-I on either mitochondrial swelling or depolarization in CGNs. Although IGF-I clearly blocked apoptosis in trophic factor-deprived CGNs, the observation that it failed to prevent mitochondrial swelling indicates that the neurons still have damaged mitochondria in the presence of IGF-I. This finding suggests that a slower nonapoptotic death process was unmasked in CGNs by blocking the more rapid apoptotic death with IGF-I. The characterization of a nonapoptotic death pathway in CGNs will require further investigation. Nonetheless, because IGF-I blocked cytochrome *c* release under conditions in which it failed to affect mitochondrial swelling or depolarization, we conclude that opening of the PTP is insufficient to promote cytochrome *c* release in trophic factor-deprived CGNs. These results are in agreement with those previously reported for hippocampal neurons exposed to staurosporine in which cytochrome *c* release and caspase-3 activation preceded mitochondrial depolarization (Krohn et al., 1999). Collectively, these results indicate that opening of the PTP may not be a principal mechanism for cytochrome *c* release in neurons.

The proapoptotic Bcl-2 family member Bax has been implicated in cytochrome *c* release and the apoptosis of CGNs *in vitro* and *in vivo* (Miller et al., 1997b; Desagher et al., 1999; Selimi et al., 2000b). The proapoptotic function of Bax is attenuated by anti-apoptotic members of the Bcl-2 family (Bcl-2, Bcl-X_L) that heterodimerize with Bax and sequester it away from mitochondria (Otter et al., 1998). Conversely, BH3-only Bcl-2 family members promote the proapoptotic effects of Bax by binding to Bcl-2, thus freeing Bax to incorporate into the mitochondrial membrane (Zong et al., 2001). In addition, BH3-only proteins also have been shown to interact with Bax and induce a conformational change that facilitates its incorporation into mitochondria (Desagher et al., 1999). These findings illustrate that BH3-only proteins serve several key functions in the Bax-dependent release of cytochrome *c* and initiation of the intrinsic death pathway.

The BH3-only protein Bim was shown recently to be induced both in sympathetic neurons subjected to NGF withdrawal and in trophic factor-deprived CGNs (Putcha et al., 2001; Whitfield et al., 2001). Sympathetic neuron apoptosis was attenuated by injection of Bim antisense oligonucleotides (Whitfield et al., 2001), and neurons from Bim knock-out mice were less sensitive to apoptosis than neurons from wild-type mice (Putcha et al., 2001). In addition, overexpression of Bim induced apoptosis in sympathetic neurons (Whitfield et al., 2001) and in CGNs in a Bax-dependent manner (Harris and Johnson, 2001). Multiple isoforms of Bim have been identified that apparently arise by alternative splicing (O'Connor et al., 1998). In the works cited above (Putcha et al., 2001; Whitfield et al., 2001), Bim_{EL} was induced during neuronal apoptosis, whereas we observed the induction of Bim_s in CGNs subjected to trophic factor withdrawal. These isoform-specific differences may be a result of the specific antibodies used to detect Bim. The polyclonal antibody used in

the current study detected primarily a single ~15 kDa protein in CGN lysates and in human embryonic kidney 293 cell lysates (data not shown), consistent with the apparent molecular weight of Bim_S. We observed an approximately threefold induction of Bim_S protein after acute trophic factor withdrawal that was prevented completely by inclusion of IGF-I in a PI3K-dependent manner. These results suggest that IGF-I suppresses the intrinsic death pathway upstream of Bim synthesis. Consistent with this conclusion, Harris and Johnson (2001) have shown recently that IGF-I was unable to rescue CGNs from apoptosis induced by overexpression of the BH3-only protein Dp5/Hrk. Thus our data are the first to identify the upregulation of Bim as a major target of IGF-I action in neurons undergoing apoptosis.

Bim expression is regulated by multiple transcription factors. In NGF-deprived sympathetic neurons dominant-negative c-Jun partially attenuated the induction of Bim mRNA and Bim_{EL} protein, inhibited cytochrome *c* release, and rescued sympathetic neurons from apoptosis (Whitfield et al., 2001). c-Jun also has been implicated in the apoptosis of CGNs (Watson et al., 1998), and an inhibitor of the JNK signaling pathway (CEP-1347) was shown recently to blunt partially the induction of Bim mRNA in CGNs subjected to trophic factor withdrawal (Harris and Johnson, 2001). In agreement with JNK/c-Jun involvement in the induction of Bim_S in CGNs undergoing apoptosis, the p38/JNK inhibitor SB203580 significantly attenuated both the activation of c-Jun and the increase in Bim_S expression. However, IGF-I failed to inhibit c-Jun activation under conditions in which it significantly blocked the induction of Bim_S. These results indicate that c-Jun plays a role in the regulation of Bim expression during CGN apoptosis, but IGF-I suppresses the induction of Bim via a mechanism that does not involve modulation of JNK/c-Jun signaling. This conclusion is in agreement with the work of Whitfield et al. (2001), who proposed that JNK/c-Jun signaling cooperates with a distinct JNK/c-Jun-independent pathway to stimulate the expression of Bim in sympathetic neurons deprived of NGF.

In this context the forkhead transcription factor FKHRL1 has been shown recently to regulate Bim expression in hematopoietic cells (Dijkers et al., 2000). Cytokine withdrawal from a pro-B cell line induced activation (dephosphorylation) of FKHRL1, induction of Bim, and apoptosis (Dijkers et al., 2000). Moreover, expression of a constitutively active mutant of FKHRL1, in which three putative AKT phosphorylation sites are mutated to alanine, induced Bim expression, cytochrome *c* release, and apoptosis in hematopoietic cells (Dijkers et al., 2002). Given that FKHRL1 has been shown to be a substrate for AKT in neurons (Zheng et al., 2000), the AKT-mediated inactivation of FKHRL1 may be one mechanism by which IGF-I inhibits apoptosis. Indeed, overexpression of a constitutively active FKHRL1 triple phosphorylation site mutant is sufficient to induce the apoptosis of CGNs (Brunet et al., 1999). In the present study we showed that trophic factor withdrawal from CGNs led to an inactivation of AKT, a corresponding activation of FKHRL1, and translocation of FKHRL1 to the nucleus. All of these effects, along with the induction of Bim, were prevented by IGF-I in a PI3K-dependent manner. In addition, adenoviral expression of a dominant-negative mutant of AKT was sufficient to activate FKHRL1 and induce Bim expression in CGNs maintained in the presence of serum and depolarizing potassium. Taken together, our data suggest that IGF-I attenuates the induction of Bim in trophic factor-deprived CGNs via a PI3K/AKT-mediated inactivation of the FKHRL1 transcription factor.

In summary, our results demonstrate that suppression of the intrinsic death signaling cascade is a principal mechanism underlying the neuroprotective effects of IGF-I. IGF-I blocks Bim induction, cytochrome *c* release, and activation of the intrinsic initiator caspase-9 and the executioner caspase-3 in CGNs deprived of trophic support. Moreover, IGF-I inhibits the actions of FKHRL1, a transcriptional regulator of Bim, suggesting a novel c-Jun-independent mechanism for the modulation of Bim in neurons.

REFERENCES

Bach MA, Shen-Orr Z, Lowe Jr WL, Roberts Jr CT, LeRoith D (1991) Insulin-like growth factor-I mRNA levels are developmentally regulated in specific regions of the rat brain. Brain Res Mol Brain Res 10:43–48.

Barber AJ, Nakamura M, Wolpert EB, Reiter CE, Seigel GM, Antonetti DA, Gardner TW (2001) Insulin rescues retinal neurons from apoptosis by a phosphatidylinositol 3-kinase/Akt-mediated mechanism that reduces the activation of caspase-3. J Biol Chem 276:32814–32821.

Bartlett WP, Li XS, Williams M, Benkovic S (1991) Localization of insulin-like growth factor-1 mRNA in murine central nervous system during postnatal development. Dev Biol 147:239–250.

Brunet A, Bonni A, Zigmond MJ, Lin MZ, Juo P, Hu LS, Anderson MJ, Arden KC, Blenis J, Greenberg ME (1999) Akt promotes cell survival by phosphorylating and inhibiting a Forkhead transcription factor. Cell 96:857–868.

Chrysis D, Calikoglu AS, Ye P, D'Ercole AJ (2001) Insulin-like growth factor-I overexpression attenuates cerebellar apoptosis by altering the expression of Bcl family proteins in a developmentally specific manner. J Neurosci 21:1481–1489.

Clarkson ED, Zawada WM, Bell KP, Esplen JE, Choi PK, Heidenreich KA, Freed CR (2001) IGF-I and bFGF improve dopamine neuron survival and behavioral outcome in parkinsonian rats receiving cultured human fetal tissue strands. Exp Neurol 168:183–191.

Coffey ET, Smiciene G, Hongisto V, Cao J, Brecht S, Herdegen T, Courtney MJ (2002) c-Jun N-terminal protein kinase (JNK) 2/3 is specifically activated by stress, mediating c-Jun activation, in the presence of constitutive JNK1 activity in cerebellar neurons. J Neurosci 22:4335–4345.

Desagher S, Osen-Sand A, Nichols A, Eskes R, Montessuit S, Lauper S, Maundrell K, Antonsson B, Martinou JC (1999) Bid-induced conformational change of Bax is responsible for mitochondrial cytochrome *c* release during apoptosis. J Cell Biol 144:891–901.

Dijkers PF, Medema RH, Lammers JW, Koenderman L, Coffer PJ (2000) Expression of the pro-apoptotic Bcl-2 family member Bim is regulated by the forkhead transcription factor FKHR-L1. Curr Biol 10:1201–1204.

Dijkers PF, Birkenkamp KU, Lam EW, Thomas NS, Lammers JW, Koenderman L, Coffer PJ (2002) FKHR-L1 can act as a critical effector of cell death induced by cytokine withdrawal: protein kinase B-enhanced cell survival through maintenance of mitochondrial integrity. J Cell Biol 156:531–542.

D'Mello SR, Galli C, Ciotti T, Calissano P (1993) Induction of apoptosis in cerebellar granule neurons by low potassium: inhibition of death by insulin-like growth factor-I and cAMP. Proc Natl Acad Sci USA 90:10989–10993.

Dudek H, Datta SR, Franke TF, Birnbaum MJ, Yao R, Cooper GM, Segal RA, Kaplan DR, Greenberg ME (1997) Regulation of neuronal survival by the serine-threonine protein kinase Akt. Science 275:661–665.

Eilers A, Whitfield J, Babij C, Rubin LL, Ham J (1998) Role of the Jun kinase pathway in the regulation of c-Jun expression and apoptosis in sympathetic neurons. J Neurosci 18:1713–1724.

Eldadah BA, Ren RF, Faden AI (2000) Ribozyme-mediated inhibition of caspase-3 protects cerebellar granule cells from apoptosis induced by serum-potassium deprivation. J Neurosci 20:179–186.

Fernandez AM, de la Vega AG, Torres-Aleman I (1998) Insulin-like growth factor-I restores motor coordination in a rat model of cerebellar ataxia. Proc Natl Acad Sci USA 95:1253–1258.

Galli C, Meucci O, Scorziello A, Werge TM, Calissano P, Schettini G (1995) Apoptosis in cerebellar granule cells is blocked by high KCl, forskolin, and IGF-1 through distinct mechanisms of action: the involvement of intracellular calcium and RNA synthesis. J Neurosci 15:1172–1179.

Garcia-Calvo M, Peterson EP, Leiting B, Ruel R, Nicholson DW, Thornberry NA (1998) Inhibition of human caspases by peptide-based and macromolecular inhibitors. J Biol Chem 273:32608–32613.

Gerhardt E, Kugler S, Leist M, Beier C, Berliocchi L, Volbracht C, Weller M, Bahr M, Nicotera P, Schulz JB (2001) Cascade of caspase activation in potassium-deprived cerebellar granule neurons: targets for treatment with peptide and protein inhibitors of apoptosis. Mol Cell Neurosci 17:717–731.

Green DR (1998) Apoptotic pathways: the roads to ruin. Cell 94:695–698.

Harada J, Sugimoto M (1999) An inhibitor of p38 and JNK MAP kinases prevents activation of caspase and apoptosis of cultured cerebellar granule neurons. Jpn J Pharmacol 79:369–378.

Harris CA, Johnson Jr EM (2001) BH3-only Bcl-2 family members are coordinately regulated by the JNK pathway and require Bax to induce apoptosis in neurons. J Biol Chem 276:37754–37760.

Heck S, Lezoualc'h F, Engert S, Behl C (1999) Insulin-like growth factor-1-mediated neuroprotection against oxidative stress is associated with activation of nuclear factor κB. J Biol Chem 274:9828–9835.

Kennedy SG, Kandel ES, Cross TK, Hay N (1999) Akt/protein kinase B inhibits cell death by preventing the release of cytochrome *c* from mitochondria. Mol Cell Biol 19:5800–5810.

Kermer P, Ankerhold R, Klocker N, Krajewski S, Reed JC, Bahr M (2000) Caspase-9: involvement in secondary death of axotomized rat retinal ganglion cells *in vivo*. Brain Res Mol Brain Res 85:144–150.

Korsmeyer SJ, Wei MC, Saito M, Weiler S, Oh KJ, Schlesinger PH (2000) Pro-apoptotic cascade activates BID, which oligomerizes BAK or BAX into pores that result in the release of cytochrome *c*. Cell Death Differ 7:1166–1173.

Krohn AJ, Wahlbrink T, Prehn JH (1999) Mitochondrial depolarization is not required for neuronal apoptosis. J Neurosci 19:7394–7404.

Kuida K, Haydar TF, Kuan CY, Gu Y, Taya C, Karasuyama H, Su MS, Rakic P, Flavell RA (1998) Reduced apoptosis and cytochrome *c*-mediated caspase activation in mice lacking caspase-9. Cell 94:325–337.

Lai EC, Felice KJ, Festoff BW, Gawel MJ, Gelinas DF, Kratz R, Murphy MF, Natter HM, Norris FH, Rudnicki SA (1997) Effect of recombinant human insulin-like growth factor-I on progression of ALS. A placebo-controlled study. The North America ALS/IGF-I study group. Neurology 49:1621–1630.

Li M, Wang X, Meintzer MK, Laessig T, Birnbaum MJ, Heidenreich KA (2000) Cyclic AMP promotes neuronal survival by phosphorylation of glycogen synthase kinase 3β. Mol Cell Biol 20:9356–9363.

Lin X, Bulleit RF (1997) Insulin-like growth factor-I (IGF-I) is a critical trophic factor for developing cerebellar granule cells. Brain Res Dev Brain Res 99:234–242.

Liu XF, Fawcett JR, Thorne RG, Frey II WH (2001) Non-invasive intranasal insulin-like growth factor-I reduces infarct volume and improves neurologic function in rats following middle cerebral artery occlusion. Neurosci Lett 308:91–94.

Martinou JC, Green DR (2001) Breaking the mitochondrial barrier. Nat Rev Mol Cell Biol 2:63–67.

Miller TM, Tansey MG, Johnson Jr EM, Creedon DJ (1997a) Inhibition of phosphatidylinositol 3-kinase activity blocks depolarization- and insulin-like growth factor-I-mediated survival of cerebellar granule cells. J Biol Chem 272:9847–9853.

Miller TM, Moulder KL, Knudson CM, Creedon DJ, Deshmukh M, Korsmeyer SJ, Johnson Jr EM (1997b) Bax deletion further orders the cell death pathway in cerebellar granule cells and suggests a caspase-independent pathway to cell death. J Cell Biol 139:205–217.

Minden A, Lin A, Smeal T, Derijard B, Cobb M, Davis R, Karin M (1994) c-Jun N-terminal phosphorylation correlates with activation of the JNK subgroup but not the ERK subgroup of mitogen-activated protein kinases. Mol Cell Biol 14:6683–6688.

Mustafa A, Lannfelt L, Lilius L, Islam A, Winblad B, Adem A (1999) Decreased plasma insulin-like growth factor-I level in familial Alzheimer's disease patients carrying the Swedish APP 670/671 mutation. Dement Geriatr Cogn Disord 10:446–451.

O'Connor L, Strasser A, O'Reilly LA, Hausmann G, Adams JM, Cory S, Huang DC (1998) Bim: a novel member of the Bcl-2 family that promotes apoptosis. EMBO J 17:384–395.

Otter I, Conus S, Ravn U, Rager M, Olivier R, Monney L, Fabbro D, Borner C (1998) The binding properties and biological activities of Bcl-2 and Bax in cells exposed to apoptotic stimuli. J Biol Chem 273:6110–6120.

Putcha GV, Moulder KL, Golden JP, Bouillet P, Adams JA, Strasser A, Johnson Jr EM (2001) Induction of Bim, a proapoptotic BH3-only Bcl-2 family member, is critical for neuronal apoptosis. Neuron 29:615–628.

Rotwein P, Burgess SK, Milbrandt JD, Krause JE (1988) Differential expression of insulin-like growth factor genes in rat central nervous system. Proc Natl Acad Sci USA 85:265–269.

Russell JW, Windebank AJ, Schenone A, Feldman EL (1998) Insulin-like growth factor-I prevents apoptosis in neurons after nerve growth factor withdrawal. J Neurobiol 36:455–467.

Selimi F, Doughty M, Delhaye-Bouchaud N, Mariani J (2000a) Target-related and intrinsic neuronal death in *lurcher* mutant mice are both mediated by caspase-3 activation. J Neurosci 20:992–1000.

Selimi F, Vogel MW, Mariani J (2000b) Bax inactivation in *lurcher* mutants rescues cerebellar granule cells but not Purkinje cells or inferior olivary neurons. J Neurosci 20:5339–5345.

Tagami M, Yamagata K, Nara Y, Fujino H, Kubota A, Numano F, Yamori Y (1997) Insulin-like growth factors prevent apoptosis in cortical neurons isolated from stroke-prone spontaneously hypertensive rats. Lab Invest 76:603–612.

Torres-Aleman I, Barrios V, Lledo A, Berciano J (1996) The insulin-like growth factor-I system in cerebellar degeneration. Ann Neurol 39:335–342.

Van Golen CM, Feldman EL (2000) Insulin-like growth factor-I is the key growth factor in serum that protects neuroblastoma cells from hyperosmotic-induced apoptosis. J Cell Physiol 182:24–32.

Watson A, Eilers A, Lallemand D, Kyriakis J, Rubin LL, Ham J (1998) Phosphorylation of c-Jun is necessary for apoptosis induced by survival signal withdrawal in cerebellar granule neurons. J Neurosci 18:751–762.

Wei MC, Zong WX, Cheng EH, Lindsten T, Panoutsakopoulou V, Ross AJ, Roth KA, MacGregor GR, Thompson CB, Korsmeyer SJ (2001) Proapoptotic BAX and BAK: a requisite gateway to mitochondrial dysfunction and death. Science 292:727–730.

White RJ, Reynolds IJ (1996) Mitochondrial depolarization in glutamate-stimulated neurons: an early signal specific to excitotoxin exposure. J Neurosci 16:5688–5697.

Whitfield J, Neame SJ, Paquet L, Bernard O, Ham J (2001) Dominant-negative c-Jun promotes neuronal survival by reducing Bim expression and inhibiting mitochondrial cytochrome *c* release. Neuron 29:629–643.

Ye P, Xing Y, Dai Z, D'Ercole AJ (1996) *In vivo* actions of insulin-like growth factor-I (IGF-I) on cerebellum development in transgenic mice: evidence that IGF-I increases proliferation of granule cell progenitors. Brain Res Dev Brain Res 95:44–54.

Zhang W, Ghetti B, Lee WH (1997) Decreased IGF-I gene expression during the apoptosis of Purkinje cells in *pcd* mice. Brain Res Dev Brain Res 98:164–176.

Zheng WH, Kar S, Quirion R (2000) Insulin-like growth factor-1-induced phosphorylation of the forkhead family transcription factor FKHRL1 is mediated by Akt kinase in PC12 cells. J Biol Chem 275:39152–39158.

Zong WX, Lindsten T, Ross AJ, MacGregor GR, Thompson CB (2001) BH3-only proteins that bind pro-survival Bcl-2 family members fail to induce apoptosis in the absence of Bax and Bak. Genes Dev 15:1481–1486.

Zou H, Li Y, Liu X, Wang X (1999) An APAF-1·cytochrome *c* multimeric complex is a functional apoptosome that activates procaspase-9. J Biol Chem 274:11549–11556.

THE JOURNAL OF BIOLOGICAL CHEMISTRY

Vol. 277, No. 27, Issue of July 5, pp. 24546–24553, 2002
Printed in U.S.A.

Suppression of Death Receptor Signaling in Cerebellar Purkinje Neurons Protects Neighboring Granule Neurons from Apoptosis via an Insulin-like Growth Factor I-dependent Mechanism*

Received for publication, February 1, 2002, and in revised form, April 3, 2002
Published, JBC Papers in Press, April 18, 2002, DOI 10.1074/jbc.M201098200

Daniel A. Linseman‡, Maria L. McClure‡, Ron J. Bouchard, Tracey A. Laessig, Ferogh A. Ahmadi, and Kim A. Heidenreich§

From the Department of Pharmacology, University of Colorado Health Sciences Center and the Denver Veterans Affairs Medical Center, Denver, Colorado 80220

Neuronal apoptosis contributes to the progression of neurodegenerative disease. Primary cerebellar granule neurons are an established *in vitro* model for investigating neuronal death. After removal of serum and depolarizing potassium, granule neurons undergo apoptosis via a mechanism that requires intrinsic (mitochondrial) death signals; however, the role of extrinsic (death receptor-mediated) signals is presently unclear. Here, we investigate involvement of death receptor signaling in granule neuron apoptosis by expressing adenoviral, AU1-tagged, dominant-negative Fas-associated death domain (Ad-AU1-ΔFADD). Ad-AU1-ΔFADD decreased apoptosis of granule neurons from 65 ± 5 to 27 ± 2% (n = 7, $p < 0.01$). Unexpectedly, immunocytochemical staining for AU1 revealed that <5% of granule neurons expressed ΔFADD. In contrast, ΔFADD was expressed in >95% of calbindin-positive Purkinje neurons (~2% of the cerebellar culture). Granule neurons in proximity to ΔFADD-expressing Purkinje cells demonstrated markedly increased survival. Both granule and Purkinje neurons expressed insulin-like growth factor-I (IGF-I) receptors, and ΔFADD-mediated survival of granule neurons was inhibited by an IGF-I receptor blocking antibody. These results demonstrate that the selective suppression of death receptor signaling in Purkinje neurons is sufficient to rescue neighboring granule neurons that depend on Purkinje cell-derived IGF-I. Thus, the extrinsic death pathway has a profound but indirect effect on the survival of cerebellar granule neurons.

Apoptosis is a type of programmed cell death characterized by a cascade of proteolytic events orchestrated by the caspase family of cysteine proteases (1). There are two principal pathways leading to apoptotic cell death. These include the "extrinsic" or death receptor-initiated pathway and the "intrinsic" or mitochondrial pathway (2). The extrinsic pathway originates with binding of death-promoting ligands (*e.g.* FasL) to their cognate death receptors (*e.g.* Fas) (3). Ligand binding induces oligomerization of death receptors and promotes their association with adapter molecules like Fas-associated death domain protein (FADD)[1] (4). The receptor-FADD interaction occurs via a protein-protein binding motif known as the death domain (5). The initiator caspase, pro-caspase 8, is then recruited to the death-inducing signaling complex via binding to the death effector domain of FADD (6). The resulting proximity of multiple pro-caspase 8 molecules facilitates their autocatalytic cleavage to the active protease caspase 8 (7). The intrinsic pathway is initiated by release of cytochrome *c* from mitochondria and its subsequent association with apoptosis-activating factor 1 and pro-caspase 9 (8). This large protein complex (the apoptosome) promotes activation of caspase 9 (9). The intrinsic pathway is regulated by both pro- and anti-apoptotic members of the Bcl-2 family (10). Each of the above initiator caspases, 8 and 9, cleave downstream executioner caspases such as caspase 3 from the pro-form to the active protease, thus resulting in the cleavage of critical cellular proteins and apoptosis (11, 12).

Neuronal apoptosis plays an essential role in the normal development of the central nervous system (13). Developmental neuronal cell death requires activation of a caspase cascade as evidenced by the substantial hyperplasia observed in many areas of the brain in caspase 3 knock-out mice (14). Aberrant apoptotic mechanisms are thought to contribute significantly to many neurodegenerative disorders including Alzheimer's and Parkinson's disease (15). Therefore, elucidation of the apoptotic signaling pathways underlying neurodegeneration is critical to enhance current therapies for these disorders. Recent findings indicate that components of both the extrinsic (death receptors or their ligands) and intrinsic (Bcl-2 family members) death pathways are regulated at the level of expression during neurodegeneration or neuronal injury *in vivo* (16, 17). Moreover, transgenic animal models or spontaneously occurring mutants of specific death receptor-signaling molecules or Bcl-2 family members provide further evidence that these pathways are involved in neuronal injury (18, 19).

To examine the signal transduction mechanisms underlying neuronal apoptosis, primary neuronal cultures have been extensively utilized. Primary cerebellar granule neurons isolated from early postnatal rats are a well characterized model system

* This work was supported by a Department of Veterans Affairs Merit Award (to K. A. H.), Department of Defense Grant DAMD17-99-1-9481 (to K. A. H.), National Institutes of Health Grant NS38619-01A1 (to K. A. H.), and a Veterans Affairs Research Enhancement Award Program (to K. A. H. and D.A.L.). The costs of publication of this article were defrayed in part by the payment of page charges. This article must therefore be hereby marked "*advertisement*" in accordance with 18 U.S.C. Section 1734 solely to indicate this fact.

‡ These authors contributed equally to this work.

§ To whom correspondence should be addressed: University of Colorado Health Sciences Center Dept. of Pharmacology (C236) 4200 E. Ninth Ave. Denver, CO 80262. Tel.: 303-399-8020 (ext. 3891); Fax: 303-393-5271; E-mail: Kim.Heidenreich@UCHSC.edu.

[1] The abbreviations used are: FADD, Fas-associated death domain protein; IGF-I, insulin-like growth factor-I; ΔFADD, Fas-associated death domain protein lacking a death effector domain; DAPI, 4,6-diamidino-2-phenylindole; m.o.i., multiplicity of infection; PBS, phosphate-buffered saline; Ad-AU1-ΔFADD, adenoviral, AU1-tagged, dominant-negative Fas-associated death domain; 25k + Ser, control medium containing serum and 25 mM potassium; 5k−Ser, apoptotic medium lacking serum and containing 5 mM potassium.

for investigating neuronal apoptosis (20). These cell cultures are highly homogeneous, with greater than 95% of the isolated cells being granule neurons (21). The remaining cells include glial cells and other neuronal cells such as Purkinje neurons, which demonstrate an interdependent relationship with granule neurons both *in vivo* and *in vitro* (22, 23). Cerebellar granule neurons require activity-dependent signals (membrane depolarization) and serum for their survival *in vitro* (20, 21, 24). After removal of serum and lowering of extracellular potassium from 25 to 5 mM (trophic factor withdrawal), granule neurons undergo rapid apoptotic cell death characterized by caspase activation and nuclear condensation and fragmentation (21). Cerebellar granule neuron apoptosis is attenuated by neurotrophic growth factors, including insulin-like growth factor-I (IGF-I) (20, 21, 24–26), or by inhibitors of the stress-activated protein kinases, c-Jun-NH_2-terminal kinase or p38 mitogen-activated protein kinase (27). Significantly, both neurotrophins and stress-activated protein kinase inhibitors also rescue neurons from apoptosis *in vivo*, thus validating the results obtained in cerebellar granule neurons *in vitro* (28, 29).

Several studies indicate that the intrinsic death pathway plays a critical role in cerebellar granule neuron apoptosis. For example, granule neurons display a rapid translocation of the pro-apoptotic Bcl-2 family member, Bax, to mitochondria and release of cytochrome *c* after trophic factor withdrawal (30). Moreover, cerebellar granule neurons isolated from Bax knockout mice exhibit a significant reduction in apoptosis in response to serum and potassium deprivation (31). In addition, expression of the BH3-only, pro-apoptotic Bcl-2 family member, Bim, is markedly increased in granule neurons during trophic factor withdrawal (32). In contrast to the above findings, relatively little is known about the involvement of the extrinsic death pathway in promoting cerebellar granule neuron apoptosis. Le-Niculescu *et al.* (33) show that FasL mRNA is induced after trophic factor withdrawal in cerebellar granule neurons, and furthermore, sequestration of FasL with FasFc attenuates granule neuron apoptosis. However, additional data supporting a role for the extrinsic death pathway in cerebellar granule neuron apoptosis have not been forthcoming.

In the present study, we examined the involvement of death receptor signaling in cerebellar granule neuron apoptosis by expressing a dominant-negative mutant of FADD (ΔFADD) in primary cultures of cerebellar granule neurons using adenoviral vectors. Our results show that adenoviral ΔFADD was expressed almost exclusively in cerebellar Purkinje cells, yet it effectively rescued granule neurons from apoptosis. The ΔFADD-mediated survival of granule neurons was dependent on their proximity to ΔFADD-expressing Purkinje cells and required Purkinje cell-derived IGF-I. These data indicate that the extrinsic death pathway significantly, but indirectly, influences the survival of cerebellar granule neurons.

EXPERIMENTAL PROCEDURES

Materials—Adenoviral-AU1-ΔFADD (34) was kindly provided by Dr. David Brenner and the adenoviral core at the University of North Carolina (Chapel Hill, NC). Dr. Sylvia Christakos at the University of Medicine and Dentistry of New Jersey (Newark, NJ) kindly provided rabbit polyclonal antibodies raised against rat calbindin D28K (35). Monoclonal antibodies to the AU1 epitope tag were purchased from Berkley Antibody Co. (Richmond, CA). Neutralizing monoclonal antibodies against the IGF-I receptor were purchased from Oncogene (Boston, MA). Fluorescein isothiocyanate- and Cy3-conjugated secondary antibodies were obtained from Jackson Immunoresearch (West Grove, PA). Hoechst dye 33258 and DAPI (4,6-diamidino-2-phenylindole) were purchased from Sigma.

Cell Culture—Primary rat cerebellar granule neurons were isolated from 7-day-old Sprague-Dawley rat pups as described previously (36). Briefly, cells were plated at a density of 2.0×10^6 cells/ml in basal modified Eagle's medium containing 10% fetal bovine serum, 25 mM KCl, 2 mM L-glutamine, and penicillin (100 units/ml)-streptomycin (100 μg/ml) (Invitrogen). Cytosine arabinoside (10 μM) was added to the culture medium 24 h after plating to limit the growth of non-neuronal cells. Experiments were performed after 7 days in culture. Apoptosis was induced by removing the plating medium and replacing it with serum-free medium containing 5 mM KCl.

Adenoviral AU1-ΔFADD Infection—The ΔFADD adenovirus was purified by cesium chloride gradient ultracentrifugation. The viral titer (multiplicity of infection (m.o.i.) was determined by measuring the absorbance at 260 nm (where 1.0 absorbance units = 1×10^{12} particles/ml), and infectious particles were verified by plaque assay. Five days after plating, neuronal cultures were infected with Ad-AU1-ΔFADD at a m.o.i. ranging from 5 to 50. After infection, cells were returned to the incubator for 48 h at 37 °C and 10% CO_2. On day 7, neurons were induced to undergo apoptosis. Twenty-four hours later, the cells were fixed for quantification of apoptosis and/or immunocytochemistry as described below (under "Experimental Procedures").

Quantitation of Apoptosis—Neuronal cultures were fixed with 4% paraformaldehyde in phosphate-buffered saline (PBS, pH 7.4) for 30 min at room temperature and washed with PBS, and nuclei were stained with either Hoechst dye or DAPI. Cells were scored as apoptotic if their nuclei were condensed or fragmented. In general, ~500 cells from at least 2 fields of a 35-mm well were counted. However, some experiments were performed on glass coverslips, and granule neuron apoptosis was quantified in relation to their proximity to AU1-positive, ΔFADD-expressing Purkinje cells. For these experiments, two techniques were utilized to prevent selective bias in defining the anti-apoptotic effect of ΔFADD and the spatial association between surviving granule neurons and ΔFADD-expressing Purkinje cells. First, 40× fields were randomly scanned under the Cy3 filter for AU1-positive Purkinje cells (see "Immunocytochemistry" in this section, below). Fields were randomly selected that contained from 0 to 4 Purkinje cells per field (where "0" Purkinje cells implied no AU1 immunoreactivity apparent in the 40× field, an area of ~100,000 μm^2). After identification of the above fields, the filter was changed to DAPI, and granule neuron apoptosis was quantified within each given field. The second technique utilized to prevent selective counting bias was that random fields were selected by two independent researchers. Ten fields containing on average 30 granule neurons per field were counted per condition from a total of three independent experiments. Data are presented as the percentage of cells in a given treatment group, which were scored as apoptotic. All experiments were performed at least in triplicate.

Immunocytochemistry—Cerebellar cultures were plated on polyethyleneimine-coated glass cover slips at a density of $\sim 1.0 \times 10^5$ cells/coverslip. Five days after plating, cells were infected with Ad-AU1-ΔFADD and subsequently induced to undergo apoptosis 48 h post-infection as described above. After treatment, cells were fixed with 4% paraformaldehyde and then permeabilized and blocked in PBS containing 0.2% Triton X-100 and 5% bovine serum albumin. Cells were then incubated overnight at 4 °C with either mouse-anti-AU1 (1:1000), rabbit-anti-calbindin (1:5000), or mouse-anti-IGF-I receptor (1 μg/ml) diluted in PBS containing 0.2% Triton X-100 and 2% bovine serum albumin. The primary antibody was aspirated, and cells were washed five times with PBS. Cells were then incubated with the appropriate Cy3-conjugated or fluorescein isothiocyanate-conjugated secondary antibody (diluted 1:500) and DAPI for 1 h at room temperature. The cells were then washed 5 times with PBS, and coverslips were adhered to glass slides with mounting medium (0.1% *p*-phenylenediamine in 75% glycerol in PBS). Fluorescence imaging was performed on a Zeiss Axioplan 2 microscope equipped with a Cooke Sensicam deep-cooled CCD camera, and images were analyzed and subjected to digital deconvolution using the Slidebook software program (Intelligent Imaging Innovations Inc., Denver, CO).

Data Analysis—Results shown represent the means ± S.E. for the number (n) of independent experiments performed. Statistical differences between the means of unpaired sets of data were evaluated using one-way analysis of variance followed by a *post hoc* Dunnett's test (54). A p value of <0.01 was considered statistically significant.

RESULTS

Adenoviral ΔFADD Attenuates Apoptosis of Cerebellar Granule Neurons Induced by Trophic Factor Withdrawal—To investigate if death receptor signaling is involved in the apoptotic cell death of primary cerebellar granule neurons subjected to trophic factor withdrawal, cerebellar cell cultures were infected with increasing titers of adenoviral, AU1-tagged, dominant-negative FADD (Ad-AU1-ΔFADD). ΔFADD is a truncated pro-

tein that lacks the death effector domain and, therefore, inhibits its coupling of liganded death receptors to the initiator caspase 8 (34, 37). Forty-eight hours after infection, cells were switched from control medium containing serum and 25 mM potassium to apoptotic medium lacking serum and containing 5 mM potassium. After an additional 24-h incubation, cells were fixed, and nuclei were stained with Hoechst dye. Granule neurons containing condensed and/or fragmented nuclei were scored as apoptotic. As shown in Fig. 1*A*, uninfected granule neurons maintained in control medium throughout the experiment demonstrated a low amount of basal apoptosis (6 ± 1%, $n = 7$). Apoptosis in uninfected granule neurons switched to apoptotic medium for 24 h measured 65 ± 5% ($n = 7$). Infection with a negative control adenovirus (Ad-cytomegalovirus (*CMV*)) at a m.o.i. of 50 had no effect on granule neuron apoptosis (69 ± 5%, $n = 7$), whereas infection with ΔFADD resulted in a significant reduction in granule neuron apoptosis to 27 ± 2% ($n = 7$, $p < 0.01$) at a m.o.i. of 50. At the adenoviral titers used in this series of experiments (m.o.i. of from 5 to 50) there was no detectable dose dependence of ΔFADD on granule neuron apoptosis (Fig. 1*A*). When granule neuron apoptosis was carefully analyzed on a field-by-field basis, it was evident that the protection observed with ΔFADD was not uniformly distributed throughout the cell culture (Fig. 1*B*). Like the apoptosis observed in uninfected cultures (Fig. 1*B*, compare the *upper right panel* (apoptotic) to *upper left panel* (control)), there were some fields in the ΔFADD-infected cultures that contained a similar high percentage of apoptotic granule neurons (Fig. 1*B*, *Field A*). However, other fields in the ΔFADD-infected cultures displayed a marked reduction in cerebellar granule neuron apoptosis (Fig. 1*B*, *Field B*). Interestingly, this localized effect of ΔFADD on granule neuron survival was invariably associated with the presence of one or more large and irregularly shaped nuclei within the field of protected granule neurons (Fig. 1*B*, *Field B*, see the nuclei indicated by the *arrows*).

The Survival of Granule Neurons Is Dependent on Their Proximity to ΔFADD-expressing Purkinje Cells—The cerebellar cell cultures utilized in this study have been extensively characterized and are deemed highly homogeneous with greater than 95% of the culture being granule neurons (21). Of the remaining cells, the most prevalent are Purkinje neurons, which display an interdependent relationship with granule neurons both *in vivo* and *in vitro* (22, 23). The calcium-binding protein, calbindin, has been utilized as a marker for Purkinje cells in the cerebellum (38). Immunocytochemical staining of our cerebellar cell cultures for calbindin revealed that the large, irregularly shaped nuclei described above in Fig. 1*B* (*Field B*) were those of Purkinje neurons (Fig. 2*A*). The identified Purkinje neurons demonstrated a classical morphology characterized by an expansive dendritic tree (39). Further immunocytochemical analysis demonstrated that Purkinje cells were very efficiently infected with Ad-AU1-ΔFADD as shown by their marked staining with anti-AU1 (Fig. 2*B*). On average, Purkinje neurons made up ~2% of the entire cerebellar cell culture, and greater than 95% of identified Purkinje cells were AU1-positive after infection with Ad-AU1-ΔFADD at a m.o.i. of from 5 to 50. The lack of concentration dependence for ΔFADD expression in Purkinje neurons over this range of adenoviral titers correlated with the lack of dose dependence for ΔFADD inhibition of granule neuron apoptosis (see Fig. 1*A*), suggesting that the protection observed was dependent on ΔFADD expression in Purkinje neurons.

As described above, the ability of ΔFADD to rescue granule neurons from trophic factor withdrawal-induced death was unevenly distributed throughout the cell culture, and the protected granule neurons were near Purkinje cells (Fig. 1*B*, *Field B*). To further examine this effect, granule neuron apoptosis was analyzed on a field-by-field basis as described in Fig. 1*B*; however, infected cultures were stained with both DAPI (to

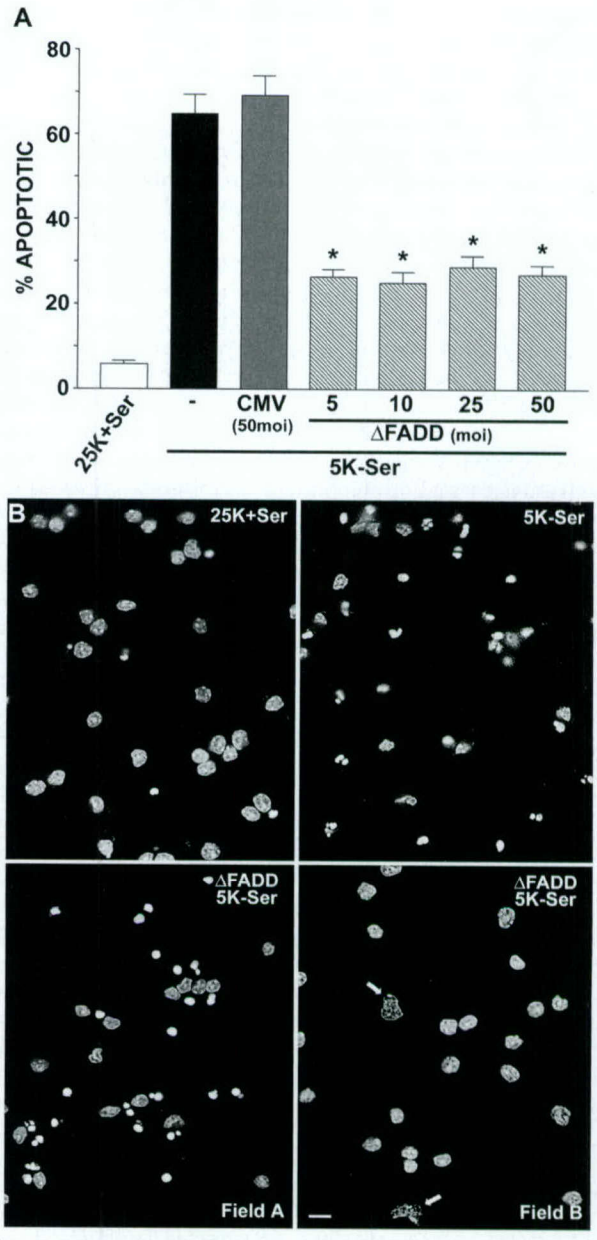

FIG. 1. **Adenoviral infection with ΔFADD attenuates cerebellar granule neuron apoptosis induced by trophic factor withdrawal; the protective effects of ΔFADD are localized.** *A*, cerebellar granule neurons were infected with either a negative control adenovirus (Ad-cytomegalovirus (*CMV*)) or Ad-AU1-ΔFADD at the m.o.i. shown on day 5 in culture. On day 7, cells were incubated in either control (*25K+Ser*) or apoptotic (*5K-Ser*) medium for 24 h. After incubation, granule neurons were fixed, and nuclei were stained with Hoechst dye. Cells containing condensed and/or fragmented chromatin were scored as apoptotic. For each experiment, at least 2 fields of ~500 granule neurons/field were counted per condition. The results shown represent data obtained from seven independent experiments. *, statistically different from 5K-Ser alone ($p < 0.01$). *B*, uninfected granule neurons (*top panels*) or granule neurons infected with ΔFADD at a m.o.i. = 50 (*bottom panels*) were incubated in either control (*25K+Ser*) or apoptotic (*5K-Ser*) medium for 24 h, and nuclei were then stained with DAPI. Nuclei with condensed and/or fragmented chromatin were abundant in uninfected granule neurons incubated in 5K-Ser medium and in some fields of granule neurons infected with ΔFADD (*Field A*). However, other fields of granule neurons infected with ΔFADD did not display a significant number of apoptotic nuclei (*Field B*). These latter fields invariably contained one or more larger and irregularly shaped nuclei (indicated by the *arrows*). *Scale bar* = 10 μm.

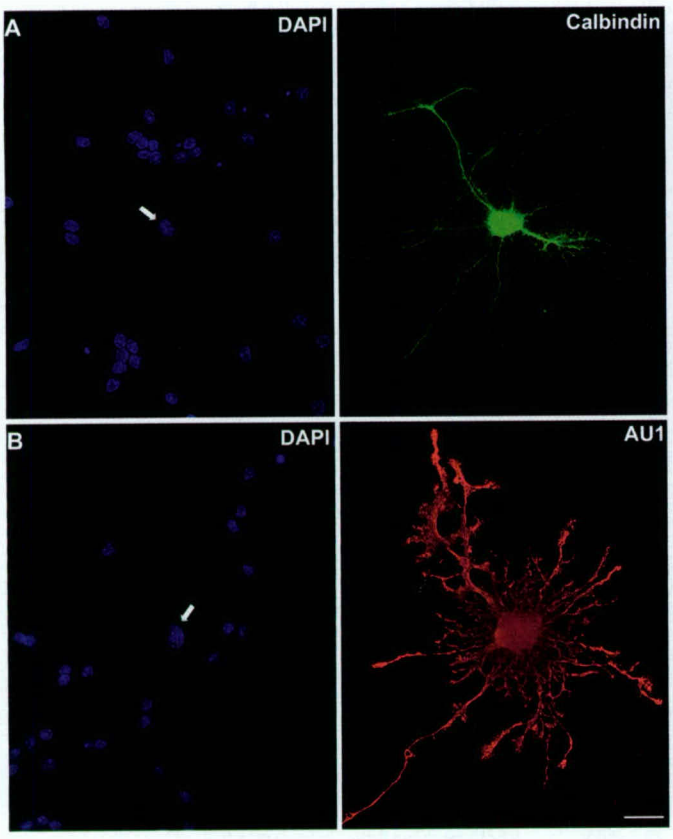

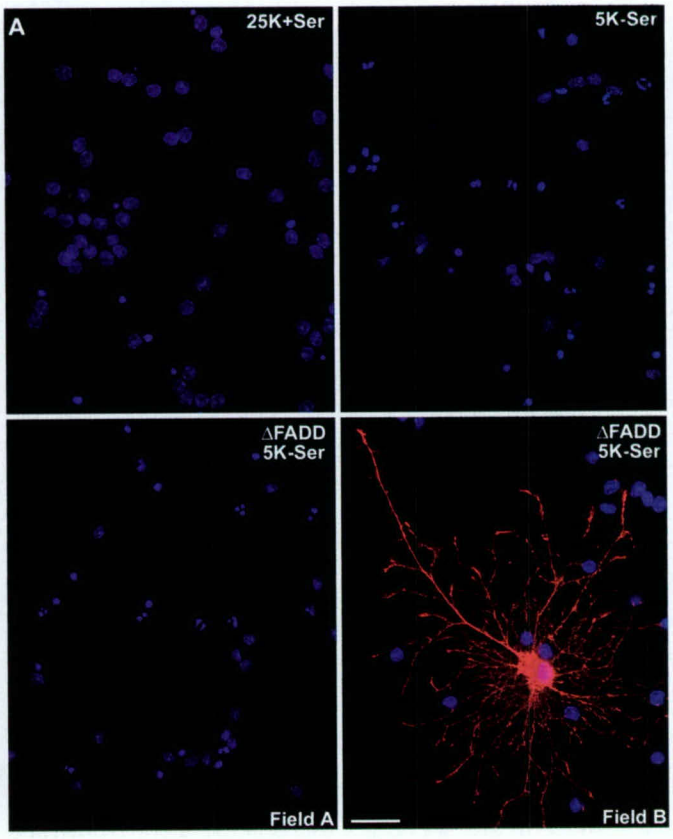

FIG. 2. **Ad-AU1-ΔFADD is expressed in calbindin-positive Purkinje neurons.** *A*, cerebellar cell cultures were maintained in control (25K+Ser) medium for 7 days. After fixation, cells were stained with DAPI (*left panel*) and anti-calbindin (*right panel*) to identify Purkinje neurons. The small nuclei are granule neurons, whereas the large irregularly shaped nucleus (identified by the *arrow*) is that of a calbindin-positive Purkinje cell. *B*, cerebellar cell cultures were infected with Ad-AU1-ΔFADD at a m.o.i. = 50 on day 5 in culture. On day 7, the cells were fixed and stained with DAPI (*left panel*) and anti-AU1 (*right panel*) to identify ΔFADD-infected cells. The small nuclei are granule neurons, whereas the large irregularly shaped nucleus (identified by the *arrow*) is that of a ΔFADD-infected Purkinje cell. *Scale bar* = 20 μm.

assess nuclear morphology) and anti-AU1 to identify ΔFADD-expressing cells. Uninfected cells displayed the expected high amount of granule neuron apoptosis after trophic factor withdrawal (Fig. 3*A*, compare the *upper right panel* (apoptotic) to the *upper left panel* (control)). Similarly, fields of infected cultures that did not contain any ΔFADD-positive Purkinje cells also exhibited significant granule neuron death after trophic factor withdrawal (Fig. 3*A*, *Field A*). In contrast, fields of infected cells that contained at least one ΔFADD-expressing Purkinje neuron displayed a marked reduction in granule neuron apoptosis (Fig. 3*A*, *Field B*). To quantitate this effect, the number of healthy *versus* apoptotic granule neurons was counted per 40× field in ΔFADD-infected cultures that were incubated in apoptotic medium for 24 h. The granule neuron apoptosis results were then subdivided into three data sets based on the number of ΔFADD-positive Purkinje cells (0, 1–2, or 3–4) identified per field by AU1 staining. As shown in Fig. 3*B*, fields of granule neurons in infected cultures that did not contain any ΔFADD-positive Purkinje cells exhibited 58 ± 1% apoptosis (n = 3 experiments, 10 fields/experiment), a value similar to that observed in uninfected cerebellar cultures. However, fields that contained either 1–2 or 3–4 ΔFADD-expressing Purkinje cells demonstrated a significant decrease in granule neuron apoptosis to 22 ± 6 or 20 ± 6%, respectively (n = 3, $p < 0.01$). These results indicate that the ΔFADD-mediated

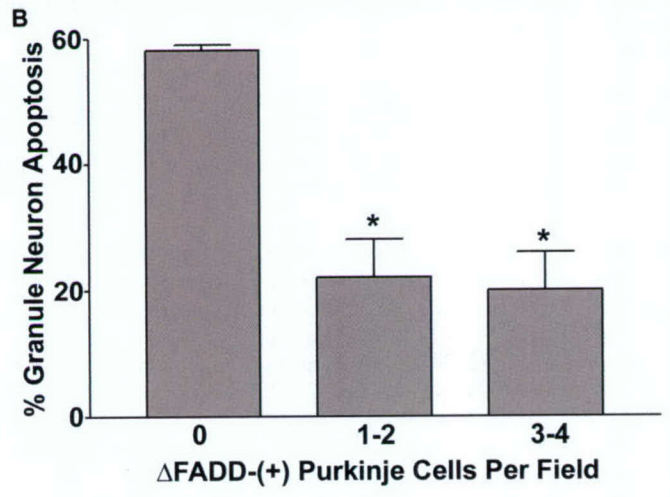

FIG. 3. **Granule neurons in proximity to ΔFADD-expressing Purkinje cells demonstrate increased survival.** *A*, uninfected granule neurons (*top panels*) or granule neurons infected with Ad-AU1-ΔFADD at a m.o.i. = 50 (*bottom panels*) were incubated in either control (*25K+Ser*) or apoptotic (*5K-Ser*) medium for 24 h and then stained with DAPI and anti-AU1. Condensed and/or fragmented nuclei were abundant in uninfected granule neurons incubated in 5K-Ser medium. Apoptotic granule neurons were also plentiful in fields infected with ΔFADD that did not contain any ΔFADD-expressing Purkinje cells (*Field A*). In contrast, fields infected with ΔFADD that contained one or more ΔFADD-positive Purkinje cells displayed a significant decrease in the number of apoptotic granule neurons after trophic factor withdrawal (*Field B*). *Scale bar* = 20 μm. *B*, ΔFADD-infected cerebellar cell cultures were incubated in apoptotic medium and stained for DAPI and AU1, as described in *A*. After staining, the number of healthy *versus* apoptotic granule neurons were counted in fields containing either 0, 1–2, or 3–4 ΔFADD-expressing Purkinje cells per field. Ten fields containing an average of 30 granule neurons/field were counted per condition. The results shown represent data obtained from three independent experiments. *, statistically different from "0" ΔFADD-(+) Purkinje cells per field ($p < 0.01$).

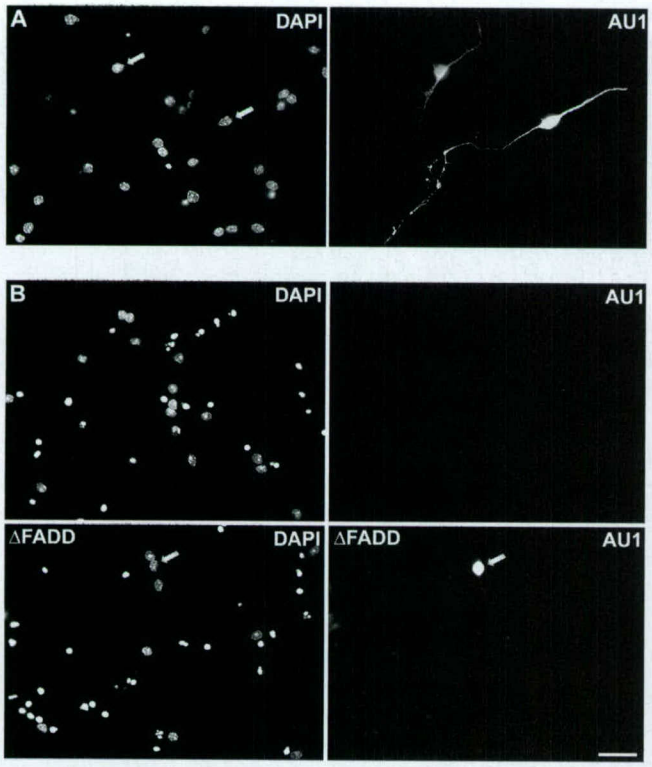

FIG. 4. **Cerebellar granule neurons do not efficiently express Ad-AU1-ΔFADD.** *A*, cerebellar cell cultures were infected on day 5 with Ad-AU1-ΔFADD at a m.o.i. = 50. On day 7, cells were fixed and stained with DAPI (*left panel*) and anti-AU1 (*right panel*). AU1 staining revealed that less than 5% of granule neurons expressed ΔFADD (identified by the *arrows*). *B*, uninfected granule neurons (*top panels*) or AU1-ΔFADD-infected granule neurons (*bottom panels*) were incubated in apoptotic (5K-Ser) medium for 24 h, fixed, and stained with DAPI (*left panels*) and AU1 (*right panels*). Trophic factor withdrawal induced a similar apoptotic response in uninfected cells and infected cells in close association with granule neurons expressing AU1-ΔFADD (indicated by the *arrow*). *Scale bar* = 20 μm.

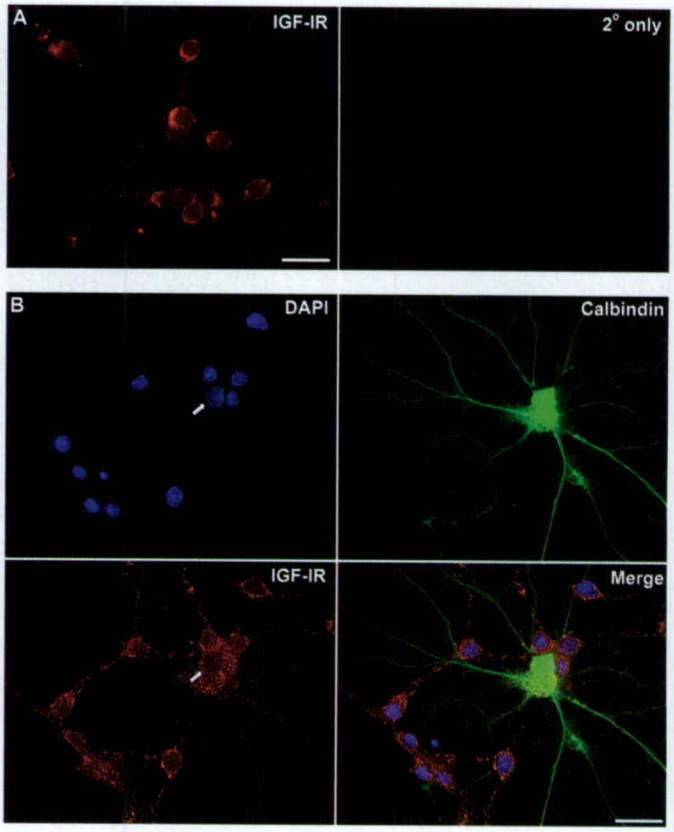

FIG. 5. **Cerebellar granule neurons and Purkinje neurons express IGF-I receptors on their cell surfaces.** *A*, cerebellar granule neurons were fixed and stained with a monoclonal antibody that recognizes the IGF-I receptor (*IGF-IR*). After incubation with a Cy3-conjugated secondary antibody, IGF-I receptors were identified by fluorescence microscopy. IGF-I receptors were expressed primarily at the cell membrane (*left panel*). Incubation with the secondary antibody alone (2° only) did not produce any positive staining (*right panel*). *B*, cerebellar cell cultures were stained as described in *A* but, in addition, calbindin-positive Purkinje cells were identified using a polyclonal antibody to calbindin D28K and a fluorescein isothiocyanate-conjugated secondary. Both granule neurons and calbindin-positive Purkinje neurons showed immunoreactivity for IGF-I receptors. Note the *overlapping yellow staining* indicative of IGF-I receptor and calbindin colocalization in Purkinje cells (*lower right panel*). *Scale bar* = 20 μm.

protection of cerebellar granule neurons from trophic factor withdrawal-induced apoptosis depends on the proximity of granule neurons to ΔFADD-expressing Purkinje cells.

Ad-AU1-ΔFADD Is Not Efficiently Expressed in Granule Neurons—Although Purkinje neurons demonstrated marked expression of Ad-AU1-ΔFADD (Fig. 2*B*), most granule neurons were devoid of AU1 staining (Fig. 4*A*). Quantitatively, when more than 2000 granule neurons were visualized from cerebellar cell cultures infected with Ad-AU1-ΔFADD (m.o.i. = 50), less than 100 stained positively for the AU1 epitope tag at 48 h post-infection (4.4 ± 0.7%, data pooled from 3 independent experiments). These results indicate that granule neurons do not efficiently express AU1-ΔFADD after adenoviral infection. Furthermore, fields of infected cultures that contained one or more AU1-ΔFADD-positive granule neurons displayed a similar amount of apoptotic granule neuron death after trophic factor withdrawal as was observed in uninfected cultures (Fig. 4*B*). This latter result further demonstrates that the ability of ΔFADD to rescue granule neurons from apoptosis is not mediated by proximity to the very few granule neurons actually expressing ΔFADD. However, it is noteworthy that essentially all of the granule neurons that were AU1-ΔFADD-positive were protected from trophic factor withdrawal-induced death regardless of their proximity to Purkinje neurons.

ΔFADD-mediated Cerebellar Granule Neuron Survival Is Dependent on IGF-I—The above data indicate that inhibition of death receptor signaling in Purkinje cells (via infection with Ad-AU1-ΔFADD) not only maintains the Purkinje neurons during trophic factor withdrawal but also results in the protection of closely neighboring granule neurons that require Purkinje cell-derived survival signals. One potent neurotrophin known to rescue cerebellar granule neurons from apoptosis is the growth factor IGF-I (20, 21, 24–26). *In situ* mRNA hybridization studies show that the principal source of IGF-I in the developing cerebellum is the Purkinje cell (40). To investigate a potential role of IGF-I in granule neuron survival, we first analyzed the expression of IGF-I receptors in the cerebellar cell cultures. Immunocytochemical staining with an antibody to the IGF-I receptor demonstrated that cerebellar granule neurons expressed IGF-I receptors primarily at the cell membrane (Fig. 5*A*, *left panel*). Incubation with the Cy3-conjugated secondary antibody alone did not produce any positive staining (Fig. 5*A*, *right panel*). When cerebellar cultures were co-immunostained for both IGF-I receptors and calbindin, both granule neurons and calbindin-positive Purkinje neurons showed immunoreactivity for IGF-I receptors on their cell surfaces (Fig. 5*B*, *lower right panel*, see the *yellow overlapping staining* for co-localized IGF-I receptors and calbindin in a representative Purkinje neuron; the surrounding cells are granule neurons).

Next, the effect of an IGF-I receptor blocking antibody on the ΔFADD-mediated protection of cerebellar granule neurons was

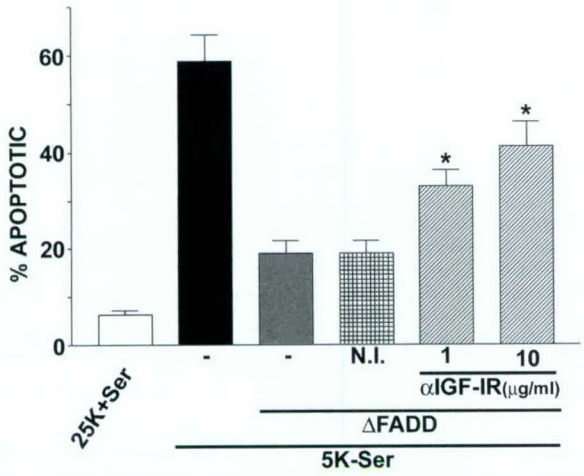

FIG. 6. **ΔFADD-mediated granule neuron survival is inhibited by an IGF-I receptor blocking antibody.** Cerebellar cell cultures were either uninfected or infected with Ad-AU1-ΔFADD (m.o.i. = 50) on day 5. On day 7, cells were incubated in either control (25K+Ser) or apoptotic (5K-Ser) medium alone or containing either an anti-IGF-I receptor blocking antibody (αIGF-IR, 1 or 10 μg/ml) or a non-immune (*N.I.*) control IgG (10 μg/ml) for 24 h. After incubation, cells were fixed, and nuclei were stained with Hoechst dye. Cells containing condensed and/or fragmented nuclei were scored as apoptotic. For each experiment, at least 2 fields of ~500 granule neurons/field were counted per condition. The results shown represent data obtained from seven independent experiments. *, statistically different from ΔFADD alone ($p < 0.01$).

assessed (Fig. 6). Ad-AU1-ΔFADD decreased apoptosis of granule neurons from 59 ± 5% ($n = 7$) to 19 ± 3% ($n = 7, p < 0.01$). Incubation with a non-immune IgG control had no effect on the ability of ΔFADD to decrease granule neuron apoptosis (19 ± 3% apoptosis, $n = 7$), whereas inclusion of a neutralizing antibody that binds to the extracellular domain of the IGF-I receptor significantly attenuated the protective effect of ΔFADD in a dose-dependent manner (41 ± 5% apoptosis at an antibody concentration of 10 μg/ml, $n = 7$, $p < 0.01$ compared with ΔFADD alone). Finally, radioimmunoassay of serum-free media obtained from cerebellar cell cultures revealed that the concentration of IGF-I was below the limits of detection (≥6 ng/ml), further confirming that the protection by IGF-I was localized in nature. Collectively, these results suggest that ΔFADD-mediated survival of cerebellar granule neurons requires local secretion of Purkinje cell-derived IGF-I.

DISCUSSION

In the present study, we investigated a role for the extrinsic death pathway in the apoptotic cell death of primary cerebellar granule neurons subjected to trophic factor withdrawal. Adenoviral expression of dominant-negative FADD (ΔFADD) rescued a significant percentage of granule neurons from trophic factor withdrawal-induced death. Initially, this result suggested that death receptor signaling may play a direct role in cerebellar granule neuron apoptosis. However, immunocytochemical analysis revealed that adenoviral ΔFADD was not efficiently expressed in granule neurons but, instead, showed marked expression in the small number of Purkinje neurons found in these cerebellar cell cultures. Moreover, the ability of adenoviral ΔFADD to rescue granule neurons from apoptosis was dependent on their proximity to ΔFADD-expressing Purkinje cells and required IGF-I. Two major conclusions can be drawn from the above results. First, although the data do not support a direct role for the extrinsic death pathway in cerebellar granule neuron apoptosis, the results are the first to demonstrate that death receptor signaling in Purkinje neurons indirectly influences the survival of granule neurons. Second, selective suppression of the extrinsic death pathway in Purkinje cells is sufficient to rescue neighboring granule neurons that depend on Purkinje cell-derived trophic support including IGF-I.

Previous studies have implicated the intrinsic death pathway in the apoptosis of cerebellar granule neurons. For example, trophic factor withdrawal-induced death of granule neurons requires the pro-apoptotic Bcl-2 family members Bax and Bim (30–32). Bim is a BH3-only Bcl-2 family member that acts in a concerted manner with Bax to promote apoptosis (41). Similar results have also been observed *in vivo* in inherited animal models of cerebellar neuronal death. The lurcher mutant mouse is characterized by a gain-of-function mutation in the Δ2 glutamate receptor that results in the death of cerebellar Purkinje cells (22). Subsequent to the loss of their target Purkinje cells, granule neurons die secondarily via an apoptotic mechanism (22). Targeted deletion of Bax has only a minor effect on Purkinje neuron death but essentially abolishes the secondary death of granule neurons in lurcher mutant mice (42, 43). Thus, Bcl-2 family members regulate cerebellar granule neuron apoptosis both *in vitro* and *in vivo*, strongly suggesting that the intrinsic death pathway plays a principal role in granule neuron apoptosis.

However, much less is known about the involvement of extrinsic death signaling in cerebellar granule neurons. Previous work illustrated that trophic factor withdrawal induces an increase in the mRNA for FasL in primary cerebellar granule neurons, and furthermore, granule neurons isolated from FasL-deficient mice (*gld* mice) demonstrate a significant decrease in their susceptibility to trophic factor withdrawal-induced death (33). Although these results suggest that the extrinsic pathway may be involved in granule neuron apoptosis, our data indicate that disruption of death receptor signaling in cerebellar Purkinje neurons is sufficient to significantly decrease apoptosis in neighboring granule neurons. Thus, the conclusions that were originally drawn from the *gld* mice may actually reflect a loss of the extrinsic death machinery in Purkinje cells that normally make up a small component of cerebellar cell cultures. Yet, it should be noted that our data do not absolutely exclude a direct role for the extrinsic death pathway in granule neuron apoptosis. In fact we observed that the small number of granule neurons that did express ΔFADD were rescued from apoptosis regardless of their proximity to Purkinje cells. However, recent data indicate that specific inhibitors of caspase 8 (an extrinsic initiator caspase) fail to rescue granule neurons from trophic factor withdrawal-induced death, whereas selective caspase 9 (an intrinsic initiator caspase) inhibitors block apoptosis (44). Although the relative selectivities of synthetic caspase inhibitors are not absolute, these findings support an intrinsic-dependent but extrinsic-independent mode of cell death in granule neurons.

The putative role of extrinsic and intrinsic death signaling in the apoptosis of Purkinje neurons is much less well defined than in granule neurons. As described above, Bax deletion did not significantly affect Purkinje neuron survival in lurcher mutant mice (42, 43). In contrast, normal mice in which Bax is knocked out show a significant increase in Purkinje cell number in the cerebellum (45). A similar increase in the number of cerebellar Purkinje cells is also observed in mice overexpressing a human Bcl-2 transgene, suggesting that the intrinsic death pathway influences the developmental death of Purkinje neurons (46). In addition, the spontaneous apoptotic death of Purkinje cells observed *in vitro* in murine cerebellar organotypic cultures is reduced in tissue isolated from Bcl-2 transgenic mice (47). This latter result indicates that the intrinsic

death pathway may also play a role in Purkinje neuron apoptosis induced by stress associated with *in vitro* culture conditions. However, a more detailed analysis of the mechanism underlying Purkinje cell death is currently lacking. Our data suggest that one important function of Purkinje neurons (*i.e.* to provide trophic support to neighboring granule neurons) is compromised after the withdrawal of trophic factors from cerebellar cell cultures. Moreover, expression of ΔFADD, an inhibitor of extrinsic death signaling, maintains Purkinje cell function during trophic factor withdrawal. Thus, extrinsic death signals in addition to intrinsic signals play a significant role in Purkinje neuron loss-of-function and ultimately death.

Finally, the ability of ΔFADD-expressing Purkinje cells to rescue neighboring granule neurons from apoptosis was inhibited by an IGF-I receptor-blocking antibody, suggesting involvement of IGF-I in the neuroprotection. Previous work has shown that Purkinje cells are the principal source of IGF-I production in the developing cerebellum *in vivo* (40), and IGF-I is a potent neurotrophin for cerebellar granule neurons *in vitro* (20, 21, 24–26). *In vivo* studies demonstrate that Purkinje-derived trophic support, including IGF-I, is essential for the proper development of cerebellar granule neurons (22, 48). For example, in Purkinje cell degeneration (*pcd*) mice, in which Purkinje cells die spontaneously before adulthood, cerebellar IGF-I mRNA expression decreases significantly as the Purkinje neurons degenerate (49). After the death of Purkinje cells in *pcd* mice, granule neurons undergo apoptosis resulting from the loss of Purkinje cell-derived IGF-I. Our cerebellar cultures were isolated from postnatal day 7 rats, and Purkinje neurons from this stage of development exhibit maximal IGF-I secretion *in vivo* (50). In addition, IGF-I secretion by Purkinje neurons is highly correlated with the differentiated phenotypes of both granule neurons and Purkinje cells, as is observed in our cultures (50–52). Collectively, the above findings are consistent with an important role for Purkinje cell-derived IGF-I in promoting the survival of cerebellar granule neurons.

Precisely how ΔFADD expression influences Purkinje cell IGF-I production or secretion is presently unclear. It may be that ΔFADD simply blocks extrinsic death signaling in Purkinje neurons and, therefore, sustains their normal function of secreting trophic factors like IGF-I. Alternatively, it is possible that ΔFADD expression somehow enhances IGF-I synthesis or secretion. Further experiments will be necessary to identify the exact mechanism underlying the regulation of Purkinje cell-derived IGF-I by death receptor signaling molecules. In addition, the molecular mechanism that mediates the neuroprotective effects of IGF-I is unclear. Recently, we have shown that exogenous IGF-I rescues cerebellar granule neurons by inhibiting the intrinsic death pathway.[2] Moreover, in transgenic mice overexpressing IGF-I, there was a marked increase in the expression of Bcl-2 in cerebellar Purkinje neurons (53). This finding indicates that Purkinje-derived IGF-I may not only promote the survival of neighboring granule neurons via a paracrine mechanism but may also support Purkinje cells directly via an autocrine mechanism, perhaps by suppressing intrinsic death signals at the mitochondria.

In conclusion, we have shown that adenoviral ΔFADD infection of cerebellar cell cultures results in the restricted expression of ΔFADD in Purkinje neurons. ΔFADD-expressing Purkinje cells rescue neighboring granule neurons from trophic factor withdrawal-induced apoptosis via secretion of IGF-I. The dependence of cerebellar granule neuron survival on Purkinje cell-derived trophic support mimics that found *in vivo* during cerebellar development. The results are the first to show that the extrinsic death pathway in Purkinje neurons indirectly but significantly influences the survival of cerebellar granule neurons.

[2] D. A. Linseman, R. A. Phelps, R. J. Bouchard, T. A. Laessig, S. S. Le, and K. A. Heidenreich, manuscript in preparation.

REFERENCES

1. Nunez, G., Benedict, M. A., Hu, Y., and Inohara, N. (1998) *Oncogene* **17,** 3237–3245
2. Green, D. R. (1998) *Cell* **94,** 695–698
3. Pinkoski, M. J., and Green, D. R. (1999) *Cell Death Differ.* **6,** 1174–1181
4. Chinnaiyan, A. M., O'Rourke, K., Tewari, M., and Dixit, V. M. (1995) *Cell* **81,** 505–512
5. Feinstein, E., Kimichi, A., Wallach, D., Boldin, M., and Varfolomeev, E. (1995) *Trends Biochem. Sci.* **20,** 342–344
6. Muzio, M., Chinnaiyan, A. M., Kischkel, F. C., O'Rourke, K., Shevchenko, A., Ni, J., Scaffidi, C., Bretz, J. D., Zhang, M., Gentz, R., Mann, M., Krammer, P. H., Peter, M. E., and Dixit, V. M. (1996) *Cell* **85,** 817–827
7. Muzio, M., Stockwell, B. R., Stennicke, H. R., Salvesen, G. S., and Dixit, V. M. (1998) *J. Biol. Chem.* **273,** 2926–2930
8. Cai, J., Yang, J., and Jones, D. P. (1998) *Biochim. Biophys. Acta* **1366,** 139–149
9. Zou, H., Li, Y., Liu, X., and Wang, X. (1999) *J. Biol. Chem.* **274,** 11549–11556
10. Tsujimoto, Y. (1998) *Genes Cells* **3,** 697–707
11. Stennicke, H. R., Jurgensmeier, J. M., Shin, H., Deveraux, Q., Wolf, B. B., Yang, X., Zhou, Q., Ellerby, H. M., Ellerby, L. M., Bredesen, D., Green, D. R., Reed, J. C., Froelich, C., and Salvesen, G. S. (1998) *J. Biol. Chem.* **273,** 27084–27090
12. Pan, G., Humke, E. W., and Dixit, V. M. (1998) *FEBS Lett.* **426,** 151–154
13. Nijhawan, D., Honarpour, N., and Wang, X. (2000) *Annu. Rev. Neurosci.* **23,** 73–87
14. Kuida, K., Zheng, T. S., Na, S., Kuan, C., Yang, D., Karasuyama, H., Rakic, P., and Flavell, R. A. (1996) *Nature* **384,** 368–372
15. Yuan, J., and Yankner, B. A. (2000) *Nature* **407,** 802–809
16. Kitamura, Y., Shimohama, S., Kamoshima, W., Ota, T., Matsuoka, Y., Nomura, Y., Smith, M. A., Perry, G., Whitehouse, P. J., and Taniguchi, T. (1998) *Brain Res.* **780,** 260–269
17. Felderhoff-Mueser, U., Taylor, D. L., Greenwood, K., Kozma, M., Stibenz, D., Joashi, U. C., Edwards, A. D., and Mehmet, H. (2000) *Brain Pathol.* **10,** 17–29
18. Martin-Villalba, A., Herr, I., Jeremias, I., Hahne, M., Brandt, R., Vogel, J., Schenkel, J., Herdegen, T., and Debatin, K. M. (1999) *J. Neurosci.* **19,** 3809–3817
19. Parsadanian, A. S., Cheng, Y., Keller-Peck, C. R., Holtzman, D. M., and Snider, W. D. (1998) *J. Neurosci.* **18,** 1009–1019
20. Galli, C., Meucci, O., Scorziello, A., Werge, T. M., Calissano, P., and Schettini, G. (1995) *J. Neurosci.* **15,** 1172–1179
21. D'Mello, S. R., Galli, C., Ciotti, T., and Calissano, P. (1993) *Proc. Natl. Acad. Sci. U. S. A.* **90,** 10989–10993
22. Selimi, F., Doughty, M., Delhaye-Bouchaud, N., and Mariani, J. (2000) *J. Neurosci.* **20,** 992–1000
23. Baptista, C. A., Hatten, M. E., Blazeski, R., and Mason, C. A. (1994) *Neuron* **12,** 243–260
24. Miller, T. M., Tansey, M. G., Johnson, E. M., Jr., and Creedon, D. J. (1997) *J. Biol. Chem.* **272,** 9847–9853
25. Gleichmann, M., Weller, M., and Schulz, J. B. (2000) *Neurosci. Lett.* **282,** 69–72
26. D'Mello, S. R., Borodetz, K., and Soltoff, S. P. (1997) *J. Neurosci.* **17,** 1548–1560
27. Harada, J., and Sugimoto, M. (1999) *Jpn. J. Pharmacol.* **79,** 369–378
28. Clarkson, E. D., Zawada, W. M., Bell, K. P., Esplen, J. E., Choi, P. K., Heidenreich, K. A., and Freed, C. R. (2001) *Exp. Neurol.* **168,** 183–191
29. Zawada, W. M., Meintzer, M. K., Rao, P., Marotti, J., Wang, X., Esplen, J. E., Clarkson, E. D., Freed, C. R., and Heidenreich, K. A. (2001) *Brain Res.* **891,** 185–196
30. Desagher, S., Osen-Sand, A., Nichols, A., Eskes, R., Montessuit, S., Lauper, S., Maundrell, K., Antonsson, B., and Martinou, J.-C. (1999) *J. Cell Biol.* **144,** 891–901
31. Miller, T. M., Moulder, K. L., Knudson, C. M., Creedon, D. J., Deshmukh, M., Korsmeyer, S. J., and Johnson, E. M., Jr. (1997) *J. Cell Biol.* **139,** 205–217
32. Putcha, G. V., Moulder, K. L., Golden, J. P., Bouillet, P., Adams, J. A., Strasser, A., and Johnson, E. M., Jr. (2001) *Neuron* **29,** 615–628
33. Le-Niculescu, H., Bonfoco, E., Kasuya, Y., Claret, F. X., Green, D. R., and Karin, M. (1999) *Mol. Cell. Biol.* **19,** 751–763
34. Streetz, K., Leifeld, L., Grundmann, D., Ramakers, J., Eckert, K., Spengler, U., Brenner, D. A., Manns, M., and Trautwein, C. (2000) *Gastroenterology* **119,** 446–460
35. Christakos, S., Rhoten, W. B., and Feldman, S. C. (1987) *Methods Enzymol.* **139,** 534–551
36. Li, M., Wang, X., Meintzer, M. K., Laessig, T., Birnbaum, M. J., and Heidenreich, K. A. (2000) *Mol. Cell. Biol.* **20,** 9356–9363
37. Bradham, C. A., Qian, T., Streetz, K., Trautwein, C., Brenner, D. A., and Lemasters, J. J. (1998) *Mol. Cell. Biol.* **18,** 6353–6364
38. Hockberger, P. E., Yousif, L., and Nam, S. C. (1994) *Neuroimage* **1,** 276–287
39. Vogel, M. W., and Prittie, J. (1995) *J. Neurobiol.* **26,** 537–552
40. Bartlett, W. P., Li, X. –S., Williams, M., and Benkovic, S. (1991) *Dev. Biol.* **147,** 239–250
41. Zong, W. X., Lindsten, T., Ross, A. J., MacGregor, G. R., and Thompson, C. B. (2001) *Genes Dev.* **15,** 1481–1486
42. Doughty, M. L., De Jager, P. L., Korsmeyer, S. J., and Heintz, N. (2000) *J. Neurosci.* **20,** 3687–3694
43. Selimi, F., Vogel, M. W., and Mariani, J. (2000) *J. Neurosci.* **20,** 5339–5345
44. Gerhardt, E., Kugler, S., Leist, M., Beier, C., Berliocchi, L., Volbracht, C.,

Weller, M., Bahr, M., Nicotera, P., and Schulz, J. B. (2001) *Mol. Cell. Neurosci.* **17,** 717–731
45. Fan, H., Favero, M., and Vogel, M. W. (2001) *J. Comp. Neurol.* **436,** 82–91
46. Zanjani, H. S., Vogel, M. W., Delhaye-Bouchaud, N., Martinou, J.-C., and Mariani, J. (1996) *J. Comp. Neurol.* **374,** 332–341
47. Ghoumari, A. M., Wehrle, R., Bernard, O., Sotelo, C., and Dusart, I. (2000) *Eur. J. Neurosci.* **12,** 2935–2949
48. Andersson, I. K., Edwall, D., Norstedt, G., Rozell, B., Skottner, A., and Hansson, H.-A. (1988) *Acta Physiol. Scand.* **132,** 167–173
49. Zhang, W., Ghetti, B., and Lee, W.-H. (1997) *Brain Res. Dev. Brain Res.* **98,** 164–176
50. Bondy, C. A. (1991) *J. Neurosci.* **11,** 3442–3455
51. Lin, X., and Bulleit, R. F. (1997) *Brain Res. Dev. Brain Res.* **99,** 234–242
52. Torres-Aleman, I., Pons, S., and Arevalo, M. A. (1994) *J. Neurosci. Res.* **39,** 117–126
53. Baker, N. L., Carlo Russo, V., Bernard, O., D'Ercole, A. J., and Werther, G. A. (1999) *Brain Res. Dev. Brain Res.* **118,** 109–118
54. Ludbrook, J. (1998) *Clin. Exp. Pharmacol. Physiol.* **25,** 1032–1037

Cellular/Molecular

The p75 Neurotrophin Receptor Can Induce Autophagy and Death of Cerebellar Purkinje Neurons

Maria L. Florez-McClure,[1] Daniel A. Linseman,[1] Charleen T. Chu,[2] Phil A. Barker,[3] Ron J. Bouchard,[1] Shoshona S. Le,[1] Tracey A. Laessig,[1] and Kim A. Heidenreich[1]

[1]Department of Pharmacology, University of Colorado Health Sciences Center, and Denver Veterans Affairs Medical Center, Denver, Colorado 80262, [2]Department of Pathology, Division of Neuropathology, and Pittsburgh Institute for Neurodegenerative Diseases, University of Pittsburgh School of Medicine, Pittsburgh, Pennsylvania 15213, and [3]Center for Neuronal Survival, Montreal Neurological Institute, McGill University, Montreal, Quebec H3A 2B4, Canada

The cellular mechanisms underlying Purkinje neuron death in various neurodegenerative disorders of the cerebellum are poorly understood. Here we investigate an *in vitro* model of cerebellar neuronal death. We report that cerebellar Purkinje neurons, deprived of trophic factors, die by a form of programmed cell death distinct from the apoptotic death of neighboring granule neurons. Purkinje neuron death was characterized by excessive autophagic–lysosomal vacuolation. Autophagy and death of Purkinje neurons were inhibited by nerve growth factor (NGF) and were activated by NGF-neutralizing antibodies. Although treatment with antisense oligonucleotides to the p75 neurotrophin receptor (p75ntr) decreased basal survival of cultured cerebellar neurons, p75ntr-antisense decreased autophagy and completely inhibited death of Purkinje neurons induced by trophic factor withdrawal. Moreover, adenoviral expression of a p75ntr mutant lacking the ligand-binding domain induced vacuolation and death of Purkinje neurons. These results suggest that p75ntr is required for Purkinje neuron survival in the presence of trophic support; however, during trophic factor withdrawal, p75ntr contributes to Purkinje neuron autophagy and death. The autophagic morphology resembles that found in neurodegenerative disorders, suggesting a potential role for this pathway in neurological disease.

Key words: **autophagy; Purkinje neuron; p75ntr; cell death; neurotrophin; vacuoles**

Introduction

Chronic neurodegenerative diseases are characterized by a selective loss of specific neuronal populations over a period of years or even decades. Although the underlying causes of most neurodegenerative diseases are unclear, the loss of neurons and neuronal contacts is a key feature of disease pathology. Elucidation of the cellular mechanisms regulating neuronal cell death is critical for developing new therapeutic strategies to slow or halt the progressive neurodegeneration in these disorders.

Purkinje neurons in the cerebellum integrate input to the cerebellar cortex from the mossy fibers and climbing fibers and subsequently generate inhibitory output to the deep cerebellar nuclei (Ghez and Thach, 2000). In addition to their essential role in proper cerebellar function, Purkinje neurons provide critical trophic support to developing cerebellar granule neurons and inferior olivary neurons (Torres-Aleman et al., 1994; Zanjani et al., 1994; Linseman et al., 2002a). Purkinje neurons are specifically lost in various neurodegenerative conditions such as spinocerebellar ataxias (Koeppen, 1998; Watase et al., 2002), ataxia telangectasia (Gatti and Vinters, 1985; Borghesani et al., 2000), autism (Ritvo et al., 1986; Bailey et al., 1998), and certain prion encephalopathies (Ferrer et al., 1991; Watanabe and Duchen, 1993; Lasmezas et al., 1997). Although Purkinje cell loss is a critical feature of disease pathology, the molecular mechanisms underlying Purkinje cell death remain poorly understood.

The Lurcher (Lc) mouse has been extensively used as an *in vivo* model of Purkinje neuron degeneration. The cell degeneration in the Lurcher cerebellum results from a single point mutation in the δ2 glutamate receptor (GluRδ2), whose expression is restricted to Purkinje neurons (Zuo et al., 1997). The degeneration and loss of Purkinje neurons in Lurcher cerebellum is followed by a secondary death of cerebellar granule neurons and inferior olivary neurons attributable to loss of trophic support normally provided by their afferent target Purkinje neurons (Wetts and Herrup, 1982). Because GluRδ2^{Lc} causes a constitutive depolarization of Purkinje neurons, it was originally thought that the death of Purkinje neurons in the Lc cerebellum was akin to excitotoxicity mediated by excessive calcium influx. However, a recent report suggested that the mechanism of GluRδ2^{Lc}-induced Purkinje cell degeneration can be dissociated from depolarization (Selimi et al., 2003). Instead, Lc Purkinje cell death is hypothesized to involve interactions between the mutant GluRδ2

Received Dec. 30, 2003; revised March 16, 2004; accepted March 17, 2004.

This work was supported by a Department of Veterans Affairs merit award (K.A.H.), Department of Defense Grant DAMD17-99-1-9481 (K.A.H.), National Institutes of Health Grants NS38619-01A1 (K.A.H.) and NS40817 (C.T.C.), a Department of Veterans Affairs Research Enhancement Program award (K.A.H., D.A.L.), and a National Research Service award (M.L.F.-M.). We thank Ardith Ries of the University of Pittsburgh electron microscopy laboratory for technical assistance and Dr. John Shelburne of the Duke University and Veterans Affairs Medical Centers (Durham, NC) for helpful discussion.

Correspondence should be addressed to Kim A. Heidenreich, Department of Pharmacology, C236, University of Colorado Health Sciences Center, 4200 East Ninth Avenue, Denver, CO 80262. E-mail: kim.heidenreich@uchsc.edu.

DOI:10.1523/JNEUROSCI.5744-03.2004

 0270-6474/04/244498-12$15.00/0

receptor and the proteins nPIST and Beclin 1, because these protein–protein interactions can lead to cell death and increase autophagy when overexpressed in heterologous cells (Yue et al., 2002). Furthermore, both groups were able to demonstrate the appearance of autophagic vacuoles in Lc Purkinje neurons before degeneration, suggesting that upregulated autophagy is an early feature of dying Purkinje neurons (Yue et al., 2002; Selimi et al., 2003).

Autophagy is a degradative pathway responsible for the bulk of proteolysis in normal cells. Autophagy is an evolutionarily conserved pathway that leads to the degradation of proteins and entire organelles in cells undergoing stress; however, in extreme cases it can result in cellular dysfunction and cell death (Klionsky and Emr, 2000). Autophagy begins with the formation of double-membrane vesicles that sequester cytoplasm and organelles in autophagosomes (autophagic vacuoles in mammalian cells). The autophagosomes fuse with lysosomes, forming autophagolysosomes. The contents of autophagolysosomes are degraded by lysosomal enzymes into basic macromolecules, which are then recycled for use in essential cellular functions (Stromhaug and Klionsky, 2001).

Dysregulation of autophagolysosomal activity can lead to cell death and is implicated in several neurodegenerative conditions, including Parkinson's disease (Anglade et al., 1997), Alzheimer's disease (Cataldo et al., 1996; Nixon et al., 2000), Lewy body dementias (Zhu et al., 2003), Huntington's disease (Kegel et al., 2000; Petersen et al., 2001), and prion encephalopathies (Boellaard et al., 1991; Liberski et al., 2002). Nutrient deprivation, including withdrawal of serum (Mitchener et al., 1976), is one stimulus known to induce autophagy. In this report, we describe an *in vitro* model to investigate signaling pathways that regulate autophagy and survival in cerebellar Purkinje neurons. We used cerebellar cultures from early postnatal rats to investigate Purkinje neuron death in response to trophic factor withdrawal. In this model, Purkinje cell loss was characterized by extensive cytoplasmic vacuolation and a marked absence of nuclear condensation or fragmentation. The vacuoles stained with markers for autophagic vacuoles and lysosomes and the presence of abundant, enlarged autophago(lyso)somes was confirmed by transmission electron microscopy. The autophagy inhibitor 3-methyladenine diminished cytoplasmic vacuolation and moderately increased the survival of Purkinje neurons. Nerve growth factor (NGF) also inhibited autophagy and death of Purkinje neurons. The protective effects of NGF were mediated by the low-affinity p75 neurotrophin receptor (p75ntr). Our data support the hypothesis that p75ntr can regulate autophagy and death in Purkinje neurons.

Materials and Methods

Materials. Polyclonal antibodies to calbindin-D28k and p75ntr, monoclonal antibodies to NGF, and purified NGF were obtained from Chemicon (Temecula, CA). Polyclonal antibodies to NGF and monoclonal antibodies to phospho-TrkA were obtained from Santa Cruz Biotechnology (Santa Cruz, CA). The monoclonal phosphotyrosine antibody (Ab) was obtained from Upstate Cell Signaling Solutions (Lake Placid, NY). A polyclonal antibody to the intracellular domain of rat p75ntr was obtained from Covance (Berkeley, CA). Cy3- and FITC-conjugated secondary antibodies for immunocytochemistry were purchased from Jackson ImmunoResearch (West Grove, PA). Horseradish peroxidase-linked secondary antibodies and reagents for enhanced chemiluminescence detection were obtained from Amersham Biosciences (Piscataway, NJ). Lysosensor blue was obtained from Molecular Probes (Eugene, OR). Monodansylcadaverine, 3-methyladenine, and 4,6-diamidino-2-phenylindole (DAPI) were from Sigma (St. Louis, MO). Adenoviral cytomegalovirus (CMV; negative control adenovirus) was from Dr. Jerry Schaack (University of Colorado Health Sciences Center, Denver, CO). The adenoviral rat p75ntr myristylated intracellular domain (p75mICD) has been described previously (Roux et al., 2001).

Cell culture. Rat cerebellar granule neurons were isolated from 7-d-old Sprague Dawley rat pups as described previously (D'Mello et al., 1993). Briefly, neurons were plated at a density of 2.0×10^6 cells/ml in basal modified Eagle's medium (BME) containing 10% fetal bovine serum, 25 mM KCl, 2 mM L-glutamine, and penicillin (100 U/ml)-streptomycin (100 μg/ml; Invitrogen, Gaithersburg, MD) Cytosine arabinoside (10 μM) was added to the culture medium 24 hr after plating to limit the growth of non-neuronal cells. Experiments were performed after 7 d in culture. Death was induced by removing the serum- and high-potassium-containing media and replacing it with serum-free and 5 mM potassium BME.

Adenoviral infection. Five days after plating, neuronal cultures were infected with either control adenovirus (adenoviral CMV) or adenoviral p75ntr, full-length or truncated, mICD, each at the indicated multiplicity of infection. After infection, cells were returned to the incubator for 48 hr at 37°C and 10% CO_2. On day 7, neurons were processed for live cell imaging or fixed for immunocytochemistry.

Antisense. The p75ntr antisense and missense oligonucleotides (both at 5 μM) were added to the cultures at the time of plating [day *in vitro* (DIV) 0] by repeatedly triturating the cells in the presence of the oligonucleotides before seeding. The oligonucleotides were present throughout the culture. Trophic factor withdrawal was performed on day 5 or 6 in culture (DIV 5 or 6) for either 24 or 48 hr. After this treatment, the cells were processed for live cell lysosensor experiments or fixed for immunocytochemistry to count Purkinje neurons. In all cases, the antisense was taken up by neurons with nearly 100% efficiency as assayed by visualization of the fluorescently labeled oligonucleotides. HPLC-purified phosphorothioate oligonucleotides were purchased from Integrated DNA Technologies (Coralville, IA). Sequences used were as follows: rat p75ntr 5′ antisense, 5′-ACCTGCCCTCCTCATTGCA-3′; and rat p75ntr 5′ missense, 5′-CTCCCACTCGTCATTCGAC-3′. The rat 5′ p75ntr antisense was also purchased with a 5′ 56-FAM fluorescent label so that uptake by the neurons could be monitored. The antisense sequence used has been characterized previously and has been shown to be effective at inhibiting p75ntr-mediated cell death both *in vitro* and *in vivo* (Barrett and Bartlett, 1994; Cheema et al., 1996; Lowry et al., 2001).

Immunocytochemistry. Neuronal cultures were plated on polyethyleneimine-coated glass coverslips. Neurons were infected and induced to undergo death as indicated previously. After treatment, the neurons were fixed with 4% paraformaldehyde and then permeabilized and blocked with PBS, pH 7.4, containing 0.2% Triton X-100 and 5% BSA. Cells were then incubated with polyclonal antibodies against calbindin (1:250), active caspase-3 (1:500), or p75ntr (1:250) overnight at 4°C diluted in PBS containing 0.1% Triton X-100 and 2% BSA. Primary antibodies were then removed, and the cells were washed at least six times with PBS at room temperature. The neurons were then incubated with Cy3-conjugated donkey anti-rabbit secondary antibodies (1:500) and DAPI (1 μg/ml) for 1 hr at room temperature. The cells were then washed at least six more times with PBS, and coverslips were adhered to glass slides with mounting medium (0.1% *p*-phenylenediamine in 75% glycerol in PBS). Imaging was performed on a Zeiss (Thornwood, NY) Axioplan 2 microscope equipped with a Cooke Sensicam deep-cooled CCD camera, and images were analyzed with the Slidebook software program (Intelligent Imaging Innovations Inc., Denver, CO).

Purkinje cell counts. Purkinje neuron numbers were measured by counting the number of calbindin-positive cells in 152 fields under 63× oil that were randomly selected by following a fixed grid pattern over the coverslip. The total area counted per coverslip was 14.6 mm^2 or ~13% of the coverslip. In addition to calbindin staining, cells were also judged on their morphology. Cells counted as Purkinje neurons had large rounded cell bodies, elaborate processes, and larger, more oval nuclei (in comparison with the smaller, rounder nuclei of granule neurons). Some very bright calbindin-positive cells that were either as small as the granule neurons, having bipolar processes, or very large flattened cells, lacking elaborate processes, were not counted because previous studies on *in vitro* differentiation of Purkinje neurons suggest that these cells may represent examples of delayed or aberrant development of Purkinje neu-

rons in culture (Baptista et al., 1994). At least three coverslips were counted per experimental condition. The numbers were averaged and expressed as a percentage of the average number counted in the appropriate controls. This was repeated for at least three independent experiments.

Live cell imaging and vacuolation measurements. Lysosensor blue and monodansylcadaverine (MDC) were added to the cultures at the end of the indicated treatments and returned to the incubator for 20 min. The cells were then washed three times with 37°C phenol red-free DMEM to remove nonspecifically bound dyes. The coverslips were mounted onto glass slides on ~10 μl of phenol red-free DMEM; excess media were aspirated; and the coverslips were sealed and imaged immediately. Purkinje neurons were identified on the basis of their morphology (large, oval nuclei, large cell body, and multiple processes) by scanning the coverslips under bright-field differential interference contrast with a 63× oil objective. Images of the lysosensor blue and MDC fluorescence were captured on the DAPI and FITC channels, respectively, with the 100× oil objective. The lysosensor blue images were used to measure the diameters of all the visible lysosomes in at least six Purkinje neurons per condition. This was usually between 100 and 200 lysosomes. This was repeated for at least three independent experiments.

Transmission electron microscopy. Cultured cells were fixed in 2% paraformaldehyde and 2.5% glutaraldehyde for 1 hr, postfixed in 1% osmium tetroxide for 1 hr at 4°C, and processed for embedding in the culture dish. Cells were then gently scraped and embedded in blocks of Eponaraldite. Thin sections were stained with 4% aqueous uranyl acetate and lead citrate and examined on a Philips CM-12 electron microscope.

Lysate preparation. After incubation for the indicated times and with the reagents specified above, the culture medium was aspirated, cells were washed once with 2 ml of ice-cold PBS (PBS, pH 7.4), placed on ice, and scraped into lysis buffer (200 μl/35 mm well) containing 20 mM HEPES, pH 7.4, 1% Triton X-100, 50 mM NaCl, 1 mM EGTA, 5 mM β-glycerophosphate, 30 mM sodium pyrophosphate, 100 μM sodium orthovanadate, 1 mM phenylmethylsulfonyl fluoride, 10 μg/ml leupeptin, and 10 μg/ml aprotinin. Cell debris was removed by centrifugation at 6000 × *g* for 3 min and the protein concentration of the supernatant was determined using a commercially available protein assay kit (Pierce, Rockford, IL). Equal amounts of supernatant protein were diluted to a final concentration of 1× SDS-PAGE sample buffer, boiled for 5 min, and electrophoresed through 7.5% polyacrylamide gels. Proteins were transferred to polyvinylidene membranes (Millipore, Bedford, MA) and processed for immunoblot analysis.

Immunoblot analysis. Nonspecific binding sites were blocked in PBS, pH 7.4, containing 0.1% Tween 20 (PBS-T) and 1% BSA for 1 hr at room temperature. Primary antibodies were diluted in blocking solution and incubated with the membranes for 1 hr. Excess primary Ab was removed by washing the membranes three times in PBS-T. The blots were then incubated with the appropriate horseradish peroxidase-conjugated secondary Ab diluted in PBS-T for 1 hr and were subsequently washed three times in PBS-T. Immunoreactive proteins were detected by enhanced chemiluminescence. In some experiments, membranes were reprobed after stripping in 0.1 M Tris-HCl, pH 8.0, 2% SDS, and

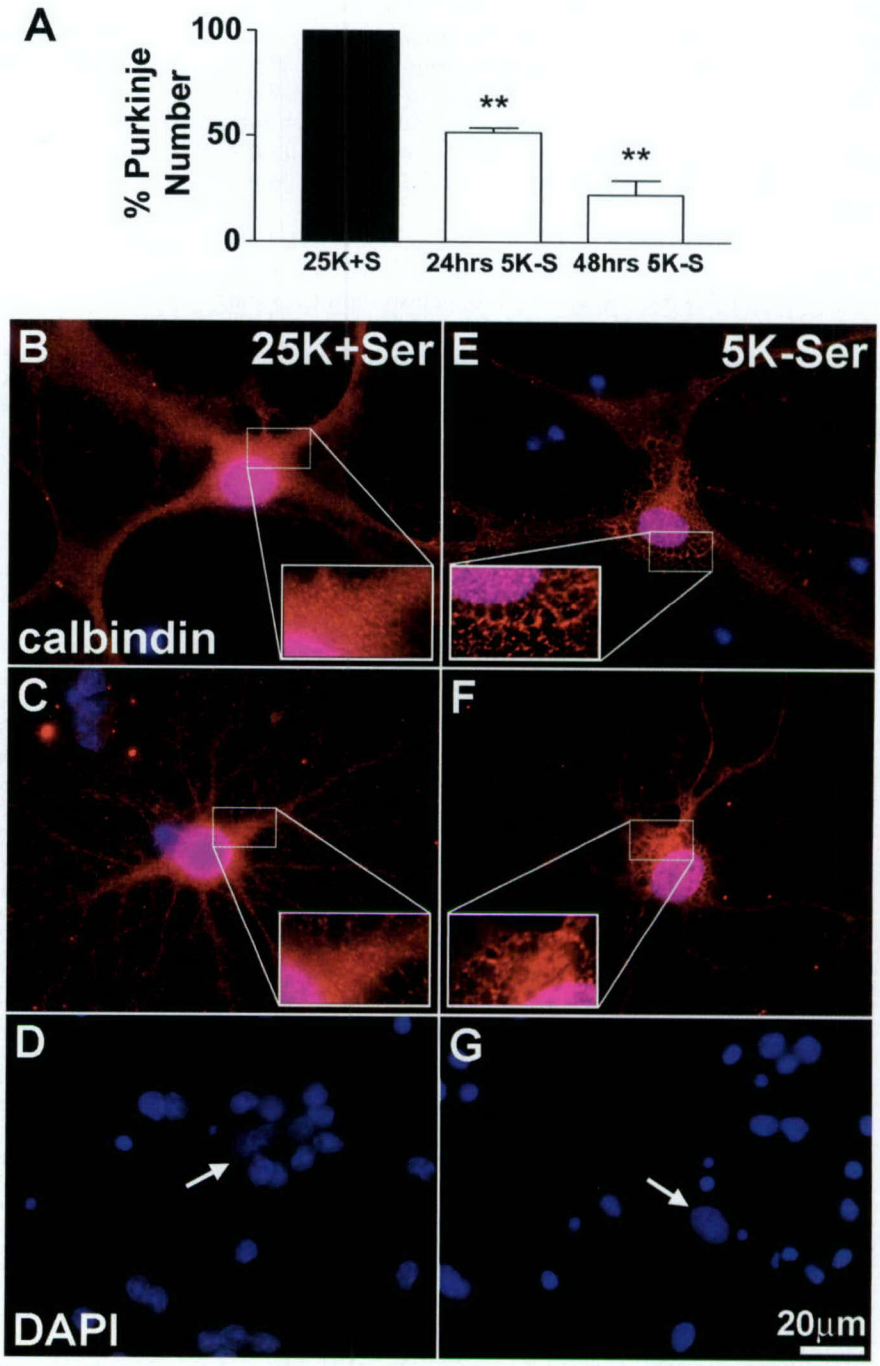

Figure 1. Trophic factor withdrawal induces a nonapoptotic death pathway in Purkinje neurons. Cultured cerebellar neurons were allowed to differentiate in medium containing 10% fetal calf serum and 25 mM potassium. On day 7, neurons were either maintained in control medium (25K+Ser) or subjected to trophic factor withdrawal medium (5K−Ser) for 24–48 hr. *A*, Purkinje number was quantified by counting the total number of calbindin-positive Purkinje cells in randomly chosen, equally sized areas per condition (total area, 14.6 mm^2). Numbers are plotted as a percentage of control. Values represent the mean ± SEM of three independent experiments each performed in triplicate. **Significant difference from 25K+S control at $p < 0.01$, one-way ANOVA, Tukey's *post hoc* test. *B–G*, Cells incubated in either control medium (*B–D*) or deprived of trophic factors (*E–G*) were fixed and stained with polyclonal antibodies against calbindin-D28k (a specific marker of Purkinje neurons; red) and the nuclear dye DAPI (blue). *B*, *C*, Purkinje neurons maintained in control medium demonstrate differentiated morphology. *D*, DAPI staining reveals the nuclei of healthy granule neurons and a Purkinje neuron (arrow). *E*, *F*, Trophic factor withdrawal induced extensive cytoplasmic vacuolation of Purkinje neurons (see magnified insets). *G*, DAPI staining reveals increased nuclear condensation and fragmentation in granule neurons, whereas there is a notable lack of nuclear condensation in Purkinje nuclei (arrow).

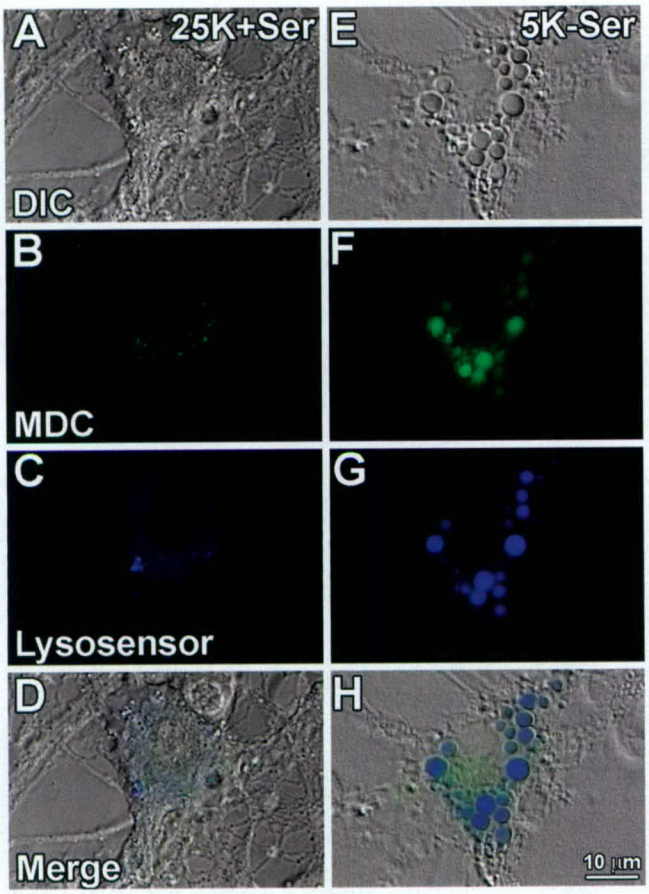

Figure 2. Autophagic and lysosomal markers stain vacuoles that form during Purkinje neuron degeneration. Purkinje neurons maintained in either control (25K+Ser) or trophic factor withdrawal (5K−Ser) media for 24 hr were stained with the autophagic marker MDC (green), and lysosensor blue, a pH-sensitive dye that fluoresces blue in acidic environments. Live cell imaging of control (*A–D*) and trophic factor-deprived (*E–H*) Purkinje neurons was performed. *A*, *E*, Bright-field images of cells identified as Purkinje neurons based on their morphology, characterized by a large cytoplasm (compared with granule neurons) and extensive neuronal processes. *B*, *F*, MDC staining demonstrating increases in autophagosomes in Purkinje neurons after trophic factor withdrawal. *C*, *G*, Lysosensor blue staining reveals acidic organelles (i.e., lysosomes) and demonstrates a marked increase in the size of lysosomes in Purkinje neurons after withdrawal of trophic factors. *D*, *H*, All three fields merged, demonstrating colabeling of some cytoplasmic vacuoles with both MDC and lysosensor blue indicative of autophagolysosomal fusion.

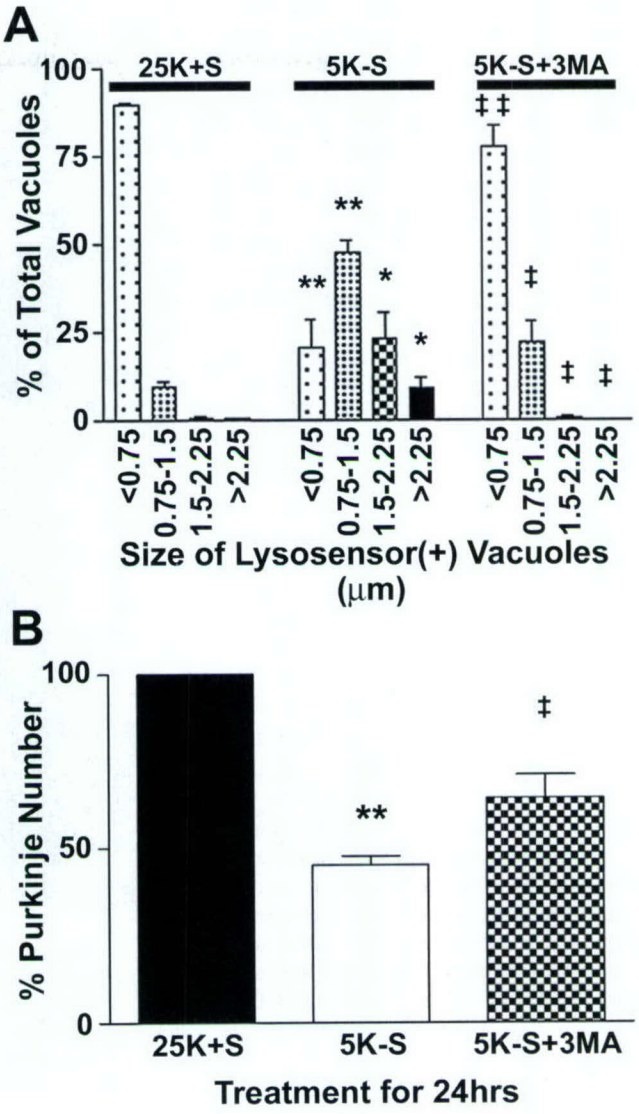

Figure 3. The autophagy inhibitor 3MA, blocks the increased vacuolation and loss of Purkinje neurons. Purkinje neurons were maintained in either control medium (25K+S) or trophic factor withdrawal medium (5K−S) in the absence or presence of 5 mM 3MA (5K−S+3MA) for 24 hr. *A*, The effects of the various treatments on vacuole size were quantified by measuring the diameters of all visible lysosensor blue-positive vacuoles in 6–12 Purkinje neurons per treatment condition in at least three independent experiments. Usually, the total number of vacuoles measured per condition was between 100 and 200. The size distribution was graphed as a percentage of total vacuoles that were within the indicated size ranges. *B*, Quantitation of the effects of 3MA on Purkinje neuron numbers demonstrate that addition of 5 mM 3MA to trophic withdrawal medium partially rescues Purkinje neurons from death after 24 hr of trophic factor withdrawal, compared with healthy controls. Numbers are mean ± SEM values of seven independent experiments, each performed in triplicate. **,*Significant difference from 25K+S (**$p < 0.01$; *$p < 0.05$). ‡‡,‡Significant difference from 5K−S (‡‡$p < 0.01$; ‡$p < 0.05$).

100 mM β-mercaptoethanol for 30 min at 52°C. The blots were rinsed twice in PBS-T and processed as above with a different primary Ab. Autoluminograms shown are representative of at least three independent experiments.

Data analysis. Results shown represent the means ± SEM for the number of independent experiments performed. Statistical differences between the means of unpaired sets of data were evaluated using one-way ANOVA followed by *post hoc* Tukey's test; $p < 0.05$ was considered statistically significant.

Results

Trophic factor withdrawal results in a loss of Purkinje neurons that is morphologically distinct from apoptosis

We have investigated Purkinje neuron death induced by trophic factor withdrawal using primary cerebellar neuronal cultures. Although these cultures have been extensively used to study signaling pathways that regulate survival of cerebellar granule neurons (D'Mello et al., 1993; Linseman et al., 2002b; Vaudry et al., 2003), they also provide a model system for studying differentiated Purkinje neurons (Baptista et al., 1994). Primary neuronal cultures are derived from dissociated cerebella of early postnatal rats. These neuronal cultures survive and differentiate when maintained in medium containing 10% fetal calf serum and a depolarizing concentration of potassium (25 mM). Granule neurons, which constitute ~98% of the cell population, undergo classical apoptosis, characterized by chromatin condensation and caspase activation, when they are deprived of serum and depolarizing potassium (trophic factor withdrawal; (D'Mello et al., 1993; Linseman et al., 2002b).

In contrast, Purkinje neurons, which make up ~2% of the

culture, undergo a distinct nonapoptotic form of cell death in response to trophic factor withdrawal. Quantification of the number of Purkinje neurons after trophic factor withdrawal is shown in Figure 1*A*. Purkinje neurons were identified by staining with antibodies to the Purkinje marker calbindin-D28k. After 24 or 48 hr of trophic factor withdrawal, Purkinje numbers were 50.4 ± 1.4 and 22.3 ± 7.0% of controls, respectively. The remaining Purkinje neurons showed markedly different morphology from that of control cells, characterized by extensive cytoplasmic vacuolation (Fig. 1, compare control cells, *B, C*, with trophic factor-deprived cells, *E, F*). In contrast to granule neurons deprived of trophic support, which demonstrated substantial nuclear condensation and fragmentation characteristic of apoptosis (Fig. 1, compare *D, G*), Purkinje neurons showed no obvious signs of nuclear condensation or fragmentation (Fig. 1, compare nuclei indicated in *D, G*, arrows). The degenerating Purkinje neurons did not stain with propidium iodide, indicating that they retained membrane integrity throughout the death process (data not shown). The maintenance of membrane integrity suggested that Purkinje death did not occur by necrosis. Vacuole formation and subsequent loss of Purkinje neurons required new RNA synthesis because addition of the transcriptional inhibitor actinomycin D (ActD) decreased vacuolation and significantly increased the numbers of Purkinje cells to 78.7 ± 1.5% compared with 50.4 ± 1.4% ($p < 0.05$) after 24 hr of trophic factor withdrawal. The ability of ActD to protect Purkinje neurons further suggested that the mechanism of death was not necrotic but was rather a regulated program of cell suicide.

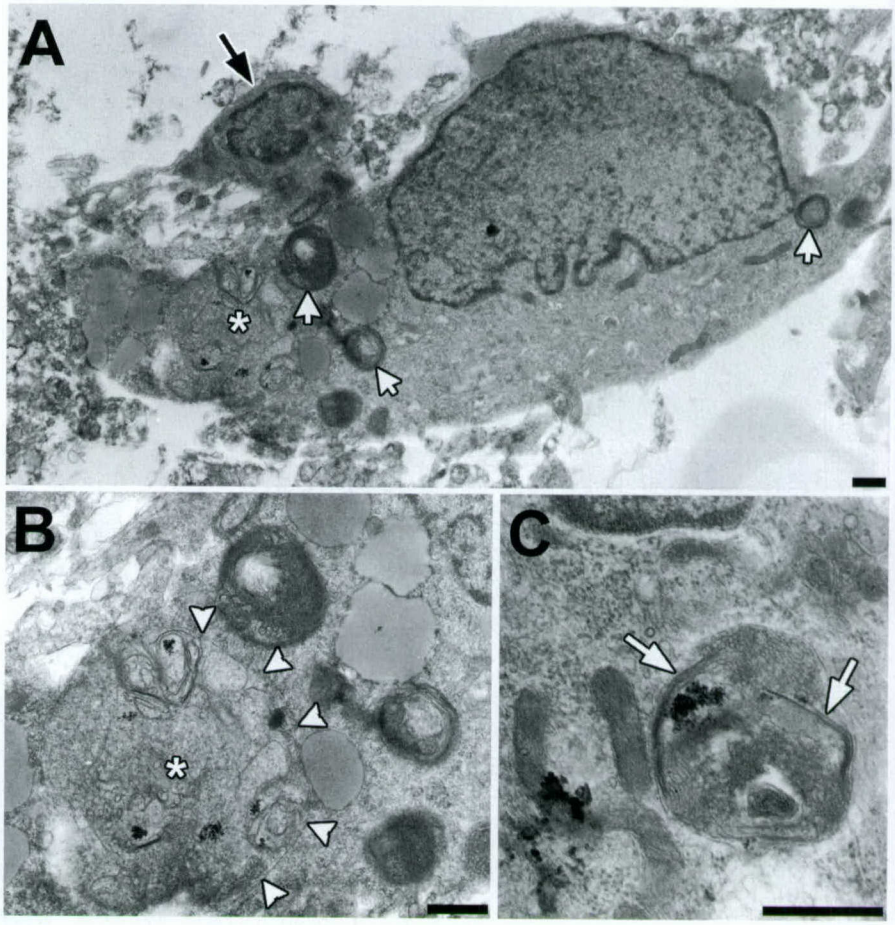

Figure 4. Transmission electron microscopy of Purkinje neurons after 24 hr of trophic factor withdrawal demonstrates ultrastructural features of autophagy. *A*, Low-power micrograph of a large Purkinje cell with multiple secondary lysosomes (white arrows) and a large autophagic vacuole (asterisk). In contrast, the smaller cerebellar granule neuron (black arrow) does not show these changes. *B*, Detail of the large autophagic vacuole indicated by the asterisk. There are disorganized membranous structures consistent with endoplasmic reticulum, ribosomes, and glycogen, delimited predominantly by a single membrane (white arrowheads). *C*, Micrograph showing an autophagosome delimited by a double membrane (white arrows). Note the similarity of the contents to adjacent mitochondria and cytoplasmic glycogen (lower left). Scale bars, 500 nm.

Purkinje neurodegeneration is associated with increased autophagy

Extensive cytoplasmic vacuolation was the most prominent morphological feature distinguishing healthy from degenerating Purkinje neurons in response to trophic factor withdrawal. To determine the mechanism underlying the loss of Purkinje neurons, we first characterized the nature of the vacuoles formed during withdrawal conditions. The formation of extensive cytoplasmic vacuoles is consistent with the upregulation of autophagy. The autofluorescent drug MDC has been shown to specifically accumulate in autophagic vacuoles (Biederbick et al., 1995; Munafo and Colombo, 2001). To determine whether autophagy was activated in Purkinje neurons subjected to trophic factor withdrawal, we incubated the cerebellar cultures with MDC and then visualized the MDC staining using live cell imaging techniques. In addition to MDC, the neurons were stained with lysosensor blue, a pH-sensitive dye that fluoresces in acidic compartments (pK_a, 5.2), thus specifically revealing lysosomes. These experiments demonstrated that control Purkinje neurons contained both lysosomal and autophagic vacuoles. However, in healthy Purkinje neurons these vacuoles were on average very small (Fig. 2*A–D*). In contrast, 24 hr of trophic factor withdrawal induced a marked increase in the sizes of autophagic and lysosomal vacuoles, as detected by MDC and lysosensor blue staining, respectively (Fig. 2*E–H*).

To determine whether augmented autophagy contributed to Purkinje neuron death, we incubated the cultures with 5 mM 3-methyladenine (3MA), a drug known to inhibit the formation of autophagosomes (Seglen and Gordon, 1982). Quantitative analysis revealed that trophic factor withdrawal significantly increased the size of vacuoles in Purkinje neurons (Fig. 3*A*). In healthy Purkinje neurons, ~89% of the lysosensor blue-positive vacuoles were <0.75 μm in diameter. After 24 hr of trophic factor withdrawal, most (~47%) of the lysosensor blue-positive vacuoles in the dying Purkinje neurons were much larger with a diameter, between 0.75 and 1.5 μm, and a significant percentage (~32%) were >1.5 μm in diameter. Addition of 5 mM 3MA to the cerebellar cultures almost completely maintained the lysosensor size profile of vacuoles in the range observed in control Purkinje neurons. The inhibition of autophagic activity by 3-methyladenine correlated with significantly increased numbers of Purkinje neurons that remained after 24 hr of trophic factor deprivation (Fig. 3*B*).

Electron microscopic analysis of autophagic vacuoles in trophic factor-deprived Purkinje neurons

Taken together, the above data suggested that autophagy is upregulated in Purkinje neurons subjected to trophic factor withdrawal. Electron microscopy was performed on cerebellar cultures to confirm that the enlarged MDC- and lysosensor-positive vacuoles observed after trophic factor withdrawal were indeed autophagic vacuoles. The electron micrographs revealed that the cytoplasm of identified Purkinje cells showed multiple autophagosomes, multivesicular bodies, and other secondary lysosomes ranging in size from 0.7 to 3.0 μm after 24 hr of trophic factor withdrawal (Fig. 4). Some of these autophagic structures contained ribosomes, glycogen, and disorganized membranous organelles (Fig. 4*A*,*B*, asterisks, *C*). Occasionally, a double membrane was observed extending around cytoplasmic contents (Fig. 4*C*, white arrows), indicative of earlier stages of autophagy (Shelburne et al., 1973). The cytoplasm of Purkinje neurons also contained lipid droplets (Fig. 4*A*). In Purkinje neurons, the nuclear chromatin was uniformly dispersed (Fig. 4*A*). In contrast to the Purkinje neurons, large autophagolysosomes were absent from the granule neurons, which instead showed mild cytoplasmic condensation and peripheral chromatin clumping (Fig. 4*A*, black arrow).

Purkinje neuron autophagy and death are caspase-independent

Previous studies have shown that trophic factor withdrawal and other death-inducing stimuli can simultaneously induce both autophagy and apoptosis (Jia et al., 1997; Xue et al., 1999; Uchiyama, 2001). In these models, caspase activation and apoptosis occurred downstream of autophagy and could be blocked by 3MA. To determine whether the autophagic death pathway in Purkinje neurons acted in concert with caspase activation, we added the broad-spectrum caspase inhibitor zVAD-FMK to Purkinje neurons undergoing trophic factor withdrawal. Addition of zVAD-FMK (100 μM), which effectively inhibits caspase activity in cerebellar granule neurons, was unable to block Purkinje vacuolation or death. The numbers of Purkinje neurons remaining after 24 hr of trophic factor withdrawal in the absence and presence of zVAD-FMK were 55.7 ± 2.8 and 54.7 ± 3.5, respectively. Furthermore, we were unable to detect increases in activated caspase-3 by immunocytochemical techniques in Purkinje neurons undergoing death induced by trophic factor withdrawal (data not shown). In contrast, activated caspase-3 immunoreactivity increases markedly in the granule neurons after trophic factor withdrawal (Linseman et al., 2003). These results suggest that neither autophagy nor death of Purkinje neurons required caspase activation.

NGF promotes survival and decreases autophagy in Purkinje neurons

Having established that trophic factor withdrawal induced autophagy and death of cerebellar Purkinje neurons, we next examined whether neurotrophin signaling could protect Purkinje neurons in this model. NGF is a neurotrophin known to promote the survival and differentiation of many types of neurons both *in vitro* and *in vivo*, including Purkinje neurons (Legrand and Clos, 1991; Cohen-Cory et al., 1993; Mount et al., 1998). We added NGF at various concentrations to the cultures at the time of trophic factor withdrawal and determined its effect on Purkinje survival. High concentrations of NGF (>50 ng/ml) significantly increased Purkinje numbers compared with trophic factor withdrawal alone (Fig. 5*E*). To determine whether NGF could prevent extensive autophagic vacuolation, cultures were subjected to trophic factor withdrawal in the absence or presence of NGF, and quantitative analysis of vacuolation was performed using live cell lysosensor measurements (Fig. 5*G*). Again, in the presence of trophic support, the majority of Purkinje neurons contained small (<0.75 μm) lysosensor-positive vacuoles. After 24 hr of trophic factor withdrawal, most Purkinje neurons contained very large vacuoles, with 49% of vacuoles between 0.75 and 1.5 μm, ~21% of vacuoles between 1.5 and 2.25 μm, and ~13% of vacuoles >2.25 μm. The addition of NGF (2.5 μg/ml) to the trophic factor withdrawal media significantly decreased the overall vacuolation of Purkinje neurons. The lysosome size profile was shifted, with the majority of vacuoles (~76%) being <0.75 μm in diameter, ~19% of vacuoles between 0.75 and 1.5 μm, ~4% of vacuoles between 1.5 and 2.25 μm, and <1% of vacuoles >2.25 μm. Images shown are representative of the overall effects of the various treatments (Fig. 5*A–C*).

To determine whether decreasing NGF in the cerebellar cultures would be sufficient to induce autophagy and death of Purkinje neurons, we added NGF-neutralizing antibodies to the media and determined the effects on Purkinje survival and vacuolation. Addition of NGF-neutralizing antibodies to the cultures for 24 hr reduced the numbers of Purkinje neurons to 70.6 ± 5.3% of controls (Fig. 5*F*). Control IgG had no effect on the number of Purkinje neurons. The effect of the NGF-neutralizing antibodies was less than the effect of complete trophic factor withdrawal, which reduced Purkinje numbers to 45.2 ± 2.7% of control (Fig. 5*F*). To determine whether the NGF-neutralizing antibodies could induce autophagic vacuolation in Purkinje neurons, we performed live cell imaging experiments to measure the sizes of Purkinje lysosomes (Fig. 5*H*). Again, control Purkinje neurons contained mostly small lysosensor-positive vacuoles, whereas 24 hr of trophic factor withdrawal markedly induced the appearance of much larger vacuoles. Addition of NGF-neutralizing antibodies similarly increased the appearance of larger vacuoles in Purkinje neurons, although not to the same extent as trophic factor withdrawal. Control IgG had no effect on the size distribution of the vacuoles. The ability of NGF-neutralizing antibodies to induce the formation of vacuoles was also observed by calbindin staining (Fig. 5, compare *A*, *D*).

The protective effects of NGF on Purkinje neurons are independent of TrkA signaling

NGF exerts its effects by binding to two distinct receptors, the TrkA receptor and p75ntr. The high concentrations of NGF required to promote Purkinje survival suggested that the p75ntr receptor mediated the neuroprotective effects of NGF in these cultures. Further data supporting this hypothesis come from experiments showing that TrkA receptor tyrosine phosphorylation is high under basal conditions and does not change on trophic factor withdrawal (up to 6 hr) or on addition of high doses of NGF (Fig. 6*A*,*B*). Furthermore, Purkinje neurons demonstrated significantly increased autophagic vacuolation (within 3–4 hr of trophic factor withdrawal, as assessed by live cell lysosensor measurements of vacuole size; Fig. 6*C*) before any significant decrease in TrkA activation.

In the presence of trophic factors, the p75ntr supports Purkinje neuron survival

The p75 neurotrophin receptor is expressed throughout the developing cerebellum and demonstrates specific spatial and temporal regulation (Yan and Johnson, 1988; Carter et al., 2003). In

particular, p75ntr is expressed in the developing Purkinje neurons by postnatal day 7, the time point at which we obtained our cerebellar cultures. p75ntr immunoreactivity gradually decreases until it becomes absent from adult cerebellum; however, injury such as axotomy of Purkinje neurons results in marked re-expression of p75ntr in the injured neurons (Martinez-Murillo et al., 1993). These data suggest that p75ntr is involved in both the development of the cerebellum and injury responses in Purkinje neurons.

To determine whether p75ntr was involved in mediating autophagy and death of Purkinje neurons, cerebellar cultures were incubated with antisense oligonucleotides directed against a 5′ region spanning the initiation codon of the rat p75ntr mRNA. This antisense sequence has been shown to be effective at preventing the NGF withdrawal or axotomy-induced death of dorsal root ganglion neurons (Barrett and Bartlett, 1994; Cheema et al., 1996) and the axotomy-induced death of spinal motor neurons (Lowry et al., 2001), which are mediated by p75ntr. Dissociated cerebellar tissue was triturated with 5 μM 56-FAM-labeled antisense or missense phosphorothioate oligonucleotides at the time of plating. The antisense entered both granule neurons and Purkinje neurons in the culture, with nearly 100% efficiency as assessed by fluorescence microscopy. The p75ntr antisense had two distinct effects on the neurons in the culture. Inclusion of the antisense in the culture medium for 7 d resulted in a significant decrease in the basal survival of both cerebellar granule and Purkinje neurons. Purkinje neuron number with the p75ntr antisense was 35 ± 2.3% of control cultures. The effect of the p75ntr antisense on cell numbers was specific because cultures treated with scrambled missense oligonucleotides did not demonstrate diminished survival. Also, the loss of cells induced by p75ntr antisense was not apparent until approximately day 4 or 5 in culture (as assed by cell density by bright-field examination of the cultures). This corresponds to the time in culture when NGF production is first detectable by Western blot analysis (data not shown). These findings suggest that p75ntr mediates survival in response to autocrine and paracrine neurotrophic factors such as NGF and possibly other neurotrophins such as brain-derived neurotrophic factor (BDNF) or neurotrophin-3 (NT-3), which are known to be secreted by cells in these cerebellar cultures (Favaron et al., 1993; Leingartner et al., 1994; Condorelli et al., 1998; Marini et al., 1998; Bhave et al., 1999).

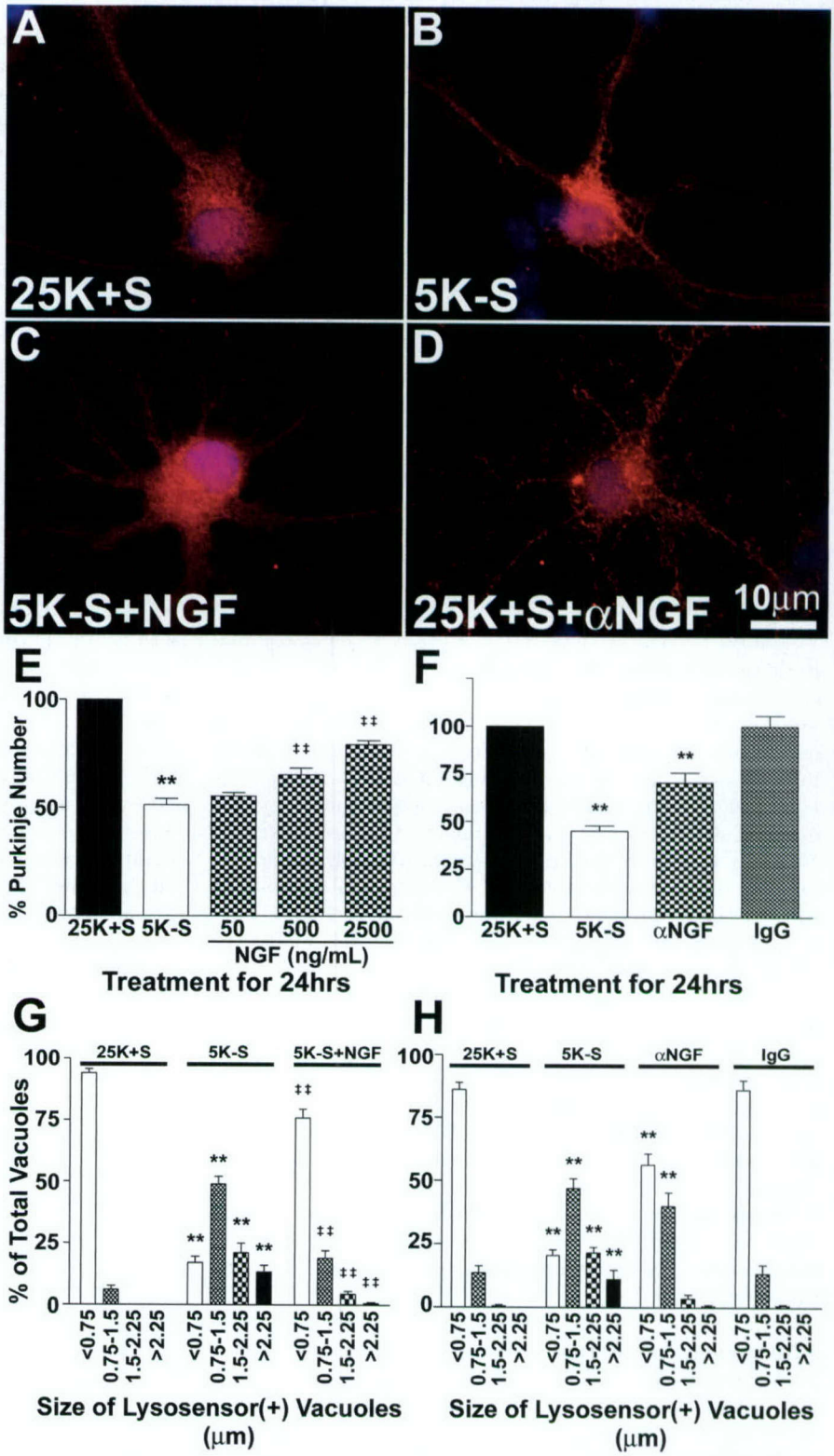

Figure 5. The neurotrophin NGF blocks the loss and the increased vacuolation of Purkinje neurons. *A–D*, Purkinje neurons maintained in various conditions were fixed and stained with antibodies to calbindin-D28k (a specific marker of Purkinje neurons; red) and the nuclear dye DAPI (blue). Images shown are representative of the effects of the various treatments. Purkinje neurons were maintained in control medium (*A*, 25K+S), trophic factor withdrawal medium (*B*, 5K−S), trophic factor withdrawal medium with 2500 ng/ml NGF (*C*, 5K−S+NGF), and control medium with 2 μg/ml NGF-neutralizing antibodies (*D*, 25K+S+αNGF) for 24 hr. *E*, Quantitation of the effects of NGF on Purkinje neuron numbers demonstrates that NGF partially rescues Purkinje neurons from death in a concentration-dependent manner after 24 hr of trophic factor withdrawal, compared with healthy controls. *F*, Quantitation of the effects of NGF-neutralizing antibodies on Purkinje neuron numbers demonstrates that depleting NGF from control media results in a loss of Purkinje neurons, whereas control antibodies had no effect on Purkinje survival. Numbers are mean ± SEM values of at least three independent experiments, each performed in triplicate. *G*, *H*, The

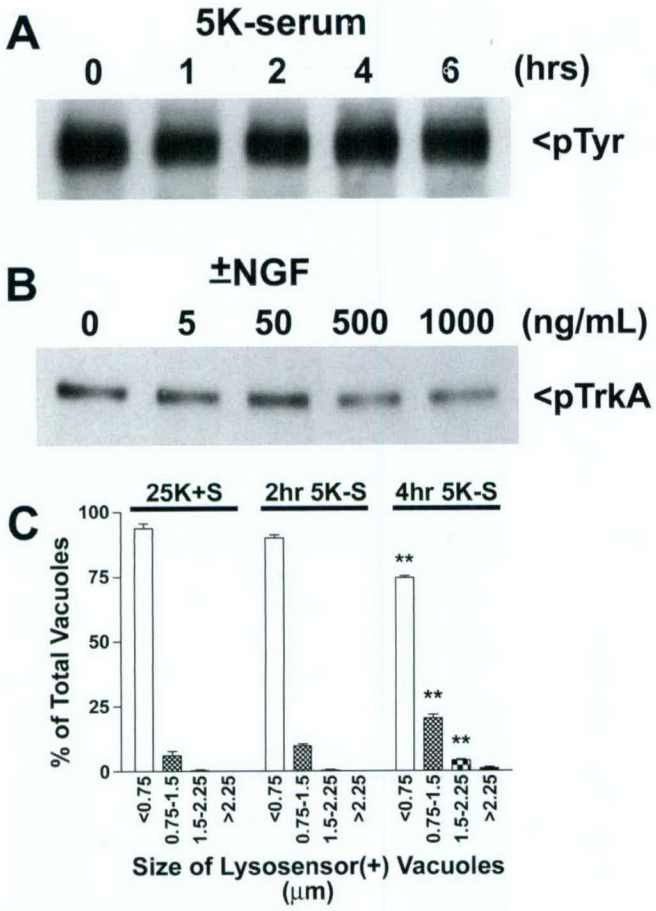

Figure 6. The protective effects of NGF are not mediated by TrkA. Immunoblot analysis was performed to determine the effects of trophic factor withdrawal and various doses of NGF on TrkA activation. *A*, Immunoblot of samples from cultures subjected to 0, 1, 2, 4, and 6 hr of trophic factor withdrawal with a phosphotyrosine-specific Ab. *B*, Immunoblot of samples from cultures subjected to acid wash, followed by 2 hr of trophic factor withdrawal and then incubation with 0, 5, 50, 500, or 1000 ng/ml of NGF for 10 min. *C*, The effects of a short time course of trophic factor withdrawal on vacuole size were quantified by measuring the diameters of all visible lysosensor blue-positive vacuoles in 6–12 Purkinje neurons per treatment condition in at least three independent experiments. Usually, the total number of vacuoles measured per condition was between 100 and 200. The size distribution was graphed as a percentage of total vacuoles that were within the indicated size ranges. **,*Significant difference from 25K+S (**$p < 0.01$; *$p < 0.05$).

p75ntr promotes autophagy and death of Purkinje neurons in the absence of trophic stimuli

In contrast to its effects on basal survival, the p75ntr antisense completely blocked the death of Purkinje neurons induced by 48 hr of trophic factor withdrawal (Fig. 7*A*). Moreover, 5 μM antisense decreased the autophagic vacuolation of Purkinje neurons elicited by 24 hr of trophic factor withdrawal (Fig. 7*B*). Again, in the presence of trophic support, most (~90%) of the Purkinje neuron lysosensor-positive vacuoles were <0.75 μm, and only ~10% of vacuoles were between 0.75 and 1.5 μm, with no vacuoles >1.5 μm in diameter After 24 hr of trophic factor withdrawal, most Purkinje neurons contained very large vacuoles, with ~49% of vacuoles between 0.75 and 1.5 μm, ~13% of vacuoles between 1.5 and 2.25 μm, and ~11% of vacuoles >2.25 μm. Cultures that were preincubated with p75ntr antisense oligonucleotides demonstrated a shifted lysosome size profile, with ~70% of vacuoles <0.75 μm in diameter, ~26% of vacuoles between 0.75 and 1.5 μm, ~4% of vacuoles between 1.5 and 2.25 μm, and <1% of vacuoles >2.25 μm. In contrast, missense oligonucleotides had no effect on the lysosome size profile of Purkinje neurons deprived of trophic support (Fig. 7*B*). Collectively, the above results indicate that antisense-mediated depletion of p75ntr decreases the basal survival of Purkinje neurons in the presence of trophic support. However, under conditions of trophic factor withdrawal, decreasing p75ntr provides a survival advantage to the remaining Purkinje neurons. The ability of p75ntr to mediate both the survival and death in the same neuron depending on cellular context is consistent with previous reports of its effects on dorsal root ganglion neuron survival (Barrett and Bartlett, 1994; Sorensen et al., 2003).

Overexpression of a truncated p75ntr lacking the extracellular domain induces Purkinje neuron autophagy and death in the presence of trophic support

To provide direct evidence that the p75ntr can induce autophagy and death in Purkinje neurons, we investigated the effects of adenoviral-mediated overexpression of a myristoylated rat p75ntr intracellular domain (p75mICD) protein. This p75ntr truncation mutant was used because it lacks the ligand-binding domain, which would complicate the interpretation of results because of the presence of endogenous neurotrophins in these cultures. It has been shown that relatively low expression levels of this p75ntr mutant mediate the survival of PC12 cells. In contrast, high levels of p75mICD expression induce efficient PC12 cell death (Roux et al., 2001). Finally, it has been demonstrated that the intracellular domain possesses the potent cell death-inducing activity of p75ntr (Majdan et al., 1997; Coulson et al., 2000; Rabizadeh et al., 2000; Murray et al., 2003). Cultures were infected with recombinant control CMV or p75mICD adenoviruses at various multiplicities of infection (moi) on day 5 in culture. After incubation for 48 hr, the cultures were fixed and stained with polyclonal antibodies raised against the intracellular domain of rat p75ntr (Majdan et al., 1997), followed by a Cy3-conjugated secondary antibody. Increases in p75ntr immunoreactivity after infection with the p75mICD adenovirus were primarily and consistently observed in cells with morphologies typical of Purkinje neurons. Semiquantitative analysis of fluorescence images indicated that p75ntr expression in p75mICD-infected Purkinje neurons was increased by 3.4-fold compared with uninfected controls or cells infected with control CMV adenovirus. To determine whether overexpression of p75mICD could induce Purkinje neuron death, infected neurons were fixed and stained with calbindin antibodies to quantify Purkinje numbers. Overexpression of p75mICD resulted in a dose-dependent loss of Purkinje neurons, with infection at 50 moi yielding similar levels of Purkinje cell loss, as was observed with trophic factor withdrawal (Fig. 8*A*). Infection with a control adenovirus at 50 moi did not induce significant Purkinje neuron death (Fig. 8*A*). To determine whether overexpression of p75mICD could induce autophagic vacuolation in Purkinje neurons, live cell quan-

←

effects of the various treatments on vacuole size were quantified by measuring the diameters of all visible lysosensor blue-positive vacuoles in 6–12 Purkinje neurons per treatment condition in at least three independent experiments. Usually, the total number of vacuoles measured per condition was between 100 and 200. The size distribution was graphed as a percentage of total vacuoles that were within the indicated size ranges. *G*, A high concentration of NGF (2500 ng/ml) significantly decreased the autophagic vacuolation of Purkinje neurons induced by 24 hr of trophic factor withdrawal. *H*, NGF-neutralizing antibodies significantly increased the vacuolation of Purkinje neurons in control media. *E–H*, **,*Significant difference from 25K+S (**$p < 0.01$; *$p < 0.05$). ‡‡,‡Significant difference from 5K−S (‡‡$p < 0.01$; ‡$p < 0.05$).

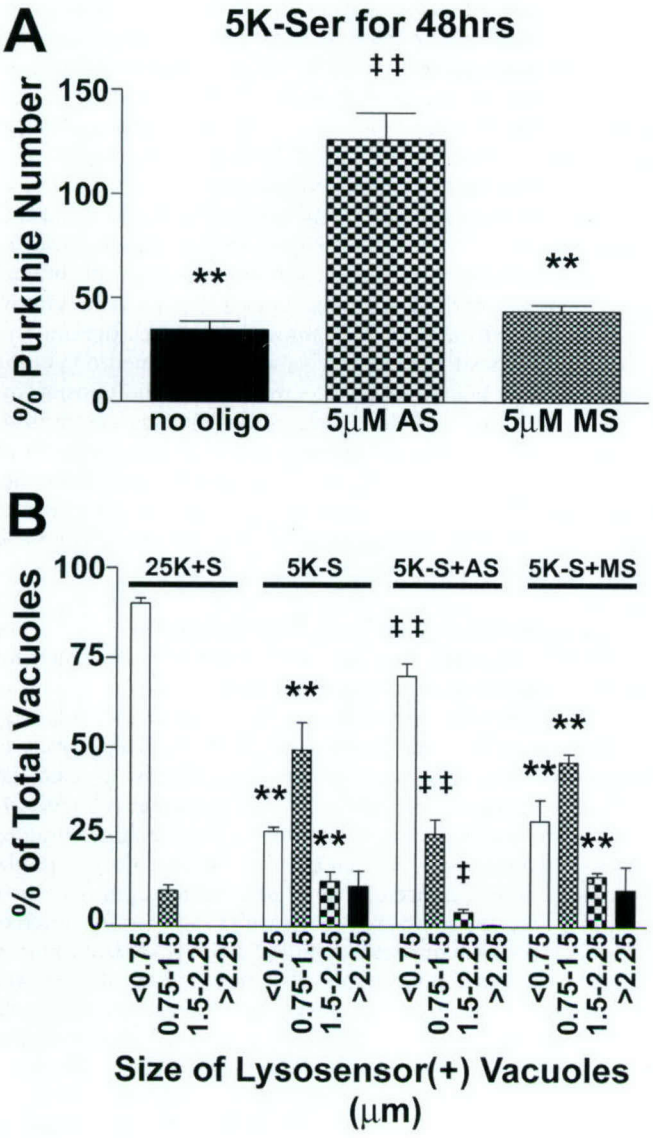

Figure 7. p75ntr antisense inhibits the loss and vacuolation of Purkinje neurons. Purkinje neurons maintained in various conditions were fixed and stained with antibodies to calbindin-D28k. *A*, Quantitation of the effects p75ntr antisense (AS) and missense (MS) oligonucleotides (oligo) on Purkinje neuron numbers expressed as the percentage of the appropriate control demonstrates that p75ntr antisense completely blocks the loss of Purkinje neurons induced by trophic factor withdrawal, whereas missense oligos had no effect on Purkinje survival. Numbers are mean ± SEM values of at least three independent experiments, each performed in triplicate. *B*, The effects of the various treatments on vacuole size were quantified by measuring the diameters of all visible lysosensor blue-positive vacuoles in 6–12 Purkinje neurons per treatment condition in at least three independent experiments. Usually, the total number of vacuoles measured per condition was between 100 and 200. The size distribution was graphed as a percentage of total vacuoles that were within the indicated size ranges. **,*Significant difference from 25K+S (**$p < 0.01$; *$p < 0.05$). ‡‡,‡Significant difference from 5K−S (‡‡$p < 0.01$; ‡$p < 0.05$).

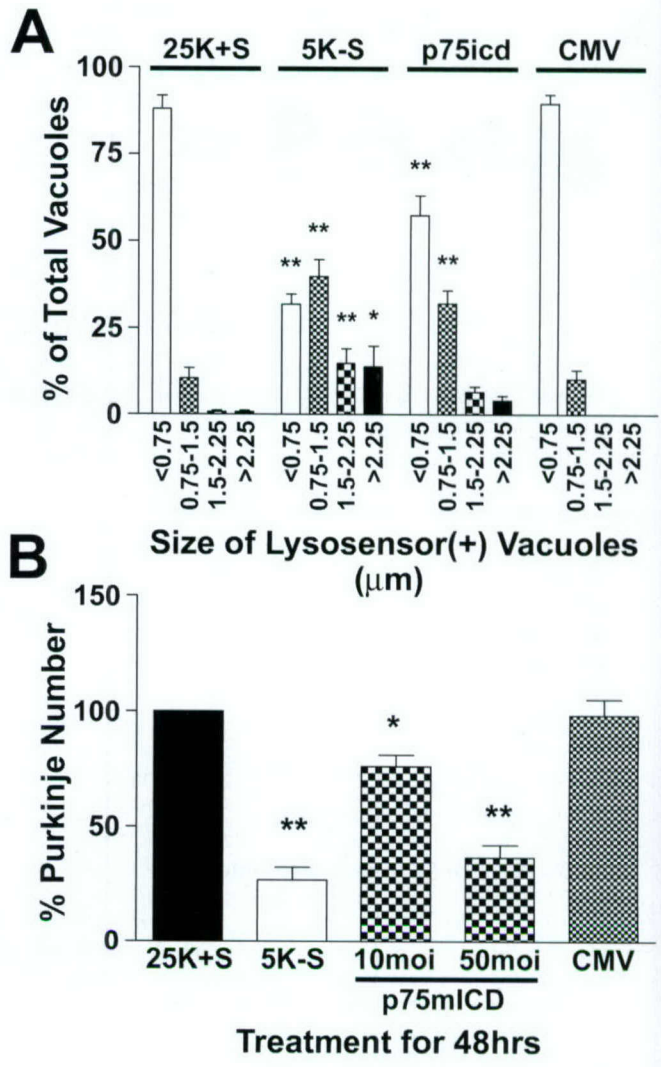

Figure 8. Overexpression of a truncated p75ntr receptor lacking the ligand-binding domain induces the loss and vacuolation of Purkinje neurons. Cultures were subjected to trophic factor withdrawal or adenoviral infection with either control CMV (at 50 moi) or myristoylated intracellular domain p75ntr (at both 10 and 50 moi) adenoviruses on DIV 5. *A*, The cells were fixed and stained with calbindin antibodies to determine Purkinje neuron numbers after the various treatments. *B*, The effects of p75mICD and CMV infection at 50 moi on vacuole size were quantified by measuring the diameters of all visible lysosensor blue-positive vacuoles in 6–12 Purkinje neurons per treatment condition in at least three independent experiments. Usually, the total number of vacuoles measured per condition was between 100 and 200. The size distribution was graphed as a percentage of total vacuoles that were within the indicated size ranges. **,*Significant difference from 25K+S (**$p < 0.01$; *$p < 0.05$).

tification of lysosome size was performed (Fig. 8*B*). Purkinje neurons that were infected with 50 moi of p75mICD adenovirus demonstrated significantly increased autophagic vacuolation, with only ~58% of vacuoles <0.75 μm, ~32% of vacuoles between 0.75 and 1.5 μm, ~7% of vacuoles between 1.5 and 2.25 μm, and ~4% of vacuoles >2.25 μm. Infection with 50 moi of control CMV adenovirus did not significantly increase Purkinje neuron vacuolation. In addition to increasing autophagic vacuolation, p75mICD infection caused notable membrane blebbing and, in some rare cases, nuclear condensation and fragmentation in Purkinje neurons. Our observations of increased autophagy with p75mICD expression are consistent with a previous report of p75ntr intracellular domain-induced death being morphologically characterized by increased vacuolation (Coulson et al., 2000), in addition to the regularly reported morphological features of apoptosis.

Discussion

Morphological studies of diseased human postmortem brain consistently reveal signs of increased autophagic activity in degenerating neuronal populations. There are multiple reports in the literature that describe autophagic vacuoles, as well as disturbances in the lysosomal degradative system in neurodegenerative conditions such as Alzheimer's disease (Cataldo et al., 1996; Nixon et al., 2000), Parkinson's disease (Anglade et al., 1997),

Huntington's disease (Kegel et al., 2000; Petersen et al., 2001), prion encephalopathies (Boellaard et al., 1991; Jeffrey et al., 1992), and diffuse Lewy body disease (Zhu et al., 2003). Extensive cytoplasmic vacuole formation, consistent with autophagy, also has been described in degenerating cerebellar Purkinje neurons in models of ischemia (Fessatidis et al., 1993; Barenberg et al., 2001) and in spinocerebellar ataxia 1 transgenic mice (Skinner et al., 2001). Recently, autophagy has been implicated in the death of cerebellar Purkinje neurons in the Lurcher mouse, which suffers from extensive Purkinje neuron degeneration caused by a point mutation in the δ2 glutamate receptor (Zuo et al., 1997). Two reports have also shown that Lurcher Purkinje neurons demonstrate ultrastructural features of autophagy at a time when they begin to degenerate (Yue et al., 2002; Selimi et al., 2003). In addition, overexpression of the mutant glutamate receptor induced autophagy and death in human embryonic kidney 293 cells (Yue et al., 2002). In the current study, we have shown that autophagy is greatly enhanced in Purkinje neurons that are dying as a result of trophic factor deprivation, and treatments that decrease autophagy are associated with increased survival, lending further support to the hypothesis that enhanced autophagy is involved in Purkinje neuron degeneration. Moreover, we have identified a role for p75ntr as a possible mediator of autophagy and death in Purkinje neurons.

It is generally accepted that the neurotrophins NGF, BDNF, NT-3, and NT-4/5 promote survival and differentiation by binding to their cognate Trk receptors (Ibanez et al., 1992). In contrast, deciphering the role of p75ntr signaling in mediating neurotrophin effects has been complicated by several factors. First, p75ntr shares structural homologies with members of the tumor necrosis factor receptor family of death receptors and lacks intrinsic tyrosine kinase activity. Second, all four neurotrophins are able to bind to p75ntr with similar affinity but display selectivity when binding to the Trk receptors (Klein et al., 1991a,b; Lamballe et al., 1991). Third, p75ntr is often coexpressed with Trk receptors, and neurotrophin effects are dependent on the relative complements of Trk and p75 neurotrophin receptors (for review, see Rabizadeh and Bredesen, 2003). In this context, it has been shown that the presence of p75ntr is required for high-affinity binding of neurotrophins to Trk receptors (Hempstead et al., 1991). Yet another layer of complexity is added when one considers that unprocessed proneurotrophins demonstrate higher-affinity binding to p75ntr but have negligible binding to Trk receptors (Lee et al., 2001). Finally, p75ntr may also function as a coreceptor with the Nogo receptor (Wang et al., 2002) or as a receptor for prion (Della-Bianca et al., 2001) and β-amyloid proteins (Yaar et al., 1997). These complexities in neurotrophin signaling may provide some explanation for the paradoxical roles ascribed to p75ntr in the literature. Expression of p75ntr is capable of inducing death, especially when neurotrophin concentrations are limited (Rabizadeh et al., 1993; Barrett and Georgiou, 1996). In addition, p75ntr signaling can result in death in response to neurotrophin binding (Casaccia-Bonnefil et al., 1996; Frade et al., 1996; Kuner and Hertel, 1998; Friedman, 2000). In contrast, other reports suggest that p75ntr plays an important and necessary role in mediating survival in response to neurotrophins (Barrett and Bartlett, 1994; Barrett et al., 1998; DeFreitas et al., 2001; Bui et al., 2002).

In the current report, we provide evidence that p75ntr plays an important role in mediating autophagy and death of cerebellar Purkinje neurons induced by trophic factor withdrawal. The promotion of survival and the reduction of autophagic vacuolation required high concentrations of NGF, suggesting the involvement of p75ntr. TrkA phosphorylation was not correlated with the autophagic vacuolation induced by trophic factor withdrawal or with neuroprotection mediated by NGF. Decreasing available neurotrophin with NGF-neutralizing antibodies induced autophagic vacuolation and death of Purkinje neurons. Antisense to p75ntr decreased autophagy and completely inhibited the loss of Purkinje neurons in response to trophic factor withdrawal. Moreover, adenoviral-mediated overexpression of a myristoylated rat p75ntr intracellular domain protein (p75mICD) resulted in significantly increased autophagic vacuolation that was also accompanied by a significant loss of Purkinje neurons. Finally, our results directly show that Purkinje neuron death induced by either trophic factor withdrawal or p75mICD overexpression is associated with increased autophagic vacuolation, suggesting an important role for autophagy during Purkinje neuron degeneration.

Our results with p75ntr antisense suggest a dual role for p75ntr in mediating both the survival and death of Purkinje neurons. Antisense to p75ntr decreased the survival of Purkinje neurons maintained in healthy conditions. The loss of neurons induced with p75ntr antisense occurred at a time when NGF synthesis becomes detectable, suggesting that p75ntr is required for the basal survival of the cerebellar neurons that is mediated by autocrine and paracrine neurotrophin production in theses cultures. In contrast, Purkinje neurons pretreated with p75ntr antisense were completely resistant to death and demonstrated decreased vacuolation in response to trophic factor withdrawal. Collectively, our results suggest that neurotrophin signaling through p75ntr can regulate the survival and death of Purkinje neurons. One can speculate that in the presence of appropriate neurotrophin, signaling from p75ntr can promote Purkinje survival, and decreasing neurotrophin levels can lead to a loss of prosurvival p75ntr signals. However, it is also possible that a loss of appropriate neurotrophins not only leads to a loss of prosurvival signals but also may result in the generation of prodeath signals from p75ntr. This concept of p75ntr as a dependence receptor has been hypothesized by others to explain the paradoxical nature of p75ntr function (Rabizadeh et al., 2000). In addition, our data have not formally ruled out the possibility that trophic factor withdrawal results in an increase of some ligand that promotes prodeath p75ntr signals because there is evidence in the literature that p75ntr may have other ligands or may also function as a coreceptor with other proteins (Yaar et al., 1997; Della-Bianca et al., 2001; Wang et al., 2002).

Despite the evidence suggesting that autophagy is upregulated in neurodegeneration, very little is known about the cellular mechanisms that regulate autophagy in neurons (for review, see Yuan et al., 2003). Several reports suggest that the activation of autophagy contributes to the death of neurons (Xue et al., 1999; Uchiyama, 2001; Borsello et al., 2003; Weeks, 2003). In contrast, other studies indicate a neuroprotective role for autophagy in Huntington's disease and α-synucleopathies (Qin et al., 2003; Webb et al., 2003). These studies demonstrate that autophagy may be a mechanism for mutant protein degradation and the prevention of plaque formation. Similarly, in cases in which mitochondria are extensively damaged, autophagy may be protective by sequestering and degrading defective mitochondria before they can release death-inducing proteins (Lemasters et al., 2002; Tolkovsky et al., 2002). One can speculate that the degree and specificity of autophagy may determine cell fate. By elucidating the molecular pathways that regulate autophagy, it may be possible to determine which components of autophagy may contribute to neurodegeneration and which may be neuroprotective. In

addition to the questions regarding autophagy as a survival or death mechanism, it will be of great importance to understand the effects of autophagy on neuronal function, such as the formation and maintenance of synapses, the transduction of electrical impulses, and neurotransmitter release.

References

Anglade P, Vyas S, Javoy-Agid F, Herrero MT, Michel PP, Marquez J, Mouatt-Prigent A, Ruberg M, Hirsch EC, Agid Y (1997) Apoptosis and autophagy in nigral neurons of patients with Parkinson's disease. Histol Histopathol 12:25–31.

Bailey A, Luthert P, Dean A, Harding B, Janota I, Montgomery M, Rutter M, Lantos P (1998) A clinicopathological study of autism. Brain 121:889–905.

Baptista CA, Hatten ME, Blazeski R, Mason CA (1994) Cell-cell interactions influence survival and differentiation of purified Purkinje cells in vitro. Neuron 12:243–260.

Barenberg P, Strahlendorf H, Strahlendorf J (2001) Hypoxia induces an excitotoxic-type of dark cell degeneration in cerebellar Purkinje neurons. Neurosci Res 40:245–254.

Barrett GL, Bartlett PF (1994) The p75 nerve growth factor receptor mediates survival or death depending on the stage of sensory neuron development. Proc Natl Acad Sci USA 91:6501–6505.

Barrett GL, Georgiou A (1996) The low-affinity nerve growth factor receptor p75NGFR mediates death of PC12 cells after nerve growth factor withdrawal. J Neurosci Res 45:117–128.

Barrett GL, Georgiou A, Reid K, Bartlett PF, Leung D (1998) Rescue of dorsal root sensory neurons by nerve growth factor and neurotrophin-3, but not brain-derived neurotrophic factor or neurotrophin-4, is dependent on the level of the p75 neurotrophin receptor. Neuroscience 85:1321–1328.

Bhave SV, Ghoda L, Hoffman PL (1999) Brain-derived neurotrophic factor mediates the anti-apoptotic effect of NMDA in cerebellar granule neurons: signal transduction cascades and site of ethanol action. J Neurosci 19:3277–3286.

Biederbick A, Kern HF, Elsasser HP (1995) Monodansylcadaverine (MDC) is a specific in vivo marker for autophagic vacuoles. Eur J Cell Biol 66:3–14.

Boellaard JW, Kao M, Schlote W, Diringer H (1991) Neuronal autophagy in experimental scrapie. Acta Neuropathol (Berl) 82:225–228.

Borghesani PR, Alt FW, Bottaro A, Davidson L, Aksoy S, Rathbun GA, Roberts TM, Swat W, Segal RA, Gu Y (2000) Abnormal development of Purkinje cells and lymphocytes in Atm mutant mice. Proc Natl Acad Sci USA 97:3336–3341.

Borsello T, Croquelois K, Hornung JP, Clarke PG (2003) *N*-methyl-D-aspartate-triggered neuronal death in organotypic hippocampal cultures is endocytic, autophagic and mediated by the c-Jun N-terminal kinase pathway. Eur J Neurosci 18:473–485.

Bui NT, Konig HG, Culmsee C, Bauerbach E, Poppe M, Krieglstein J, Prehn JH (2002) p75 neurotrophin receptor is required for constitutive and NGF-induced survival signalling in PC12 cells and rat hippocampal neurones. J Neurochem 81:594–605.

Carter AR, Berry EM, Segal RA (2003) Regional expression of p75NTR contributes to neurotrophin regulation of cerebellar patterning. Mol Cell Neurosci 22:1–13.

Casaccia-Bonnefil P, Carter BD, Dobrowsky RT, Chao MV (1996) Death of oligodendrocytes mediated by the interaction of nerve growth factor with its receptor p75. Nature 383:716–719.

Cataldo AM, Hamilton DJ, Barnett JL, Paskevich PA, Nixon RA (1996) Properties of the endosomal-lysosomal system in the human central nervous system: disturbances mark most neurons in populations at risk to degenerate in Alzheimer's disease. J Neurosci 16:186–199.

Cheema SS, Barrett GL, Bartlett PF (1996) Reducing p75 nerve growth factor receptor levels using antisense oligonucleotides prevents the loss of axotomized sensory neurons in the dorsal root ganglia of newborn rats. J Neurosci Res 46:239–245.

Cohen-Cory S, Elliott RC, Dreyfus CF, Black IB (1993) Depolarizing influences increase low-affinity NGF receptor gene expression in cultured Purkinje neurons. Exp Neurol 119:165–175.

Condorelli DF, Dell'Albani P, Timmusk T, Mudo G, Belluardo N (1998) Differential regulation of BDNF and NT-3 mRNA levels in primary cultures of rat cerebellar neurons. Neurochem Int 32:87–91.

Coulson EJ, Reid K, Baca M, Shipham KA, Hulett SM, Kilpatrick TJ, Bartlett PF (2000) Chopper, a new death domain of the p75 neurotrophin receptor that mediates rapid neuronal cell death. J Biol Chem 275:30537–30545.

DeFreitas MF, McQuillen PS, Shatz CJ (2001) A novel p75NTR signaling pathway promotes survival, not death, of immunopurified neocortical subplate neurons. J Neurosci 21:5121–5129.

Della-Bianca V, Rossi F, Armato U, Dal-Pra I, Costantini C, Perini G, Politi V, Della Valle G (2001) Neurotrophin p75 receptor is involved in neuronal damage by prion peptide-(106–126). J Biol Chem 276:38929–38933.

D'Mello SR, Galli C, Ciotti T, Calissano P (1993) Induction of apoptosis in cerebellar granule neurons by low potassium: inhibition of death by insulin-like growth factor I and cAMP. Proc Natl Acad Sci USA 90:10989–10993.

Favaron M, Manev RM, Rimland JM, Candeo P, Beccaro M, Manev H (1993) NMDA-stimulated expression of BDNF mRNA in cultured cerebellar granule neurones. NeuroReport 4:1171–1174.

Ferrer I, Saracibar N, Gonzalez G (1991) Spongiform encephalopathy and multisystemic degeneration. Neurologia 6:29–33.

Fessatidis IT, Thomas VL, Shore DF, Hunt RH, Weller RO (1993) Neuropathological features of profoundly hypothermic circulatory arrest: an experimental study in the pig. Cardiovasc Surg 1:155–160.

Frade JM, Rodriguez-Tebar A, Barde YA (1996) Induction of cell death by endogenous nerve growth factor through its p75 receptor. Nature 383:166–168.

Friedman WJ (2000) Neurotrophins induce death of hippocampal neurons via the p75 receptor. J Neurosci 20:6340–6346.

Gatti RA, Vinters HV (1985) Cerebellar pathology in ataxia-telangiectasia: the significance of basket cells. Kroc Found Ser 19:225–232.

Ghez C, Thach WT (2000) The cerebellum. In: Principles of neuroscience (Kandel ER, Schwartz JH, Jessell TM, eds), pp 832–852. New York: McGraw-Hill.

Hempstead BL, Martin-Zanca D, Kaplan DR, Parada LF, Chao MV (1991) High-affinity NGF binding requires coexpression of the trk proto-oncogene and the low-affinity NGF receptor. Nature 350:678–683.

Ibanez CF, Ebendal T, Barbany G, Murray-Rust J, Blundell TL, Persson H (1992) Disruption of the low affinity receptor-binding site in NGF allows neuronal survival and differentiation by binding to the trk gene product. Cell 69:329–341.

Jeffrey M, Scott JR, Williams A, Fraser H (1992) Ultrastructural features of spongiform encephalopathy transmitted to mice from three species of bovidae. Acta Neuropathol (Berl) 84:559–569.

Jia L, Dourmashkin RR, Allen PD, Gray AB, Newland AC, Kelsey SM (1997) Inhibition of autophagy abrogates tumour necrosis factor alpha induced apoptosis in human T-lymphoblastic leukaemic cells. Br J Haematol 98:673–685.

Kegel KB, Kim M, Sapp E, McIntyre C, Castano JG, Aronin N, DiFiglia M (2000) Huntingtin expression stimulates endosomal-lysosomal activity, endosome tubulation, and autophagy. J Neurosci 20:7268–7278.

Klein R, Jing SQ, Nanduri V, O'Rourke E, Barbacid M (1991a) The trk proto-oncogene encodes a receptor for nerve growth factor. Cell 65:189–197.

Klein R, Nanduri V, Jing SA, Lamballe F, Tapley P, Bryant S, Cordon-Cardo C, Jones KR, Reichardt LF, Barbacid M (1991b) The trkB tyrosine protein kinase is a receptor for brain-derived neurotrophic factor and neurotrophin-3. Cell 66:395–403.

Klionsky DJ, Emr SD (2000) Autophagy as a regulated pathway of cellular degradation. Science 290:1717–1721.

Koeppen AH (1998) The hereditary ataxias. J Neuropathol Exp Neurol 57:531–543.

Kuner P, Hertel C (1998) NGF induces apoptosis in a human neuroblastoma cell line expressing the neurotrophin receptor p75NTR. J Neurosci Res 54:465–474.

Lamballe F, Klein R, Barbacid M (1991) trkC, a new member of the trk family of tyrosine protein kinases, is a receptor for neurotrophin-3. Cell 66:967–979.

Lasmezas CI, Deslys JP, Robain O, Jaegly A, Beringue V, Peyrin JM, Fournier JG, Hauw JJ, Rossier J, Dormont D (1997) Transmission of the BSE agent to mice in the absence of detectable abnormal prion protein. Science 275:402–405.

Lee R, Kermani P, Teng KK, Hempstead BL (2001) Regulation of cell survival by secreted proneurotrophins. Science 294:1945–1948.

Legrand C, Clos J (1991) Biochemical, immunocytochemical and morphological evidence for an interaction between thyroid hormone and nerve growth factor in the developing cerebellum of normal and hypothyroid rats. Dev Neurosci 13:382–396.

Leingartner A, Heisenberg CP, Kolbeck R, Thoenen H, Lindholm D (1994) Brain-derived neurotrophic factor increases neurotrophin-3 expression in cerebellar granule neurons. J Biol Chem 269:828–830.

Lemasters JJ, Qian T, He L, Kim JS, Elmore SP, Cascio WE, Brenner DA (2002) Role of mitochondrial inner membrane permeabilization in necrotic cell death, apoptosis, and autophagy. Antioxid Redox Signal 4:769–781.

Liberski PP, Gajdusek DC, Brown P (2002) How do neurons degenerate in prion diseases or transmissible spongiform encephalopathies (TSEs): neuronal autophagy revisited. Acta Neurobiol Exp (Warsz) 62:141–147.

Linseman DA, McClure ML, Bouchard RJ, Laessig TA, Ahmadi FA, Heidenreich KA (2002a) Suppression of death receptor signaling in cerebellar Purkinje neurons protects neighboring granule neurons from apoptosis via an insulin-like growth factor I-dependent mechanism. J Biol Chem 277:24546–24553.

Linseman DA, Phelps RA, Bouchard RJ, Le SS, Laessig TA, McClure ML, Heidenreich KA (2002b) Insulin-like growth factor-I blocks Bcl-2 interacting mediator of cell death (Bim) induction and intrinsic death signaling in cerebellar granule neurons. J Neurosci 22:9287–9297.

Linseman DA, Bartley CM, Le SS, Laessig TA, Bouchard RJ, Meintzer MK, Li M, Heidenreich KA (2003) Inactivation of the myocyte enhancer factor-2 repressor histone deacetylase-5 by endogenous Ca^{2+}/calmodulin-dependent kinase II promotes depolarization-mediated cerebellar granule neuron survival. J Biol Chem 278:41472–41481.

Lowry KS, Murray SS, Coulson EJ, Epa R, Bartlett PF, Barrett G, Cheema SS (2001) Systemic administration of antisense p75(NTR) oligodeoxynucleotides rescues axotomised spinal motor neurons. J Neurosci Res 64:11–17.

Majdan M, Lachance C, Gloster A, Aloyz R, Zeindler C, Bamji S, Bhakar A, Belliveau D, Fawcett J, Miller FD, Barker PA (1997) Transgenic mice expressing the intracellular domain of the p75 neurotrophin receptor undergo neuronal apoptosis. J Neurosci 17:6988–6998.

Marini AM, Rabin SJ, Lipsky RH, Mocchetti I (1998) Activity-dependent release of brain-derived neurotrophic factor underlies the neuroprotective effect of *N*-methyl-D-aspartate. J Biol Chem 273:29394–29399.

Martinez-Murillo R, Caro L, Nieto-Sampedro M (1993) Lesion-induced expression of low-affinity nerve growth factor receptor-immunoreactive protein in Purkinje cells of the adult rat. Neuroscience 52:587–593.

Mitchener JS, Shelburne JD, Bradford WD, Hawkins HK (1976) Cellular autophagocytosis induced by deprivation of serum and amino acids in HeLa cells. Am J Pathol 83:485–491.

Mount HT, Elkabes S, Dreyfus CF, Black IB (1998) Differential involvement of metabotropic and p75 neurotrophin receptors in effects of nerve growth factor and neurotrophin-3 on cultured Purkinje cell survival. J Neurochem 70:1045–1053.

Munafo DB, Colombo MI (2001) A novel assay to study autophagy: regulation of autophagosome vacuole size by amino acid deprivation. J Cell Sci 114:3619–3629.

Murray SS, Bartlett PF, Lopes EC, Coulson EJ, Greferath U, Cheema SS (2003) Low-affinity neurotrophin receptor with targeted mutation of exon 3 is capable of mediating the death of axotomized neurons. Clin Exp Pharmacol Physiol 30:217–222.

Nixon RA, Cataldo AM, Mathews PM (2000) The endosomal-lysosomal system of neurons in Alzheimer's disease pathogenesis: a review. Neurochem Res 25:1161–1172.

Petersen A, Larsen KE, Behr GG, Romero N, Przedborski S, Brundin P, Sulzer D (2001) Expanded CAG repeats in exon 1 of the Huntington's disease gene stimulate dopamine-mediated striatal neuron autophagy and degeneration. Hum Mol Genet 10:1243–1254.

Qin ZH, Wang Y, Kegel KB, Kazantsev A, Apostol BL, Thompson LM, Yoder J, Aronin N, DiFiglia M (2003) Autophagy regulates the processing of amino terminal Huntingtin fragments. Hum Mol Genet 12:3231–3244.

Rabizadeh S, Bredesen DE (2003) Ten years on: mediation of cell death by the common neurotrophin receptor p75(NTR). Cytokine Growth Factor Rev 14:225–239.

Rabizadeh S, Oh J, Zhong LT, Yang J, Bitler CM, Butcher LL, Bredesen DE (1993) Induction of apoptosis by the low-affinity NGF receptor. Science 261:345–348.

Rabizadeh S, Ye X, Sperandio S, Wang JJ, Ellerby HM, Ellerby LM, Giza C, Andrusiak RL, Frankowski H, Yaron Y, Moayeri NN, Rovelli G, Evans CJ, Butcher LL, Nolan GP, Assa-Munt N, Bredesen DE (2000) Neurotrophin dependence domain: a domain required for the mediation of apoptosis by the p75 neurotrophin receptor. J Mol Neurosci 15:215–229.

Ritvo ER, Freeman BJ, Scheibel AB, Duong T, Robinson H, Guthrie D, Ritvo A (1986) Lower Purkinje cell counts in the cerebella of four autistic subjects: initial findings of the UCLA-NSAC Autopsy Research Report. Am J Psychiatry 143:862–866.

Roux PP, Bhakar AL, Kennedy TE, Barker PA (2001) The p75 neurotrophin receptor activates Akt (protein kinase B) through a phosphatidylinositol 3-kinase-dependent pathway. J Biol Chem 276:23097–23104.

Seglen PO, Gordon PB (1982) 3-Methyladenine: specific inhibitor of autophagic/lysosomal protein degradation in isolated rat hepatocytes. Proc Natl Acad Sci USA 79:1889–1892.

Selimi F, Lohof AM, Heitz S, Lalouette A, Jarvis CI, Bailly Y, Mariani J (2003) Lurcher GRID2-induced death and depolarization can be dissociated in cerebellar Purkinje cells. Neuron 37:813–819.

Shelburne JD, Arstila AU, Trump BF (1973) Studies on cellular autophagocytosis: cyclic AMP- and dibutyryl cyclic AMP-stimulated autophagy in rat liver. Am J Pathol 72:521–540.

Skinner PJ, Vierra-Green CA, Clark HB, Zoghbi HY, Orr HT (2001) Altered trafficking of membrane proteins in purkinje cells of SCA1 transgenic mice. Am J Pathol 159:905–913.

Sorensen B, Tandrup T, Koltzenburg M, Jakobsen J (2003) No further loss of dorsal root ganglion cells after axotomy in p75 neurotrophin receptor knockout mice. J Comp Neurol 459:242–250.

Stromhaug PE, Klionsky DJ (2001) Approaching the molecular mechanism of autophagy. Traffic 2:524–531.

Tolkovsky AM, Xue L, Fletcher GC, Borutaite V (2002) Mitochondrial disappearance from cells: a clue to the role of autophagy in programmed cell death and disease? Biochimie 84:233–240.

Torres-Aleman I, Pons S, Arevalo MA (1994) The insulin-like growth factor I system in the rat cerebellum: developmental regulation and role in neuronal survival and differentiation. J Neurosci Res 39:117–126.

Uchiyama Y (2001) Autophagic cell death and its execution by lysosomal cathepsins. Arch Histol Cytol 64:233–246.

Vaudry D, Falluel-Morel A, Leuillet S, Vaudry H, Gonzalez BJ (2003) Regulators of cerebellar granule cell development act through specific signaling pathways. Science 300:1532–1534.

Wang KC, Kim JA, Sivasankaran R, Segal R, He Z (2002) P75 interacts with the Nogo receptor as a co-receptor for Nogo, MAG and OMgp. Nature 420:74–78.

Watanabe R, Duchen LW (1993) Cerebral amyloid in human prion disease. Neuropathol Appl Neurobiol 19:253–260.

Watase K, Weeber EJ, Xu B, Antalffy B, Yuva-Paylor L, Hashimoto K, Kano M, Atkinson R, Sun Y, Armstrong DL, Sweatt JD, Orr HT, Paylor R, Zoghbi HY (2002) A long CAG repeat in the mouse Sca1 locus replicates SCA1 features and reveals the impact of protein solubility on selective neurodegeneration. Neuron 34:905–919.

Webb JL, Ravikumar B, Atkins J, Skepper JN, Rubinsztein DC (2003) α-Synuclein is degraded by both autophagy and the proteasome. J Biol Chem 278:25009–25013.

Weeks JC (2003) Thinking globally, acting locally: steroid hormone regulation of the dendritic architecture, synaptic connectivity and death of an individual neuron. Prog Neurobiol 70:421–442.

Wetts R, Herrup K (1982) Interaction of granule, Purkinje and inferior olivary neurons in lurcher chimaeric mice. I. Qualitative studies. J Embryol Exp Morphol 68:87–98.

Xue L, Fletcher GC, Tolkovsky AM (1999) Autophagy is activated by apoptotic signalling in sympathetic neurons: an alternative mechanism of death execution. Mol Cell Neurosci 14:180–198.

Yaar M, Zhai S, Pilch PF, Doyle SM, Eisenhauer PB, Fine RE, Gilchrest BA (1997) Binding of beta-amyloid to the p75 neurotrophin receptor induces apoptosis: A possible mechanism for Alzheimer's disease. J Clin Invest 100:2333–2340.

Yan Q, Johnson Jr EM (1988) An immunohistochemical study of the nerve growth factor receptor in developing rats. J Neurosci 8:3481–3498.

Yuan J, Lipinski M, Degterev A (2003) Diversity in the mechanisms of neuronal cell death. Neuron 40:401–413.

Yue Z, Horton A, Bravin M, DeJager PL, Selimi F, Heintz N (2002) A novel protein complex linking the delta 2 glutamate receptor and autophagy: implications for neurodegeneration in lurcher mice. Neuron 35:921–933.

Zanjani HS, Herrup K, Guastavino JM, Delhaye-Bouchaud N, Mariani J (1994) Developmental studies of the inferior olivary nucleus in staggerer mutant mice. Brain Res Dev Brain Res 82:18–28.

Zhu JH, Guo F, Shelburne J, Watkins S, Chu CT (2003) Localization of phosphorylated ERK/MAP kinases to mitochondria and autophagosomes in Lewy body diseases. Brain Pathol 13:473–481.

Zuo J, De Jager PL, Takahashi KA, Jiang W, Linden DJ, Heintz N (1997) Neurodegeneration in Lurcher mice caused by mutation in delta2 glutamate receptor gene. Nature 388:769–773.